PHARMACOGENOMIC MODELING OF BORTEZOMIB RESISTANCE IN B CELL MALIGNANCIES

A DISSERTATION
SUBMITTED TO THE FACULTY OF THE GRADUATE SCHOOL
OF THE UNIVERSITY OF MINNESOTA
BY

HOLLY ANNETTE-FESER STESSMAN

IN PARTIAL FULFILLMENT OF THE REQUIREMENTS
FOR THE DEGREE OF
DOCTOR OF PHILOSOPHY

BRIAN VAN NESS, PHD
ADVISOR

APRIL 2013

Acknowledgements

Claude Lévi-Strauss once said that “the scientist is not a person who gives the right answers, he’s one who asks the right questions” which is why I must first thank my mentor, Brian Van Ness, Ph.D., because he has always encouraged me to ask the next question. Your guidance over the past five years has made me a more mature and confident scientist. I will ever be grateful for the opportunities that you have given me to be involved in writing, presenting, and developing our work which makes leaving all the more bittersweet. Thank you for taking a chance on me and allowing me to grow.

I cannot thank Brian without also thanking my fellow lab mates who have shared this journey with me. Aatif Mansoor has been my right-hand through the majority of the projects that we have undertaken. I would not be here without you, and I wish you all the best as you pursue your medical degree. Thank you also to Samantha Quandahl, Amit Mitra, Ph.D., Taylor Harding, Amanda Farris, and Tsu (Greg) Wu, Ph.D. who contributed greatly to the completion of this work. Also, a special thank you to Trina Kuriger, M.S. and Anthony Rizzardi from the neighboring Nelson and Schmechel Labs for your guidance and for picking me up when I have needed it most. I have been truly blessed to have such amazing friends as colleagues.

I would also like to thank my preliminary and final committee including my chair, David Largaespada, Ph.D., William Oetting, Ph.D., Bonnie LeRoy, M.S., C.G.C., Jatinder Lamba, Ph.D. and Nikunj Somia, Ph.D. for always pushing me to question my work. By taking the time to meet with me, you have made me a more rigorous scientist.

Through this process, I have had the great fortune to work in multiple collaborative groups that have proven to be fruitful partnerships and have provided some amazing professional mentors. I would not be where I am now without the help,

kindness, and friendship of Linda Baughn, Ph.D., Michael Linden, M.D., Ph.D., Chad Myers, Ph.D., Siegfried Janz, M.D., Nathan Dolloff, Ph.D., and Fenghuang (Frank) Zhan, M.D., Ph.D. I also must thank all of the support staff at the University of Minnesota Biomedical Genomics Center, the Masonic Cancer Center Cytogenetics Core, the BioNet Histology and IHC Laboratory, and the University of Iowa PET Imaging Core without whom my work would not have been possible.

In the five years that I have been in Minnesota, there have been many friends who have shared in my successes and failures even amidst their own personal trials. Firstly, I must thank Heather Zierhut for being my closest confidant. Going through this process together has made the road immeasurably better. I would also like to thank Kristin Anderson, Jessica Fiege, Theresa Edelman, Sarah Bloch, Aziza Khatib, Tiffany MacKenzie, and Moony Tseng whose love and support have meant so much.

Finally, I need to thank my family who has been my biggest cheering section. Thank you, Bob, Lois, Andy, Jim, and Katie Stessman, for being the most loving and supportive in-laws. Thank you to Kelsey Feser and Zack Feser, the most amazing siblings a sister could ask for – you motivate me every day to live up to your image of me. Also, a huge thank you to my mom, Mary Melton, who has laughed and cried with me and always helped me make lemonade from life's lemons. Mostly, thank you to my husband, Brian Stessman, who has never stopped believing in me. We have grown so much in the past five years, and I can't think of anyone that I would rather have shared this journey with.

This has been a long hard road, but with such an amazing support structure, I am emerging strong. I know that I will never have all the answers, but I have learned to never be afraid to question – this is what makes a true scientist.

Dedication

This dissertation is dedicated to my mother. Even when I was too young to know the difference, you were advocating for me and allowing me to blossom. Through all the logic puzzles, science fairs, and frustrating college classes, you were there. I am here today because of you.

Abstract

Proteasome inhibitors are a class of drugs that have been largely successful in the treatment of cancer patients, particularly those with the plasma cell malignancy, multiple myeloma. The most successful of these drugs, bortezomib (Bz), has paved the way for the development of next-generation proteasome inhibitors. Although Bz has significantly contributed to improved outcomes in myeloma patients, acquired resistance to Bz is imminent. Furthermore, a portion of patients never initially respond to the drug. Therefore, the goal of these studies was to further characterize Bz resistance with the aim to better predict secondary therapies that may be used successfully with Bz to recapture drug sensitivity.

In the first study, we describe the creation of an *in vitro* malignant mouse plasma cell system from which we create isogenic pairs of Bz-sensitive and -resistant cell lines. We further characterize the transcriptional responses of these cell line pairs to identify both conserved and unique expression signatures. Using the expression signatures that are unique to each pair of cell lines, we identify secondary therapies that may be useful for treatment of the Bz-refractory cell line using an *in silico* database called Connectivity Map (CMAP). This analysis predicted a unique response to histone deacetylase inhibitors, a class of drugs that are currently being tested for efficacy in myeloma, in only one mouse cell line pair. Indeed, we find that the predicted Bz-resistant cell line has increased sensitivity to this class of drugs (including the drug panobinostat). When these cells were transferred back into syngeneic recipient mice, panobinostat treatment could successfully extend the life of Bz-resistant animals suggesting that the Bz-resistant phenotype may select also for increased sensitivity to other drugs that may be identified through *in silico* approaches.

In the second study, we follow up these observations by investigating other CMAP prediction patterns, such as those that are conserved across all cell line pairs. A second prediction of one class of these CMAP-predicted drugs using high-throughput drug screening of the cell lines revealed that a combination of these approaches may be highly successful for accurate prediction of secondary therapies. Based on these predictions, we further investigate the efficacy of topoisomerase inhibitors in combination with Bz for the treatment of Bz-resistant cell lines.

In the third study, we provide further immunophenotypic characterization of the Bz-sensitive and -resistant mouse cell lines revealing not only cell surface markers that are associated with “acquired” and “innate” Bz resistance but perhaps a mechanism of resistance. Although Bz-sensitive mouse cells display a classic myeloma phenotype, homing to the bone marrow *in vivo* and expressing classic plasma cell markers, Bz-resistant mouse cells present as extramedullary disease and express a more B cell-like immunophenotype. We identify that differences in migration may be linked to the differential expression of the bone marrow homing protein, CXCR4. Lower expression of this gene in a Bz human clinical trial was also associated with inferior survival. Immunophenotypic characterization of these cell populations further revealed that forced differentiation of the Bz-resistant population could restore Bz-sensitivity.

The final study investigates the acquisition of Bz-resistance in a B cell malignancy, Burkitt lymphoma, that is currently undergoing Bz clinical trials. In this particular malignancy, a DNA mutator, AID, is known to be expressed that may contribute to other types of drug resistance. Here, we identify that this is unlikely a mechanism for developing resistance to Bz. Furthermore, we provide evidence that AID activity is reduced in Bz-resistant clones and, in fact, that high AID expression may be selectively eliminated during Bz selection.

Table of Contents

Page

Page

Page

List of Tables

Page

List of Figures

Page

Page

List of Abbreviations

NK	natural killer
T	thymus
B	bursa-derived
(p)BCR	(pre) B cell receptor
HSC(s)	hematopoietic stem cell(s)
CLP	common lymphoid progenitor
V(D)J	variable (diverse) joining
(Ig)H	immunoglobulin heavy chain
RAG	recombination activating genes
RSS	recombination signal sequences
μ	IgM
LC	light chain
MCL	mantle cell lymphoma
FL	follicular lymphoma
MALT	mucosal-associated lymphoid tissues
SLPCs	short-lived plasma cells
GC	germinal center
AID	activation induced cytidine deaminase
SHM	somatic hypermutation
CSR	class switch recombination
PC	plasma cell
IL-6	interleukin 6
UPR	unfolded protein response
BL	Burkitt lymphoma
DLBCL	diffuse large B cell lymphoma
LPL	lymphoplasmacytic leukemia (Waldenström's macroglobulinemia)
MGUS	monoclonal gammopathy of undetermined significance
MM	multiple myeloma
MZL	mantle zone lymphoma
NHL	non-Hodgkin lymphoma
AL	amyloid light chain
BM	bone marrow
SMM	smoldering multiple myeloma
FISH	fluorescence in situ hybridization
CT	computed tomography
MRI	magnetic resonance imaging
FDG/FLT-PET	fluorodeoxyglucose/fluoro-L-thymidine-positron emission tomogrphy
Auto/Allo SCT	autologous/allogeneic stem cell transplant
IMiD	immunomodulators (thalidomide, lenalidomide, pomalidomide)
PI	proteasome inhibitors
Bz	bortezomib
Cz	carfilzomib
ER	endoplasmic reticulum
HMCLs	human myeloma cell lines
HDAC(i)	histone deacetylase (inhibitors)
(MM)-BMSC	(multiple myeloma)-bone marrow stromal cells

CSC	cancer stem cells
Hh	Hedgehog
UPS	ubiquitin proteasome system
GEP(s)	gene expression profile(s)
CMAP	Connectivity map
BzS	bortezomib -sensitive
BzR	bortezomib-resistant
GSEA	gene set enrichment analysis
PFS	progression free survival
IPA	Ingenuity pathway analysis
IC_{50}	inhibitory concentration 50
SAHA	vorinostat
EFS	event-free survival
OS	overall survival
Topo(s)	topoisomerase(s)
HTS	high-throughput screening
Fa	fraction affected
CI	combination index
DRI	drug reduction index
CPT	camptothecin
VRC2	Velcade re-sensitizing compound 2
ELISA	enzyme-linked immunosorbent assay
RT-PCR	real time-polymerase chain reaction
I-BzR	innate-bortezomib resistant
LPS	lipopolysaccharide
MRD	minimal residual disease
PRD	primary refractory disease

CHAPTER 1

INTRODUCTION

Normal lymphocyte development is a tightly regulated process that is necessary for the creation and maintenance of a healthy immune system. A class of white blood cells, the lymphocyte, is classified as one of three main cell types: natural killer cells (NK) cells, thymus (T) cells or bursa-derived (B) cells. While all three cell types are essential for a healthy immune system and the subsequent clearing of antigen infections from the body, only B cells interact directly with antigen targets through a B cell receptor (BCR) complex that stimulates the production of antigen-specific antibodies (1). These functions require incredible antigen specificity; however, creating this diversity comes at the price of compromised genomic integrity over the course of B cell development that may contribute to neoplastic transformation (2).

B cell development

All lymphocytes originate from a small, self-renewing, multi-potent stem cell progenitor population called hematopoietic stem cells (HSCs) which, in human adults, reside in bone marrow compartments that, after adolescence, are limited to the femurs, pelvis, sternum and other long bones (3). HSCs are characterized as $CD34^{+}CD59^{+}$ $CD90^{+}CD38^{lo}CD117^{+}$ but most importantly lack lineage-specific markers (4). HSCs perform 2 main functions: 1) maintaining the stem cell pool and 2) creating large amounts of daughter cell progeny that can differentiate into multiple lineages. The fate of a HSC daughter cell depends on its lineage bias (toward lymphoid or myeloid cells). The common lymphoid progenitor (*a.k.a.* pre-pro B cells), along with expressing HSC markers also express c-kit, IL-7Rα, CD45R/B220, CD11b/Mac-1, GR1, Ter119, and Flt3 but specifically lack CD19 whose expression is restricted to later B cell stages (5-7). Following B lineage commitment, these cells progress through a linear differentiation process to define and perfect their antigen specificity in order to become valuable

Figure 1. Stages of B cell differentiation. Linear differentiation of B cells from hematopoietic stem cells (HSCs) through plasma cells including cell-surface markers at each stage and organ localization. Highlighted in blue are stages at which malignant transformations are predicted to occur. CLP = common lymphoid progenitor; MALT = mucosal-associated lymphoid tissues; SLPC = short-lived plasma cell; GC = germinal center; ALL= acute lymphoblastic leukemia; CLL = chronic lymphocytic leukemia; MCL = mantle cell lymphoma; MZL = mantle zone lymphoma; FL = follicular lymphoma; BL = Burkitt lymphoma; NHL = non-Hodgkin lymphoma; DLBCL = diffuse large B cell lymphoma; SHM = somatic hypermutation; CSR = class switch recombination; LPL = lymphoplasmacytic lymphoma (Waldenström macroglobulinemia); MGUS = monoclonal gammopathy of undetermined significance; MM = multiple myeloma.

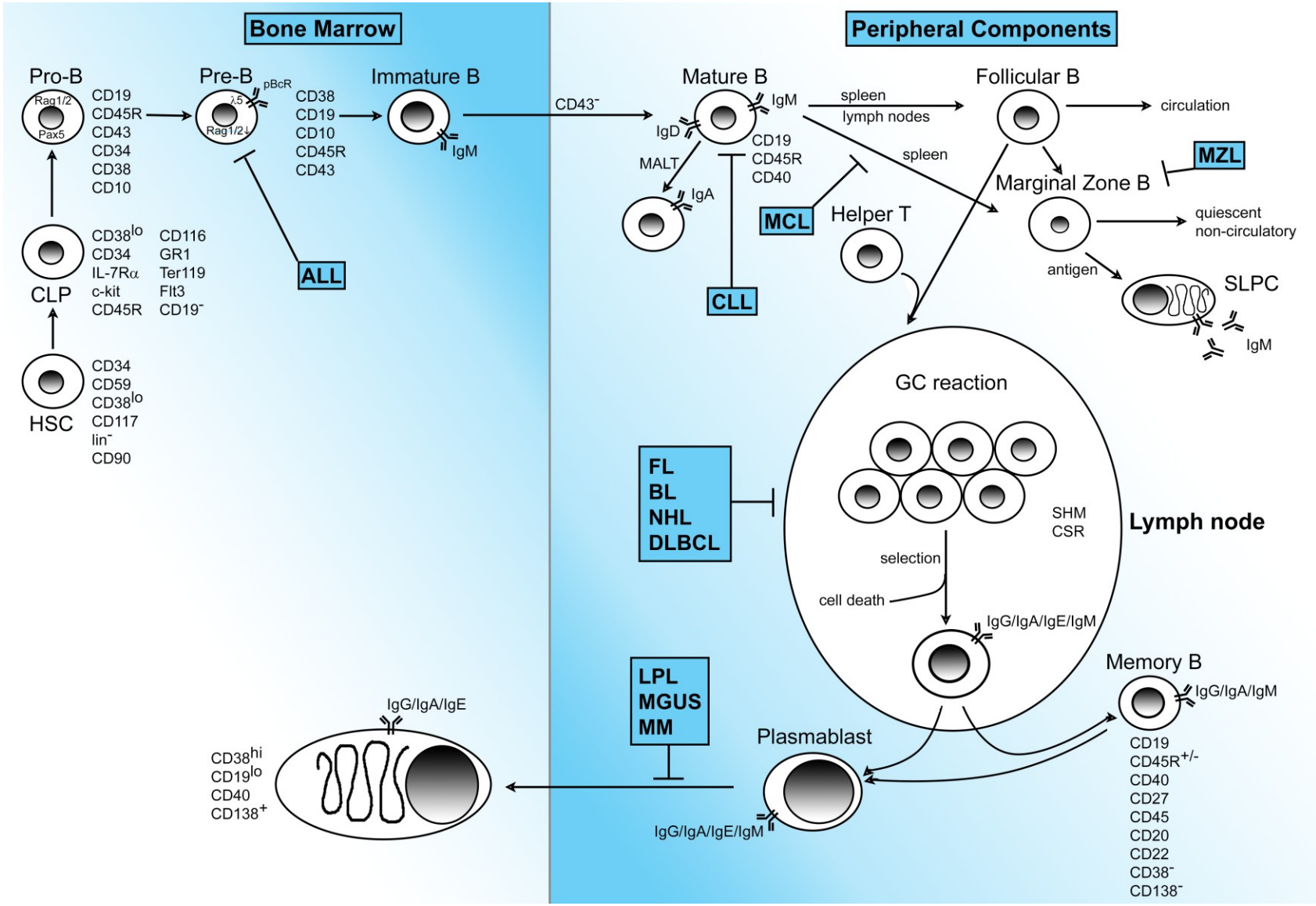
Bone Marrow
Peripheral Components
Pro-B
Rag1/2
Pax5
CD19
CD45R
CD43
CD34
CD38
CD10
Pre-B
pBcR
λ5
Rag1/2↓
CD38
CD19
CD10
CD45R
CD43
Immature B
IgM
CD43⁻
Mature B
IgM
IgD
CD19
CD45R
CD40
MALT
IgA
spleen
lymph nodes
Follicular B
circulation
spleen
MZL
Marginal Zone B
quiescent
non-circulatory
antigen
SLPC
IgM
MCL
Helper T
CLL
ALL
CLP
CD38lo
CD34
IL-7Rα
c-kit
CD45R
CD116
GR1
Ter119
Flt3
CD19⁻
HSC
CD34
CD59
CD38lo
CD117
lin⁻
CD90
GC reaction
SHM
CSR
Lymph node
selection
cell death
IgG/IgA/IgE/IgM
FL
BL
NHL
DLBCL
LPL
MGUS
MM
Memory B
IgG/IgA/IgM
CD19
CD45R+/-
CD40
CD27
CD45
CD20
CD22
CD38⁻
CD138⁻
Plasmablast
IgG/IgA/IgE/IgM
IgG/IgA/IgE
CD38hi
CD19lo
CD40
CD138+

effectors of the immune system as mixed B, T, and NK cells only (8).

Creating the B-cell receptor (BCR) complex

Still residing within the bone marrow due to the expression of CD19, CD45R and CD43 on the developing B cell (9), pro B cells begin the first step toward antigen specificity by rearranging the "variable" (V), "diversity" (D), and "joining" (J) regions of the heavy chain locus. Beginning at one of the two immunoglobulin heavy chain (IgH) loci, lymphocyte-specific recombination activating genes (RAG) 1 and 2 proteins recognize and stimulate recombination at recombination signal sequences (RSS) which flank the V, D, and J gene segments (10). One D_H and one J_H segment are combined through excision of the excess DNA between these two regions and repair by non-homologous end-joining machinery (11). This can occur with or without full commitment to B-cell lineage. Late pro B cell stage follows shortly after where the newly-created (D)J segment is recombined with one V_H segment (12). However, this final step can only occur in committed B cells (10, 13) and is marked by Pax5 expression (5) which is thought to contribute to successful V to (D)J recombination at the level of histone modification (14).

Successful V(D)J arrangement on one allele results in the expression of μ polypeptide which is important for forward B cell development. Unsuccessful V(D)J arrangement can result in a second attempt by the cell for a successful rearrangement at the IgH locus on the other chromosome homolog (15). A successful V(D)J recombination transitions the developing B cell to the large pre-B cell stage. At this time, heavy chain μ expression is primarily localized within the cytoplasm and, perhaps to a small degree, on the cell surface accompanied by a surrogate light chain (λ5 or VpreB) as a pre-BCR (pBCR) complex (10, 16). This signals the cell to halt further V_H (D)J recombination through a process called allelic exclusion, and to proliferate. This ensures that only one μ heavy chain is expressed per B cell resulting in single antigen

specificity; this regulatory event likely involves chromatin remodeling (17) to render the second IgH locus inaccessible to further recombination by RAG proteins (1) which are themselves downregulated at the level of transcription following successful recombination (18).

With a successful μ heavy chain in production, the cell moves to the next stage of development, the small pre-B cell stage. At this stage, the developing BCR gains further antigen specificity by recombining either the κ or the λ light chain (LC) locus. Light chain rearrangement occurs at either the κ or the λ locus through a recombination process similar to heavy chain rearrangement. The recombination machinery can move to the second locus if there is a failure to successfully recombine at the first. The successful recombination of one LC locus results in the expression of IgM on the cell surface and is a milestone of development indicating that the cell has reached the immature B cell stage. Together with the accessory proteins Igα and Igβ, this is termed the BCR complex. Immature B cells then undergo a selection process to eliminate cells with self-antigen specificity or that are unable to survive independent of bone marrow support (19). Cells that fail these tests may re-activate RAG-1/2 for BCR editing where rearrangement of a second, un-recombined locus may create a successful BCR that can be expressed and allow the cell to survive selection (19, 20).

V(D)J recombination is an imperfect process and can sometimes lead to aberrant expression of oncogenes and transformation when translocations relocate these genes to the heavy or light chain loci placing them under the control of immunoglobulin regulatory elements. For example, two translocations t(11;14) linking cyclin D1 and *IGH* in mantle cell lymphoma (MCL) and t(14:18) linking *BCL2* and *IGH* in follicular lymphoma (FL) have recombination structures that are consistent with RAG recombination and are observed prior to the activated B cell stage (21-23).

A mature immune reaction: an Achilles' heel for transformation?

As immature B cells lose CD43 expression and leave the bone marrow, they transition to mature (naïve) B cells surviving in the periphery while expressing both IgM and IgD on their cell surfaces. Some mature B cells localize to mucosal-associated lymphoid tissues (MALT) where they commit to expression of IgA. However, many mature B cells will migrate to follicles in the spleen or lymph nodes and enter circulation of the peripheral tissues as follicular B cells. Furthermore, some mature B cells will remain within splenic follicles settling in the marginal zones found at the border of the white pulp of the spleen becoming resting, marginal zone B cells. Marginal zone B cells do not re-enter circulation but instead may be involved in quick immune responses by becoming short-lived plasma cells as described below (1).

T cell-independent activation of marginal zone and circulating follicular B cells following exposure to an antigen, can stimulate these cells to proliferate and differentiate into short-lived plasma cells (SLPCs) (24). SLPCs are part of the early immune response that secrete mostly low affinity IgM and are short-lived (1). SLPCs are likely formed in the marginal zone and lack expression of BCL-6 but do express the PC "master regulator", BLIMP-1(1, 25). T-cell dependent antigen-activation can also trigger a more robust and long-term immune response within follicular B cells. This interaction causes the B cell to proliferate and undergo further antigen specification through a germinal center (GC) reaction (24). Although the GC reaction is necessary for the long-term immune response, the processes that occur at the GC make cells especially vulnerable to malignant transformation as discussed in detail below.

The germinal center and beyond

Follicular B cells that have been activated for a GC reaction migrate to lymph node follicles where they form large germinal centers of proliferation and BCR diversification (15). At this stage, cells upregulate the expression of BCL-6 and STAT3

which act to repress the plasma cell markers, BLIMP1 and IRF4, delaying terminal differentiation (1, 26). A large burst of proliferation caused by the upregulation of cell cycle genes but not cell growth genes (27) decreases cell doubling time to seven hours (28). This is accompanied by the expression of the DNA-damaging enzyme activation-induced cytidine deaminase (AID) which creates single-base point mutations within the V region of the heavy chain defining a process called somatic hypermutation (SHM). This process results in a large, diverse pool of BCR complexes which are further selected by a process call affinity maturation for those cells with the greatest specificity for the antigen. Following specification, AID also contributes to a process of isotype switching from IgM to IgG or IgA termed class-switch recombination (CSR) (16). Those cells that survive selection are primarily destined to become highly antigen-specific long-lived PCs that produce and secrete large amounts of switched isotype Abs that will contribute to clearing the antigen infection (29).

A minor population of cells that survive the germinal center reaction will become long-lived memory B cells which can function to quickly clear the body in cases of repeated antigen exposure (24, 30). Importantly, normal memory B cells lack large-scale Ig secretory capabilities. Memory cells are thought to exist as two subtypes: $B220^{+}$ cells which are highly proliferative and $B220^{-}$ pre-plasma memory B cells which are less proliferative but may serve as a transitional cell type that can quickly become a mature plasma cell (PC) following a second infection (31); however, the proposed transition from a proliferative GC B cells to a B220+ memory to a B220- memory B cell to a secreting, non-proliferative, fully differentiated PC is still not well understood.

Those cells that are destined for terminal PC differentiation are thought to exit the GC reaction in an intermediate or plasmablastic cell stage that may intersect with the memory cell phenotype (31). At this stage, cells are still rapidly dividing due to the lingering GC transcriptional program, but increasing expression of PC genes begins to

increase the cell size and expand the antibody secretion machinery (32). A full transition to the PC transcriptional program results in terminally differentiated, non-dividing cells that make and secrete antigen-specific antibodies and migrate back to the BM compartment where the secretion of growth factors and stimulatory cytokines like interleukin 6 (IL-6) from the stromal microenvironment act to sustain these properties for months to years (33-35).

The transition from a GC B cell to a PC is a process that is largely regulated by a small number of transcription factors that are often used to delineate these distinct stages of B cell development (Figure 2). The proliferative capacity required of GC B cells is primarily driven by the expression of BCL-6 and PAX-5 at this stage. Part of their role in driving cell cycle progression is through the repression of genes like XBP-1 and BLIMP-1 that are necessary for terminal differentiation. As cells leave the GC reaction becoming plasmablasts, there is an increase in the expression of IRF4 and NF-κB which, besides increasing the Ig secretory capabilities of these intermediate cells, also positively regulate BLIMP-1 expression (32, 36). BLIMP-1, termed the “master regulator” of PC differentiation, is the transcription factor that is ultimately responsible for executing the terminal differentiation program during normal PC development.

BLIMP-1 is sufficient for induction of plasmacytic differentiation (37) acting through multiple processes. First, by the direct repression of PAX-5 transcription, CSR is halted as is BCR signaling and the expression of the B cell transcriptional program (38). Secondly, by repressing c-MYC, cell proliferation is arrested (24, 39-42). Thirdly, the expression of BLIMP-1 allows developing PCs to leave the lymph nodes and home back to the bone marrow through the repression of follicular homing signals (43). The culmination of these events allows the developing PCs to switch from membrane-bound to secreted Ig which is required for the sustained immune response (41).

The inhibition of PAX-5 by BLIMP-1 is a particularly important regulatory step in

Figure 2. Transcription factor regulation network controlling the transition from GC B cells to PCs. A schematic of the key transcription factors known to regulate the transition from a proliferating germinal center (GC) B cell to an intermediate/ plasmablastic cell stage where antibody secretion increases through to the terminally differentiated plasma cell (PC) stage.

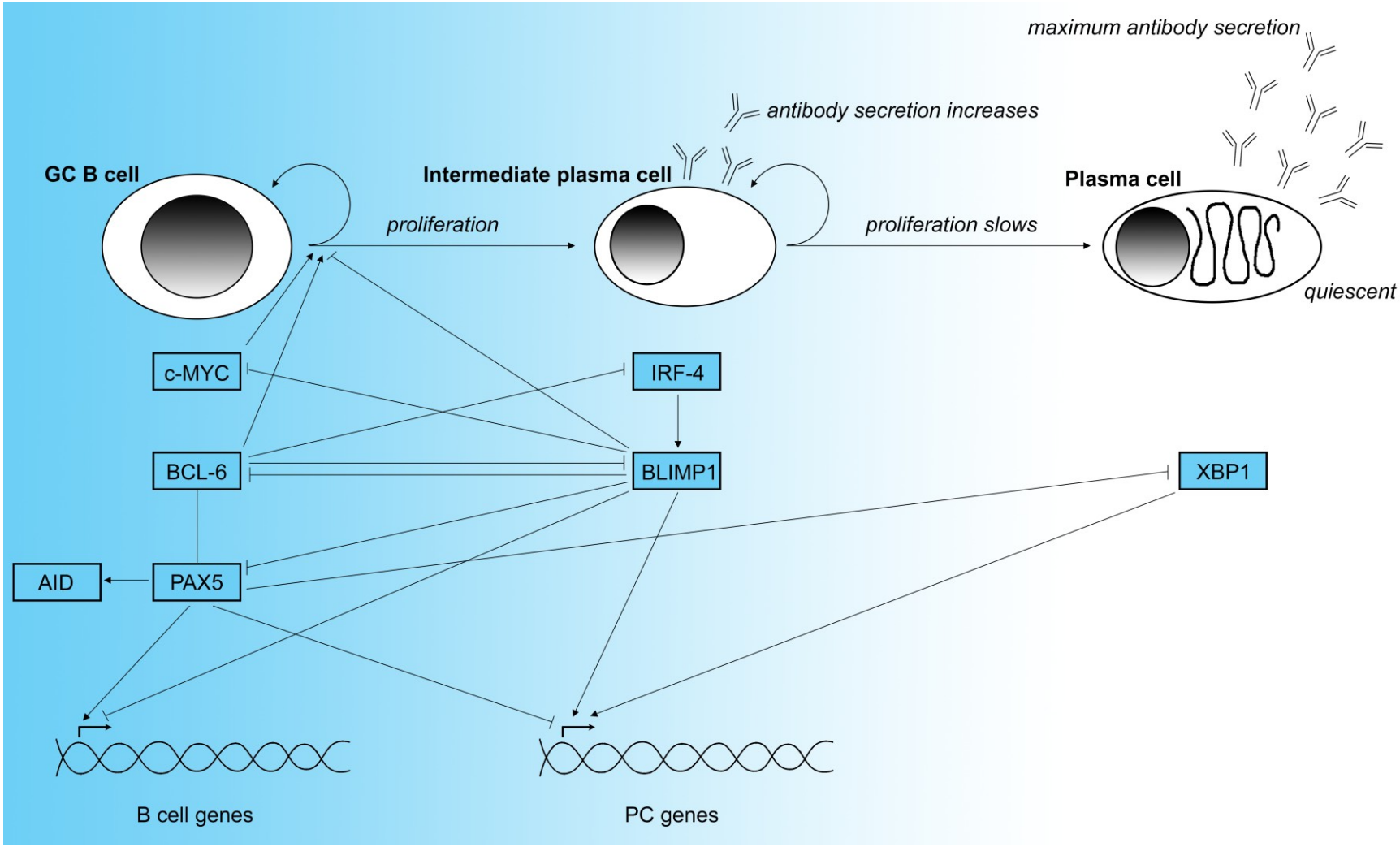
maximum antibody secretion
antibody secretion increases
GC B cell
Intermediate plasma cell
Plasma cell
proliferation
proliferation slows
quiescent
c-MYC
IRF-4
BCL-6
BLIMP1
XBP1
AID
PAX5
B cell genes
PC genes

PC development because it allows X box binding protein-1 (XBP-1) to be expressed which is required for PC formation and maintenance (38, 44, 45). Due to the high antibody load at the PC stage, restructuring of the cell's energy usage and secretory ability must occur, which in many ways is similar to an unfolded protein response (UPR) (46). XBP-1 is a gene involved in the mammalian UPR (46) and is, therefore, involved in later stages of PC differentiation with BLIMP-1. However, to what extent XBP-1 is involved in cellular remodeling during terminal differentiation is not fully understood (1, 47, 48). Ultimately, the expression of BLIMP-1 and XBP1 and the repression of BCL-6 and PAX-5 are required for normal PC maintenance (49, 50).

The danger zone

The highly-active DNA damage machinery present at the GC reaction, as well as the complexity involved in the transcriptional shift from GC B cells to PCs is thought to act as a promoter of malignant transformation. In many cases, genomic evidence of V(D)J recombination and the GC reaction (SHM or CSR) serve as markers for the staging of B cell malignancies such as FL, Burkitt lymphoma (BL), diffuse large B-cell lymphomas (DLBCL), Waldenström's macroglobulinemia (LPL), monoclonal gammopathy of undetermined significance (MGUS), multiple myeloma (MM) and MCL. Gene expression profiling and, in some cases, presence of ongoing SHM has showing that FL, BL, and some DLBCLs are likely derived from GC B cells (51-53) whereas LPL, MGUS and MM are all thought to be derived from post-GC cells as variability at the Ig locus remains constant throughout the course of the disease (54-56). MCL, while having undergone V(D)J recombination, lacks evidence of SHM and CSR placing its cell of origin prior to the GC reaction (57). What differs between these malignant B cells and their normal cells of origin is their ability to 1) proliferate, 2) evade programmed cell death, and 3) avoid terminal differentiation, which suggests that the malignant stage of differentiation is not fixed or linear as in a normal B cell.

In many cases, characteristics of the cell of origin may contribute to aberrations that hallmark cancer diagnosis and progression such as upregulation of oncogenes and downregulation of tumor suppressor genes. For example, the presence of t(8;14/2/22) lesions in endemic BL results in translocations between *C-MYC* and the *IGH*, κ LC, or λ LC loci, respectively, which may be attributed to off-target activity of the SHM machinery (58-63). CSR, which also targets the IGH locus, is thought to likely be responsible for most of the translocations involving this locus in MM and sporadic BL (64, 65). In addition, key players in the GC to PC transition are often hijacked for their oncogenic properties. This has been well-illustrated through events that have been identified in lymphoma. C-MYC often expressed in BL, is an oncogenes that promotes cell growth and clonal expansion (66) as does NF-κB which is activated in DLBCL, marginal zone lymphoma (MZL), and Hodgkins lymphoma (HL). In addition, activation of anti-apoptotic genes like BCL2 in FL and DLBCL allow cells to escape death. Finally, translocations that result in BCL-6 in non-Hodgkins lymphoma (NHL) and PAX-5 in LPL allow proliferation to continue by inhibiting plasmacytic differentiation (2).

Multiple myeloma: a history at the bedside

Of these B cell-derived malignancies, perhaps none is more devastating than MM which is the second most common hematologic malignancy in the United States, accounting for approximately 20% of deaths from blood and bone marrow cancer each year (67). The earliest reports of MM date as far back as the 1840's and were characterized by the pathological detection of large, oval cells with prominent nucleoli in the bone marrow of patients suffering from "soft bones" (68). These observations were followed closely by the description of abnormal urinary proteins in these same patients termed Bence Jones proteins, named for the physician who discovered them (69). It was not until 1900 that these characteristics were found to embody the malignancy now termed "multiple myeloma" (70). The further characterization of these Bence Jones

proteins paved the way to our current understanding of the role that abnormal Ig secretion plays in the pathophysiology of the disease (71) and led to the development of detection methods for identifying monoclonal antibodies (paraproteins) in the serum of patients. Using protein electrophoresis, increased paraprotein load could now be identified through the detection of a "church-spire" that we today term the "M-spike" (72). From this work, pioneers in the field were able to distinguish polyclonal from monoclonal disease leading to the discovery of MGUS, LPL, and amyloid light-chain (AL)-amyloidosis (73).

Currently, MM is characterized in the clinic by clonal PC expansion in the bone marrow (BM) with excessive serum paraproteins/Ig. The disease can be further characterized by the presence of osteolytic bone disease, hypercalcemia, immunodeficiency, anemia, renal failure, and peripheral neuropathy (74). A combination of increased osteoclast activity and decreased osteoblast activity causes the bone resorption seen in up to 60% of MM patients (75-77). This bone resportion contributes greatly to the hypercalcemia seen in patients as much of the calcium from the bones is released into the extracellular fluid (78). The increased serum Ig levels contribute directly to the renal impairment observed in these patients as the light chain can bind Tamm-Horsfall protein within the distal tubule of the kidneys leading to obstructions (79).

In many ways MM is considered a spectrum disorder preceded by a pre-condition call MGUS (80). MGUS is thought to be present in 1% of adults over the age of 25 years and likely progresses to MM at a rate of 0.5-3% per year (81, 82). MGUS is characterized by low disease burden and an absence of organ involvement which means that many patients likely go undiagnosed until progression to MM occurs (83). Progression to the earliest stage of MM, smoldering MM (SMM), is accompanied by increased serum paraprotein and/or increased clonal PC in the bone marrow but this is not accompanied by organ dysfunction (84). The rate of progression from SMM to

intramedullary MM is 10% in the first 5 years following diagnosis (85); however, the majority of patients progress in 2-3 years (86). Diagnosis of intramedullary MM is followed by extramedullary disease and finally plasma cell leukemia at end stages.

Newer technologies have allowed clinicians to analyze bone marrow aspirates from MM patients at different stages of disease to study PC morphology and clonality and to FISH for common MM mutations and translocations (87, 88). Gene expression profiling is sometimes performed for ongoing clinical studies to further identify genetic variant within patient samples (89). Because MM staging relies heavily on paraprotein production and organ involvement, the extent of bone disease is often monitored by computed tomography (CT), magnetic resonance imaging (MRI), fluorodeoxyglucose positron emission tomography (FDG)-PET or dual-energy X-ray absorptiometry (90, 91). Depending on the institution, a combination of these data may be used to predict patient outcomes and select chemotherapeutic agents.

Classification of MM by genetic abnormalities

MM patients are also often also classified based on the genetic lesions present at diagnosis which are detected in as many as 90% of patients (92). A combinations of ploidy status and the translocations present at diagnosis can be used to classify disease and predict outcome (93). These lesions are generally divided into two group, hyperdiploids and non-hyperdiploids. Hyperdiploids, which include trisomies, generally affect the odd-numbered chromosomes 3, 5, 7, 9, 11, 15, 19, and 21 whereas the non-hyperdiploids include those karyotypes that are hypodiploid, near-diploid, pseudodiploid, or near-tetraploid (*e.g.* fewer than 48 or more than 74 chromosomes) (94-96). Ploidy status is thought to be fixed at transformation and does not generally change throughout the course of the disease (97). Hyperdiploidy is considered a better prognosis than non-hyperdiploidy (89, 98); however, a subset of patients within the hyperdiploid population with 1q gains and/or losses of chromosome 13 have been shown to have a worse

prognosis than even non-hyperdiploid patients (99). Using gene expression profiling, Shaughnessy et al. identified a 70 gene signature that could predict poor prognosis is MM patients. Interestingly, 30% of the genes identified by this approach were located on chromosome 1 either downregulated on 1p or upregulated on 1q further validating the importance of chromosomal changes on chromosome 1 in MM patient outcomes (100).

Several decades of work has allowed researchers and physicians to classify common genetic lesions into those that are likely involved in primary disease or progression. Analysis of common translocation events in both MGUS and MM have identified that recombination between Ig elements (65, 101) and genes such as cyclin D1 (102), cyclin D3 (103), MMSET/FGFR3 (104, 105), and MAF (106, 107) are likely involved in early pathogenesis and perhaps the transition from MGUS to MM. Cyclin D1 has particularly been implicated in early stages of the disease as it is found to be highly expressed at the level of gene expression in both hyper and non-hyperdiploid groups (108). Although these primary lesions appear to be mutually exclusive, 5% of MGUS and 25% of advances MM cases possess two translocations (109). Secondary lesions appear to target oncogenes activation (RAS, C-MYC) and tumor suppressor silencing (*i.e.* phosphatase and tensin homolog (PTEN), p16INK4a, and TP53) resulting in advanced disease (110) . For reasons unknown, translocations are more common in non-hyperdiploid patients (101) with the except of chromosome 13 monosomy, chromosome 17p loss (including the TP53 locus), chromosome 1p loss, and 1q gains which have all been associated with poor prognostic outcome (89, 96, 99, 111, 112) (Table 1).

Additional genetic events likely contribute to the transformation of post-GC MGUS cells into MM. For example, the Wnt pathway may be targeted during transformation (113, 114) as evidenced by the aberrant expression of frizzled-related protein (FRZB) (115) and Dickkopf-related protein 1 (DKK1) (an inhibitor of Wnt/β-

Table 1. Common translocations in MM associated with outcome.

Gene 1	Gene 2	Frequency	Prognosis[a]
IGH (14q32)	CCND1 (11q13)	15-20%[b]	Best
IGH (14q32)	CCND3 (6p21)	5%[c]	Standard
IGH (14q32)	MMSET/FGFR3 (4p16.3)	15%[d]	Poor
IGH (14q32)	MAF (16q23)	5-10%[e]	Poor
IGH (14q32)	MAFB (20q11)	5%[f]	Poor

[a]As reported by Laubach, et al. (112) and Fonseca, et al. (92).

[b]As reported by Gabrea, et al. (102).

[c]As reported by Shaughnessy, et al. (103).

[d]As reported by Chesi, et al. (104).

[e]As reported by Chesi, et al. (106).

[f]As reported by Hurt, et al. (107).

catenin) in MM cells which may contribute to the destructive nature of MM cells toward neighboring bone (116). Epigenetic and microRNA modifiers may also contribute to transformation (117-120). Mutations in tumor suppressors like TP53, PTEN, the cyclin-dependent kinase inhibitors CDKN2A and CDKN2C (110), tumor necrosis factor (TNF), receptor-associated factor 3 (TRAF3), and cylindromatosis (CYLD) (121) and the RAS oncogenes family (110, 122) may also be targeted in MM cells. The aberrant expression of normal B cell transcription factors like XBP1 (45, 123), MYC (110, 124, 125) and IRF4 (126, 127) also likely play a role in MM pathogenesis. However, as illustrated here, MM disease is largely heterogeneous, and further characterization of these genes may reveal new drug targets for some but perhaps not all patients.

Therapy: classical meets next-generation

The standard of care for MM patients since the 1960's has been and continues to include alkylating agents and corticosteroids in cocktail which has been shown to reduce disease burden but not cure patients (128-130). Over the years, this cocktail regimen has come to include additional treatment options such as newer drugs (131) and autologous (autoSCT) (132) or allogeneic stem cell transplantation (alloSCT) from a close relative (*i.e.* a sibling) (133, 134). Patients who are eligible for either autoSCT or alloSCT undergo aggressive chemotherapy with vincristine, doxorubicin, and dexamethasone (135) prior to transplant and followed by high-dose treatment with stem cell support.

Patients who are ineligible for SCT due to age or comorbidities often undergo chemotherapy to reduce the tumor burden and preserve or improve organ health. This is followed by a treatment-free period until relapse occurs which is often characterized as a spike in serum and/or urine M-protein levels. A new cocktail treatment regimen will ensue until the disease can again be controlled. However, most patients acquire reduced sensitivity to drugs over time meaning that the time between treatment-free

periods is reduced over the course of the disease until continuous treatment is required at end stages of the disease (112).

The greatest advances in treating MM have been made over the last two decades with the discovery of next-generation drugs (IMiDSs and proteasome inhibitors) that, in combination with classical agents (corticosteroids, alkylating agents, anthracyclines, mitotic inhibitors), have drastically improved the outcomes for patients (136). One such drug, the IMiD thalidomide, has made a valiant return in MM after being abandoned for its teratogenic effects in the early 1960's. Thalidomide, as well as its derivatives lenalidomide and pomalidomide, negatively impacts MM cell growth by limiting growth cytokine and blood vessel production in the bone marrow and by promoting MM cell death by inhibiting E3 ubiquitin ligase complexes (137, 138) (Figure 3). IMiDs have been shown to be especially effective in combination therapies for both newly-diagnosed and relapsed patients (139, 140).

Proteasome inhibitors (PIs) have also vastly improved patient outcomes in MM led primarily by bortezomib/VELCADE® (Bz) (Millennium Pharmaceuticals). Bz targets chymotrypsin-like proteasome activity through reversible binding of the PSMB5 subunit of the 20S proteasome core (141) (Figure 3). Early work with this compound showed that Bz induces apoptosis by inhibiting NF-κB signaling, disrupting IL-6 induced signaling pathways, and cleaving DNA repair enzymes (142, 143). The earliest drug trials showed its efficacy in mouse models (144) and relapsed and refractory MM patients (145). Bz is currently used in cocktail for newly-diagnosed MM and has proven very effective; however, potential side effects such as peripheral neuropathy, thrombocytopenia, and shingles can negatively contribute to patient quality of life and make the use of this drug in some patients impossible (146-149). Further descriptions of the cellular consequences of Bz treatment will be provided in each chapter of this thesis.

Figure 3. Pathway targets of MM drugs. A diagram of the MM cell highlighting those unique characteristics that may be targeted by therapeutic agents. Also shown are supporting cell types and structures that contribute to MM cell viability (*i.e.* osteoclasts, bone marrow stromal cells (BMSCs), and blood vessels which may also be targeted for MM cell killing. The secretion of cytokines by the MM cell including VEGF contribute to the recruitment of supporting vasculature, a process thought to be inhibited by IMiD compounds. The reciprocal growth stimulation between the MM cell and neighboring osteoclasts may be targeted by bisphosphonates which inhibit osteoclasts and decrease bone disease in MM patients. Pathways that contribute to cellular homeostasis within MM cells are often targeted by chemotherapeutic agents (*e.g.* proteasomal degradation, cell growth, replication, and stress response). Newer agents may also target MM cells more specifically using monoclonal antibodies (mAb) toward proteins uniquely expressed on the surface of MM cells. HDAC = histone deacetylase inhibitor; Topo = topoisomerase inhibitor; HSP = heat shock protein.

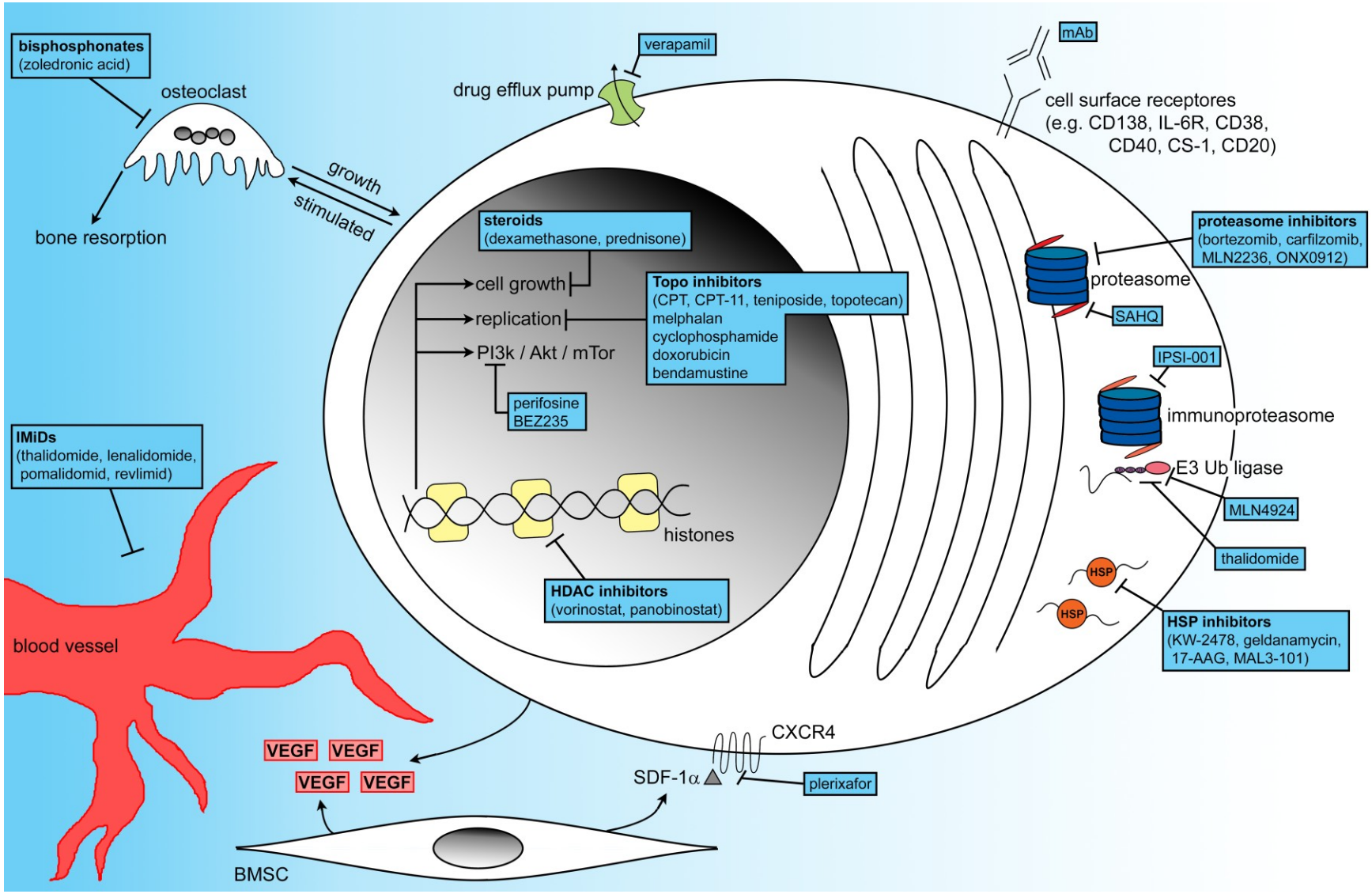
bisphosphonates
(zoledronic acid)
osteoclast
bone resorption
growth
stimulated
drug efflux pump
verapamil
mAb
cell surface receptores
(e.g. CD138, IL-6R, CD38,
CD40, CS-1, CD20)
steroids
(dexamethasone, prednisone)
cell growth
replication
PI3k / Akt / mTor
perifosine
BEZ235
Topo inhibitors
(CPT, CPT-11, teniposide, topotecan)
melphalan
cyclophosphamide
doxorubicin
bendamustine
proteasome inhibitors
(bortezomib, carfilzomib,
MLN2236, ONX0912)
proteasome
SAHQ
IPSI-001
immunoproteasome
E3 Ub ligase
MLN4924
thalidomide
HSP
HSP
HSP inhibitors
(KW-2478, geldanamycin,
17-AAG, MAL3-101)
IMiDs
(thalidomide, lenalidomide,
pomalidomid, revlimid)
histones
HDAC inhibitors
(vorinostat, panobinostat)
blood vessel
VEGF
VEGF
VEGF
VEGF
CXCR4
SDF-1α
plerixafor
BMSC

Recent FDA approval of the PI carfilzomib/KYPROLIS® (Cz) (Figure 3) has shown that irreversible inhibition of the proteasome may also be useful in treating MM; therefore, novel PIs are currently being developed including MLN2238 and ONX0912. Interestingly, genetic lesions that were once associated with poor prognosis on classical treatments, such as loss of chromosome 13 and constitutive activation of FGFR3 by Lys650Glu mutation, have been met with great success on Bz treatment (150, 151). In fact, some of this work has suggested new classes of drugs that might be developed for the treatment of MM. One example of this is the development of endoplasmic reticulum (ER) stress response pathway agonists that enhance the activation of this pathway resulting in increased Bz sensitivity (152-154). Heat shock protein 90 (HSP90) is a chaperone protein family that is involved in many pathways required for homeostasis by interacting with proteins such as AKT, TP53, MEK and STAT3. Inhibition of HSP90 using NVP-HSP90 has been shown to kill human myeloma cell lines (HMCLs) and may synergize with azacytidine and Bz (155). In addition, the inhibition of HSP90 by IPI-504 or GRP78/BiP knockdown was able to kill Bz-resistant MCL cell lines *in vitro* and *in vivo* because the HSP90/BiP association was lost (156). Additional drugs, such as the calcium channel blocker, verapamil, plus Bz have also shown synergistic killing by upregulation of ER stress (157). Clinical trials are currently underway for the use of the HSP90 inhibitor tanespimycin in combination with Bz (158) (Figure 3).

Additional studies of the Bz mode of action have also shown that inhibition of histone deacetylase inhibitors (HDACs) is an effective synergist strategy for enhanced Bz killing. Panobinostat (*a.k.a.* LBH589) has been shown to be a potent killer of drug resistant (classical treatment) MM cells and is synergistic with Bz (159, 160). This synergy is thought to occur through the inhibition of cell cycle progression and anti-apoptotic factors (*e.g.* BCL-2 and BCL-X (161)) and the upregulation of p21, p53 and p57 killing cells through intrinsic cell death pathway activation. An additional HDAC

inhibitor, vorinostat (SAHA), has also shown promise in combination with Bz in early clinical trials (162) with a 42% response rate in refractory MM (163) (Figure 3). Interestingly, Bz has been shown to down-regulate the mRNA expression of class I HDACs (*HDAC1*, *HDAC2*, *HDAC3*) in HMCLs and primary MM cells resulting in histone hyperacetylation via caspase-8-dependent degradation of Sp1 protein (a potent HDAC transactivator) while HDAC1 overexpression conferred Bz resistance in MM cells suggesting a mechanism for synergy (162). Yet, no matter the treatment regimen, still MM remains an incurable disease.

Causes of bortezomib resistance in MM patients

How and why cancer patients become resistant to treatment is not well understood. This problem is particularly pertinent to the use of Bz in MM patients. Although over 50% of patient may respond favorably to initial Bz treatment, all patients will eventually relapse from Bz therapy, and still a small percentage of patients never initially respond presenting with primary Bz refractory disease (164). The basis of these "acquired" and "innate" Bz resistant phenotypes are not well understood. However, studies that have utilized multiple model systems have provided evidence as to three main mechanisms through which Bz-refractory disease occurs: microenvironment protection, drug active site mutations, and pathways mutations that increase cell viability.

Perhaps the most widely-accepted cause of differences in MM cell sensitivity to chemotherapeutic agents is due to cell-cell interactions with the bone marrow microenvironment (165-168) (Figure 4). Like normal plasma cells, MM cells thrive in the bone marrow compartment due to a nearly endless supply of extracellular matrix proteins (*i.e.* fibronectin, collagen, laminin and osteoponotin) and supporting cell types (*i.e.* HSCs, progenitor and precursor cells , immune cells, erythroid cells, bone marrow stromal cells (BMSCs), endothelial cells, adipocytes, osteoclasts and osteoblasts). These cells produce and secrete growth cytokines like interleukin 6 (IL-6), insulin-like

growth factor 1 (IGF-1), B cell-activating factor, fibroblast growth factor (FGF), SC-derived factor 1α (SDF-1α), tumor necrosis factor α (TNF-α), transformation growth factor β (TGF-β), and vascular endothelial growth factor (VEGF) (169). In addition to supporting normal PC survival, these growth factors are also required for BM osteoclastogenesis (170) and angiogenesis (171), both of which are negatively impacted by MM cell growth (172, 173). Physical interactions between MM and supporting cell types, particularly BMSCs through cell-surface molecules like CD40, CXCR4, and P-selectin glycoprotein ligand-1 (PSGL-1) increase the secretion of these cytokines by BMSCs which, in turn, stimulate the phosphatidylinositol-3 kinase (PI3K)/AKT, RAS/RAF/MAPK kinase (MEK)/extracellular signal-regulated kinase (ERK), and Janus kinase 2 (JAK)/signal transducers and activators of transcription 3 (STAT3) downstream survival by decreasing drug sensitivity, enhancing cell migration and antibody secretion, upregulating cell cycle regulatory proteins, and increasing telomerase activity (169, 174-177) (Figure 4).

Because normal PCs also utilize these same interactions with BMSCs for survival, there has been some discussion about whether those BMSCs that support MM cell survival are themselves somewhat transformed to better support malignant PC growth and hence have been termed by some as MM-BMSCs. *In vitro* studies of MM-BMSCs have shown that they express much higher levels of IL-6 and VEGF than their healthy BMSC counterparts; they also may modulate the expression of microRNA within MM cells that may be involved in drug sensitivity (178-180). Interestingly, Bz resistance has been associated with MM cell secretion of growth cytokines (181, 182) suggesting that MM cells can mimic the bone marrow milieu for enhanced survival (Figure 4). Furthermore, constitutively activating mutations within growth cytokine signaling pathways, such as those for IL-6, within MM cells have been identified that confer resistance to classical drugs. These changes that allow MM cells to thrive away from the bone marrow

Figure 4. Effects of MM cell interactions with the bone marrow microenvironment. Illustration of the MM cell interaction with the bone marrow microenvironment including bone marrow stromal cells (BMSCs), osteoblasts, and osteoclasts which stimulate the production of growth cytokines from BMSCs and MM cells.

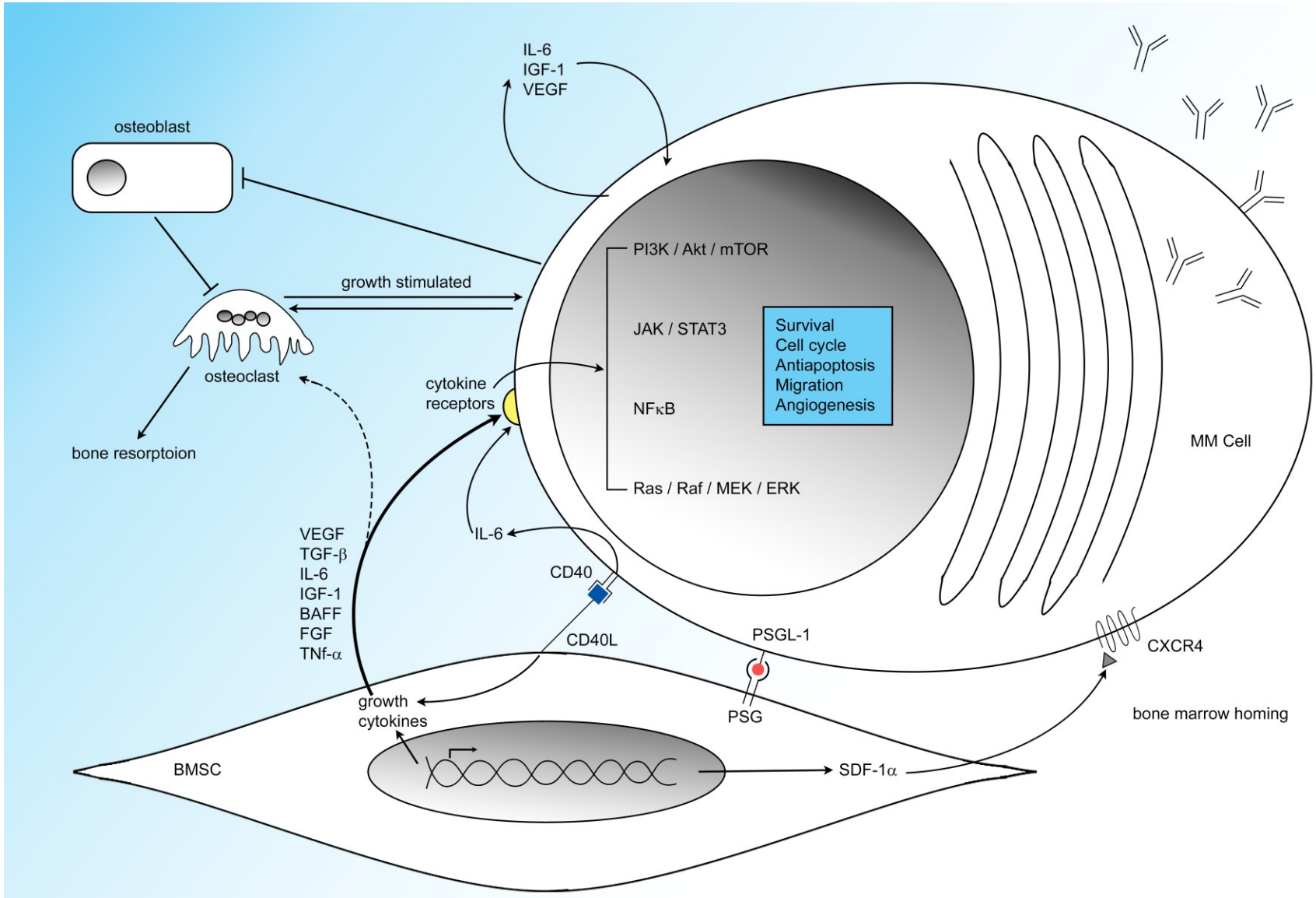
IL-6
IGF-1
VEGF
osteoblast
growth stimulated
osteoclast
bone resorptoion
PI3K / Akt / mTOR
JAK / STAT3
NFκB
Ras / Raf / MEK / ERK
Survival
Cell cycle
Antiapoptosis
Migration
Angiogenesis
MM Cell
cytokine
receptors
VEGF
TGF-β
IL-6
IGF-1
BAFF
FGF
TNf-α
IL-6
CD40
CD40L
PSGL-1
PSG
CXCR4
bone marrow homing
growth
cytokines
BMSC
SDF-1α

compartment may further explain how extramedullary masses arise in end-stage patients (166).

Although differences in Bz sensitivity due to BMSC interactions is considered by some as controversial, several studies have shown that disruption of this interaction may be a useful therapeutic approach for targeting MM cell growth (183). Indeed, studies have shown that antibody inhibition of the CD40/CD40L interaction (184) and chemical inhibition of the CXCR4/SDF-1α axis disrupt MM/BMSC binding and may even sensitize cells to Bz treatment (185). However, mutations resulting in the loss of adhesion proteins and increased migratory capabilities have been associated with reduced PI sensitivity (186). In addition, there have been several reports on MM patients where Bz resistance was associated with the development of extramedullary masses (187, 188). Interestingly, MM cells with ectopic cyclin D1 expression but not t(11;14) which depend on BMSC support for survival are underrepresented in extramedullary stages of disease (189). Together, these data suggest that there is a dependence on the bone marrow milieu for survival in early but not advanced stages of the disease and that this might be further informed by the presence of certain genetic alterations.

The most common mechanism for acquired Bz resistance in *in vitro* model systems is attributed to mutations at the drug active site within the protein, PSMB5. PSMB5 is a β subunit of 20S catalytic core responsible for chymotrypsin-like proteasome activity (190). Many human cell line models have been dose-escalated with Bz over time to create resistance that has been attributed to *PSMB5* mutations. Most of these mutations have been identified within the PSMB5 binding pocket resulting in Met56Ile, Cys63Phe, Ala49Thr, Met45Val and Cys52Phe, or Ala49Val changes. One study reported an additional propeptide region mutation resulting in an Arg24Cys change. These mutations were often associated with increases in *PSMB5* transcript and protein as well as proteasome chymotrypsin-like activity. In some cases, these mutations were

also associated with increases in immunoproteasome activity which was associated with cross-resistance to other next-generation PIs. In many of these cases, synthetic knock-down of PSMB5 expression or chemical inhibition of α proteasomal subunits restored Bz sensitivity (191-203). However, what is perhaps most intriguing about these studies is that although non-synonymous coding PSMB5 variants have been identified in Bz-refractory MM patients, none of these have been associated with survival or differences in proteasome activity. Furthermore, none of the mutations that have been identified in Bz-resistant cells *in vitro* have been identified in Bz-refractory MM patient samples (191, 204-206).

In addition to contributions from the bone marrow microenvironment and drug active site mutations, there remains a large body of literature that attributes Bz resistance to cellular changes that overall promote malignant cell viability in the face of extreme cellular stress (*i.e.* the inability to degrade excess and/or misfolded proteins). One such example of this is through inhibition of NOXA upregulation following Bz treatment. NOXA is a pro-apoptotic gene that acts though the BAK/BAX axis to promote cell death. Downregulation of NOXA expression as well as other factors in this pathway (*i.e.* RAD) as well as loss of wild-type TP53 activity have been implicated in Bz resistance (159, 160, 207-209). Overexpression of anti-apoptotic genes, such as BCL-2, MCL-1, and BAG3, has also been associated with reduced Bz sensitivity (210-213).

Besides changes in cell death, onocogenic activation has also been suggested by many as a mechanism for MM cells to avoid Bz-induced cell death. Constitutive activation of NOTCH, PI3K/AKT/mTOR, Hedgehog, NF-κB, MEK/ERK and/or JAK/STAT3 signaling pathways has been observed in multiple model systems of Bz-resistance (214-222) (223). The overexpression of the receptor tyrosine kinase c-MET in Bz-resistant HMCLs led to upregulation of cell proliferation (224) and survival. This finding is particularly interesting given the normal metastatic function of c-MET, the

upregulation of which may explain the development of extramedullary disease at Bz relapse (187, 188).

Finally, reduced cellular stress has also come to the forefront of the Bz-resistance literature. Reducing oxidative stress by increasing the baseline expression of stress response proteins (*i.e.* HSPA2, GRP78/BiP, NRF2, HSP27, HSP70, HSP90) may help Bz-resistant cells maintain homeostasis even in the presence of Bz (225-231). The activation of alternative pathways, like autophagy, in Bz-resistant cell may help shunt unfolded and/or misfolded proteins toward degradation, allowing intracellular stress to remain low in these cells (186, 232-234). Also, increased expression of drug efflux pumps like P-glycoprotein/multidrug resistance 1 (MDR1) may contribute to reduced Bz sensitivity by keeping intracellular levels of Bz low (193).

Mouse modeling of MM

Because patient samples are relatively rare, a number of mouse model systems have been utilized to identify the genetic variants that are associated with disease progression, severity, and drug resistance. These models can generally be divided into mouse myeloma-like models and xenograft models. Each model possesses certain advantages and disadvantages for studying different components of the disease.

The earliest mouse MM model utilized BALB/cAn and BALB/cJ strain mice which were susceptible to plasmacytomas when injected with the inflammatory agent, pristane (235). The formation of these localized tumors could be further expedited by co-injection with retroviruses (236). Although these tumors do secrete Ig, greater than 95% possess IgH/Myc translocations which are not that common in the MM patient population. However, this model has proven useful for studying BL where this translocation is most common (237).

Although IGH/MYC translocations are not that common in MM (occurring in only approximately 3% of the patient population (238)), the deregulation of MYC is found in

53-85% of patients (239-241). One commonly used mouse model, the Vk*myc C57Bl6/J mouse, spontaneously develop a post-GC MGUS-like condition with PC expansion in the bone marrow. In this model, c-Myc activation occurs by SHM of the myc locus by AID. A low percentage of Vk*myc mice progress to a MM-like disease at advanced ages. This presents with a monoclonal M-spike, low proliferative index, anemia, and decreased bone density. Importantly, Vk*myc mice are responsive to drugs commonly used to treat MM (125).

Another transgenic model, developed in our laboratory, utilizes the dual overexpression of the oncogene, c-Myc, and the anti-apoptotic gene, Bcl-xL, by hijacking regulatory components of the Ig machinery. The double transgenic progeny succumb to disease quickly with complete penetrance. In addition to an *in vivo* phenotype that closely recapitulates the human disease, as shown in this thesis, stable cell lines can be created from these animals that can be manipulated and adoptively transferred back into syngeneic recipients resulting in the same disease phenotype (124, 242). This is currently the only mouse model from which stable cell lines can be created which may be highly advantageous for certain approaches.

An additional transgenic mouse model expresses the spliced, active form of the PC gene XBP-1 controlled by the Ig V_H promoter and E_m enhancer elements. This pEμXBP-1s model is prone to MM development which presents as elevated IgM and IgG, PC expansion in the BM, the development of plasmacytic tumors resembling MGUS or MM, and bone lesions; however, this occurs at advanced ages in only a small percent of the patient population (123).

Interestingly, some strains of mice, like C57BL, spontaneously develop murine MGUS-like disease that will progress to MM at elderly ages; the C57BL/KaLwRij stain develops idiopathic paraproteinemia at the highest frequency and has since been termed the 5T mouse model. At 2 years of age, 50% of these mice develop MGUS and

0.5% develop MM (243). Cells from these animals can be serially transferred into recipient C57BL/KaLwRij mice resulting in secondary plasma cell disease and death (244). This adoptive transfer process has been used to create three additional related models: 5T2MM, 5T33MM, and 5THL (245). These models possess similar cell-surface marker expression but have different rates of growth and homing properties *in vivo* (246, 247). This mouse model has contributed greatly to understanding of the pathophysiology and cell biology of MM (248-259) and particularly to the discovery of bisphosphonate drugs for the treatment of bone disease in MM patients (260-268).

The Vk*myc, Bcl-X_L/Myc, pEμXBP-1s, and 5T mouse models have proven especially useful given that the bone marrow microenvironment plays a key role in cell growth, proliferation and drug sensitivity in MM (269). Perhaps the biggest advantage is the ability to study the disease in an immunocompetant host species (237). However, the problem remains that no single model provides the spectrum of heterogeneity that is present in the patient population (270, 271). While Vk*myc, pEμXBP-1s and 5T mice represent MGUS and can progress to MM, this is a very latent disease that transforms at a low frequency making large-scale studies using these models cost-prohibitive. In contrast, the Bcl-X_L/Myc model may represent aggressive disease. While this may be useful for studying refractory disease which is often aggressive, it does not necessarily inform disease progression.

For these reasons, some researchers favor xenograft models where MM patient cells can be injected into immunocompromised mice (SCID, NOD/SCID, or SCID-beige) creating palpable plasmacytoma that can be measured for easy quantification of growth over time (272). Higher levels of engraftment may be reached in this model by the addition of matrigel with the tumor cells to temporarily mimic a microenvironment (144). This cancer model system has been utilized for pre-clinical anti-MM drug development successfully for a variety of drug classes (144, 273-287). Several drugs commonly used

to treat MM patients, including Bz (144) and thalidomide (273), were first tested in this model system. However, for drugs that are considerably affected by MM-BMSC interactions (*i.e.* dexamethasone, alkylating agents, anthracyclines), this model system may not be suitable (177, 269). The absence of bone disease in these models means that an end point of death is not useful. Because of this, over-estimates of the efficacy of new drugs, especially those that may be affected by the MM-BMSC interaction, may be predicted by this model that will not translate to the clinic.

These limitations led to modifications of this methodology to include fetal bone fragments at the tumor cell injection site, a system now called the SCID-hu model. Implantation of these bone fragments provide a human bone marrow-like microenvironment instead of direct BM injection into mouse BM as the microenvironments may be different enough to limit human MM cell growth (288). Human MM cells show bone engraftment, marrow infiltration, and classic MM symptoms including an M-spike in the serum and LC renal involvement in these mice. Importantly, this model provides a much higher rate of engraftment for primary MM samples than traditional subcutaneous xenograft models, perhaps as high as 80% (289). Pre-clinical testing of many MM drugs has been performed in this model system (290-297). Because of the bone involvement phenotype (298), this system has also been used extensively to study bone resportion common to MM patients (172, 291). The lack of palpable tumor in this xenograft system means that other markers such as Ig or soluble IL-6 receptor must be used to quantify disease burden (288, 296, 299). Yet, death remains a useless endpoint in these mice as the human MM cells cannot infiltrate and cause extramedullary disease in the endogenous mouse tissues (237). The use of fetal bone has been highly controversial, and there is not a clear understanding of the differences (if any) of MM growth in fetal versus adult bone marrow; however, we do know that infants and children have never been diagnosed with MM. A more-recent

modification of this model uses rabbit bone marrow inserted into SCID mice (SCID-rab). This approach is much less controversial but has not been used as extensively although it does show promise (300).

Besides primary patients samples, established and well-described HMCLs are often used in the xenograft model systems for drug discovery (301-308). There are approximately 40 cell lines created from end-stage MM patients that were established over 20 years ago (309, 310). When injected into immunodeficient mice, these cells lines home primarily to the bone marrow but have also been shown capable of infiltrating lymph nodes and soft tissues similar to what is seen in extramedullary disease in MM patients (110, 269, 301, 302, 311-313). However, many studies have reported drug efficacy using these cell lines which cannot be recapitulated in MM clinical trials. Perhaps this is due to the fact that they cell lines represent only a small portion of the disease population. For example, the majority of these cell lines have TP53 mutations and lack hyperdiploidy which are relatively rare events in the MM patient population (310, 314-316). Even so, many elegant studies have utilized these cell lines for *in vitro* approaches (*e.g.* RNAi screens) that have revealed druggable targets for translational studies aimed toward identifying drugs that will synergize with Bz (317).

Clonal evolution and the myeloma cancer stem cell

Although the last two decades have brought marked improvements in MM patient treatment and understanding of drug resistance primarily through the use of model systems, MM remains an incurable disease suggesting that no treatments currently on the market are able to deplete the myeloma cancer stem cell (CSC) population. The development of drugs that target this population has been a challenge as this cell type is not well-defined. The first description of a potential MM CSC population came from mouse studies of serially propagated pristane-induced mouse plasmacytoma tumors which showed that only a small percentage of the tumor cells were capable of

clonogenic growth both *in vitro* and *in vivo* while the bulk of the tumor cells were quiescent (318, 319). These clonotypic B cell were also observed in MM patient samples, albeit at a frequency of 0.2-0.8% from total B cells, and had clonogenic growth properties when tested *in vitro* (320-327); however, further characterization of these cell populations was necessary in order to distinguish it from the bulk tumor.

The most well-defined marker of MM cells is CD138, a surface transmembrane heparin sulfate-bearing proteoglycan. CD138 binds type I collagen inducing the expression of matrix metalloproteinase 1 (MMP-1) and aids MM progression by promoting bone resorption and tumor invasion. Increased soluble CD138 promotes MM tumor growth *in vivo* and is considered a marker of poor prognosis (328, 329). In fact, targeting MM cells using CD138-specific antibodies has been described as a potentially successful approach for killing MM cells *in vivo* (330). Interestingly, CD138 status has come to the forefront of MM CSC literature based on studies performed by Matsui *et al*. They observed that small fractions of $CD138^-$ cells isolated from both MM cell lines as well as patients had greater clonogenic potential than their $CD138^+$ counterparts when transferred into NOD/SCID mice (331). $CD138^-$ cells also expressed CD19, CD20, CD22 and CD45 and higher levels of Ki67, a proliferation marker, as well as surface Ig with restricted LC expression (either κ or λ) (331) which was the same as the greater MM cell population (332). Further characterization of the $CD138^-$ population showed that clonally-related memory B cells which are $CD19^+CD27^+$ found in the peripheral blood of MM patients could also produce disease in primary NOD/SCID animals as well as secondary recipients and could contribute $CD138^+$ cells to the host BM (327, 333, 334). *In vitro* colony-forming assays as well as *in vivo* transfer experiments showed that $CD138^-/CD34^-$ cells could give rise to $CD138^+$ cells suggesting that transformation is a post-GC event that gives rise to a B cell-like CSC which can then give rise to the bulk $CD138^+$ cell population that is detected in MM patients at diagnosis (331). Rituximab,

humanized monoclonal CD20 antibody originally developed originally for B-cell NHLs, was especially effective in inhibiting the growth of the $CD138^-$ population which was generally cross-resistant to all other MM therapies (331, 333). Hedgehog (Hh) signaling has been implicated as a player in MM CSCs and is a known player in stem cell self-renewal. Hence, this may be a druggable target for eliminating CSCs in MM patient populations. The Hh signaling pathway is significantly upregulated in $CD138^-$ cells; inhibition of this pathway using the drug cyclopamine killed these cells, induced terminal differentiation and inhibited clonogenic growth; however, the expression of Hh *in vivo* may be dependent on stromal interactions (335, 336). These data suggest that although the bulk of the MM tumor cells may not be affected by these particular drugs, drugs that target cancer stem cells may be important moving forward in combination therapies to achieve eradication of all MM cells.

Defining the MM CSC population has revealed that these cells may be more B cell-like than was previously thought which does make sense given that B cells possess the ability to proliferate and are not restricted to the bone marrow compartment (337-340). Clonally-related mature B cell-like cells have been identified in peripheral blood and BM of MM patients (323, 341-345). Characterization of this clonogenic MM cell population has shown that these cells do in fact express markers of B cells rather than terminally differentiated PCs. These clonogenic B cells have many similar characteristics to normal adult stem cells including higher expression of detoxifying enzymes and membrane-bound drug transporters (346), persisting through drug treatment and increase during relapse in MM patients (347-350). Interestingly, increased numbers of peripheral blood malignant circulating PCs have been associated with negative outcome due to relapsed or refractory disease in MM patients (351). Significant decreases in CD138 in patients with relapsed/progressive disease have also been observed compared to drug naïve patients (352) leading many to ask whether the

expression of a B cell program, while being associated with the MM CSC phenotype, may also be associated with Bz refractory disease. The intersection of these two themes could mean that MM CSCs are resistant to Bz treatment which is thought to be true (333), but it could also mean that MM cells are capable of reverting to a CSC-like phenotype to survive Bz treatment.

In studies of CD138 status associated with outcomes, Gu *et al.* found that patients with low CD138 had a worse overall survival than patients with high CD138. These studies described two MM cell lines derived from the same patient, one with high and the other with low CD138 expression. The cell line with low CD138 expressed high levels of the B cell transcription factors BCL-6 and PAX-5 while the CD138 high cells expressed the PC regulators IRF4, BLIMP-1, and XBP1 suggesting that the CD138 cells were less PC-like (Figure 2). Importantly, forced PC differentiation of the CD138 low cells increased their sensitivity to Bz (353). Complimentary work in MCL has shown that the expression of BLIMP-1 is required for Bz sensitivity in MCL cell lines and primary tumor cells (354). Another cell line model of Bz resistance shows that the MM CSC marker CD20 is upregulated in Bz-resistance increasing sensitivity to rituximab (192). These lines of evidence point toward a loss of PC maturation markers and a gain in B cell identity in Bz-refractory disease. Whether these B cell types are selected for or induced by the drug is still unknown.

Investigation of the MM CSC and Bz resistant populations may be leading to smarter treatment strategies but it has also changed the way that physicians and researchers are thinking about clonal evolution. Classically, MM has been thought of as a linear cancer progression from MGUS through to plasma cell leukemia. More recent, large-scale cytogenetic and genome sequencing studies of MM patients through the course of disease progression has provided evidence that myelomas may be categorized into three categories: 1) genetically stable, 2) linearly evolving, or 3)

heterogeneous clonal mixtures which may contribute greatly to drug sensitivity and outcomes (355, 356). The earliest evidence of heterogeneous clonal mixtures in disease was reported as a switch in a patient after treatment from hyperdiploid to a near-tetraploid abnormal clone (357). This population may represent as high as 42% of the population (355) and shows that in fact clones may wax and wane with different therapeutic regimens (356). Perhaps not surprisingly, this heterogeneous phenotype was associated with high-risk myeloma as it was genetically unstable (355), but these studies warrant further characterization of emerging clones following relapse underscoring the desperate need for better personalized medicine approaches in MM.

Although many mechanisms of Bz resistance have been described, PIs are still considered a front-line treatment for patients with MM (358). The success of Bz treatment in MM patients has now led to investments by many research groups to determine whether Bz can be utilized in other types of cancer, particularly solid tumors (359-370). With this potential expansion in the use of Bz, understanding of the evolution of refractory disease and synergist drug combinations to combat Bz-resistance are vital.

Statement of thesis

This thesis will combine *in vitro*, *in silico*, and *in vivo* approaches to further characterize Bz resistance within the MM cancer cell population. The first study describes the establishment of *in vitro* MM-like mouse cell lines which is the model system that we favor for studying Bz-refractory disease in MM. We further investigate both the conserved and unique transcriptional signatures of Bz-sensitive and -resistant cell lines *in vitro* which may provide predictive power for the *in silico* selection of secondary therapies using a database called Connectivity Map. The second study further investigates the predictive power of combining *in silico* predictions with high-throughput compound screening for secondary drug predictions of compounds that may synergize effectively with PIs. The third study involves further immunophenotypic

characterization of the Bz-sensitive and -resistant mouse cells lines in order to identify unique cell surface markers that might be used diagnostically or targeted successfully by secondary therapy to regain Bz sensitivity. The final study investigates BL, a malignancy that is currently undergoing Bz clinical trials, to determine what role ongoing SHM might play in acquiring Bz resistance. These studies provide a more thorough characterization of the Bz-resistant phenotype and together describe new approaches that may be successfully implemented in the future for the treatment of patients with refractory MM.

CHAPTER 2

DEVELOPMENT OF AN *IN VITRO* MOUSE PLASMA CELL TUMOR SYSTEM

Prior to my joining the Van Ness laboratory in 2009, a number of mouse model systems of multiple myeloma (MM) had been established and well-described (as illustrated in Chapter 1). However, the characterization of pharmacogenomic mechanisms for cancer drugs has traditionally been explored using cell line models which are not limited by cell number, as is the case with primary tumor samples. Although a number of human myeloma cell lines (HMCLs) were available, we did not feel that these were particularly representative of current MM disease phenotypes due to the caveats described above. Therefore, the first aim of the studies described in this thesis was to establish a robust malignant plasma cell (PC) culture system.

For this system, we chose to utilize the Bcl-X_L/Myc double transgenic mouse model of MM developed previously in our laboratory and described in Chapter 1. Not only do these mice express a fully-penetrant MM-like phenotype, but the PCs that can be isolated from moribund animals possess karyotypic and gene expression signatures that align with the human disease (124, 242, 371). Furthermore, malignant cells from these animals can be isolated and established to create stable cell lines that do not require Epstein-Barr virus (EBV)-transformation for immortalization. This is an advantage that is distinct to our mouse model which we believe is particularly powerful for pharmacogenomic applications that require repeated *in vitro* studies.

Isolating malignant mouse plasma cell lines

In order to create a library of malignant mouse PC lines, we participated in a large-scale double transgenic breeding scheme that was performed to test the pre-clinical efficacy of a next-generation proteasome inhibitor (PI). In this study, 90 age-matched double transgenic mice were created and divided among three treatment arms to receive vehicle, bortezomib (Bz), or MLN2238 beginning at nine weeks of age for six

consecutive weeks (372). When mice in the vehicle or Bz treatment groups became moribund, they were sacrificed and dissected. Multiple tissues including bilateral femurs and tibias, spleen, liver, lymph nodes and tumor masses were shipped to our laboratory from each mouse overnight in culture medium. We established single-cell suspensions from each individual tissue and waited for stable malignant clones to emerge over the course of approximately six months as has been previously described (124). The growth of PCs in these cultures was aided by the addition of the cytokine, IL-6 which has been shown to stimulate MM cell growth (373). This produced a panel of close to 200 cell suspensions from which approximately 60 independent cell lines emerged.

Characterizing candidate mouse cell lines

Of the cell lines that emerged, a small percentage appeared to be dependent on transformed stromal cells that also emerged with the malignant PCs from the mouse tissues resulting in mixed cell cultures (data not shown). In addition, although the majority of the cell lines represented clonal populations (data not shown), many consisted of cells with a mixture of both B cell and PC-like morphologies (Figure 1). Interestingly, a small number of mice gave rise to independently-derived cell lines from different tissues (*i.e.* one cell line from the bone marrow and one from the spleen) that were also clonal (Figure 2, Supplemental Materials and Methods) suggesting that a malignant clone had emerged in the bone marrow and spread to the soft tissues at end-stage disease. We did not identify any clear cases of animals with biclonal disease from the obtained stable cell lines; however, this result may not have been surprising given that 100% of double transgenic mice develop PC disease. We further performed GEP on a number of our most-aggressive cell lines and identified that the gene expression pattern among independently-derived cell lines was largely similar. Not surprisingly, the cell lines that clustered most tightly were those that were derived from the same mouse (but different tissues) (data not shown). We describe many of these results in Chapter 3.

Importantly, these GEPs did not appear to drift when tested six months and up to a year later (data not shown).

In the following studies, we utilize these malignant mouse PC lines for the pharmacogenomic characterization of drug resistance, which is a major problem within the MM patient community, and for the prediction and validation of secondary therapies.

Figure 1. Cell morphologies of mouse cell lines by pathologic staining.

A representative formalin-fixed and paraffin embedded hematoxylin and eosin stained malignant mouse PC line (60X magnification) where black arrows indicate PC morphology, red arrows indicate B cell morphology, and the blue arrow indicates a binucleated cell morphology.

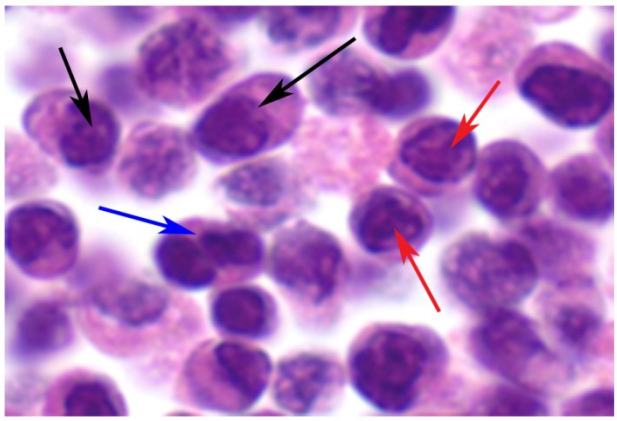

Figure 2. Stable malignant mouse plasma cell lines are clonal.

A PCR-based assay (see Supplemental Materials and Methods) for mouse D(J) rearrangement shows by gel electrophoresis that independently-derived cell lines from different tissues from the same moribund animal are likely clonal (595BM = bone marrow-derived, 595SP = splenic-derived). A well-described mouse pristane-induced plasmacytoma cell line (MPC11) was used as a positive control as was *GAPDH*. JH bands indicate the presence of either the JH2 or JH4 joining segments in each cell line. The presence of a single band indicates clonality.

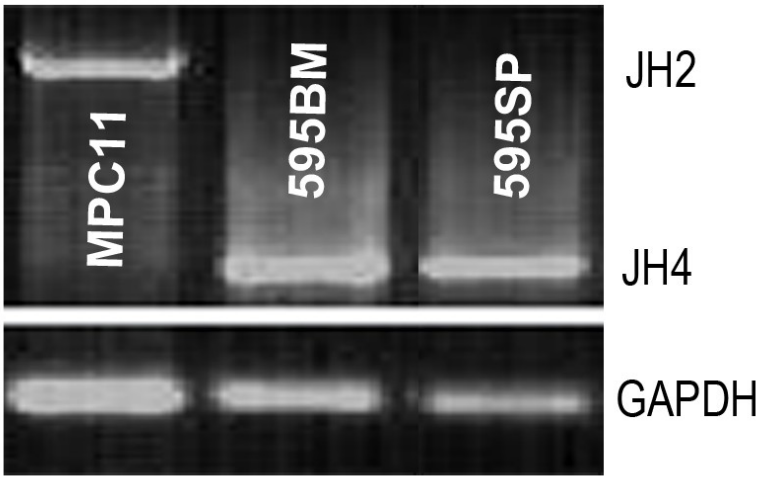
MPC11
595BM
595SP
JH2
JH4
GAPDH

Supplemental Materials and Methods

Clonality assay. Cell culture clonality was determined using a PCR-based assay for heavy chain (D)J rearrangements where the forward primer binds a conserved (D) region sequence and the reverse primer bind the constant region adjacent to the final J segment. Rearrangement was determined by endpoint PCR using the GeneAmp PCR System 9700 (Applied Biosystems, Carlsbad, CA) and GoTaq Green DNA polymerase (Promega) using 35 cycles of 94°C for 30 sec, 58°C for 30 sec and 72 °C for 2 min. The following primers used: (D)J, 5'-CTGCAACCGGTG TACATTCCSAGGTSMARCTGSAGSAGTCWGG-3' (5' primer), 5'-TGCGAAGTCGACCCTGAGGAGACGGTGACTGAGG-3' (3' primer). PCR products were resolved on a 1.5% agarose gel (BioExpress, Kaysville, UT), visualized using the ChemiDoc™ XRS+ Imager (Bio-Rad, Hercules, CA).

CHAPTER 3

PROFILING BORTEZOMIB RESISTANCE IDENTIFIES SECONDARY THERAPIES IN A MOUSE MYELOMA MODEL

Holly A. F. Stessman[1], Linda B. Baughn[1], Aaron Sarver[2], Tian Xia[3ψ], Raamesh Deshpande[3], Aatif Mansoor[1], Susan A. Walsh[4], John J. Sunderland[4], Nathan G. Dolloff[5], Michael A. Linden[6], Fenghuang Zhan[7], Siegfried Janz[8], Chad L. Myers[3], Brian G. Van Ness[1*]

From the [1]Department of Genetics, Cell Biology and Development, [2]Masonic Cancer Center Bioinformatics Support and Services, and [3]Department of Computer Science and Engineering, University of Minnesota, Minneapolis, MN, USA; [4]Department of Radiology, University of Iowa, Iowa City, IA, USA; [5]Department of Medicine, Penn State Hershey Medical Center, Hershey, PA, USA; [6]Department of Laboratory Medicine and Pathology, University of Minnesota, Minneapolis, MN, USA; [7]Department of Internal Medicine and [8]Department of Pathology, University of Iowa, Iowa City, IA, USA.

Supported by Millennium Pharmaceuticals: The Takeda Oncology Company and Onyx Pharmaceuticals.

Reproduced from *Molecular Cancer Therapeutics*, in press, 2013, by permission of the American Association for Cancer Research.

AUTHOR CONTRIBUTIONS

H. A. F. S. coordinated studies, designed and performed *in vitro* experiments, and wrote the manuscript.

L. B. B. edited the manuscript.

A. S. analyzed the GEP data.

T. X. performed the GSEA and CMAP analyses.

R. D. performed the CMAP analyses.

A. M. performed *in vitro* experiments, designed the figures, and contributed to writing the manuscript.

S. A. W. performed and analyzed the PET imaging experiments.

J. J. S. oversaw the PET imaging experiments.

N. G. D. edited the manuscript.

M. A. L. contributed to the *in vivo* study design, performed the pathologic analysis of mouse tissues, and edited the manuscript.

F. Z. analyzed all human clinical trial data.

S. J. helped to design and oversaw the *in vivo* experiments and edited the manuscript.

C. L. M. helped to design and oversaw the GSEA and CMAP approaches and edited the manuscript.

B. G. V. N. contributed to the design and oversaw all studies and contributed to writing the manuscript.

ABSTRACT

Multiple myeloma (MM) is a hematologic malignancy characterized by the proliferation of neoplastic plasma cells in the bone marrow. While the first-to-market proteasome inhibitor bortezomib/VELCADE® has been successfully used to treat myeloma patients, drug resistance remains an emerging problem. In this study, we identify signatures of bortezomib sensitivity and resistance by gene expression profiling (GEP) using pairs of bortezomib-sensitive and -resistant cell lines created from the Bcl-X_L/Myc double transgenic mouse model of MM. Notably, these bortezomib-resistant cell lines show cross-resistance to the next-generation proteasome inhibitors, MLN2238 and carfilzomib/KAPROLIS® but not to other anti-myeloma drugs. We further characterized the response to bortezomib using the Connectivity Map database revealing a differential response between these cell lines to histone deacetylase (HDAC) inhibitors. Furthermore, *in vivo* experiments using the HDAC inhibitor panobinostat confirmed that the predicted responder showed increased sensitivity to HDAC inhibitors in the bortezomib-resistant line. These findings demonstrate that GEP may be used to document bortezomib resistance in myeloma cells and predict individual sensitivity to other drugs classes. Finally, these data reveal complex heterogeneity within MM and suggest that resistance to one drug class reprograms resistant clones for increased sensitivity to a distinct class of drugs. This study represents an important next step in translating pharmacogenomic profiling and may be useful for understanding personalized pharmacotherapy of MM patients.

INTRODUCTION

Multiple myeloma (MM) is a hematopoietic neoplasm characterized by the proliferation of malignant plasma cells (PCs) in the bone marrow (374). Each year about 22,000 new cases arise in the U.S., accounting for approximately 2% of all cancer deaths (67). Standard treatments for MM patients utilize combination chemotherapies (*i.e.* alkylating agents and corticosteroids) along with autologous stem cell transplants. However, in the past decade a number of novel classes of agents have been developed for the treatment of MM, including the proteasome inhibitor (PI), bortezomib (Bz)/VELCADE® (Millennium Pharmaceuticals, Inc.) which is approved for the treatment of MM and relapsed mantle cell lymphoma (375). Despite the initial success of Bz therapy, MM remains incurable due in part to the emergence of Bz-resistant cells in the majority of patients (376, 377).

The primary target of Bz, the proteasome, is part of the highly regulated ubiquitin-proteasome system (UPS) necessary for intracellular proteolysis. The UPS plays a critical role in cellular homeostasis, cell cycle progression and DNA repair (378, 379). The constitutive proteasome, a primary UPS player, is composed of the catalytic 20S core barrel and 19S regulatory caps (together called the 26S proteasome). Bz is a boronic acid dipeptide that is highly selective for inhibition of the chymotryptic activity of the 26S proteasome via reversible binding of its target, PSMB5, a subunit of the 20S catalytic core (144, 380). Bz treatment has been shown to inhibit the transcriptional activity of NF-κB as well as trigger the unfolded protein response (UPR), leading to cell stress and apoptosis (45, 190, 381). With the advent of next-generation PIs, it has become imperative that the Bz response and signatures that are associated with Bz-resistance be further defined in order to identify those patients that 1) will most benefit from PI treatment, 2) will show signs of emerging resistance, and 3) will benefit from selective secondary therapies.

Double-transgenic Bcl-X_L/Myc mice develop plasma cell tumors (mean onset of 135 days) with full (100%) penetrance that possess many of the karyotypic, phenotypic, and gene expression features of human MM (124, 242). Furthermore, malignant PCs can be isolated from these animals, expanded, modified *in vitro*, and subsequently transferred back into syngeneic mice for drug treatment in the presence of an active immune system which includes a complete bone marrow microenvironment (124, 242). We have chosen to utilize this system to model Bz response in order to better understand acquired Bz-resistance within malignant PCs for potential application to the human MM patient population. While therapeutic response in human MM is likely dependent on a combination of tumor genetic variation and inherited population variation, the mouse model provides a common strain background, allowing us to focus on tumor variation and tumor evolution that lead to drug-resistance.

In this study, we have used gene expression profiling (GEP) in the mouse model system to identify Bz-responsive genes *in vitro*. In order to identify signatures of Bz-resistance, we created Bz-resistant mouse cell lines and examined their response to Bz compared to sensitive controls by GEP, revealing signatures of Bz-resistance over the course of Bz treatment. Finally, we used the Connectivity Map (CMAP) database to further identify individual differences in Bz resistance in our representative Bz-sensitive and -resistant lines which identified a unique response to histone deacetylase (HDAC) inhibitors, a class of drugs currently in early clinical trials for the treatment of MM (382-388).

MATERIALS and METHODS

Mouse and human plasma cell lines. The mouse cell lines 595, 589 and 638 were isolated from three individual Bcl-X_L/Myc double transgenic mice and cultured in CST media as previously described (124) and cultured for greater than 40 passages prior to any experimentation after which no changes in rate of growth, clonal drift, response to drug or gene expression were observed. The human myeloma cell lines MM1.S and U266 (obtained from ATCC) were maintained in HMCL media: RPMI 1640 (Lonza) supplemented with 15% fetal bovine serum (Cellgro), 50 µmol/L beta-mercaptoethanol (Sigma-Aldrich), 50 units/ml of penicillin and streptomycin (Hyclone), and 2 mmol/L $_L$-glutamine (Life Technologies). Cell lines were not authenticated.

Drugs and treatment conditions. Bortezomib (Bz) (Millennium Pharmaceuticals) was dissolved in serum-free RPMI-1640 (Lonza) and stored at -80°C. MLN2238 (Millennium Pharmaceuticals), MG-132 (American Peptide Company), trichostatin A (Cell Signaling Technology), and vorinostat (SAHA) (LC Laboratories) were dissolved in dimethyl sulfoxide (DMSO) (Sigma-Aldrich), melphalan (Sigma-Aldrich) was dissolved in EtOH, and panobinostat (LC Laboratories) was dissolved in ddH_20; all drugs were stored at -20°C.

Bortezomib resistant (BzR) cells were generated by dose escalation of Bz over 6 months by once weekly treatment with Bz starting at 16 nM; the Bz concentration was doubled every 3 weeks until a final growth concentration of 64 nM was reached. Cultures were removed from Bz for 14 days or 6 months prior to analysis and cultured in a manner consistent with the parental lines.

Cell viability assay. Cells were seeded at a concentration of $4x10^5$ cells per mL. After 24 hours the cells were treated with the indicated concentrations of drug for 48 hours. Cell viability was measured by CellTiter-Glo® Luminescent cell viability assay according

to manufacturer's instructions (Promega) using the Synergy 2 Microplate Reader (Biotek). Values were normalized to untreated controls and IC_{50} values were estimated by calculating the nonlinear regression using the sigmoidal dose-response equation (variable slope) in GraphPad (Prism). In some experiments, cell growth was calculated by trypan blue (Life Technologies) exclusion with a hemocytometer.

Preparation of RNA for gene expression profiling. The mouse cell lines 595 BzS, 595 BzR, 638 BzS and 638 BzR, removed from Bz selection for 14 days, were plated at a density of 4 x 10^5 cells per mL in CST media with mIL-6. In addition, 595 BzS (595.2), 595 BzR (BzR 595.2), 589 BzS and 589 BzR, removed from Bz selection for 6 months, were plated at a density of 4 x 10^5 cells per mL in CST media with mIL-6. After 24-hour incubation, 66 nM Bz was added to each well, and the cells were collected at 0, 2, 8, 16 and 24 hours after treatment. Similarly, MM1.S and U266 were plated 24 hours prior to 33 nM Bz treatment and cells were collected at 0, 16 and 24 hours. Cells were lysed, and total RNA was extracted using QIAshredder and RNeasy RNA purification columns (Qiagen). RNA concentration and integrity were analyzed using the Nanodrop-8000 (Thermo Scientific) and 2100 Bioanalyzer (Agilent Technologies). cDNA was prepared and labeled with the Illumina TotalPrep- 96 RNA Amplification Kit (Life Technologies). Samples were hybridized to the Illumina MouseWG-6 v2.0 Expression BeadChip according to manufacturer protocols and read on the Illumina iScan (Illumina). Microarray data have been made available at the Gene Expression Omnibus (GEO) web site (accession no. GSE41930).

Normalization of gene expression data. Fluorescence values obtained from the Illumina detection system without background subtraction and without normalization were analyzed for quality control as previously described (389). Quantile normalization was applied to the data that passed quality control using GeneData Analyst Software (Genedata Inc.). Following normalization, multiple probes were averaged to obtain a

single value for each gene. Statistical analyses and relative normalization was carried out as described within the draft using GeneData Analyst Software.

Enrichment analyses. Gene set enrichment analysis software (GSEA, Broad Institute, www.broadinstitute.org/gsea/) was used to test for enrichment between the differentially expressed genes in mouse and the MM patient gene set (390). Specifically, the 24hr time point after Bz treatment was compared to the 0hr time point for all Bz-sensitive mouse cell lines and the resulting differential expression values were evaluated for enrichment for the Shaughnessy, et al. gene set (390), using default GSEA parameters. In addition, variant transcripts were analyzed using Ingenuity Pathway Analysis (IPA) (Ingenuity Systems, www.ingenuity.com) to identify canonical pathways that were enriched in each set of genes. The significance of each association was determined by the Fisher exact test.

CMAP drug prediction. Genes were assigned a binary distinction of “up” or “down” respectively by selecting genes with at least 2-fold higher or lower expression in the BzS cell lines relative to the derived BzR lines at the 24hr time point (post Bz treatment). These “up” and “down” sets were queried against the Connectivity Map (CMAP) database (391, 392). The given connectivity score estimates the similarity between the input and database expression signatures. A positive score indicates that the input signature is similar to, and a negative score indicates that the input signature is opposite to what would be expected by the predicted compound. Predicted compounds were ranked in ascending order of p-value and viable compounds were chosen based on significance of correlation with the input signature ($p < 0.05$).

Quantitative PCR analysis. 1 µg of total RNA was reverse transcribed using the Transcriptor First Strand cDNA Synthesis Kit (Roche) with anchored-oligo$(dT)_{18}$ primers. Quantitative RT-PCR of cDNA was performed in triplicate on the LightCycler 480 (Roche) using LightCycler 480 Probes Master (Roche) with a pre-amplification

incubation of 95°C for 10 minutes, followed by 45 cycles of 95°C for 10 sec and 55°C for 30 sec (single acquisition). The following primers were used: *Ddit3*, 5'-GCGACAGAGCCAGAATAACA-3' (left), 5'-GATGCACTTCCTTCTGGAACA-3' (right). The Universal ProbeLibrary Mouse GAPD Gene Assay (Roche) was used as the reference gene. Data were analyzed using the LightCycler 480 software (Roche), and relative fold changes in cDNA levels were calculated with the *Gapd* reference gene as normalization using the $2^{-\Delta\Delta Ct}$ method (393). All data were normalized to total RNA extracts from the mouse B cell lymphoma cell line, CH12 (a gift from Dr. Matthew Scharff, Albert Einstein College of Medicine, NY). This cell line was not authenticated. CH12 cells were maintained in RPMI 1640 (Lonza) supplemented with 10% fetal bovine serum (Cellgro), 50 μmol/L beta-mercaptoethanol (Sigma-Aldrich), 50 units/ml of penicillin and streptomycin (Hyclone), and 2 mmol/L $_L$-glutamine (Life Technologies). Statistical significance was determined using a Student's t-test.

Animal care, tumor injection and drug treatment. FVBN/Bl6 recipient mice were generated as previously described (124, 242). Mice were maintained in a controlled environment receiving food and water ad libitum. Fresh, ficolled (Ficoll-Paque™ PLUS, GE Healthcare) 595 BzS and BzR cells (1×10^6) suspended in 100 μL of serum-free RPMI-1640 media were injected into 6 mice per group (3 groups per cell line) via the lateral tail vein of age-matched recipient mice. Mice were weighed and treated by intraperitoneal injection twice per week starting 5 days after cell transfer with vehicle (5% dextrose in water), Bz (1.2 mg/kg dissolved in 0.9% saline), or panobinostat (10 mg/kg suspended in vehicle) until moribund. Kaplan-Meier curves were generated using GraphPad (Prism). Statistical significance was determined using a Student's t-test. Tumor cell homing was monitored by positron emission tomography (PET) imaging (see Supplemental Methods). All mouse veterinary care, colony maintenance, and PET

imaging experiments were carried out in accordance with University of Iowa Institutional Animal Care and Use Committee guidelines and approvals.

FDG-PET imaging. MicroPET studies were conducted at The University of Iowa Small Animal Imaging Core. Non-fasted mice (n=2 per treatment group) were anesthetized with 2.8% (v/v) isoflurane and body weight was recorded. Blood glucose (95.4 +/- 15.7 mg/dl) was measured prior to injection of 18F-FDG using a Freestyle glucometer (Abbott Labs, Naperville, Il). A subcutaneous injection of 0.1 ml 0.9% sterile normal saline was given to ensure adequate hydration. 18F-FDG (8.4 MBq ± 0.9) or 18F-FLT (8.5 MBq ± 0.5) was injected via the lateral tail vein. The mice were allowed to wake and placed in individual warmed cages for the 60 min. uptake period. Anesthetized mice (2.8% isoflurane) were then placed prone in a heated multimodality imaging chamber (M2M imaging Corp) and positioned in the gantry of the INVEON PET/CT/SPECT multimodality animal imaging system (Siemens, Knoxville, TN). Listmode PET mages were acquired for 15 minutes and in the same workflow a microCT image was acquired for attenuation correction purposes. All decay corrected PET images were reconstructed using OSEM3D/OP-MAP with scatter correction. Visualization and SUV analysis of datasets were performed using Siemens Inveon Research Workplace software version 3.0 and PMOD version 3.3 (PMOD Technologies Ltd, Zurich Switzerland).

Histology. Tissues (femur, liver, spleen, kidney) were dissected from euthanized, moribund mice and fixed in 10% formalin. Gross examination was performed by M.A.L and H.A.F.S. – sections of each tissue were placed in cassettes for routine histologic processing. Bones were decalcified in EDTA prior to processing. After processing, samples were paraffin-embedded and sectioned. Sections were stained with hematoxylin and eosin and scored for evaluation of plasma cell neoplasm by a board-certified hematopathologist (author – M.A.L).

RESULTS

Bcl-X_L/Myc transgenic mouse plasma cell tumor lines show similar significant shifts in gene expression upon bortezomib treatment as human myeloma

In this study, three representative clonal cell lines isolated from the Bcl-X_L/Myc double transgenic mouse model of plasma cell malignancy were utilized (124, 242) to identify transcriptional responses to bortezomib in Bz-sensitive and -resistant cells *in vitro*. The 595, 589 and 638 plasma cell lines derived from individual mice showed IC_{50} values within a 22-32 nanomolar range to Bz by cell viability assay following 48 hours of drug treatment (Supplemental Figure S1A). Consistent with previous reports (142), Bz treatment of these cell lines resulted in programmed cell death as evidenced by caspase 3 cleavage and annexin V-positive/propidium iodide-negative staining by flow cytometry (data not shown). This cytotoxic profile was similar to two representative, well-described Bz-sensitive human myeloma cell lines (HMCLs), MM1.S and U266 (310, 394, 395) (Supplemental Figure S1B). Taken together, these data suggest that, like in human MM, the treatment of these mouse cell lines *in vitro* with Bz induces a cytotoxic response.

We next asked whether the transcriptional profile induced over time by exposure to Bz was similar across both species. The three Bz-sensitive (BzS) mouse lines (595 shown in duplicate as 595.2) were treated with a sublethal 66 nM dose of Bz over a time course of 24 hours and analyzed using gene expression profiling (GEP). This dose was chosen because it resulted in less than 20% death at 24 hours (Supplemental Figure S1C) but greater than 50% death at 48 hours (data not shown) suggesting that it was an optimal concentration for collecting kinetic data within a 24-hour timeframe. In addition, the HMCLs, U266 and MM1.S, were also treated with a sublethal 33 nM dose (Supplemental Figure S1D) of Bz (equitoxic to the dose used on the mouse cell lines) and analyzed by time course GEP. The variant transcripts identified from these human (genes=1421, variance > 0.1) and mouse (genes=1021, variance > 0.1) time course

data shared 132 genes in common, 58% of which also shared a common, kinetic pattern of response to Bz across all cell lines analyzed across both species (Figure 1B, Supplemental Table S1).

This transcriptional response was further validated using GEP data from a recently published human MMTT3 drug trial by Shaughnessy, et al. where RNA was collected from newly-diagnosed MM patients prior to and following a single, 48 hour test dose of Bz (390). Gene set enrichment analysis (GSEA) of the mouse *in vitro* transcriptional response to Bz (24hr vs. 0hr) showed remarkable enrichment (NOM p-value < 0.05, FDR < 25%) for the Shaughnessy, et al. 80 gene model. This 80 gene model included those genes that were 1) most changed among all patients by the Bz treatment at 48 hours and 2) were associated with progression free survival (PFS) of which 46 genes were unique and shared a gene symbol with mouse (Supplemental Figure S2A) (390). 29 genes were shown to significantly contribute to the enrichment between the mouse *in vitro* and the human *in vivo* data (Supplemental Figure S2B) many of which are known components of the proteasome ubiquitination pathway (390) which was found to be enriched in this dataset by Ingenuity Pathway Analysis (IPA). In addition, the kinetic GEP response in both the human and mouse cell lines was enriched for downstream targets of the transcription factor NFE2L2 (NRF2) ($p < 1 \times 10^{-10}$, z-score > 4, IPA) a transcription factor known to be involved in the oxidative stress response to proteasome inhibition (396). Taken together, these data demonstrate a robust transcriptional response to Bz that is conserved not only between mouse and human PC malignancies but also within isolated tumor cells *in vitro* and tumor cells in their native microenvironment in human patients.

Generation of clonally-related bortezomib sensitive and resistant cell line pairs

Because the mouse model provides a drug-naïve system with a common strain background and the ability to transfer cells back into syngeneic animals with a

competent immune system, we chose to further profile the transcriptional response associated with Bz-resistance within the tumor cell using this model system. The three BzS mouse cell lines characterized above, were dose-escalated with Bz over 6 months to obtain resistant (BzR), clonally-related (data not shown), daughter cell lines with a 2-fold to 5-fold increase in IC_{50} in response to Bz (Figure 2A, Table 1). Doubling rates for the pairs of cell lines were similar (data not shown) suggesting that the increased IC_{50} in BzR lines is not due to an increase in cell growth. To determine whether these BzR mouse cell lines were capable of maintaining their Bz-resistance over time, the cells were removed from drug selection, and Bz cell viability assays were performed after one year. The BzR lines maintained their resistant phenotype showing virtually identical IC_{50} values (data not shown).

Others have reported that Bz-resistance is often associated with increases in chymotrypsin-like proteasome activity (194, 195, 397). Indeed, we find that two representative BzR cell lines have significantly increased chymotrypsin-like activity while trypsin- and caspase-like activity is decreased (Supplemental Figure S3A-B) compared to their BzS counterparts. This observation directly correlated with a similar increase in PSMB5 protein expression by Western blotting in the BzR cells (data not shown) in the absence of *Psmb5* mutations by sequencing (data not shown) suggesting that higher baseline proteasome activity (via increased PSMB5 protein expression), not *Psmb5* inactivating mutations, likely contribute to the resistance observed in these BzR lines. In addition, these BzR lines showed cross-resistance to the boronic acid next-generation proteasome inhibitor, MLN2238, as well as the epoxyketone next-generation proteasome inhibitor, carfilzomib/KYPROLIS®. While the 595 BzR line also showed cross-resistance to the classical aldehyde proteasome inhibitor, MG-132, this line showed increased sensitivity to the MM drug, melphalan whereas the 589 BzR line maintained sensitivity to these compounds (MG-132, melphalan) (Table 1, Figure 1A).

Neither the BzS nor the BzR lines responded to drugs known to be ineffective as single agents against MM: vincristine, hydroxyurea and fludarabine (data not shown). These data suggest that not only is the resistance observed in the BzR lines specific to Bz and its next-generation derivative (MLN2238) and sustained over time but that the resistant phenotype may be overcome with other drugs.

Bz-resistance is associated with changes in transcription that are predictive of patient outcomes

We were particularly interested in determining the transcriptional differences in gene expression between these BzS and BzR cells lines and, thus, examined time courses of response by GEP following the same, sublethal Bz treatment in BzR lines (Supplemental Figure S1E) as used on their BzS counterparts (Figure 1). To globally visualize these expression patterns, we analyzed the BzR transcriptional response to Bz as we had the BzS cell lines described above.

Firstly, a pair wise comparison of the BzS and BzR baseline gene expression in the absence of Bz treatment was performed revealing a 51-gene expression signature that statistically distinguished (fold change > 2, $p < 0.05$, Student's t-test) sensitive and resistant lines (Supplemental Figure S3C). Of these 51 mouse genes, 23 had human homologs. To test the predictive power of this 23-gene model, we queried the gene expression signatures of 210 patients from the MMTT3 human drug trial (390). Unsupervised clustering of these patients based on the 23-gene model identified 2 groups whose progression-free and overall survival were significantly different (log rank test) (Figure 2B). These results suggest that our *in vitro* mouse model of Bz-resistance has predictive value in human MM drug trials which include Bz.

To further define the differences in the transcriptional response to Bz in BzS and BzR cell lines, we performed a combined analysis of the BzS and BzR Bz transcriptional profiles identifying 219 genes that changed significantly in both the sensitive or the

resistant group in response to drug ($p < 0.001$, |fold change| > 2, pairwise two group t-test) (Supplemental Table S2). Examination of heatmap clusters showed that the majority of the response to Bz in the sensitive cell lines was conserved in the resistant cell lines (Figure 2C, Supplemental Table S2), illustrating a common programmed transcriptional response of cell lines to Bz regardless of their overall sensitivity (measured by IC_{50}) to the compound. However, 29 genes were differentially responsive to Bz *in vitro* between BzS and BzR lines ($p < 0.001$, |fold change| > 2) (Figure 2D). Among these were the upregulation of a cluster of NRF-2 mediated oxidative stress response genes: *Hspb1, Dnajb1, Hspa1a, Hspa1b*, and *Ddit3* (*a.k.a.* CCAAT/Enhancer-Binding Protein Homologous Protein *(CHOP*)) (396) which has been observed in other Bz sensitive human cell lines (381, 396), suggesting that these may serve as a signature of Bz-mediated cell death which is unique to BzS compared to derived BzR cells.

Using CMAP to identify drugs with high correlation to Bz-associated death by GEP

Biomarkers that are associated with emerging resistance to Bz and yet may define sensitivity to alternative therapies, remain ill-defined (358). Although we do see a common gene signature of response to Bz and have identified similar biomarkers across Bz-resistant cell lines compared to their sensitive counterparts, we have also observed differences in response to secondary therapies across Bz-resistant cell lines (Table 1). Indeed, not all Bz-refractory MM patients respond similarly to secondary therapies. Given these differences we aimed to use the individual cell line GEP data described above to identify non-PI drugs that could target BzR cell populations using Connectivity Map (CMAP, Broad Institute) (391). The CMAP database contains treatment-induced transcriptional signatures from 1,309 bioactive compounds in 4 human cancer cell lines. An input signature can be used to query the database for correlated drug signatures. To create these input signatures, gene set enrichment analysis was used to identify in individual paired mouse GEPs those genes that were most different in BzS versus BzR

lines following drug treatment (24hr vs. 0hr data comparison, |fold change| > 2). These genes were then used to query CMAP to identify drugs that induced expression signatures that were similar (positive correlation) or dissimilar (negative correlation) to the differential expression response of each BzS lines relative to its BzR line when treated with Bz. We hypothesized that such drugs, particularly those with positive correlations to the differential response, may have the potential to kill the BzR lines.

The CMAP query produced a number of compounds with signatures that were predicted as significantly correlated (positive) or anti-correlated (negative) with the BzS/BzR differential response (Table 2, Supplemental Table S3). Broadly, drugs promoting inhibition of the proteasome-ubiquitin pathway, NF-κB, HSP90, protein synthesis and microtubules showed positive correlation, while drugs that inhibit the cell cycle showed negative correlation with the differential responses in all pairs (Table 2, Supplemental Table S3). These predictions were not surprising given the known modes of action for Bz (398). Interestingly, several HDAC inhibitors (HDACis), were significantly positively correlated with the differential Bz response in one of the three pairs of cell lines, 595 ($p < 2 \times 10^{-5}$) (Table 2, Supplemental Table S3), but were not predicted in the other two highlighting some heterogeneity among these cell line pairs. In fact, this was the only drug family with consistent drug predictions for each drug across the three cell lines queried (Supplemental Table S3). Since HDACis have been reported as having synergistic effects when combined with other MM treatments (398) and are currently in clinical trials for refractory MM (399), we chose to evaluate this result further. We hypothesized that the 595 pair of lines would respond differently to HDACi treatment than the other pairs of lines based on the CMAP results.

Based on the HDACi prediction, three HDAC inhibitors were chosen to test two representative pairs of BzS and BzR mouse lines (595 and 589) for *in vitro* sensitivity. The 595 BzR line showed enhanced sensitivity to the HDACis trichostatin A (TSA) and

vorinostat (SAHA) (Figure 3A & B, upper panels), which were chosen from the CMAP predicted drug list (Supplemental Table S3), as well as panobinostat (Figure 3C, upper panel). This was a cytotoxic response as evidenced by *CHOP* induction (381, 398, 400) (Supplemental Figure S4A). In contrast, the 589 BzR line (not predicted for enhanced sensitivity to HDACis by CMAP) showed cross-resistance to all three HDACi compounds compared to the BzS line (Figure 3A-C, lower panels). This panobinostat-sensitive phenotype has been observed in an additional BzR mouse cell line (Bz IC_{50}s: 34 nM (BzS) and 63 nM (BzR); panobinostat IC_{50}s: 37 nM (BzS) and 22 nM (BzR)) and indicates that CMAP may have the ability to identify differences in secondary drug response in these cell line models.

A subset of Bz-resistant mouse cell lines have greater in vivo sensitivity to HDAC inhibitors

It is well-documented that the myeloma response to some chemotherapeutic agents is dependent not only on the stromal microenvironment of the bone marrow (401) but on a complete immune system (402) highlighting the utility of our immunocompetent mouse model system. To determine whether the differential *in vitro* drug responses were maintained *in vivo*, the 595 BzS and BzR cell lines were adoptively transferred back into syngeneic recipients. The untreated BzS mouse phenotype appeared to be significantly less severe compared to BzR mice which reached moribundity quickly at a median time of 16 days ($p = 0.033$).

To better compare the disease burden in these animals, both FDG- and FLT-positron emission tomography (PET) imaging were used. FDG-PET imaging of representative animals from each group showed that the BzS cells home to the bone marrow whereas the BzR cells are dispersed in moribund animals with fewer characteristic “hot spots” in the long bones (Figure 4A). Representative histopathological analyses of bone marrows and soft tissues from these animals showed

that the malignant PCs were present in the marrows of both animals but were notably absent or minimal in the soft tissues of BzS mice (Supplemental Figure S4B). Those BzS and BzR cells that did home to the bone marrow had similar metabolic activity (FDG-PET); however, BzS cells had significantly higher rates of proliferation (FLT-PET) *in vivo* even though the BzS and BzR growth rates were similar *in vitro* (Figure 4B). Treatment of BzS and BzR mice with Bz *in vivo* (n=6 mice per group) showed that BzS mice received a significantly greater survival advantage with Bz treatment than their BzR counterparts (Figure 4C) whose survival did not differ from BzR vehicle-treated mice (data not shown) in agreement with our *in vitro* data (Figure 2A). This was directly correlated with significantly decreased tumor burden (FDG-PET) in BzS mice treated with Bz compared to vehicle (Figure 4D). These results indicate that myeloma cell homing may play a role in Bz sensitivity and that the immunophenotype associated with extramedullary homing may be associated with Bz resistance *in vivo*.

To specifically determine whether 595 BzR mice receive a survival advantage from panobinostat treatment as predicted *in vitro*, mice were injected with BzR cells and treated with either vehicle (n=5) or panobinostat (n=6), and the time to death for each group was compared. Consistent with our *in vitro* findings (Figure 2A & 3C), panobinostat treatment significantly increased the overall survival of BzR mice (Figure 4E) and decreased the tumor burden (Figure 4F) in these animals. These *in vivo* results not only confirm our *in vitro* findings but further suggest that there may be a greater benefit from HDAC inhibitor therapy as a salvage therapy in some refractory myelomas.

DISCUSSION

In this study, we defined the malignant PC response to Bz and characterized signatures of Bz-sensitivity and -resistance by GEP using cell lines derived from the Bcl-X_L/Myc double transgenic mouse model. Although a number of Bz treatment studies using HMCLs, primary patient samples, and non-myeloma primary patient samples have been reported (390, 394, 403-405), they did not provide a kinetic analysis of Bz-sensitive and -resistant cells exposed to Bz over time nor did they explore individual differences in Bz-resistance that may contribute to secondary drug efficacy. In addition, the availability of published Bz data has allowed us to validate the Bcl-X_L/Myc cell lines' response to drugs *in vitro* further illustrating their utility as a preclinical tool for asking pharmacogenomic questions.

Malignant PCs isolated in cell culture from these animals were generally sensitive (nanomolar concentrations) to Bz. In addition, we found evidence of a robust, conserved and likely complex response to Bz in our mouse cell lines consistent with recent reports (390, 396, 403). This response was highly conserved in well-characterized HMCLs and in human patient clinical trial samples. Perhaps the most striking trend was the coordinated upregulation of the majority of the constitutive proteasomal subunits in response to Bz treatment in both Bz-sensitive and -resistant cell lines which has been previously described (390, 396, 403) further validating our model system.

The transcriptional response to Bz that we observed in all cells regardless of their sensitivity to the drug included the induction of the gene *Psmd4* which is part of the 19S proteasomal cap complex that selectively targets and binds ubiquitinated substrates for degradation by the 20S proteasome and whose amplification has been associated with high-risk myeloma (390). We did not identify higher baseline *Psmd4* expression in our Bz-resistant cell lines; nor did we identify increases in copy number at the mouse *Psmd4*

locus by array comparative genomic hybridization (mouse 3qF2.1 syntenic to human 1q21) (data not shown). Therefore, although 1q21 amplification has been associated with a high-risk MM phenotype in patients, our data would suggest variations in Bz response may be more complex than *Psmd4* expression levels alone. Interestingly, we do observe differences in baseline expression of *Eno1* and *Cxcr4* in BzR compared to BzS cell lines, both of which have been associated with a poor prognostic outcome in MM patients (100, 406). We believe that these data further highlight the utility of this system and underscore the need for companion analyses to validate these potential biomarkers using clinical samples which we are currently developing.

We found it particularly interesting that HDACis were predicted by CMAP in this study because Bz is known to downregulate the expression of class I HDACs (162), and HDACis have been shown to decrease the 20S chymotryptic activity of the proteasome (407), both mediating cell death through the induction of CHOP and NOXA (408). In addition, HDAC6 has been shown to be a key regulator of aggresome activity, an alternative pathway for protein degradation in the absence of proteasome activity (409). Bz response is correlated to the HDAC inhibitor response in only one of the three pairs of mouse cell lines suggesting that 1) we might further identify a small, very specific gene signature that is associated with an HDAC inhibitor response *in vitro* in these mouse cell lines and that 2) not all drug resistant myelomas will respond similarly to HDACis highlighting some heterogeneity within our *in vitro* system that is also likely present in the Bz-refractory patient population. Although there is a conserved transcriptional response to Bz between these 2 pairs of Bz-sensitive and -resistant cell lines, they respond very differently to HDACi compounds suggesting that a more-favorable response might be achieved with HDACis such as panobinostat or vorinostat as a secondary therapy in some, but not all relapsing myelomas. Indeed, we have identified those genes that uniquely predicted the HDACi response in the 595 cell lines

(Supplemental Table S4). Interestingly, these genes were enriched for biosynthetic and metabolic pathways (IPA) which we are currently investigating in Bz-resistant disease. We did not include a dual treatment (Bz and panobinostat) arm in our *in vivo* study; however, dual treatment of the cell lines *in vitro* indicates that there is synergy between these two compounds (data not shown) which has been shown in another mouse model of MM (410). The mechanism of this synergy may be further informed by these studies.

Although CMAP produced additional predictions to other classes of drugs, the true predictive power of this approach remains unclear. For example, alkylating agents were predicted by CMAP but did not include melphalan for which we have observed differential response between our Bz-resistant cell lines. In fact, HDACis were the only drug family that had a consistent prediction pattern across all three cell line pairs for all drugs predicted. This suggests that perhaps the most viable secondary drug candidates will be those with consistent predictions. It remains to be seen if there are similar predictions of response in subsets of patients receiving Bz/panobinostat combination therapy; however, our data suggest that refinement of this model may be effective for predicting these cases in advance.

With the initial success of combination Bz and HDACi treatments for refractory patients in the clinic (163) and our indication of differential response to HDACis *in vitro* and *in vivo*, our model system provides additional opportunities to characterize sensitivity and resistance to HDACis *in vitro* and *in vivo*. It is apparent that the approach taken in this study identifies a novel use for gene expression profiling in the repurposing of drugs as secondary therapies in myeloma. The prediction of HDACis as a secondary therapy here suggests that a panobinostat response profile of emerging resistance might be further elucidated that could provide preclinical support for personalized medicine approaches in MM.

Table 1. Drug IC_{50}[a] table for Bz-sensitive (BzS) and Bz-resistant (BzR) mouse lines.

Drug	595 BzS	595 BzR	Fold Δ[b]	589 BzS	589 BzR	Fold Δ[b]	638 BzS	638 BzR	Fold Δ[b]
Bortezomib, nM	23	112	4.9	22	96	4.4	36	102	2.8
MLN2238, nM	28	154	5.5	39	180	4.6	N/A	N/A	N/A
Carfilzomib, nM	28	71	2.5	41	77	1.9	N/A	N/A	N/A
MG-132, nM	42	95	2.3	80	85	1.1	N/A	N/A	N/A
Melphalan, μM	240	50	0.2	80	100	1.3	N/A	N/A	N/A

[a]IC_{50} calculations were determined by a sigmoidal dose-response equation in triplicate over multiple experiments.

[b]Fold change (Δ) is representative of the BzR line normalized to its BzS control.

Table 2. Families of drugs with expression patterns significantly correlated to the Bz response in mouse lines using CMAP.

Drug Family	Prediction[a]		
	595sp[b]	638bm	589bm
Proteasome inhibitors and UPS modulators	+	+	+
NF-κB inhibitors	+	+	+
Alkylating Agents	+	+	+
HSP90 inhibitors	+	+	+
Protein synthesis inhibitors	+	+	+
Microtubule inhibitors	+	+	+
CDK/TopoI/TopoII/Cell cycle inhibitors	–	–	–
HDAC inhibitors	+	np	np

[a]Significant predictions ($p < 0.05$) were made for each of the mouse line pairs individually. A positive prediction indicates that the drug family induces a similar expression signature to the BzS signature. A negative prediction indicates that the drug family induces an opposite expression signature to the BzS signature. An "np" indicates that no drug prediction was made.

[b]595 is a combination of the 595 and 595.2 datasets.

Figure 1. Identification of Bz-responsive genes by gene expression profiling. A) Chemical structures of the proteasome inhibitors bortezomib (Bz), MLN2238, and carfilzomib (Cz) and the alkylating agent, melphalan. B) Heat map of Bz-responsive genes common to mouse and human plasma cell malignancy *in vitro* using 3 BzS mouse lines (595 in duplicate as 595.2) treated with 66 nM Bz and 2 HMCLs treated with 33 nM Bz. Mouse cells were collected at 0, 2, 8, 16 and 24 hours and human cells at 0, 16 and 24 hours after Bz treatment. Columns represent time points and rows represent genes. Columns are ordered firstly by cell line and secondly by ascending time; genes are ordered by hierarchical cluster analysis. Color indicates fold change which was determined for each gene by comparing the average of the 16 and 24 hour time points to the 0 hour time point in each time course. A full gene list has been provided in Supplemental Table S1.

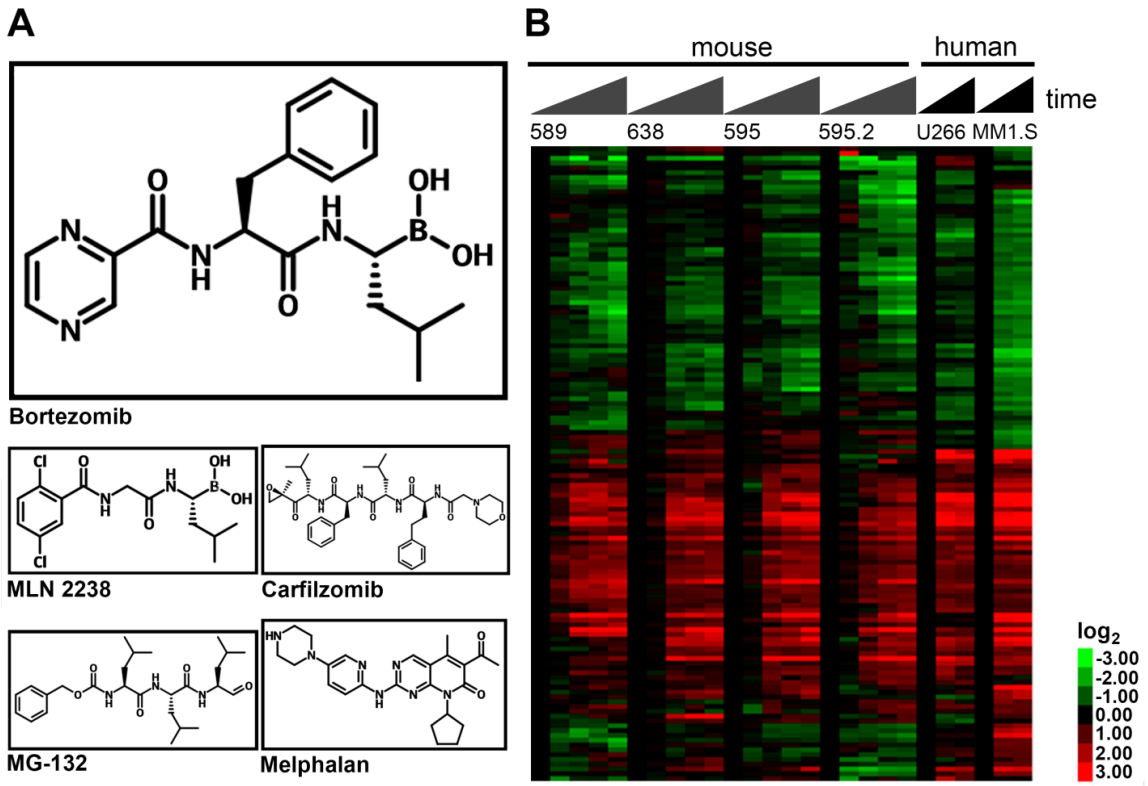
A
Bortezomib
MLN 2238
Carfilzomib
MG-132
Melphalan
B
mouse
human
time
589
638
595
595.2
U266
MM1.S
log2
-3.00
-2.00
-1.00
0.00
1.00
2.00
3.00

Figure 2. Kinetic similarities and differences in Bz response in BzS and BzR mouse lines. A) Kill curve analysis of 3 representative pairs of Bz-sensitive and -resistant mouse cell lines (595, left panel; 589, middle panel; 638, right panel). Cell viability data were collected over a range of 0-128 nM Bz. Open squares represent Bz-sensitive (BzS) lines and filled squares represent Bz-resistant (BzR) lines. All data points shown were normalized to untreated controls. Error bars, which are shown but are smaller than the data symbols, represent the standard deviation of triplicate reads over each experiment. B) Kaplan-Meier curves showing significant differences in event-free (EFS, left) and overall (OS, right) survival in patients from the MMTT3 drug trial clustered based on the expression of the genes that most distinguished mouse BzS and BzR cell lines (Supplemental Figure S3C). Heat maps of C) Bz-responsive genes across the 3 BzS mouse lines and their BzR counterparts (595 in duplicate) treated with 66 nM Bz and collected at 0, 2, 8, 16 and 24 hours after treatment highlighting D) those genes whose responses are most significantly different between BzS and BzR lines. Columns represent time points and rows represent the genes. Columns are ordered firstly by sensitivity and secondly by sample; genes are ordered by hierarchical cluster analysis. Colors indicate fold change which was determined for each gene by comparing the average of the 16 and 24 hour time points to the 0 hour time. A full gene list for part B has been provided in Supplemental Table S2.

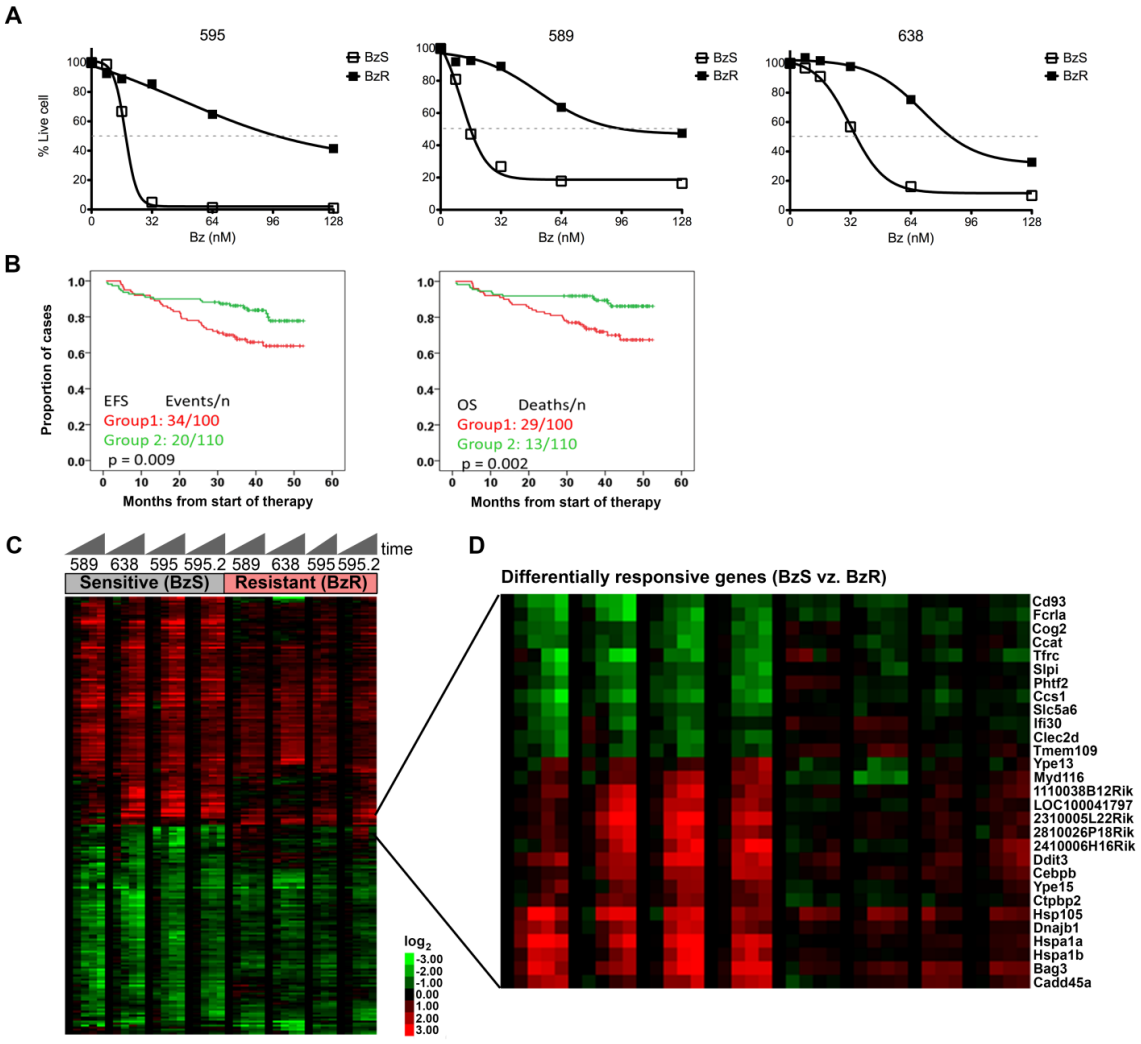
A
595
589
638
BzS
BzR
% Live cell
Bz (nM)
B
Proportion of cases
EFS Events/n
Group1: 34/100
Group 2: 20/110
p = 0.009
OS Deaths/n
Group1: 29/100
Group 2: 13/110
p = 0.002
Months from start of therapy
C
time
589 638 595 595.2 589 638 595 595.2
Sensitive (BzS)
Resistant (BzR)
log2
-3.00
-2.00
-1.00
0.00
1.00
2.00
3.00
D
Differentially responsive genes (BzS vz. BzR)
Cd93
Fcrla
Cog2
Ccat
Tfrc
Slpi
Phtf2
Ccs1
Slc5a6
Ifi30
Clec2d
Tmem109
Ype13
Myd116
1110038B12Rik
LOC100041797
2310005L22Rik
2810026P18Rik
2410006H16Rik
Ddit3
Cebpb
Ype15
Ctpbp2
Hsp105
Dnajb1
Hspa1a
Hspa1b
Bag3
Cadd45a

Figure 3. Mouse cell lines respond differently to HDAC inhibitors. A-C) Kill curve analysis of 2 representative pairs of BzS and BzR mouse cell lines (595, top panels; 589, bottom panels). Cell viability data were collected over a range of A) 0-100 nM trichostatin A, B) 0-4 μM vorinostat, or C) 0-128 nM panobinostat. Open squares represent BzS lines and filled squares represent BzR lines. All data points shown were normalized to untreated controls. Error bars, which are shown but are smaller than the data symbols, represent the standard deviation of triplicate reads over each experiment. Drug structures are shown below corresponding kill curves.

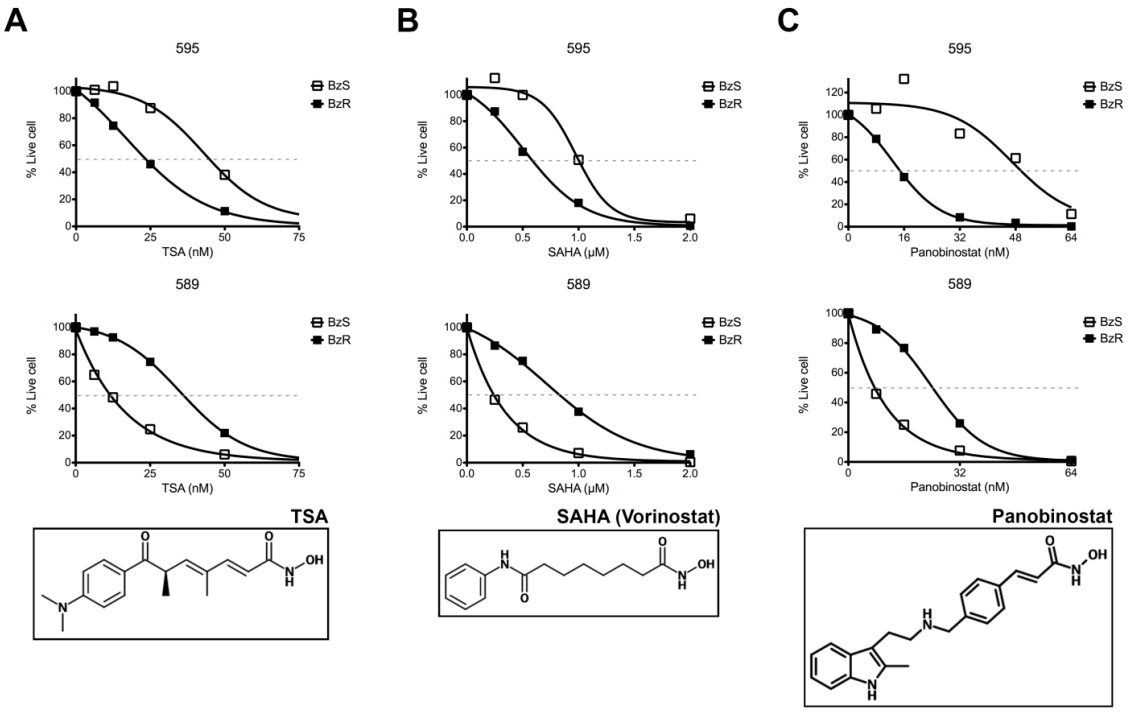
A
595
BzS
BzR
% Live cell
TSA (nM)
589
TSA
B
595
SAHA (μM)
589
SAHA (Vorinostat)
C
595
Panobinostat (nM)
589
Panobinostat

Figure 4. Bz-resistant cells respond favorably to panobinostat *in vivo*. A) Representative FDG-PET imaging of untreated 595 BzS and BzR cell-injected FVBN/Bl6 syngeneic mice (one mouse shown from each group). Red arrows indicate tumor "hotspots". B) Quantification of FDG- (blue) and FLT-PET (red) imaging of untreated BzS and BzR mice (n=2 per group (4 tissue sites scored from each), * $p < 0.05$). C) Kaplan-Meier curve of BzS (black) and BzR (red) cell-injected mice treated with Bz. Statistical significance was determined using a one-tailed Student's t-test. D) Quantification of FDG-PET-imaged BzS mice treated with either vehicle (left, white bar) or Bz (right, gray bar) (n=2 per group (4 tissue sites scored from each), *** $p < 0.0005$). E) Kaplan-Meier curve of BzR cell-injected mice treated with vehicle (n=5, black) or panobinostat (n=6, blue) until death. Statistical significance of both Kaplan-Meier curves was determined using a one-tailed Student's t-test. F) Quantification of FDG-PET-imaged BzR mice treated with either vehicle (left, white bar) or panobinostat (right, gray bar) (n=2 per group (4 tissue sites scored from each), * $p < 0.05$). Statistical significance of all PET imaging was determined using a two-tailed, nonparametric Mann-Whitney test (95% CI).

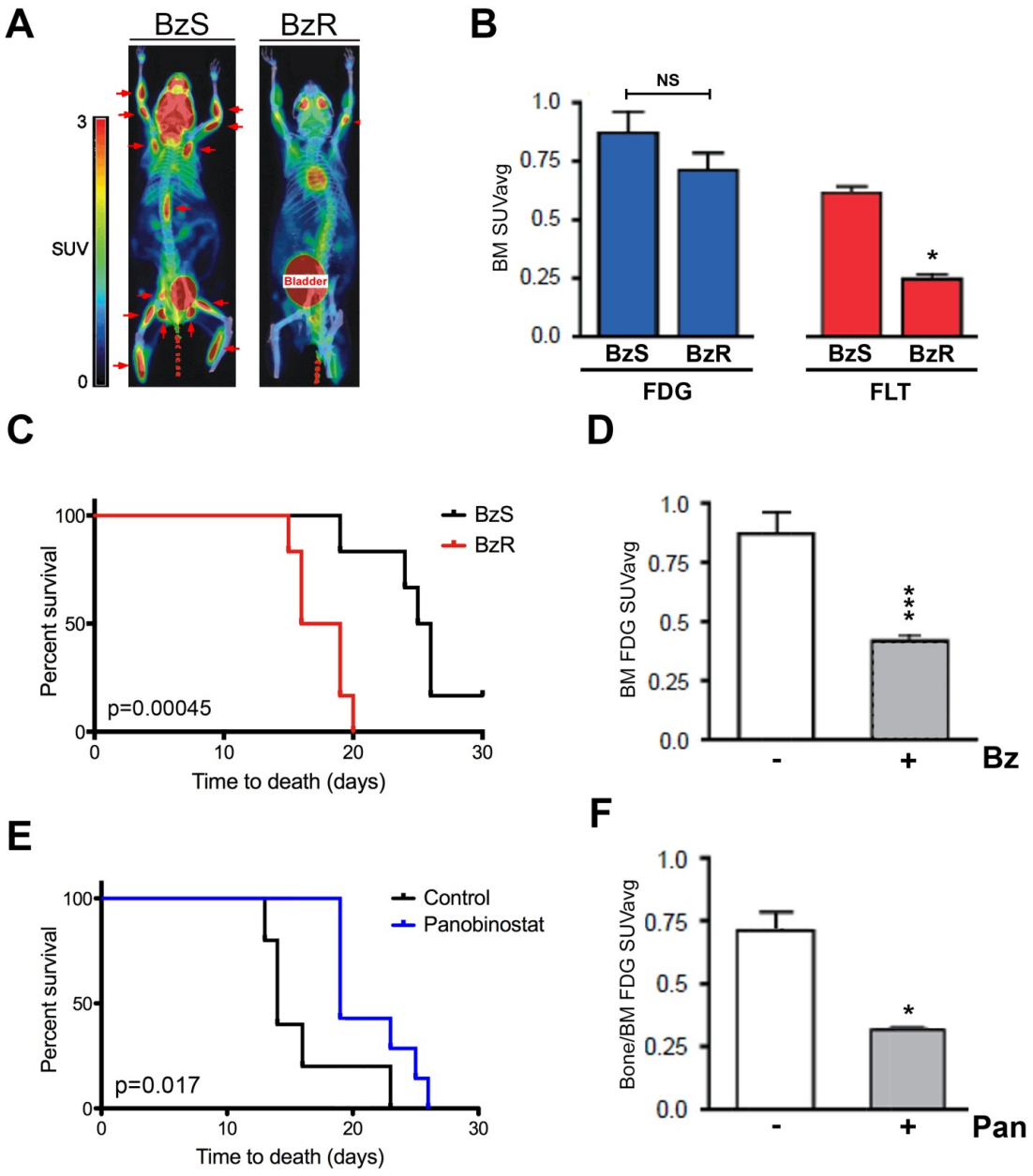
A
BzS
BzR
3
SUV
0
Bladder
B
NS
1.0
0.75
0.5
0.25
0.0
BM SUVavg
*
BzS
BzR
FDG
BzS
BzR
FLT
C
100
50
0
Percent survival
BzS
BzR
p=0.00045
0
10
20
30
Time to death (days)
D
1.0
0.75
0.5
0.25
0.0
BM FDG SUVavg
***
-
+
Bz
E
100
50
0
Percent survival
Control
Panobinostat
p=0.017
0
10
20
30
Time to death (days)
F
1.0
0.75
0.5
0.25
0.0
Bone/BM FDG SUVavg
*
-
+
Pan

Supplemental Figure S1. Mouse and human plasma cell lines respond to Bz *in vitro*. Kill curve analysis of A) 3 representative Bz-sensitive mouse cell lines (595, 589 and 638, left panel) and B) 2 human myeloma cell lines (U266 and MM1.S, right panel). Cell viability data were collected 48 hours post-treatment over a range of 0-128 nM Bz. All data points shown were normalized to untreated controls. Error bars, which are shown but are smaller than the data symbols, represent the standard deviation of triplicate reads over each experiment. Viable cell percentages in C) 2 representative BzS mouse cell lines following 24 hours of 66 nM bortezomib treatment, D) 2 representative, HMCLs following 24 hours of 33 nM bortezomib treatment, and E) 2 representative BzR mouse cell lines following 24 hours of 66 nM bortezomib treatment. Viable percentages are indicated (filled bars) relative to an untreated control (open bars) by trypan blue exclusion using a hemacytometer in triplicate.

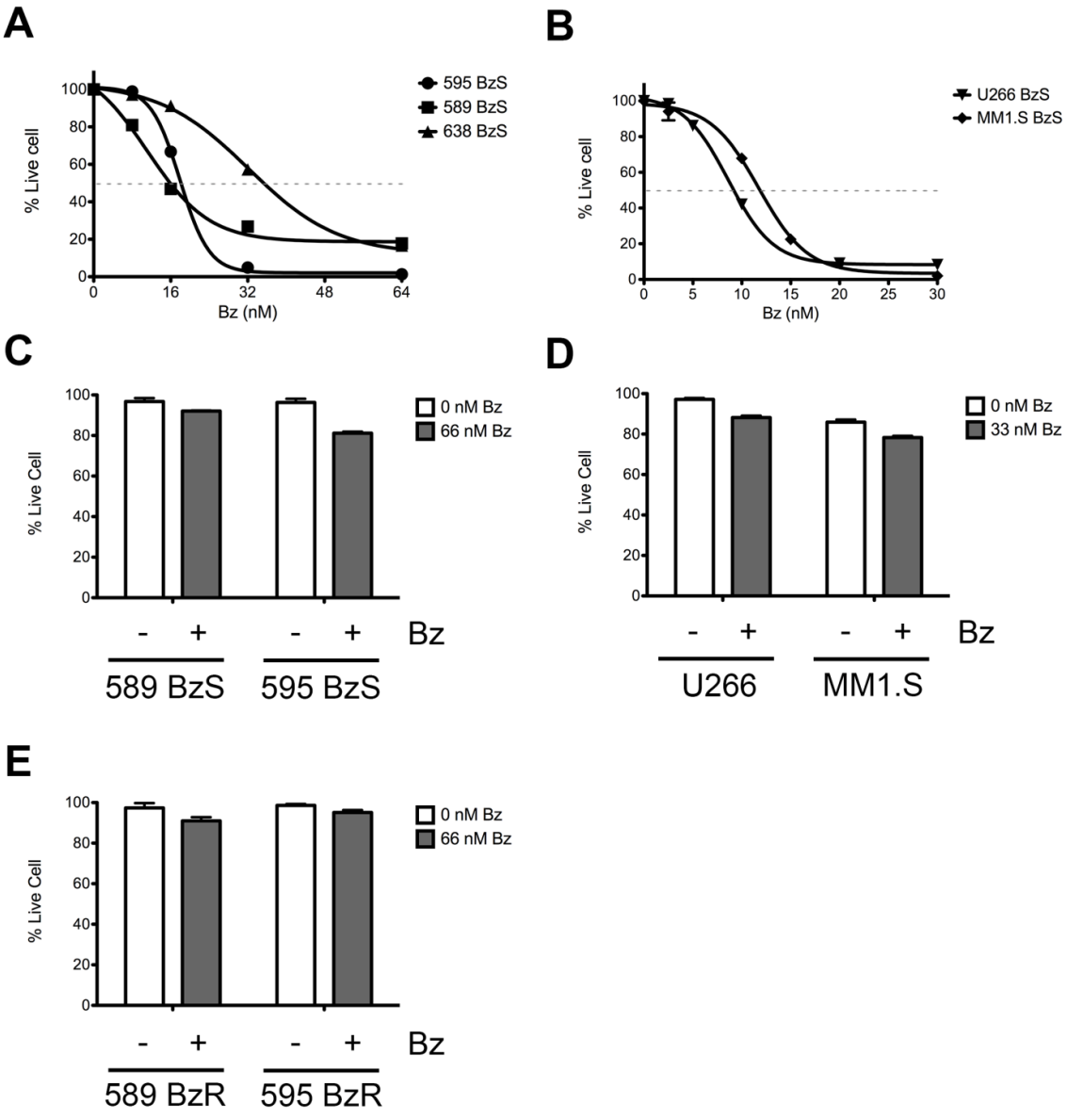
A
% Live cell
Bz (nM)
595 BzS
589 BzS
638 BzS
B
% Live cell
Bz (nM)
U266 BzS
MM1.S BzS
C
% Live Cell
0 nM Bz
66 nM Bz
- + - + Bz
589 BzS
595 BzS
D
% Live Cell
0 nM Bz
33 nM Bz
- + - + Bz
U266
MM1.S
E
% Live Cell
0 nM Bz
66 nM Bz
- + - + Bz
589 BzR
595 BzR

Supplemental Figure S2. Gene Set Enrichment Analysis (GSEA) shows enrichment between mouse *in vitro* and human *in vivo* data. A) Enrichment plot comparing the transcriptional response of the BzS cell lines *in vitro* with 66 nM Bz (24hr vs. 0hr) to the Shaughnessy, et al. 80 gene model patient data. The dashed line represents the enrichment score, and the filled arrow represents the leading edge genes contributing to this enrichment. B) Heatmap illustrating the kinetic response of the 29 leading edge genes over the course of 24 hour 66 nM Bz treatment in 3 BzS cell lines (595 in duplicate shown as 595.2). Mouse cells were collected at 0, 2, 8, 16 and 24 hours. Columns represent time points and rows represent genes. Columns are ordered firstly by cell line and secondly by ascending time; genes are ordered by hierarchical cluster analysis. Color indicates fold change which was determined for each gene and time point by comparing to the 0 hour time point.

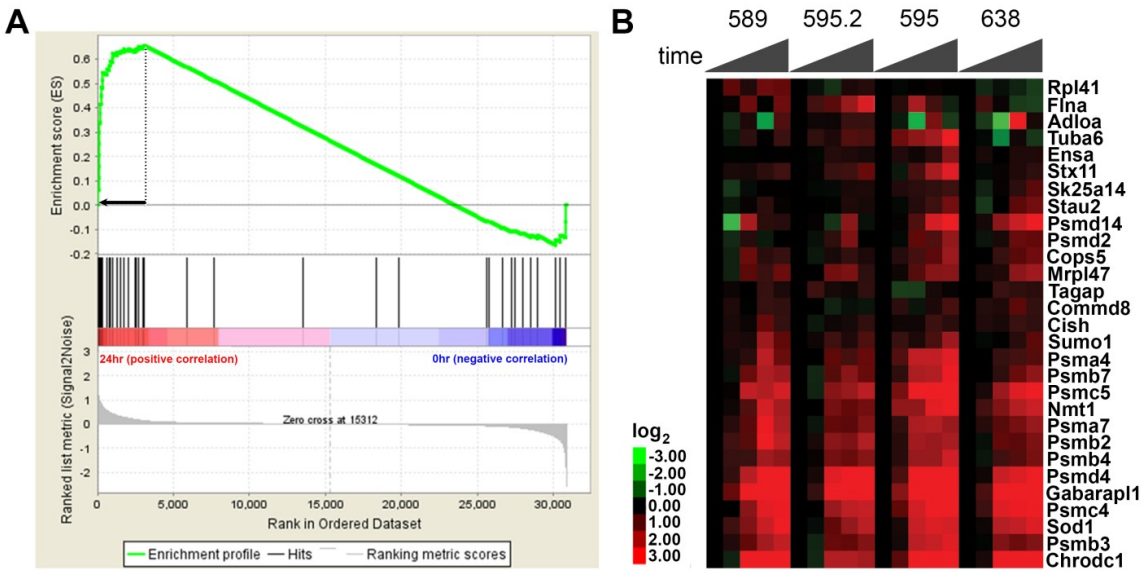
A
Enrichment score (ES)
0.6
0.5
0.4
0.3
0.2
0.1
0.0
-0.1
-0.2
Ranked list metric (Signal2Noise)
3
2
1
0
-1
-2
24hr (positive correlation)
0hr (negative correlation)
Zero cross at 15312
0
5,000
10,000
15,000
20,000
25,000
30,000
Rank in Ordered Dataset
Enrichment profile
Hits
Ranking metric scores
B
589
595.2
595
638
time
log2
-3.00
-2.00
-1.00
0.00
1.00
2.00
3.00
Rpl41
Flna
Adloa
Tuba6
Ensa
Stx11
Sk25a14
Stau2
Psmd14
Psmd2
Cops5
Mrpl47
Tagap
Commd8
Cish
Sumo1
Psma4
Psmb7
Psmc5
Nmt1
Psma7
Psmb2
Psmb4
Psmd4
Gabarapl1
Psmc4
Sod1
Psmb3
Chrodc1

Supplemental Figure S3. Baseline differences in BzS and BzR cells in the absence of drug. Proteasome activity assay of A) 595 and B) 589 BzS and BzR mouse cell lines in the absence of Bz. Open bars represent BzS lines and filled bars represent BzR lines for chymotrypsin-, trypsin- and caspase-like assays. All data points shown were normalized to their representative BzS line. Error bars represent the standard deviation of triplicate reads over each experiment, and statistical significance was determined using a two-tailed Student's t-test (** $p < 0.005$; *** $p < 0.0005$). C) Heat map of the 51 genes that differ significantly ($p < 0.05$, $|\text{fold change}| > 2$) in BzR cell lines (right) normalized to their BzS counterparts (left) in the absence of drug selection. Columns represent cell lines; rows represent the genes which are ordered by hierarchical cluster analysis. Genes in bold where those with a human homolog.

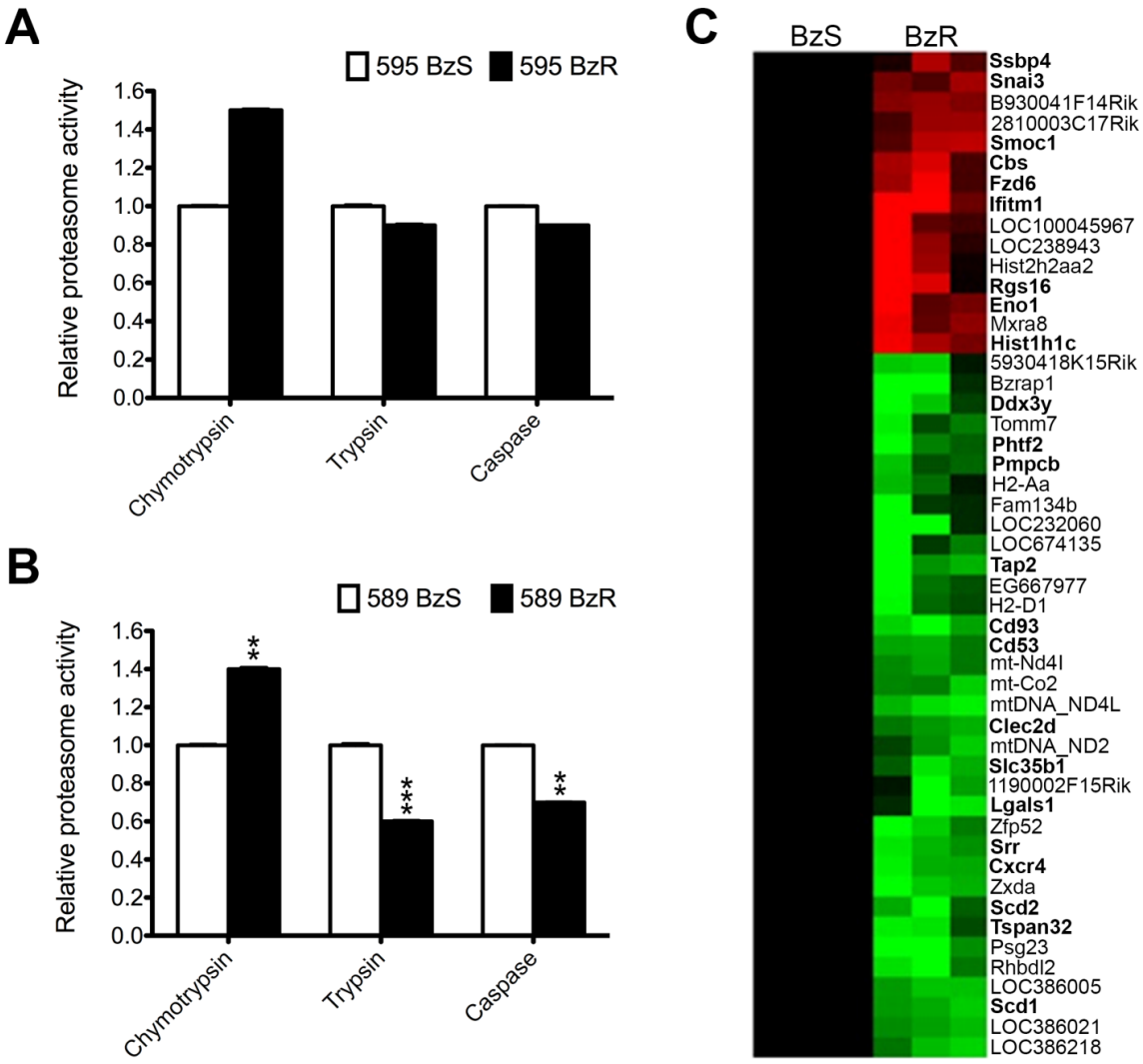
A
595 BzS
595 BzR
Relative proteasome activity
1.6
1.4
1.2
1.0
0.8
0.6
0.4
0.2
0.0
Chymotrypsin
Trypsin
Caspase
B
589 BzS
589 BzR
Relative proteasome activity
**
***
**
Chymotrypsin
Trypsin
Caspase
C
BzS
BzR
Ssbp4
Snai3
B930041F14Rik
2810003C17Rik
Smoc1
Cbs
Fzd6
Ifitm1
LOC100045967
LOC238943
Hist2h2aa2
Rgs16
Eno1
Mxra8
Hist1h1c
5930418K15Rik
Bzrap1
Ddx3y
Tomm7
Phtf2
Pmpcb
H2-Aa
Fam134b
LOC232060
LOC674135
Tap2
EG667977
H2-D1
Cd93
Cd53
mt-Nd4l
mt-Co2
mtDNA_ND4L
Clec2d
mtDNA_ND2
Slc35b1
1190002F15Rik
Lgals1
Zfp52
Srr
Cxcr4
Zxda
Scd2
Tspan32
Psg23
Rhbdl2
LOC386005
Scd1
LOC386021
LOC386218

Supplemental Figure S4. The analysis of BzS and BzR properties in vitro and *in vivo*. Quantitative RT-PCR of Ddit (CHOP) expression prior to ("-") or following ("+") 66 nM Bz (top panel) or 55 nM panobinostat (bottom panel) treatment for 24 hours. Open bars represent BzS lines and filled bars represent BzR lines. All data points shown were normalized to an untreated control mouse B cell lymphoma cell line, CH12 (not shown). Error bars represent the standard deviation of triplicate reads over each experiment, and statistical significance was determined using a two-tailed Student's t-test (* $p < 0.05$; ** $p < 0.005$; *** $p < 0.0005$). B) Representative hematoxylin and eosin stained bone marrow (50X with oil), liver (20X), spleen (50X with oil) and kidney (20X) sections from moribund 595 BzS (top panels) and BzR (bottom panels) cell-injected animals receiving vehicle treatment showing the presence or absence of malignant plasma cell infiltrates.

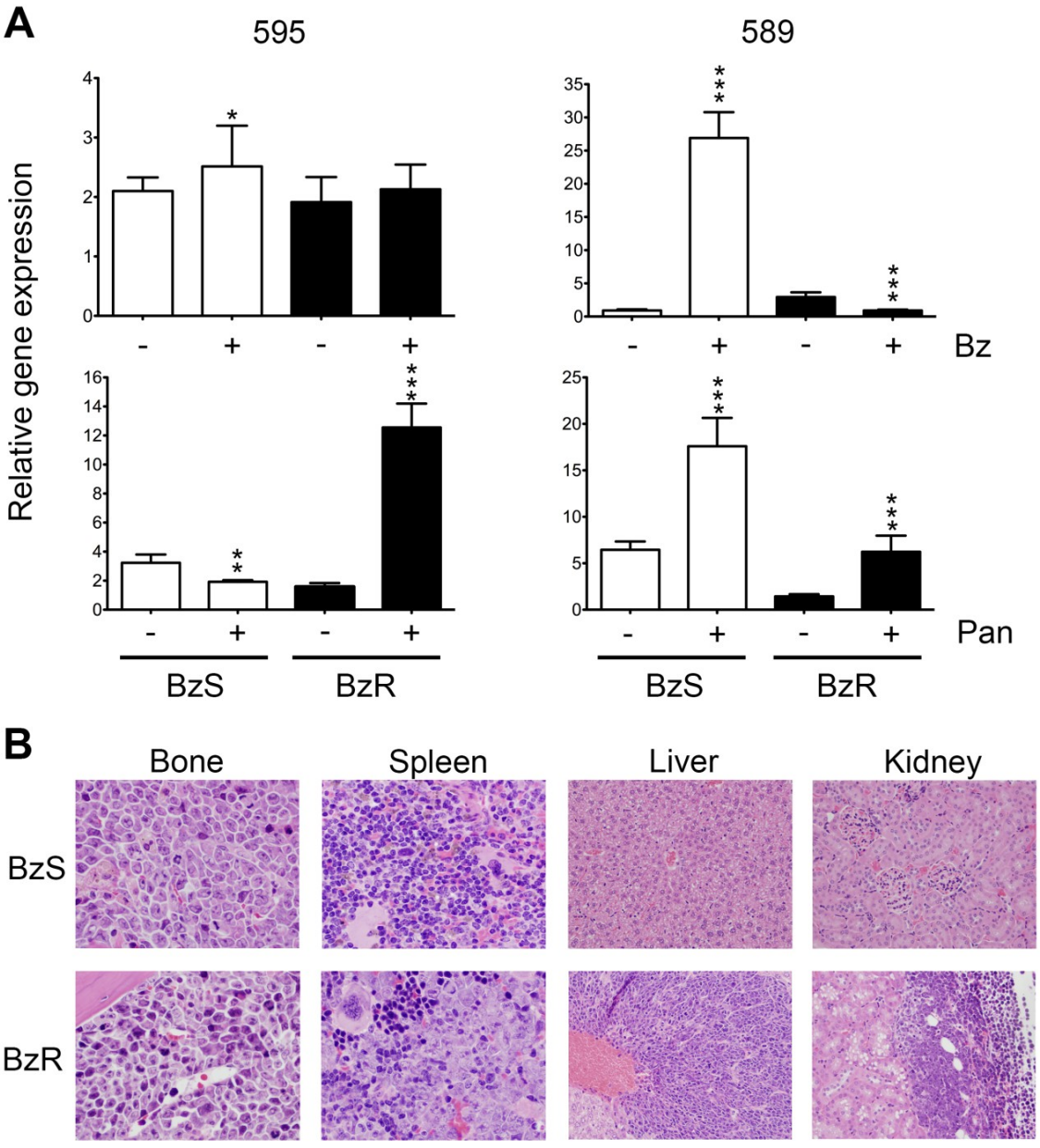
A
595
589
Relative gene expression
Bz
Pan
BzS
BzR
B
Bone
Spleen
Liver
Kidney
BzS
BzR

Supplemental Table S1. Significant Bz-responsive genes common to human and mouse corresponding to Figure 1B.

Gene Symbol
CD9
SLC7A7
ANKRD37
FOS
LDLR
AHNAK
IFI27
HVCN1
SELPLG
ACSS1
DBI
FAIM3
ITGB5
SIDT2
PON2
EBPL
MKI67
NUP210
CCND1
KLF13
PAFAH1B3

GALK1
LDHA
CYSLTR1
DHCR7
CD47
ICAM2
ATP2A3
OXCT1
CST3
CYBASC3
GLT25D1
SLC35B2
GUSB
TFRC
SLC5A6
TMEM109
SLC19A1
STT3A
SLC29A1
UNC93B1
CD52
COQ2

IDH2
RASSF4
MFNG
EVL
CALM2
STMN1
PRPS2
PLAC8
MAT2A
PDXP
SFRS7
SRM
CXCR4
TAP1
TLR7
TMEM51
ALDH18A1
CSTB
STARD5
TUBB2B
DDIT4
JUN

P4HA2
BLVRB
BSCL2
MAFG
ATF4
HSP90AA1
HSPA8
DNAJB1
HSPA1B
GADD45A
DEDD2
DDIT3
BAG3
ZFAND2A
DNAJB2
RNF181
GABARAPL1
TBC1D15
PSMC4
ATF5
IER3
NPLOC4
ADRM1

PSMC3
PSMD4
SQSTM1
GCLM
PSMD1
PSMC5
STK40
TTC1
YPEL5
HSPA1A
MLLT11
MVP
HSPB1
UCHL1
ATF3
CEBPB
TSC22D3
SARS
TRIB3
CYB5R1
SESN2
STIP1
EIF4EBP1

SNX10
GADD45G
KLF6
VIM
PSAT1
PSMD14
ST13
SGK1
VPS37B
EMP3
CBR3
KLF2
SLC2A3
SLC38A2
RHBDL2
S100A10
NDRG1
PIK3IP1
DUSP1
TOB1
STC2

Supplemental Table S2. Significant Bz-responsive genes corresponding to Figure 2C.

Gene Symbol
Maged1
Nploc4
Mlkl
Vcp
Zwint
Gclm
Psmd12
Tax1bp1
Wdr1
Ier3
Pdlim7
Bach1
Sod1
Psmc2
Atp6v1h
Psmd4
Hspb6
2500002L14Rik
Mad2l1bp
Oraov1
Ttc1

8430410K20Rik
scl0002315.1_12
Ufd1l
Whdc1
Ccdc77
Dnajb2
Slc25a38
Gch1
Mocs1
Rnf181
2310004I24Rik
2310004N11Rik
Nars
Napb
Cdr2
Dnajb1
Stip1
Hspa8
Chordc1
Hsp105
Rnu6
Prmt2

4930504E06Rik
Mvp
Tbc1d15
2310005E10Rik
LOC100047261
Mns1
Dedd2
Zyx
Bag3
Gadd45a
C130022K22Rik
Hspa1a
Hspa1b
Cebpb
1500012F01Rik
2410006H16Rik
Stx5a
Ddit3
Ypel5
Zfand3
Gtpbp2
LOC100045005

4932441N08Rik
Angptl6
Soat2
1110038B12Rik
E430031D18Rik
LOC100041797
2310005L22Rik
2810026P18Rik
Csprs
Mib2
Slc6a9
4930431B09Rik
Rassf1
Atf3
Myd116
Lpxn
Ypel3
Tubb6
Hsp90aa1
LOC100048105
Ubg
Fos
mtDNA_ND2
mtDNA_ND4L
mt-Nd4l

LOC381365
Idh2
LOC100044779
LOC207685
Plac8
LOC245892
LOC329750
Bhlhb8
Dbp
Pdk1
Ak3l1
Fam162a
IGLC2_J00595_Ig_la mbda_constant_2_14
Bcl11a
LOC386520
Psg23
Slc15a3
Retsat
3110056O03Rik
Car12
H2-DMa
Crlf1
Ltbp4
Cercam

Gm2a
Cyp51
Nrm
Cnp
Selpl
Selplg
Atp2a3
Pld4
Elovl6
9130415E20Rik
Cd47
Scd1
Prodh
Scd2
Cd22
Plxnb2
Abcd1
Cd93
Fcrla
Oxct1
Kcnn4
Napsa
Hvcn1
Ptprcap
Ifi30

LOC100047579
Cd72
Ahnak
Cst3
LOC669658
Tnni2
Ly6e
LOC100047815
Ng23
1700052O22Rik
LOC100044948
Ifi27
Slc35b2
1110001J03Rik
Grcc10
Clec2d
Tmem109
Camkv
Glt25d1
Gusb
Tfrc
Slpi
Mpeg1
Phtf2
Cybasc3

LOC100045882
Gcs1
Slc5a6
H2-Aa
Nola3
Coq2
Gcat
Vpreb3
9630015D15Rik
Eno3
2210411K11Rik
Arhgdig
Cd3g
Nudt19
Aars
Chac1
Trib3
Atf5
Nupr1
Hspb1
Cd151
Impact
Uchl1
Mllt11
Casp1

Psmc4
Psmc5
EG432448
Psmd1
Psmc3
Adrm1
Trafd1
Zfand2a
Rit1
Gabarapl1
Sqstm1
Ankrd37
Mist1
LOC100044439
B930041F14Rik
H2afx
Rsph1
1600014C23Rik
Hist1h2bf
Rgs16
Hist2h2aa1
Hist2h2aa2
2310039H08Rik
Macrod1
Slc7a3

BC028528	Atf4	Stk40
LOC630729	Glipr1	

Supplemental Table S3. Individual drug predictions by CMAP analysis.

			Correlation[c]		
Drug Family[a]	**Drug**	**Degree[b]**	595	638	589
Proteasome inhibitors and UPS modulators	disulfiram	++	+	+	+
	MG-262	+++	np	+	+
	mometasone	++	np	+	+
NFκB inhibitors	15-delta prostaglandin J2	++	+	+	+
	thiostrepton	++	+	+	np
	parthenolide	++	+	+	np
	withaferin A	++	+	+	+
HSP90 inhibitors	geldanamycin	++	+	+	np
	alvespimycin	++	+	np	+
	monorden	+	+	np	+
	tanespimycin	+	+	np	np
Protein synthesis inhibitors	puromycin	+++	+	+	+
	anisomycin	+++	np	+	+
	emetine	++	np	+	+
	cephaeline	+++	np	+	+
	cicloheximide	++	+	+	+
CDK/TopoI/TopoII/Cell cycle inhibitors	doxorubicin	– – –	np	-	-
	resveratrol	++	+	np	np
	camptothecin	– – –	np	-	np

	ellipticine	– –	np	-	np
	etoposide	– –	np	-	np
	mitoxantrone	– –	np	-	np
	harmine	– –	np	np	-
	luteolin	– –	np	np	-
	staurosporine	–	np	np	-
Sodium/calcium modulators and calcium channel blockers	tetrandrine	+	+	+	+
	gossypol	++	+	+	+
	econazole	++	+	+	np
	perhexiline	++	+	+	np
	clomifene	++	+	+	np
	bepridil	++	+	+	np
	felodipine	+	np	+	+
	nitrendipine	– –	-	np	np
	cyproheptadine	++	+	np	np
Na+/K+ - ATPase membrane pump inhibitors	helveticoside	++	np	+	+
	lanatoside C	++	np	+	+
	digoxin	++	np	+	+
	digitoxigenin	++	np	+	+
	digoxigenin	+	np	np	+
	strophanthidin	+	np	np	+

	ouabain	+	np	np	+
Antihistamines and Anticholinergics	terfenadine	+++	+	+	+
	astemizole	++	+	+	np
	proadifen	++	+	np	+
	spiperone	++	np	+	+
	atropine	– –	np	np	-
	mefloquine	++	+	np	+
	clemastine	++	np	+	np
Microtubule inhibitors	mebendazole	++	+	+	np
	nocodazole	++	+	np	+
	fenbendazole	++	+	+	np
Alkylating agents	semustine	++	+	+	+
	lomustine	++	+	+	np
PI3K inhibitors	LY-294002	++	+	np	np
HDAC inhibitors	trichostatin A	++	+	np	np
	vorinostat	++	+	np	np
	rifabutin	++	+	np	np
	scriptaid	++	+	np	np
	valproic acid	++	+	np	np
Antipsychotics	thioridazine	++	+	+	np
	prochlorperazine	++	+	+	np
	pimozide	++	+	+	np
	fluphenazine	++	+	+	np
	Metergoline	++	+	np	np

	chlorcyclizine	+	+	+	np
	trifluoperazine	++	+	+	np
	metixene	++	np	np	+
	cloperastine	++	+	np	np
	perphenazine	++	+	np	np
	thioproperazine	++	+	np	np
Antidepressants	desipramine	++	+	+	np
	doxepin	++	+	np	np
	norcyclobenzaprine	++	+	np	np
	imipramine	++	+	np	np
Antivirals	mycophenolic acid	– –	np	-	-
	methotrexate	–	np	-	np

[a]Drugs families determined from previous literature (411).

[b]Indicates the degree to which a drug is positively or negatively correlated (by correlation score output from CMAP) calculated as the average correlation score across the 3 lines where: |0-0.33| = +/-; |0.34-0.66| = ++/--; |0.67-1| = +++/---.

[c]Output given by CMAP indicating the relatedness of the input profile to the database profile where "–" is a strong opposite response and "+" is a strong similar response by gene expression profiling. "np" indicates that no prediction was made for this drug in this cell line. Prediction are significant with a $p < 0.05$.

Supplemental Table 4. Genes driving HDACi predictions[a] by CMAP in mouse cell lines.

Genes Symbol	DCTD	CKB
ANP32A	USP1	ENO2
NCBP2	UMPS	EMP1
PWP1	DTYMK	MVP
CTCF	STC2	TAP1
CTPS	PDCD2	TRAFD1
CAD	GEMIN4	GMPR
TMPO	PPP1R8	RAB11FIP5
COIL	UCK2	LMNA
RCC1	LMNB2	GNS
IFRD2	USP16	GM2A
COQ7	NIP7	RNASE4
MCM7	POLR3B	SLC2A14 /// SLC2A3
SUV39H1	TSEN2	
TTC27	SETD6	NAGK
MRTO4	IPP	ABCA7
PEX14	PPAN	PLEKHO2
MBD3	PSAP	STK17B

[a]Genes shown were common to the trichostatin A and vorinostat predictions uniquely in the 595 cell line made available through the CMAP portal.

CHAPTER 4

IDENTIFIATION OF NOVEL DRUG COMBINATIONS TO COMBAT BORTEZOMIB-RESISTANT MYELOMA BY *IN SILICO* AND HIGH-THROUGHPUT SCREENING APPROACHES

Holly A. F. Stessman[1], Amit Mitra[1], Amriti Lulla[2], Taylor Harding[1], Aatif Mansoor[1], Brian G. Van Ness[1]*, Nathan G. Dolloff[2]*

From the [1]Department of Genetics, Cell Biology and Development, University of Minnesota, Minneapolis, MN and the [2]Department of Medicine, Penn State Hershey Medical Center, Hershey, PA, USA.

*Co-corresponding authors

Supported by Millennium Pharmaceuticals: The Takeda Oncology Company and Onyx Pharmaceuticals.

AUTHOR CONTRIBUTIONS

H. A. F. S. coordinated studies, designed and performed *in vitro* experiments, and designed figures.

A. M. performed *in vitro* experiments.

A. L. performed *in vitro* experiments.

T. H. performed *in vitro* experiments and analyzed drug synergy data.

A. M. performed *in vitro* experiments and analyzed drug synergy data.

N. G. D. designed and performed all HTS experiments.

B. G. V. N. contributed to the design and oversaw all studies.

ABSTRACT

Bortezomib/VELCADE® (Bz) is a proteasome inhibitor that has been used successfully in the treatment of multiple myeloma (MM) patients. However, acquired resistance to Bz is an emerging problem. Thus, there is a need for novel therapeutic combinations that enhance Bz sensitivity or re-sensitize Bz resistant MM cells to Bz. The Connectivity Map (CMAP; Broad Institute) database contains treatment-induced transcriptional signatures from 1,309 bioactive compounds in 4 human cancer cell lines. An input signature can be used to query the database for correlated drug signatures, a technique that has been used previously to identify drugs that combat chemoresistance in cancer. In this study we used *in silico* bioinformatics screening as well as a high-throughput drug screening assay system to compare pairs of isogenic Bz sensitive and resistant mouse cell lines derived from the iMycCα/Bcl-x_L mouse model of plasma cell malignancy, to identify compounds that combat Bz resistance. The intersection of these two approaches provided evidence that topoisomerase inhibitors may in fact target Bz-resistant MM cells and re-sensitize them to Bz. Indeed, we found that multiple topoisomerase inhibitors were significantly more active against Bz-resistant than Bz-sensitive cells as single agents and restored sensitivity to Bz when combined with Bz as a cocktail regimen. This work demonstrates the potential synergy of these approaches for identifying novel therapeutic combinations that may overcome Bz resistance in MM. Furthermore, it identifies topoisomerase inhibitors, drugs that are already approved for clinical use, as agents that may have utility in combating Bz resistance in refractory MM patients.

INTRODUCTION

Bortezomib/VELCADE® (Bz) is a proteasome inhibitor (PI) that has been used successfully in the treatment of the malignant plasma cell malignancy, multiple myeloma (MM). Despite the recent success of Bz therapy, MM is still incurable due in part to the emergence of Bz-resistant cells in the majority of patients, which likely contributes to the fact that only 41% of patients survive past 5 years (67). Bz is often used in combination with other drugs to target and kill malignant plasma cells in patients (412); however, the pool of therapeutic options available for cocktail regimens remains limited. Thus, there is a need for novel therapeutic combinations that enhance Bz sensitivity and/or target Bz-resistant MM cells to maximize the efficacy of the combination therapy approach.

The Connectivity Map (CMAP; Broad Institute) database provides an *in silico* platform for drug discovery (391, 413) that has been previously used to identify cancer salvage therapies (392). This database contains treatment-induced transcriptional signatures from 1,309 bioactive compounds in 4 human cancer cell lines. An input signature can be used to query the database for correlated or anti-correlated drug signatures. A correlated (+) connectivity score indicates pathways that are likely targeted by the drug of interest used to create the input signature, whereas an anti-correlated (-) score could have two interpretations: 1) this could indicate simply that this pathway is inversely regulated by the drug of interest or 2) this could be interpreted as a difference in pathway regulation between two disease states if a paired transcriptional analysis was used to crease the input signature. Although early studies explored primarily the predictive value of correlated signatures (392, 414), a recent push has been made to decipher the value of anti-correlated drug predictions (415, 416).

Recent analysis of the differential transcriptional response in isogenic pairs of Bz-sensitive and derived Bz-resistant mouse cell lines showed that treatment of the Bz-sensitive line correlated with genes expression profiles (GEPs) of drugs that target the proteasome, NF-κB, HSP90 and microtubules, as indicated by positive connectivity scores using the CMAP approach (Chapter 3, Table 2). Defining the mechanism of action for a drug is a well-described function of this *in silico* approach (417) and here displays a proof-of-principle. However eight compounds, all classified as topoisomerase (Topo) I and/or II inhibitors, were negatively correlated to the same input signatures by CMAP analysis (Chapter 3, Supplemental Table 3) (418). Because the input signature, in this case, was a comparison of the response to Bz in Bz-sensitive versus resistant cells lines, the negative connectivity score here could be interpreted as 1) an upregulation of Topos by Bz treatment in Bz sensitive lines, which has been previously reported (419) or 2) as an inhibition of Topos in Bz resistant cells upon Bz treatment.

In this study we investigate whether Topo inhibitors, as negatively predicted drugs by the CMAP approach, may be viable candidates for secondary therapy in Bz-resistant MM. By merging *in silico* CMAP data with a high throughput drug screening (HTS) assay system, we identify that Topo inhibitors may synergize with Bz for greater killing of Bz-resistant cells. In addition, a new compound was identified through the high-throughput drug screening approach that is highly effective at killing Bz-resistant cells.

MATERIALS AND METHODS

Mouse and human plasma cell lines. The mouse cell line pairs 595 and 589 were cultured in CST media as previously described (418). The human myeloma cell lines MM1.S and U266 (obtained from ATCC) and their BzR counterparts were maintained in HMCL media: RPMI 1640 (Lonza) supplemented with 15% fetal bovine serum (Cellgro), 50 μmol/L beta-mercaptoethanol (Sigma-Aldrich), 50 units/ml of penicillin and streptomycin (Hyclone), and 2 mmol/L $_{L}$-glutamine (Life Technologies).

Drugs and treatment conditions. Bortezomib (Bz) (Millennium Pharmaceuticals) was dissolved in serum-free RPMI-1640 (Lonza) and stored at -80°C. MLN2238 (Millennium Pharmaceuticals), carfilzomib (Onyx Pharmaceuticals), camptothecin (CPT), CPT-11, topotecan and teniposide (all from Selleck Chemicals) were dissolved in dimethyl sulfoxide (DMSO) (Sigma-Aldrich); all drugs were stored at -20°C.

Bortezomib resistant (BzR) MM1.S and U266 cells were generated by dose escalation of Bz over 4 months by once weekly treatment with Bz starting at 5 nM; the Bz concentration was increased by 5 nM every 2 weeks for the MM1.S line and every 4 weeks for the U266 line.

Cell viability assay. Cells were seeded at a concentration of $4x10^5$ cells per mL. After 24 hours the cells were treated with the indicated concentrations of drug(s) for 48 hours. Cell viability was measured by CellTiter-Glo® Luminescent cell viability assay according to manufacturer's instructions (Promega) using the Synergy 2 Microplate Reader (Biotek). Values were normalized to untreated controls and IC_{50} values were estimated by calculating the nonlinear regression using the sigmoidal dose-response equation (variable slope) in GraphPad (Prism). Drug synergy was determined by calculating the combination index (CI) value for each drug combination using Chou-Talalay

methodology which has been previously described (420). The dose reduction index (DRI) was calculated using Compusyn software (ComboSyn, Inc.).

Flow cytometric analysis. To detect intracellular cleaved caspase 3, BzS and BzR cells were treated with either 0-100 nM Bz or media for 48 Bz. The cells were then fixed using the Cytofix/Cytoperm Fixation/Permeabilization kit (BD Biosciences), blocked in buffer containing 30% FBS, 0.1% Saponin and 20 mM HEPES, and stained using an anti-caspase 3 antibody (BD Pharmingen). Samples were analyzed using an EPICS Elite (Beckman Coulter) and are presented as relative to the media-treated controls.

High-throughput drug screening assay. Screening was conducted using the NCI Diversity Set II small molecule chemical library of ~1500 compounds that were selected for their broad structural diversity and drug-like properties. One pair (595) of isogenic BzS and BzR mouse cell lines was used to query this library. Cells were seeded at a density of $3x10^4$ cells per well of a 96-well plate. Compounds were screened at 5 μM final concentration for a duration of 48 hours, after which cell viability was measured using CellTiter-Glo® Luminescent cell viability assay according to manufacturer's instructions (Promega). Three groups were incorporated into the screening: (1) BzS cells were treated with single-agent Diversity Set compounds to identify compounds with general anti-MM activity; (2) BzR cells were treated with single-agent Diversity Set compounds to identify compounds with greater activity in BzR cells than in the BzS cells; (3) BzR cells were treated with a combination of Diversity Set compounds in the presence of 25 nM Bz to identify compounds that re-sensitize resistant cells to Bz. Bz was added to one of the blank wells as an internal standard on each plate. For analysis, the luminescent signal from the untreated 4 corner wells of each plate were averaged and set as 100%. All other viability scores were reported relative to these controls.

Positive hits were verified in follow-up cell viability assays that were performed using triplicate wells. The false positive rate for the screening was ~25%.

RESULTS

Based on previously reported CMAP data (418), we queried an isogenic pair of mouse Bz-sensitive (BzS) and -resistant (BzR) cell lines against the NCI Diversity Set II small molecule library (421) to identify drugs with overlapping sensitivity profiles using both *in silico* and screening approaches. We hypothesized that common drug "hits" would be highly effective in combination with Bz for the treatment of Bz refractory disease. The BzS cells were tested against the single-agent drug library and the BzR cell lines were tested under two conditions, 1) against the single-agent library and 2) against the library in the presence of 25 nM Bz (the concentration at which only approximately 10% of these cells are killed after 48 hours of exposure as evidence by caspase-3 cleavage (Figure 1)).

Drug library screening provided multiple compounds of interest that had varied patterns of efficacy. While some drugs showed equal sensitivity across all tests suggesting no synergy with Bz, still others showed only synergy with Bz or even antagonism despite superb single-agent activity in BzS and BzR cell lines. However, we were most interested in those drugs that showed increased sensitivity in the BzR cell lines and synergy with Bz (Figure 2A). Interestingly, three of the top four drug library candidate drugs for potential BzR salvage were Topo inhibitors. Camptothecin (CPT) and teniposide both displayed patterns of increased sensitivity in the BzR cell line and synergy in combination with Bz (Figure 2B). Given that CMAP also predicted Topo inhibitors through anti-correlated gene expression signatures in this mouse model system of Bz-resistance (Chapter 3, Supplemental Table 3) (418), we chose to evaluate Topo inhibitors for efficacy in refractory MM further.

Two representative and previously-described pairs of BzS and BzR isogenic mouse cell lines (Chapter 3) (418) were used to determine IC_{50} values for each of four clinically-relevant Topo inhibitors: CPT, CPT-11, topotecan, and teniposide. Three of the four Topo inhibitors tested had consistently greater single-agent efficacy in the BzR cell lines than their BzS counterparts (Table 1) even though the rates of growth between cell line pairs were similar (data not shown). Only CPT-11 did not share this pattern having greater efficacy in the 595 but not the 589 BzR cell line (Table 1). Two agent kill curves were then performed to identify the most synergist combinations of Topo inhibitors and proteasome inhibitors.

For each drug duo (PI + Topo inhibitor) five concentrations of each drug were used. Each concentration combination was plated in a separate cell culture well creating a 25-well grid which included the range of single-agent wells for each drug and all two-agent combinations. Cell viability for each well was determined after 48 hours of drug treatment, and these data were used to calculate the faction of affected (Fa) cells at each single-agent and combination treatment. To assess drug synergy, Chou-Talalay plots (420) were created using these Fa values for each PI (Bz, carfilzomib or MLN2238) combined with each of the four Topo inhibitors (CPT, CPT-11, Topotecan, or teniposide). This analysis provides a metric of drug synergy termed the combination index (CI) score where a CI of < 1 is considered synergistic and a CI > 1 is considered antagonistic (420). Interestingly, although the BzR cell lines display general cross-resistance to the next-generation PIs, MLN228 and carfilzomib/KYPROLIS®, all three PIs showed synergy with the Topo II inhibitor, teniposide in these cell lines (Figure 2C). This is illustrated by CI values that are less than 1 through much of each dataset (Figure 2C).

Using these CI values together with the single-agent data, we were further able to extrapolate whether, due to synergy, the dosage of PIs may be reduced in the presence of teniposide for optimal killing. This dose reduction index (DRI) is calculated using the fixed IC_{50} concentration of the PI inhibitors (Bz, carfilzomib, or MLN2238) over the range of teniposide concentrations (422). We find, in some cases, that PI IC_{50} concentrations (Table 2) may be reduced as much as 95% in the presence of teniposide to achieve an Fa=0.5 (*i.e.* 50% death) (Table 2). Validation of this dose reduction index (DRI) for the most synergist combination concentrations are currently underway as are the companion drug synergy studies using Bz-sensitive and derived Bz-resistant human myeloma cell lines. Activity assays will also be required to further define the mechanism(s) behind this synergy. Finally, *in vivo* experiments will be used to validate this response and explore the translational applicability of this approach.

In addition to well-described drugs, the Diversity Set II drug library also contains multiple compounds whose functions are currently unknown. Interestingly, one of these compounds showed modest yet significant single agent activity in the mouse Bz-resistant cell line and potent synergy when combined with Bz. These results were confirmed using additional Bz-resistant mouse (589) and human (MM1.S and U266) cell line pairs. We have named this compound Velcade Re-sensitizing Compound 2 (VRC2). Importantly, IC_{50} values for VRC2 in normal mouse and human fibroblasts were 100-fold higher than those observed in malignant human and mouse plasma cells (data not shown), suggesting that this drug may have a low toxicity profile *in vivo*. We are currently evaluating the activity of VRC2 in animal models of MM, alone and in combination with Bz. We are also utilizing kinetic gene expression profiling and yeast screening assays to

establish the precise mechanism of action for VRC2. However, these preliminary data suggest that VRC2 may have clinical relevance in Bz-refractory MM.

DISCUSSION

In this study, we used complimentary *in silico* and high-throughput drug screening methods to identify drug families that may be effective in target Bz-refractory MM cells. The intersection of these approaches revealed that Topo inhibitors might be useful for this purpose. Not only did many Topo inhibitors display increased single-agent sensitivity in Bz-resistant cell lines compared to their Bz-sensitive counterparts, but this activity appears to be synergist with Bz modes of action. Indeed, Congdon *et al.* reported that treatment of a human MM cell line with Bz results in increased Topo expression and double-strand DNA breaks, which led to increased sensitivity to a Topo inhibitor (419). Therefore, a thorough assessment of the baseline DNA-damage, Topo activity, and Topo expression in Bz-sensitive and -resistant cell lines may be required to elucidate the mechanism behind our observed PI and teniposide synergy further.

Interestingly, a number of Topo inhibitors are already used in the clinic for the treatment of cancer (423). These drugs fall generally into two categories, Topo I or Topo II inhibitors, depending on their protein target. Although the function of topoisomerases is to relieve DNA supercoiling during replication and transcription, the mechanism by which this occurs between Topo classes varies. Human Topo I (TOP1) binds and generates single-stranded breaks in the DNA allowing the cleaved strand to rotate around the opposite strand and recruits repair proteins to re-ligate the backbone (424). The Topo II complex (TOP2A/B) performs a similar function but through the creation of double-strand breaks in the DNA (425). Topo inhibitors function by inhibiting the disassociation of the Topo proteins from the DNA strand after supercoiling is relieved. Hindrance from the Topo protein stops ligation from occurring resulting in unresolved DNA breaks that trigger apoptosis (419). TOP1 inhibitors include camptothecin (CPT)

and its derivatives CPT-11 and topotecan, whereas teniposide inhibits TOP2A/B. Furthermore, a number of approved MM drugs, (*i.e.* etoposide and doxorubicin) have Topo II inhibiting properties (426). The use of newer Topo inhibitors has been proposed for refractory MM, however, this was prior to the approval and widespread use of Bz (427, 428). Notably, these data suggest that newer Topo inhibitors may be especially effective for the treatment of Bz refractory MM.

One potential caveat of utilizing Topo inhibitors may be the presence of UGT1A1*28 variants which are present in as high as 37.5% of some patient populations (429). The UGT1A1*28 variant has been associated with changes in the metabolism of CPT-11 and adverse events related to treatment (*i.e.* bone marrow toxicity) of patients (429). UGT1A1 genotyping is currently available and recommended by the FDA for CPT-11 use, however, testing has yet to be fully implemented in the clinic (430).

Finally, these studies illustrate the utility of combined approaches for drug discovery to combat refractory MM. Interestingly, we have identified both well-described (Topo inhibitors) and novel compounds of interest (VRC2) to this effect. Furthermore, the availability of additional libraries including the FDA-Approved Oncology Drug Library (from the NCI Developmental Therapeutics Program) means that drug repurposing may be utilized successfully by this methodology. Given the severe side effects (*i.e.* peripheral neuropathy) that can be associated with Bz treatment (431), the identification of drugs that can significantly reduce the concentrations of Bz required for the same effect may have tremendous clinical utility. In this case, we used these combined approaches to identify drugs that are capable of re-sensitizing Bz-resistant cells to Bz *in vitro*, outlining a potentially useful pre-clinical pipeline for the treatment of refractory disease.

Table 1. Single-agent IC_{50} comparison of Bz-sensitive and -resistant mouse cell lines.

Drug	595BzS	595BzR	Log (fold change)[a]	589BzS	589BzR	Log (fold change)[a]
Bortezomib, nM	23	112	2.3	22	96	2.1
MLN2238, nM	28	154	2.5	39	180	2.2
Carfilzomib, nM	28	71	1.3	41	77	0.9
Camptothecin (CPT), μM	> 15	0.8	-4.3	0.7	0.6	-0.2
CPT-11, μM	44	35	-0.3	33	20	-0.7
Topotecan, μM	> 15	0.8	-4.3	0.8	0.6	-0.3
Teniposide, μM	3	0.6	-2.3	0.2	0.05	-1.7

[a]IC_{50} value of the BzR relative to the BzS cell line.

Table 2. Drug reduction index for decreasing PI concentrations.

Drug combination	Cell line	% Reduction[a]
Cz + Teniposide	589 BzS	N/A
	589 BzR	92
	595 BzS	N/A
	595 BzR	42
MLN2238 + Teniposide	589 BzS	45
	589 BzR	75
	595 BzS	71
	595 BzR	95

[a]Percent reduction in PI concentration that can be used to obtain the same IC_{50} in combination with teniposide compared to the PI alone.

Figure 1. Cell death by Bz is associated with caspase 3 cleavage.

Flow cytometric analysis of BzS (gray bars) and BzR (black bars) cells treated with a range of 0-100 nM Bz for 48 hours stained with a cleaved caspase 3 antibody. All treatment data shown were normalized to untreated controls.

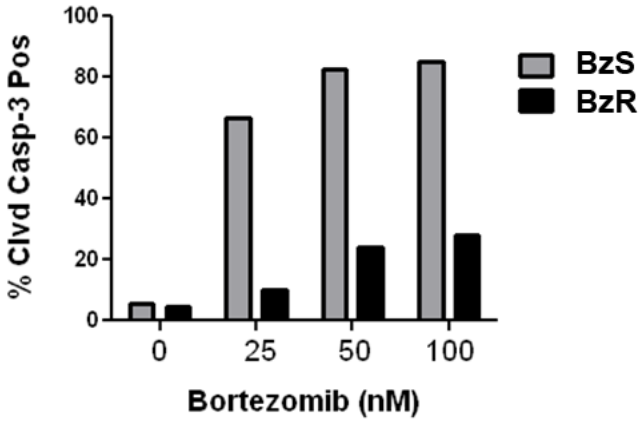
% Clvd Casp-3 Pos
100
80
60
40
20
0
0
25
50
100
Bortezomib (nM)
BzS
BzR

Figure 2. Drug screening identifies topoisomerase inhibitors as candidate drugs for Bz synergy.

High-throughput drug screening independently identifies topoisomerase inhibitors as potentially effective secondary therapies in Bz-resistant mouse lines. A) The NCI Diversity Set II of approximately 1,800 small molecules was screened using one pair (595) of isogenic BzS (grey bars) and BzR (black bars) mouse cell lines. The library was screened for single-agent activity (5 μM concentrations used). In addition to screening for single-agent sensitivity, the BzR line was screened with the same compounds in the presence of 50 nM Bz (red bars) for synergistic combinations. Of the top drug hits, two were Topo inhibitors, camptothecin (CPT) and teniposide. Cell viability was measured in triplicate and is shown as a percent of the control. C) Chou-Talalay (420) combination index (CI) plots for two independent mouse BzR cell lines (595 on the left, 589 on the right) for the combination of the Topo inhibitor, teniposide, with either Bz (top), carfilzomib (middle) or MLN2238 (bottom). Cell viability was measured in triplicate at each drug combination following 48 hours of treatment *in vitro*. The fraction of affected cell (Fa) is indicated on the X-axis and the log(CI) on the Y-axis. Combination index values (CI) < 1 are considered synergist combinations.

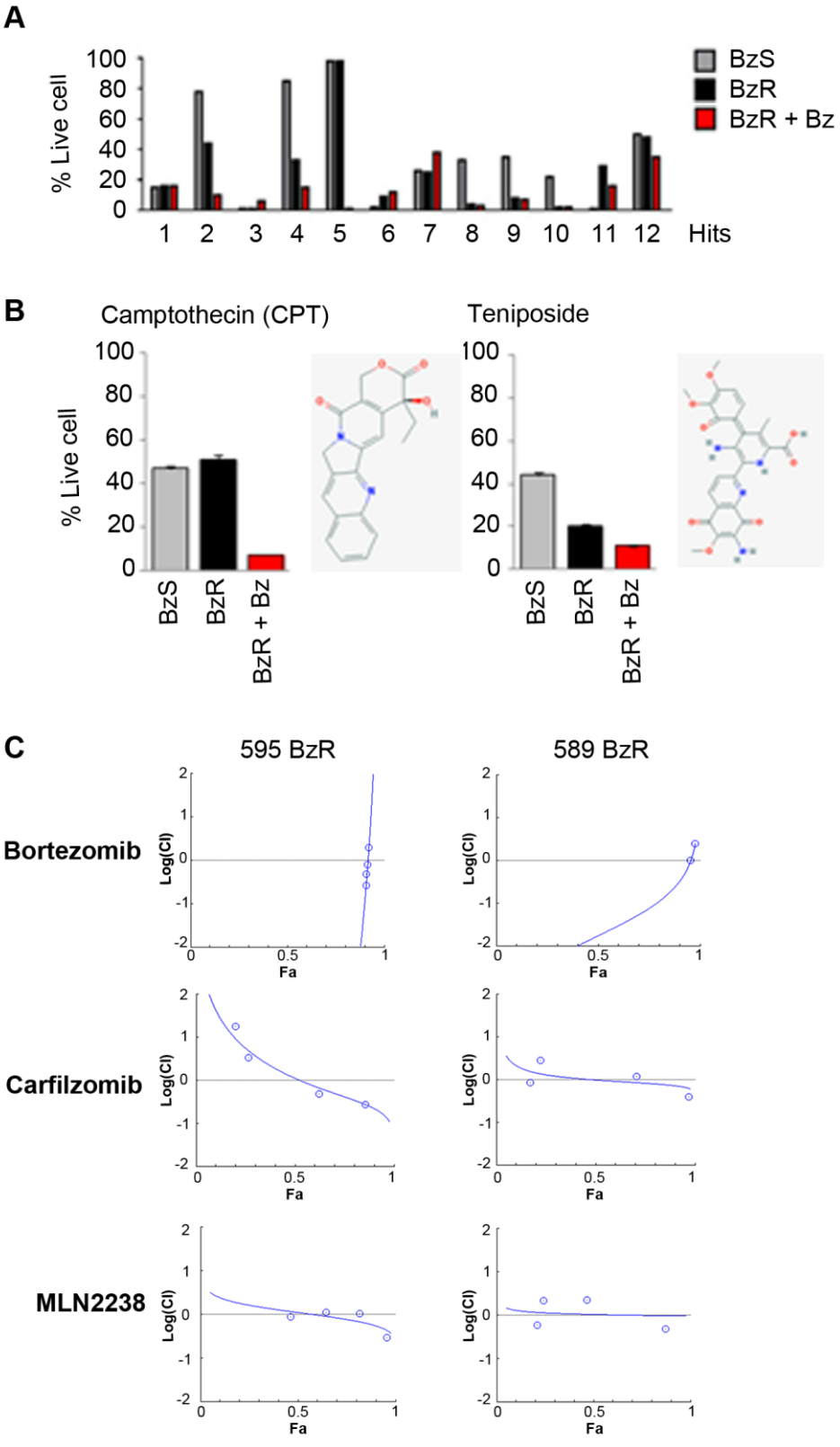
A
% Live cell
100
80
60
40
20
0
1 2 3 4 5 6 7 8 9 10 11 12
Hits
BzS
BzR
BzR + Bz
B
Camptothecin (CPT)
Teniposide
% Live cell
BzS
BzR
BzR + Bz
C
595 BzR
589 BzR
Bortezomib
Carfilzomib
MLN2238
Log(CI)
Fa

CHAPTER 5

LOSS OF PLASMA CELL COMMITMENT CONFERS BORTEZOMIB RESISTANCE IN A MOUSE MYELOMA MODEL

Holly A. F. Stessman[1], Aatif Mansoor[1], Aaron L. Sarver[2], Fenghuang Zhan[3], Guido Tricot[3], Siegfried Janz[4], Michael A. Linden[5], Brian G. Van Ness[1,*], Linda B. Baughn[1,*]

From the [1]Department of Genetics, Cell Biology and Development and [2]Masonic Cancer Center Bioinformatics Support and Services, University of Minnesota, Minneapolis, MN, USA; [3]Department of Internal Medicine, Division of Hematology, Oncology, and Blood & Marrow Transplantation and [4]Department of Pathology, The University of Iowa Roy J. and Lucille A. Carver College of Medicine, Iowa City, IA, USA; [5]Department of Laboratory Medicine and Pathology, University of Minnesota, Minneapolis, MN, USA.

[*]Co-corresponding authors

Supported by Millennium Pharmaceuticals: The Takeda Oncology Company and University of Minnesota Grant-In-Aid. Cytogenetic analyses performed at the University of Minnesota Cytogenetics Core Laboratory with support from the Masonic Cancer Center Grant P30CA077598-09 and flow cytometry was performed at the Flow Cytometry Core Facility of the Masonic Cancer Center supported by P30CA77598. The PET imaging was supported by P30CA086862 from the NCI.

Manuscript submitted for publication.

AUTHOR CONTRIBUTIONS

H. A. F. S. coordinated studies, designed and performed *in vitro* experiments, and wrote the manuscript[Ψ].

A. M. performed *in vitro* experiments, designed the figures, and contributed to writing the manuscript.

A. L. S. analyzed the mouse GEP data.

F. Z. analyzed all human clinical trial data.

G. T. contributed clinical trial data.

S. J. oversaw *in vivo* experiments and edited the manuscript.

M. A. L. edited the manuscript

B. G. V. N. contributed to the design and oversaw all studies and contributed to writing the manuscript.

L. B. B. contributed to the design, oversaw the project, performed *in vitro* experiments, and wrote the manuscript[Ψ].

[Ψ]These authors contributed equally to writing this manuscript.

ABSTRACT

Multiple myeloma (MM), the second most common hematopoietic malignancy, remains an incurable plasma cell (PC) neoplasm. While the proteasome inhibitor, bortezomib (Bz) has increased patient survival, resistance represents a major treatment obstacle as most patients ultimately relapse becoming refractory to additional therapy. Current tests fail to detect emerging resistance; by the time patients acquire resistance, tumor burden is substantial. To establish immunophenotypic signatures that predict Bz sensitivity, we utilized Bz-sensitive and -resistant cell lines derived from tumors of the Bcl-X_L/Myc mouse model of PC malignancy. We identified the reduced expression of 3 markers (CD93, CD69 and CXCR4) in "acquired" (Bz-selected) resistant cells. Using this genetic signature, we isolated a subpopulation of cells from a drug-naïve, Bz-sensitive culture that immunophenotypically resemble "acquired" Bz resistant cells yet display "innate" resistance to the drug. Of these markers, *CXCR4* expression was most predictive of outcome in patients, as reduced *CXCR4* expression was significantly associated with poorer survival in Bz-treated MM patients. Although these genes were identified as biomarkers, they may indicate a mechanism for Bz-resistance through the loss of PC maturation markers which may be induced and/or selected by Bz. Most importantly, induction of PC differentiation in both "acquired" and "innate" resistant cells restored Bz sensitivity suggesting a novel therapeutic approach for targeting Bz refractory MM.

INTRODUCTION

Multiple myeloma (MM) is a plasma cell (PC) malignancy representing the second most common hematopoietic cancer. Unlike normal PCs, which are fully differentiated, malignant PCs retain their self-renewing capabilities and, in myeloma patients, accumulate in the bone marrow resulting in a fatal malignancy (432, 433). Over the last decade, remarkable advances have been made in the treatment of MM that have improved patient survival, including bone marrow transplant and the discovery of novel chemotherapeutic agents including proteasome inhibitors. Proteasome inhibitors block the ability of the proteasomal complex to degrade overabundant, misfolded or damaged polyubiquitinated proteins (434, 435). The large-scale production of antibodies by PCs requires the systematic degradation of excess peptides to maintain cellular homeostasis making the proteasome complex a successful chemotherapeutic target for MM (377).

Bortezomib (Bz)/VELCADE® (Millennium Pharmaceuticals, Inc.) was the first clinically approved, specific inhibitor of the proteasome and is a member of a growing family of proteasome inhibitors including next-generation compounds such as MLN2238 (Millennium Pharmaceuticals, Inc.) and the recently FDA-approved carfilzomib (Onyx Pharmaceuticals) (377). Bz reversibly inhibits the PSMB5 subunit of the proteasome, primarily targeting its chymotrypsin-like activity (436). Bz has been widely used to treat MM in combination with agents such as melphalan, dexamethasone, thalidomide and other newer IMiD-derivatives such as lenalidomide (377).

MM patients treated with Bz alone or in combination with other agents achieve high response rates (437). Despite this initial success, the majority of patients eventually relapse; some maintaining sensitivity to further Bz therapy, while others

develop refractory disease due to “acquired” drug resistance. Furthermore, some patients never respond to Bz having primary refractory disease and, therefore, displaying “innate” resistance to the drug (438). However, the similarities and differences between innate and acquired Bz resistance remain ill-defined. Currently, there are no reliable diagnostic predictors to determine whether a patient will respond to Bz treatment. By the time MM patients are classified as drug resistant, their tumor burden is often substantial and the prognosis is poor. Therefore, diagnostic tests that could predict Bz sensitivity or resistance prior to treatment are critically needed.

Our previous studies, which utilized *in vitro* cell lines created from the Bcl-X_L/Myc mouse model of plasma cell malignancy, highlighted by gene expression profiling a number of genes that may distinguish Bz-sensitive from -resistant cells *in vitro* (418). The goal of this study was to identify and validate those immunophenotypic markers that best distinguish Bz-sensitive from -resistant cells to establish signatures that predict Bz sensitivity as preclinical support for the development of a future diagnostic test for MM patients. We utilized these previously described Bz-sensitive (BzS) and Bz-resistant (BzR) mouse cells lines (418) derived from tumors of this Bcl-X_L/Myc double transgenic mouse model (124, 242). We employ this model because PC tumor lines isolated from these mice closely resemble human MM based on GEP, chromosomal abnormalities and progression of disease in the bone marrow (124, 242, 372, 418). Here we identify the loss of plasma cell maturation markers as a component of an immunophenotype that is associated with both innate and acquired Bz resistance. This is a highly regulated network that may prove vulnerable in the case of Bz resistance.

MATERIALS AND METHODS

Mouse tumor cell lines and treatment conditions. Mouse cell lines 595BzS, 595BzR, 589BzS and 589BzR were cultured in murine PC media containing RPMI 1640 (Lonza, Allendale, NJ), 15% fetal bovine serum (FBS) (Cellgro, Mediatech, Manassas, VA), 25 mmol/L HEPES (Lonza), 1mmol/L sodium pyruvate, 50 µmol/L beta-mercaptoethanol (Sigma-Aldrich, St. Louis, MO), 50 units/ml of penicillin and streptomycin (Thermo Fisher Scientific, Waltham, MA), 2 mmol/L $_{L}$-glutamine (Gibco Life Technologies, Grand Island, NY) and 0.5 ng/ml interleukin (IL)-6 (R&D Systems, Minneapolis, MN). Cells were split every 3 days and maintained at concentrations between 2-5x10^6 cells/mL. In some experiments, live cells were isolated by Ficoll-Hypaque (GE Healthcare, Piscataway, NJ) prior to analysis.

Bortezomib (Bz) (Millennium Pharmaceuticals, Inc., Cambridge, MA) was dissolved in serum-free RPMI 1640, and lipopolysacharide (LPS) (E-Coli 0111:B4, Sigma-Aldrich) was dissolved in PBS. Bz and LPS were added to the media at the concentration and for the time indicated.

Cytotoxicity assay. Cells were cultured at 4x10^5 cells/mL and treated with indicated concentrations of Bz for 48 hours. Cells were subjected to CellTiter-Glo® Luminescent cell viability assay according to manufacturer's instructions (Promega, Madison, WI). Values were normalized to untreated controls. Numbers of total live cells were determined by trypan blue exclusion and counting in triplicate using a hemacytometer.

Fluorescence analysis and sorting. Cells were stained with the following anti-mouse antibodies: CD69 FITC (clone H1.2F3), CD93 APC (clone AA4.1), CD138/syndecan-1 PE (clone 281-2), B220 APC (clone RA3-6B2) (all from BD Biosciences, Franklin Lakes, NJ), CD38 PE (BioLegend, San Diego, CA) and analyzed using the FACSCalibur (BD

Biosciences, Franklin Lakes, NJ). For fluorescence activated cell sorting experiments, at least $2x10^7$ cells were used, stained as described above using anti-mouse CD93 APC (clone AA4.1) and sorted using a FACSAria (BD Biosciences). To detect both intracellular and cell-surface CXCR4 expression, cells were first stained with anti-mouse CD184/CXCR4-PE (clone 2B11, eBioscience) antibody or Rat IgG2b kappa-PE isotype control (eBiosccience) and then fixed using the Cytofix/Cytoperm Fixation/Permeabilization kit (BD Biosciences), blocked in buffer containing 30% FBS, 0.1% Saponin and 20 mM HEPES, and stained a second time with the same antibodies. Samples were analyzed using the FACSCalibur and FlowJo Software (Tree Star, Ashland, OR).

Enzyme linked immunosorbant assay (ELISA). Cells (4×10^5 cells/ml) were plated in murine PC media for 48 hours. Supernatants were harvested and cells were lysed using buffer containing 10 mM Tris (pH 7.8), 150 mM NaCl, 1 mM EDTA, 1% Nonidet P-40. Ig kappa ELISA (Thermo Fisher Scientific) was performed according to the manufacturer's instructions, and Ig kappa levels were determined by subtracting the value from medium alone or lysis buffer control and normalized according to CellTiter-Glo® Luminescent values.

Array-comparative genomic hybridization. Genomic DNA was extracted from 10x10^6 cells in log phase growth for each cell line in the absence of drug selection using the PerfectPure DNA Blood Kit (5 PRIME Inc., Gaithersburg, MD). DNA was heat fragmented and DNA from BzR lines was labeled with fluorochrome Cyanine-5 using random primers and exo-Klenow fragment DNA polymerase. Control DNA from parental lines was labeled concurrently in Cyanine-3. The sample and control DNA were combined and array-based comparative genomic hybridization (a-CGH) was performed

with a microarray constructed by Agilent Technologies that contains approximately 170,000 distinct biological oligonucleotides spaced at an average interval of 10.9 kb.

The ratio of sample to control DNA for each oligo was calculated using Feature Extraction software 10.5 (Agilent Technologies, Santa Clara, CA). The abnormal threshold was applied using Genomics Workbench 7.0 (Agilent Technologies). A combination of several statistical algorithms were applied. A minimum of three oligonucleotides that have a minimum absolute ratio value of 0.1 [based on a log(2) ratio] is required for reporting of a copy number loss or gain.

Extraction of RNA and RT-PCR. RNA was extracted using QIAshredder and RNeasy RNA purification columns (Qiagen, Valencia, CA). RNA was reverse transcribed using the Transcriptor First Strand cDNA Synthesis Kit (Roche, San Francisco, CA). Quantitative RT-PCR was performed in triplicate using the LightCycler 480 and Probes Master (Roche) using 45 cycles of 95°C for 10 sec and 55°C for 30 sec (single acquisition). The primers used are presented in supplemental materials. Data were analyzed using LightCycler 480 software (Roche), and relative fold changes were calculated using the $2^{-\Delta\Delta Ct}$ method with the GAPD reference gene for normalization.

The ratio of spliced to unspliced Xbp1 was determined by endpoint PCR using GeneAmp PCR System 9700 (Applied Biosystems, Carlsbad, CA) and GoTaq Green DNA polymerase (Promega) using 35 cycles of 95°C for 30 sec, 50°C for 30 sec and 72 °C for 1 min. The XBP1 primers used were as previously described (47) and have been included in the supplemental methods: PCR products were resolved on a 2.5% agarose gel (BioExpress, Kaysville, UT), visualized using the ChemiDoc™ XRS+ Imager (Bio-Rad, Hercules, CA), and quantified by Image Lab Software.

Quantitative RT-PCR primers. The following primers were used: Cd93, 5'-

TGAAATAGACGCCCTGAAAAC-3' (5' primer), 5'-AATCAAAGCCTGGGTTTAGGA-3' (3' primer); Cd69, 5'-GGAAAATAGCTCTTCACATCTGG-3' (5'primer), 5'-TGATGCTTCTCAAAATGTATACTGG-3' (3' primer); Irf4, 5'-ACAGCACCTTATGGCTCTCTG-3' (5' primer), 5'-ATGGGGTGGCATCATGTAGT-3' (3' primer); Blimp-1, 5'-TGCGGAGAGGCTCCACTA-3' (5' primer), 5'-TGGGTTGCTTTCCGTTTG-3' (3' primer); Chop, 5'-GCGACAGAGCCAGAATAACA-3' (5' primer), 5'-GATGCACTTCCTTCTGGAACA-3' (3' primer); Cxcr4, 5'-TGGAACCGATCAGTGTGAGT-3' (5' primer), 5'- GGGCAGGAAGATCCTATTGA-3' (3' primer). The primers included in the Universal ProbeLibrary Mouse Gapd Gene Assay (Roche) were used as the reference gene.

Xbp1 primers. Xbp1, 5'-ACACGCTTGGGAATGGACAC-3' (5' primer), 5'-CCATGGGAAGATGTTCTGGG-3' (3' primer).

Cell lines and culture. CH12F3-2 (CH12) and MPC11 were kindly provided by Matthew Scharff (Albert Einstein College of Medicine, Bronx, NY). CH12 cells were maintained in RPMI 1640 supplemented with 10% FBS, 50 □mol/L 2-mercaptoethanol and 5% NCTC (BioWhittaker, Walkersville, MD), and MPC11 cells were cultured in murine PC media described above without IL-6.

Human gene expression profiling analysis. Plasma cell purifications and gene expression profiling, using the Affymetrix U133Plus2.0 microarray (Affymetrix, Santa Clara, CA), were performed as previously described (390). GEP of $CD138^{+}$ bone marrow plasma cells from 214 MM patients were used from this study. Signal intensities were pre-processed and normalized by GCOS1.1 software (Affymetrix). We performed permutation analyses to correlate *CXCR4* expression with patient survival in the total therapy 3 trial (TT3, n=214); the presented p value was based on the best cut-off (50%

patients in high- or low-*CXCR4* group) between these 2 parameters. All statistical analyses were performed with the use of the statistical software R (Version 2.6.2) (http://www.r-project.org).

RESULTS

Acquired bortezomib resistance is associated with immunophenotypic changes.

To identify immunophenotypic biomarkers in Bz-resistant PCs, we utilized the previously described *in vitro* double transgenic Bcl-X_L/Myc mouse cell lines (124, 242, 418). In a previous study, Bz-sensitive (BzS) mouse cell lines were dose escalated with bortezomib *in vitro* to create Bz-resistant (BzR) daughter cell lines which were further characterized using gene expression profiling (GEP) (418). We selected the most Bz-resistant of these pairs, 589 (4.4-fold increase in IC_{50}) and 595 (4.9-fold increase in IC50), for further immunophenotypic characterization. Both the 595 and 589 BzS and BzR lines were characterized by flow cytometry and found to be $CD38^+CD138^+$ (Supplemental Figure S1) and $CD20^-CD27^-$ (data not shown) compared to isotype controls (Supplemental Figure S2A), characteristic of early plasma cells (439). These cells also express mature B cells markers such as B220, most strongly in the 595 BzS line (Supplemental Figure S1).

Three cell-surface markers CD93, CD69 and CXCR4 had consistently reduced expression in the BzR compared to the BzS cell lines (Figure 1A). Using quantitative RT-PCR, we validated the reduced expression of these genes in all cell lines tested (Figure 1B). The differences in the cell surface mean fluorescence intensity between BzS and BzR cells were most well-defined by CD93 and CD69 protein and mRNA expression (Figure 1A-B); BzS cells were $CD93^+CD69^+$ (double positive) and BzR cells were $CD93^-CD69^-$ (double negative) (Figure 1C).

Innate and acquired bortezomib resistant cells have similar immunophenotypes.

CD93 and CD69 most clearly distinguished mouse BzS from BzR cells. Because MM cultures are known to be heterogeneous, we asked whether Bz-resistant $CD93^-$

$CD69^-$ cells are present within drug naïve, BzS cultures. While the majority of BzS cultures stained double positive for CD93 and CD69, approximately 0.1% of 595 and 12% of 589 BzS cells were double negative for CD93 and CD69 (Figure 1C, left panels). Characterization of 4 other BzS cell lines derived from the same double transgenic mouse model displayed 2-6% CD93/CD69 double negative cells (data not shown).

To further characterize this potentially "innate" Bz-resistant population, we isolated $CD93^-CD69^-$ cells from the 589 BzS culture, which displayed the highest percentage of double negative cells, by flow sorting and performed Bz dose response assays, quantitative RT-PCR and flow cytometry for the immunophenotyic markers above. Dose response assays using Bz revealed that this drug naïve, $CD93^-CD69^-$ sorted population (I-BzR) had an IC_{50} (Figure 2A) and growth rate (Supplemental Figure S2B) comparable to the 589 BzR cell line. As expected, I-BzR cells expressed reduced levels of CD93 and CD69 protein (Figure 2B) and mRNA (Figure 2C). Moreover, the I-BzR cells displayed a moderate reduction in the expression of CXCR4 (Figure 2B) similar to BzR cells (Figure 1A). Interestingly, this "innate" Bz-resistant, immunophenotype was persistent as long as 1 year post-sort (data not shown), characteristic of primary refractory disease seen in MM patients. These results demonstrate that "innate" Bz-resistant cells (I-BzR) isolated from a drug naïve, heterogeneous culture display similar immunophenotypic characteristics to cells with an acquired (drug-selected) resistance to Bz.

Bz promotes loss of CD93 and CD69.

To characterize the emergence of the $CD93^-CD69^-$ double negative Bz-resistant population, BzS cells were treated with drug to determine whether the loss of CD93 and CD69 expression is selected for and/or modulated by Bz treatment. As expected, BzS

cells treated with a high-dose of Bz resulted in approximately 95% (595BzS, data not shown) and 80% (589BzS, Figure 2A) death. After gating on live cells, we observed reduced expression of CD93 and CD69 by flow cytometry compared to untreated controls (Figure 3A). Shifts in CD93 and CD69 cell surface expression were more pronounced in the 589 BzS line, the remaining live cells displaying a BzR cell immunophenotype (Figure 3A, Supplemental Figure S2C). The maintenance of these double negative cells is not likely due to variable growth rates as CD93 and CD69 double positive and double negative populations divide at similar rates (0.8-0.9 cell divisions/day, Supplemental Figure S2B). Quantitative RT-PCR analysis of BzS cells following sub-lethal Bz treatment, a condition not associated with substantial cell death (Supplemental Figure S2D), resulted in significantly reduced expression of *Cd93* in both the 595 and 589 BzS lines and *Cd69* in the 595 BzS line (Figure 3B). These results demonstrate that Bz treatment may both select for the CD93 and CD69 double negative population as well as induce the loss of these cell-surface markers at the level of mRNA regulation.

Low CXCR4 expression may be of diagnostic value in predicting human Bz-resistant MM.

The data described above define a strong role for CD93, CD69, and CXCR4 as biomarkers of both “innate” and “acquired” Bz-resistance in our mouse plasma cell *in vitro* system. Using a publicly available MM dataset, we sought to determine whether these markers were associated with survival in patients treated with Bz. The total therapy 3 (MMTT3) drug trial reported by Shaughnessy, et al. provides GEP data in MM patients prior to and following a single, 48 hour test-dose of Bz. Following this Bz treatment, patients were placed on drug cocktail regimens and survival was reported

(390). High expression of both CD93 and CD69 has not been described in human MM. Indeed we find that the expression of these markers is very low in patient samples (data not shown). However, CXCR4 is highly expressed in human MM (440). In fact, as a single biomarker, low *CXCR4* expression was able to significantly distinguish those MM patients with poorer event free (EFS; $p = 0.013$) and overall (OS; $p = 0.010$) survival in this clinical trial (Supplemental Figure S3A-B). Therefore, although the consistent reduction in CXCR4 that we observe in our mouse cell lines is moderate, CXCR4 may be a viable diagnostic target associated with clinical outcome in MM patients being treated with Bz.

The Bz-resistant immunophenotype implicates a role for B cell differentiation.

Given our analysis of human MM GEP data, there appears to be utility in the immunophenotypic characterization of the mouse BzS and BzR cell lines for identifying biomarkers of Bz-resistance; however, whether these biomarkers play a role in the mechanism of Bz-resistance remains ill-defined. In the mouse, we have identified that low CD93/CD69/CXCR4 expression best define Bz-resistant cells (Figure 1 & 2). We have also observed minimal losses in other cell-surface markers including CD38 in these populations (data not shown). Mouse PCs are known to express higher levels of *Cd93*, *Cxcr4* and *Cd38* mRNA relative to germinal center (GC) B cells (441). In addition, high CD93 expression has been shown to be necessary for the maintenance of normal, long-lived plasma cells in mice (442). Loss of these markers in both the BzR and I-BzR populations led us to hypothesize that, besides their roles as biomarkers, the loss of CD93, CD69, CXCR4 and CD38 in Bz-resistant cells is associated with a loss of PC maturation markers in MM.

Using a human MM clinical trial reported by Mulligan, et al. where GEP was performed on patients prior to treatment with either high-dose dexamethasone or Bz as a single agent (APEX drug trial) (403), we compared the expression profiles for genes known to be highly involved in PC maturation between Bz responders and nonresponders. A combination of these data and the available mouse GEP data (418) showed that there indeed appeared to be reduced expression in some of the genes known to be "master regulators" of PC differentiation, *XBP1* and *PRDM1* (*BLIMP-1*) in Bz nonresponders (data not shown). These markers were further validated *in vitro* where we found reduced Xbp1 splicing in the Ig-secreting mouse 595 BzR cell line relative to its BzS counterpart but not in the 589 line which lacks heavy chain expression (Supplemental Figure S4A). A lack of spliced XBP1 was also present in PCs isolated from human Bz-resistant MM patients (Rodger Tiedemann, personal communication). Taken together, these data suggest a certain plasticity in the PC commitment of Bz-resistant cells which may be induced by Bz selection.

Lipopolysaccharide treatment re-sensitizes Bz-resistant cells to Bz.

Because the Bz-resistant cells in our model system display features of lost PC commitment, we next determined whether we could therapeutically target this process by promoting PC differentiation of BzR cells to restore the immunophenotype of the BzS population and re-sensitize cells to Bz-induced death. The toll like receptor (TLR)-4 ligand, bacterial lipopolysaccharide (LPS), is a known inducer of B cell differentiation (443-445). Previous studies have shown that differentiation of B cells to $CD138^{+}$, immunoglobulin-secreting PCs requires the coordinated induction of the transcription factor IRF4 (24) and its downstream transcriptional target, BLIMP-1 (30) (Figure 4A). Consistent with these studies, LPS treatment of 589 cells for 72 hours resulted in a 6-

fold increase in *Irf4* in both BzR lines (Figure 4B, top panel) and a 3-fold (I-BzR) to 6-fold (BzR) increase in *Blimp-1* (Figure 4B, bottom panel) mRNA levels. Interestingly, increased expression of *Irf4* and *Blimp-1* were only observed in BzR cells as these transcription factors did not increase in the LPS-treated BzS culture (Figure 4B) suggesting that the BzS population is insensitive to further LPS-mediated PC differentiation despite similar expression of *Tlr4* mRNA (data not shown).

BLIMP-1 is required for XBP1 induction and activation of the physiological unfolded protein response (UPR) pathway in preparation for immunoglobulin secretion (30, 43, 47). This UPR pathway is responsible for further processing of *XBP1* mRNA into its spliced form with the assistance of IRE1α (47) (Figure 4A). Consistent with LPS-induced PC differentiation, we observed increased *Xbp1* splicing in the BzR cells but not in the BzS population (Figure 4C). *Xbp1* splicing corresponded to increased Ig kappa secretion only in the I-BzR population (Figure 4D). This lack of Ig kappa secretion (Figure 4D) and undetectable intracellular Ig kappa in the BzR cells (Supplemental Figure S4B) correlated with a deletion within the kappa gene locus as evidenced by array comparative genomic hybridization (Supplemental Figure S4C). Increased BLIMP-1 has also been associated with CHOP expression (24) (Figure 4A). Consistent with this, we observed increased *CHOP* in BzR cells (Figure 4B) as well as increased sensitivity to LPS treatment (data not shown).

We next asked whether LPS stimulation promoted the re-expression of CD93, CD69 and CXCR4 in BzR populations. We observed a modest increase in *Cd93* mRNA (Supplemental Figure S5A) and cell surface expression (Supplemental Figure S5B) only in the I-BzR population consistent with the modest increase in Ig kappa secretion (Figure 4D) demonstrating a positive correlation between CD93 expression and Ig secretion,

which has been previously reported (442). LPS stimulation resulted in increased *Cd69* and *Cxcr4* mRNA (Figure 4E) and CD69 cell-surface expression (Figure 4F) in both BzR lines.

Finally we asked whether this re-commitment of an PC immunophenotype restores Bz sensitivity in BzR cells. Following LPS pre-treatment, live cells were re-plated for Bz treatment. Consistent with our previous findings, we observed reduced viability of the non-LPS treated BzS population and little death in BzR cells following Bz treatment (Figure 5). However, LPS pre-treatment prior to Bz treatment significantly reduced the viability in all cultures including the previously Bz-resistant populations (BzR and I-BzR) (Figure 5).

Taken together, we have identified an immunophenotype that can segregate Bz-sensitive and -resistant mouse PC lines *in vitro*. Furthermore, these distinguishing markers suggest that BzR cells represent a population with reduced PC commitment which is perhaps both selected and induced by Bz treatment. This lack of commitment may prove to be a therapeutic target in Bz refractory MM.

DISCUSSION

In this study we utilized tumor lines derived from the Bcl-X_L/Myc transgenic mouse model of PC malignancy to immunophenotypically characterize neoplastic Bz-sensitive and -resistant PCs in order to identify biomarkers associated with acquired and innate Bz resistance. Although these pairs of cell lines shared many common markers of PC expression, we found that Bz-sensitive cells are predominately CD93/CD69 (88-99.9%) double positive cells (6 independently derived transgenic mouse lines analyzed), whereas BzR cells display a striking reduction in the expression of both of these markers. In fact, CD93 and CD69 are the two cell-surface proteins that best distinguished Bz-sensitive from -resistant, both “innate” and “acquired”, cells. While CD93 is expressed during early B cell development, this expression is lost in GC B cells and is again induced as B cells differentiate into PCs (442). CD93/CD138 expression has been shown to be restricted to antibody-producing cells and is required for the maintenance of long-lived plasma cells in the bone marrow in mice (442). Expression of CD93 and CD138 on Bz-sensitive cells is consistent with their PC differentiation stage and Ig secretion; however, we see a loss of CD93 in Bz-resistant cells. Stessman, et al. reported that a GEP analysis of the BzS and BzR lines in the absence of drug showed enrichment for downstream targets of the transcription factors, XBP1 and BLIMP-1, both of which are involved in PC commitment (418). These findings, as well as our use of the APEX clinical trial to further analyze the expression of PC markers in Bz-refractory MM patients, suggest that there is an association between Bz-resistance and a loss of PC commitment.

LPS stimulation induced the re-expression of CD93 in about 27% of I-BzR cells which is positively correlated with a 30% increase in Ig secretion, suggesting that these

two events are likely occurring together within the CD93+ population. Since LPS pre-treatment did not uniformly increase CD93 expression, re-sensitization of BzR cells may not always correlate with CD93 expression. However, expression of the activation marker CD69 increased uniformly following LPS treatment suggesting that CD69 may in fact be a better marker for predicting Bz sensitivity although little is known about the function of this protein during PC differentiation (441). Future studies are required to determine the precise role of CD69 in Bz sensitivity, specifically, whether this is simply a biomarker or perhaps playing a larger mechanistic role in resistance.

While BzR cells maintain some features of PCs, still others are reduced; however, BzR cells do not share a complete shift by GEP to a GC B cell stage (441) (data not shown). It is possible and, based on our data, in fact likely that the loss of PC commitment may serve as not only a biomarker of Bz resistance but as a direct therapeutic target in refractory MM. The loss of PC commitment may confer a selective advantage for evading Bz-mediated death via the reduction of the unfolded protein response (UPR). GC B cells, which express and secrete fewer immunoglobulin molecules than PCs, are less sensitive to endoplasmic reticulum stress and display a reduced UPR (45, 47). We demonstrate that BzR cells secrete reduced immunoglobulin proteins compared to BzS cells, consistent with the observation that BzR cells have lost some of their PC commitment. This raises the possibility that BzR cells are resistant because of reduced antibody production suggested previously by others (446). While LPS stimulation re-sensitized both BzR and I-BzR cells to Bz, re-sensitization correlated minimally with increased Ig secretion in I-BzR cells arguing, at least in this context, that Bz sensitivity does not always require Ig synthesis and secretion. On the other hand, LPS stimulation increased XBP1 splicing and CHOP expression, two components

necessary for the UPR, suggesting that Bz sensitivity may require the initiation of the UPR signaling cascade which may occur independently of Ig synthesis.

Although low CD93 and CD69 best distinguish our Bz-resistant mouse cell lines, these markers are not highly expressed on human PCs. However, using this model system we have demonstrated that an immunophenotype may exist that could be used diagnostically to identify Bz-sensitive and -resistant patients prior to treatment. In fact, reduced expression of CXCR4 and CD38 were also identified as components of our Bz-resistant immunophenotype and are expressed on human MM cells. Reduced expression of CXCR4 is thought to play a role in PC homing to the bone marrow (447), and, when injected back into syngeneic mice, BzR cells fail to home to the marrow compared to their BzS counterparts (418). These data suggest that reduced CXCR4 expression correlates with increased disease severity. This is consistent with our analysis of the MMTT3 trial (390) which showed that low *CXCR4* expression was significantly associated with reduced event free and overall survival compared to patients with high *CXCR4* expression treated with Bz. These data suggest that Bz selection may promote the loss of CXCR4 which in turn may decrease the reliance of the MM cells on the bone marrow microenvironment promoting extramedullary disease.

The re-sensitization of previously Bz-resistant cells to Bz following LPS pretreatment supports the hypothesis that BzR cells have lost some of their PC commitment distinct from Bz-sensitive cells. While LPS promoted PC differentiation of BzR cells, BzS cells were unaffected by LPS stimulation similar to *in vitro* adapted plasmacytoma tumors (448). Re-sensitization of Bz-resistant MM lines following PC differentiation using 2-methoxyestrodiol or all-trans-retinoic acid was recently described

(353). Combined, these studies argue that augmentation of PC differentiation may be a logical chemotherapeutic approach in Bz-refractory MM.

These studies outline the immunophenotypic characterization of Bz-sensitive and -resistant PCs using a mouse model which has identified the loss of PC commitment in Bz-resistant cells compared to Bz-sensitive cells. By therapeutically forcing Bz-resistant cells to differentiate back into PCs, we have shown that we can re-sensitize these cells to Bz treatment. Of the Bz-resistant markers identified, low *CXCR4* best correlates with poor MM patient clinical outcomes suggesting that this could be a useful biomarker for developing a diagnostic test to identify Bz resistance. The positive impact of such a diagnostic tool in patient care could mean the early detection of Bz resistance and improved overall survival through individualized medical treatment. In addition, if in fact these immunophenotypic biomarkers are involved in the drug-resistant mechanism, this may provide novel drug targets for the synthesis of new compounds aimed at reversing resistance by promoting PC differentiation prior to Bz treatment. This highlights a unique therapeutic option for the treatment of relapsed and primary refractory MM patients.

Figure 1. Immunophenotypic characterization of acquired bortezomib resistant lines.

A. Fluorescence-activated cell sorting analysis of BzS (solid black line) and BzR (dark grey histogram) cells stained with indicated antibodies. B. Quantitative RT-PCR analysis of *Cd93* and *Cd69* relative mRNA expression in 595 and 589 BzS and BzR lines. Values were normalized to *Gapd* mRNA and error bars represent PCR triplicates. Significance was determined using a one-tailed Student's t-test (* $p < 0.05$; ** $p < 0.01$; **** $p < 0.0001$). C. Fluorescence-activated cell sorting dot plot analysis of BzS and BzR cells double stained with CD93 and CD69 antibodies.

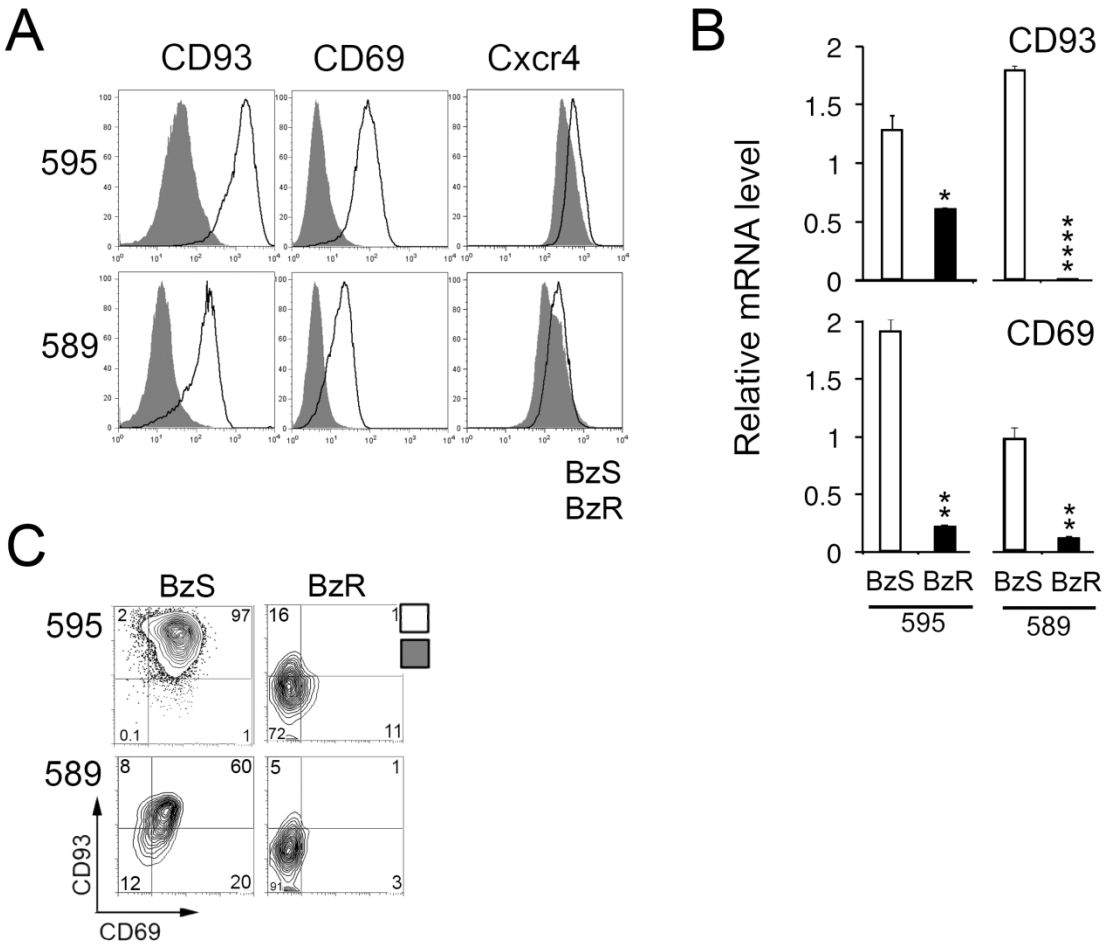
A
CD93
CD69
Cxcr4
595
589
BzS
BzR
B
CD93
CD69
Relative mRNA level
2
1.5
1
0.5
0
*
****
**
**
BzS BzR
BzS BzR
595
589
C
BzS
BzR
595
589
2
97
0.1
1
16
1
72
11
8
60
12
20
5
1
91
3
CD93
CD69

Figure 2. Establishment and characterization of innate bortezomib resistant lines.

A. 589 BzS, BzR, and I-BzR lines were cultured in the presence of indicated concentrations of Bz for 48 hours and percentage of live cells determined by CellTiter-Glo® values normalized to untreated controls. Error bars represent three independent CellTiter-Glo® readings. B. Fluorescence-activated cell sorting analysis of BzS (solid black line) and I-BzR (light grey histogram) stained with indicated antibodies. C. Quantitative RT-PCR analysis of *Cd93* and *Cd69* relative mRNA expression in 589 BzS and I-BzR lines. Values were normalized to *Gapd* mRNA and error bars represent PCR triplicates. Significance was determined using a one-tailed Student's t-test (** $p < 0.01$; **** $p < 0.0001$).

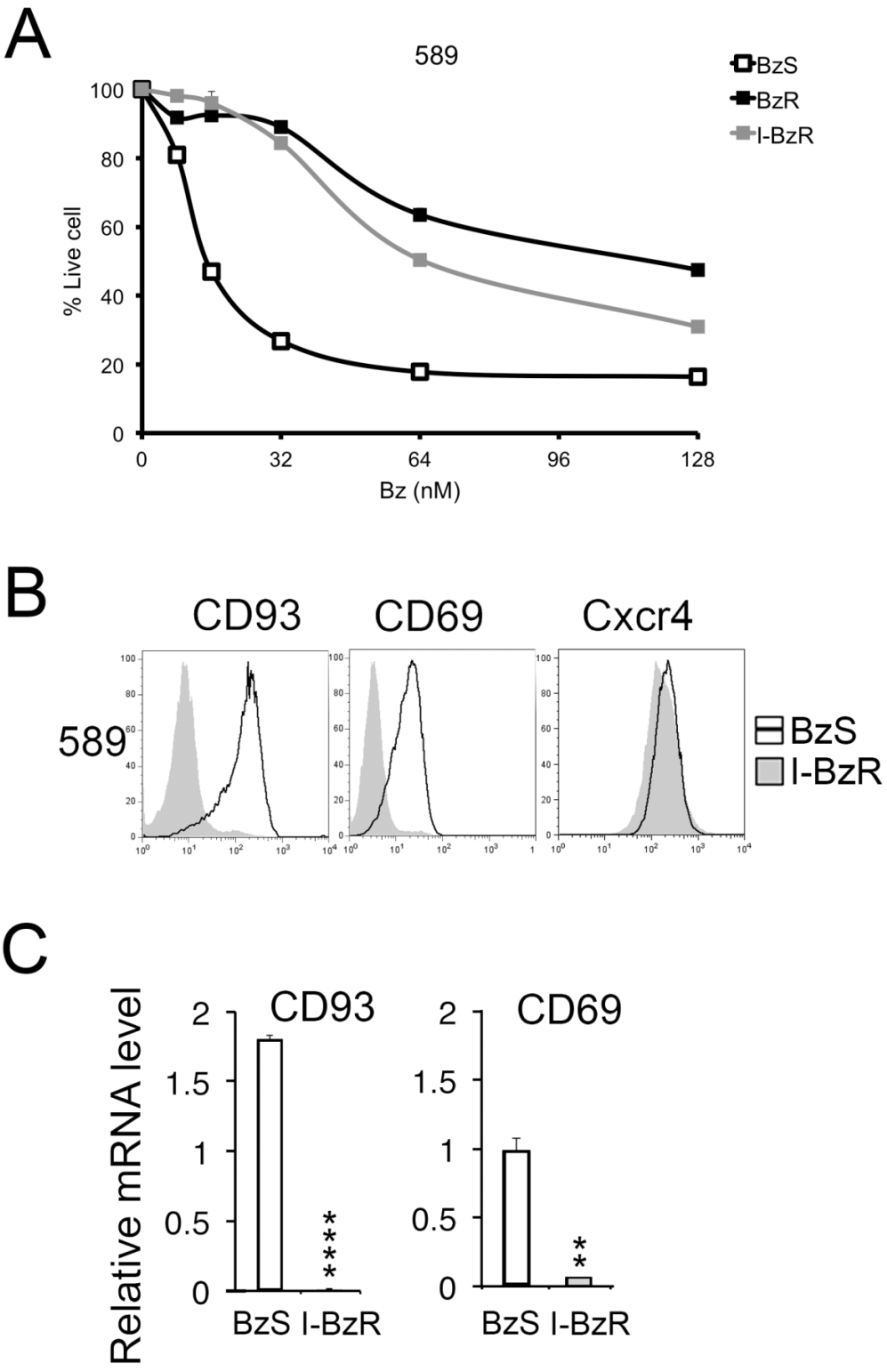
A
589
BzS
BzR
I-BzR
% Live cell
100
80
60
40
20
0
0
32
64
96
128
Bz (nM)
B
CD93
CD69
Cxcr4
589
BzS
I-BzR
C
Relative mRNA level
CD93
CD69
2
1.5
1
0.5
0
****
**
BzS
I-BzR

Figure 3. Bortezomib promotes loss of CD93 and CD69.

A. Fluorescence-activated cell sorting analysis of live untreated BzS cells (solid black line), BzS cells treated with 64 nM Bz for 48 hours (dotted black line) and untreated BzR cells (dark grey histogram) stained with CD93 and CD69 antibodies. Live cells were gated using forward and side scatter. B. Quantitative RT-PCR analysis of *Cd93* and *Cd69* mRNA in 595 and 589 lines. Values were normalized to *Gapd* mRNA and error bars represent PCR triplicates. Significance was determined using a one-tailed Student's t-test (** $p < 0.01$; *** $p < 0.001$; **** $p < 0.0001$).

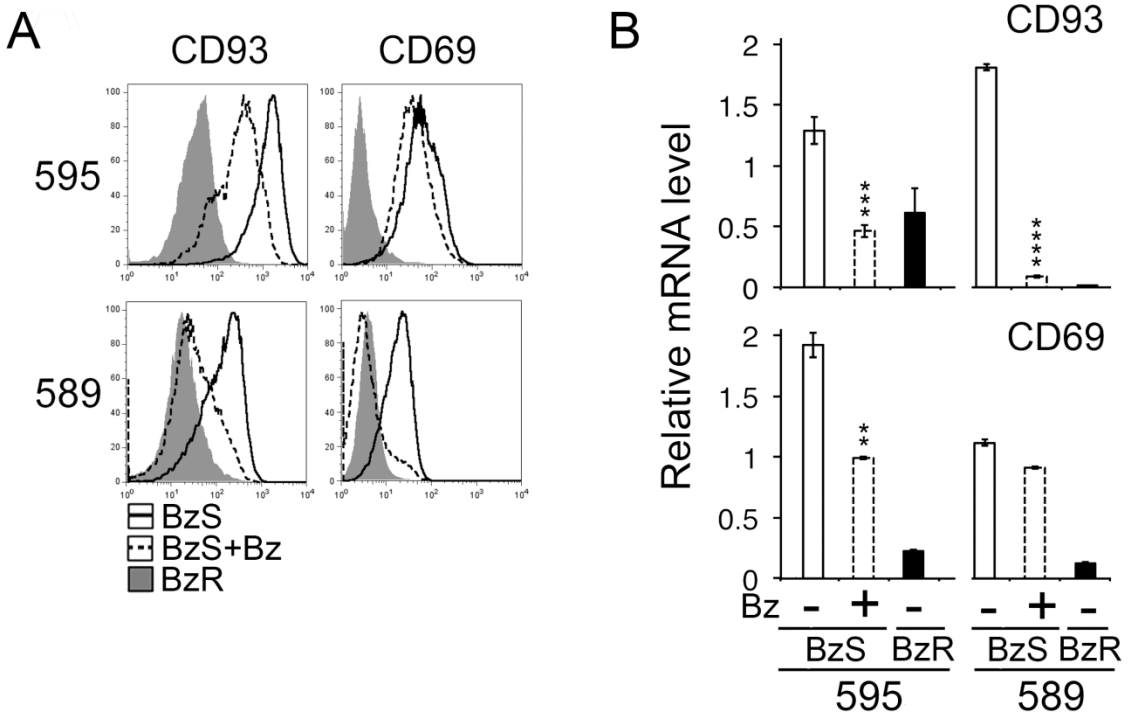
A
CD93
CD69
595
589
BzS
BzS+Bz
BzR
B
CD93
CD69
Relative mRNA level
Bz
BzS
BzR
595
589

Figure 4. LPS induces plasma cell differentiation in Bz-resistant cells.

A. Schematic of genes normally expressed highly at the plasma cell (PC) developmental stage shown relative to germinal center (GC) and plasmablast/intermediate plasma cell (iPC) stages. B. Quantitative RT-PCR analysis of *Irf4*, *Blimp1*, and *CHOP* mRNA in 589 untreated cells and 72 hour LPS-treated cells. Values were normalized to *Gapd* mRNA, and error bars represent PCR triplicates. C. Densitometry values representing the percentage of spliced/unspliced *Xbp1* in 589 BzS, BzR and I-BzR cells untreated or treated with LPS for 72 hours. D. ELISA of Ig kappa light chain secreted into the media following 72 hour LPS treatment, cells were ficolled and incubated for an additional 24 hours. The error bars represent three independent ELISA readings, and values were normalized to total live cells determined by CellTiter-Glo®. E. Quantitative RT-PCR analysis of *Cd69* and *Cxcr4* mRNA in 589 untreated cells and 72 hour LPS-treated cells. Values were normalized to *Gapd* mRNA and error bars represent PCR triplicates. Significance was determined using a one-tailed Student's t-test (* $p < 0.05$; ** $p < 0.01$; *** $p < 0.001$; **** $p < 0.0001$). F. Fluorescence-activated cell sorting analysis of untreated BzS (solid black line), BzR (dark grey line), or I-BzR (light grey line) and LPS-treated (dotted lines) stained with CD69.

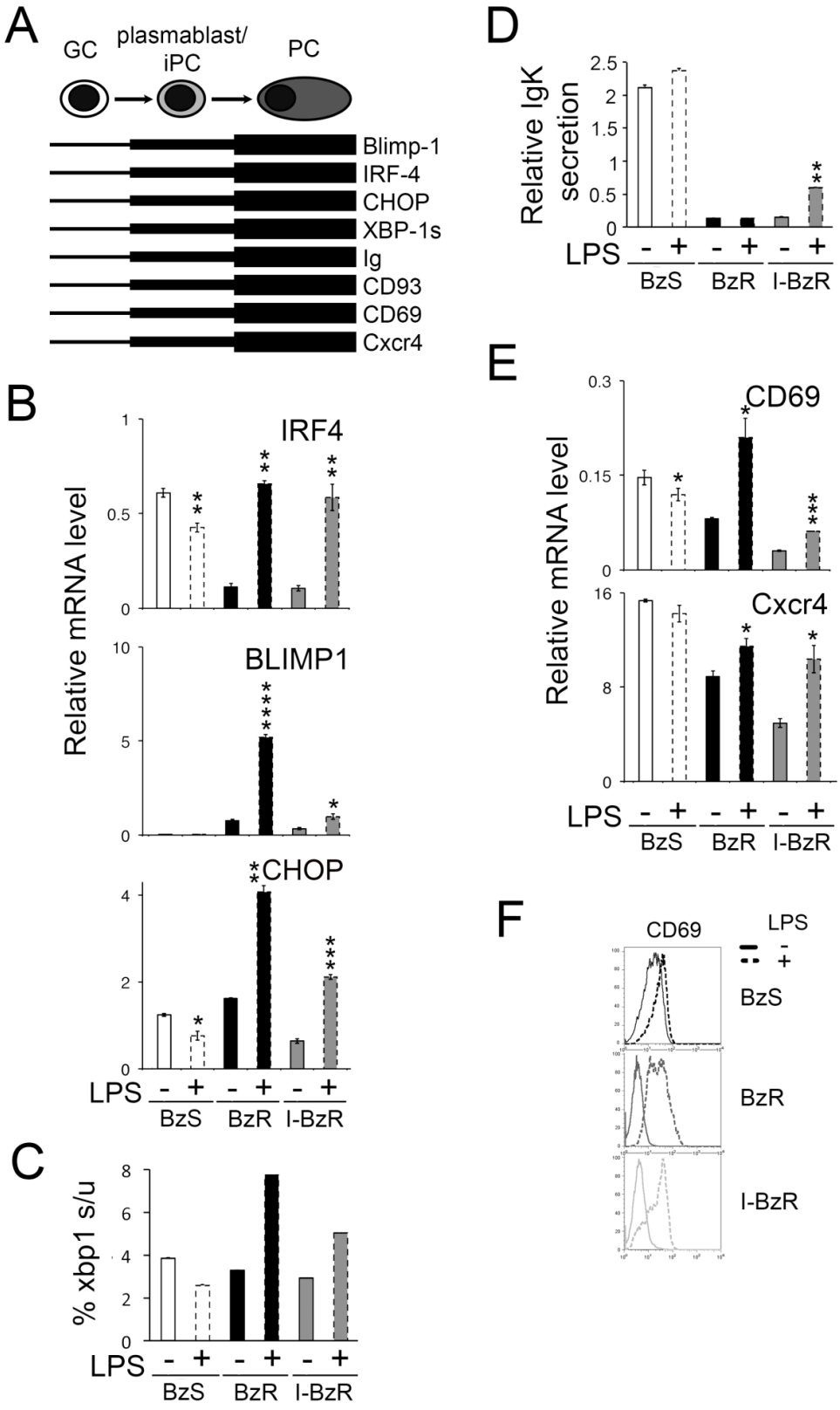
A
GC
plasmablast/
iPC
PC
Blimp-1
IRF-4
CHOP
XBP-1s
Ig
CD93
CD69
Cxcr4
B
IRF4
BLIMP1
CHOP
Relative mRNA level
LPS
BzS
BzR
I-BzR
C
% xbp1 s/u
D
Relative IgK secretion
E
CD69
Cxcr4
F
CD69
LPS

Figure 5. LPS re-sensitizes Bz-resistant cells to bortezomib treatment.

72 hour LPS-treated or untreated BzS and BzR lines were ficolled and re-plated in the presence or absence of 60 nM Bz for 48 hours. The percentage of live cells determined by CellTiter-Glo® values normalized to untreated controls (*i.e.* In the absence of Bz, LPS-treated were normalized to non-LPS-treated cells, and following LPS treatment, Bz-treated were normalized to non-Bz-treated cells) are shown. Error bars represent three independent CellTiter-Glo® readings.

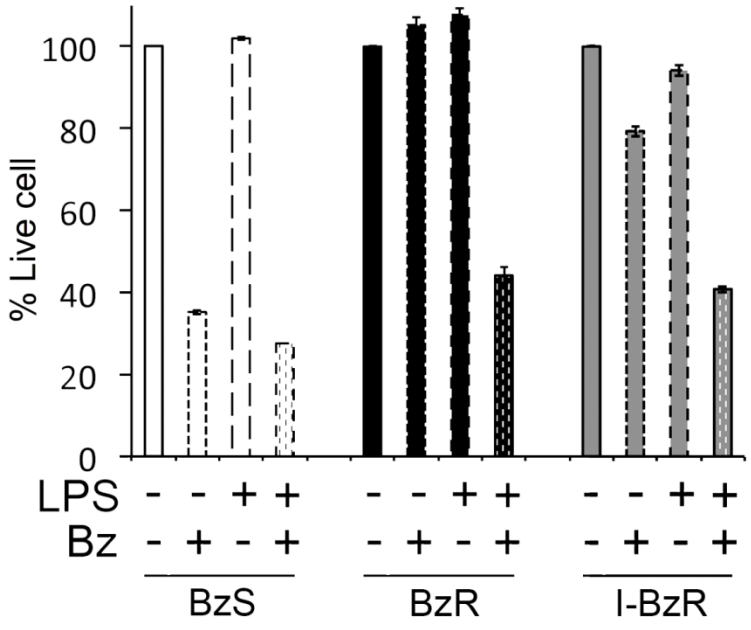
% Live cell
100
80
60
40
20
0
LPS - - + + - - + + - - + +
Bz - + - + - + - + - + - +
BzS
BzR
I-BzR

Supplemental Figure S1.

Fluorescence-activated cell sorting analysis of 595 BzS (solid black line) and 589 BzS (dotted black line) cells compared to GC B cell, CH12 (dark grey histogram), and plasmacytoma, MPC11 (light grey histogram), reference cell lines stained with indicated antibodies.

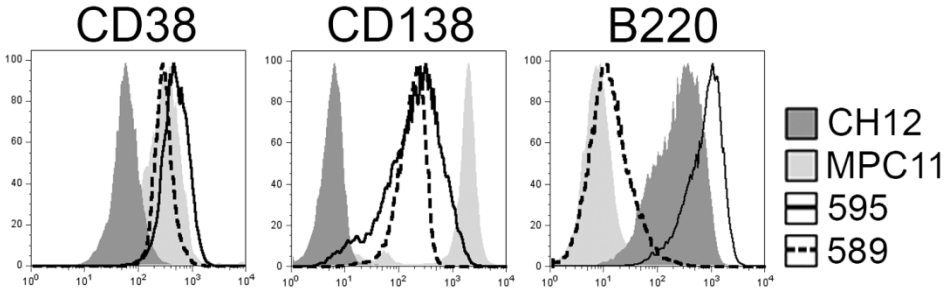
CD38
CD138
B220
CH12
MPC11
595
589

Supplemental Figure S2.

A. Fluorescence-activated cell sorting analysis of 589 BzS and BzR cells either unstained (top panel) or stained with isotype control antibodies (lower panels). B. Total live 589 BzS, BzR, and I-BzR cells were determined by trypan blue exclusion by three independent cell counts. C. Fluorescence-activated cell sorting analysis of 589 BzS cells in the presence or absence of 64 nM (high dose) Bz for 48 hours double stained with CD93 and CD69. Live cells were gated based on FSC and SSC. The gated populations are reflected in dot plots below. D. 595 and 589 BzS and BzR lines were incubated in the presence or absence of 33 nM (low dose) Bz for 24 hours. The percentage of live cells determined by CellTiter-Glo® values were normalized to untreated controls. Error bars represent three independent CellTiter-Glo® readings.

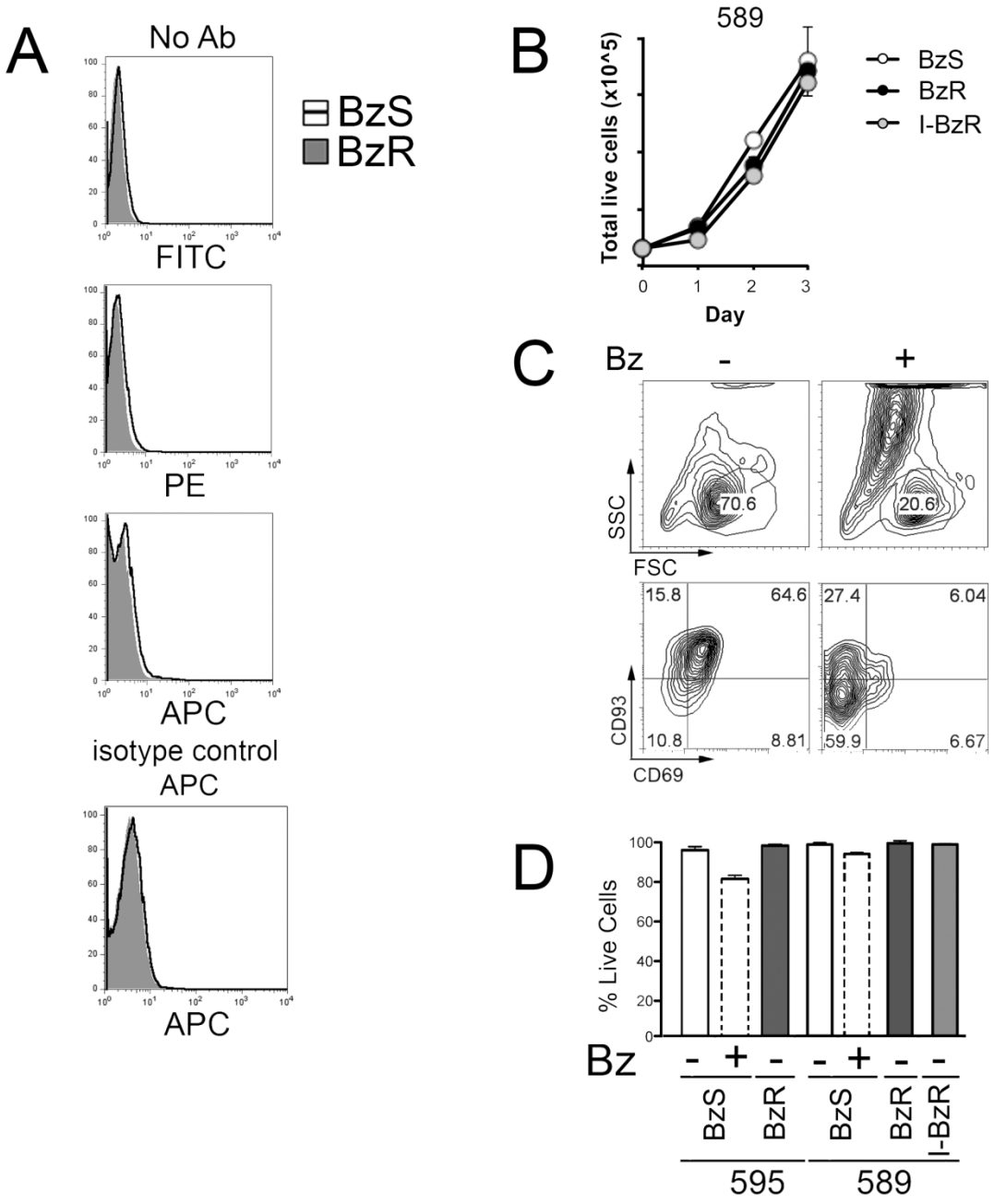
A
No Ab
BzS
BzR
FITC
PE
APC
isotype control
APC
APC
B
589
Total live cells (x10^5)
Day
BzS
BzR
I-BzR
C
Bz
-
+
SSC
FSC
70.6
20.6
15.8
64.6
27.4
6.04
10.8
8.81
59.9
6.67
CD93
CD69
D
% Live Cells
Bz
BzS
BzR
BzS
BzR
I-BzR
595
589

Supplemental Figure S3.

A. Event-free (EFS) and B. overall survival (OS) analysis of high and low *CXCR4* expressing MM patient groups taken from the total therapy 3 (TT3) drug trial (390). The p value represents significant difference by one-way ANOVA. The number of cases analyzed is indicated.

A

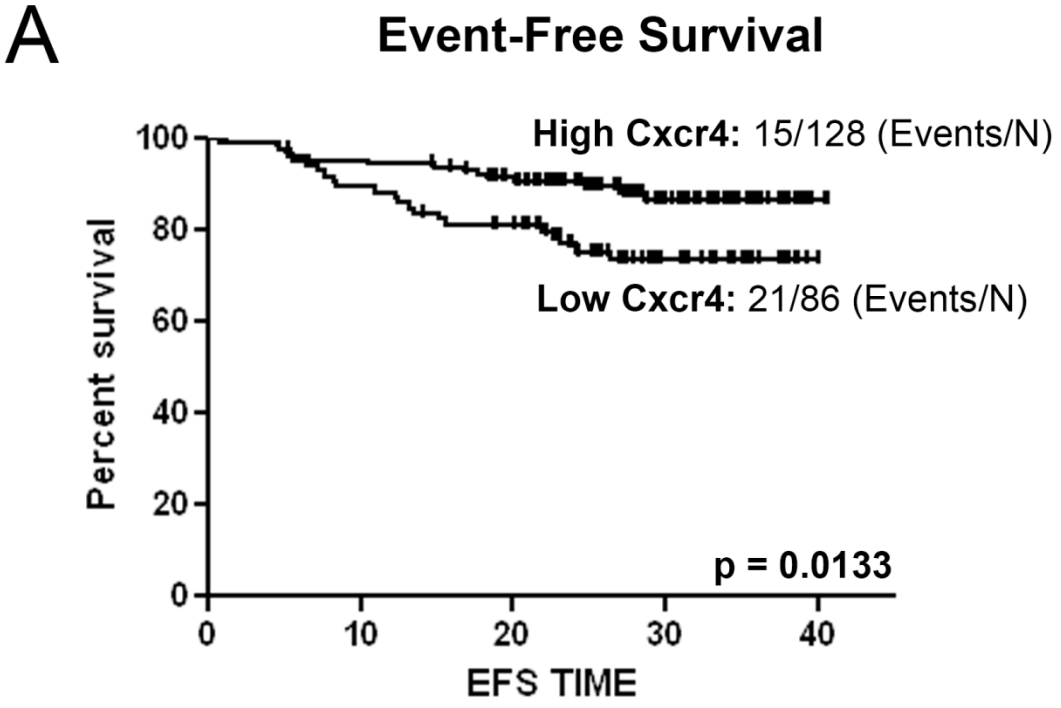
Event-Free Survival
High Cxcr4: 15/128 (Events/N)
Low Cxcr4: 21/86 (Events/N)
p = 0.0133
Percent survival
100
80
60
40
20
0
0
10
20
30
40
EFS TIME

B

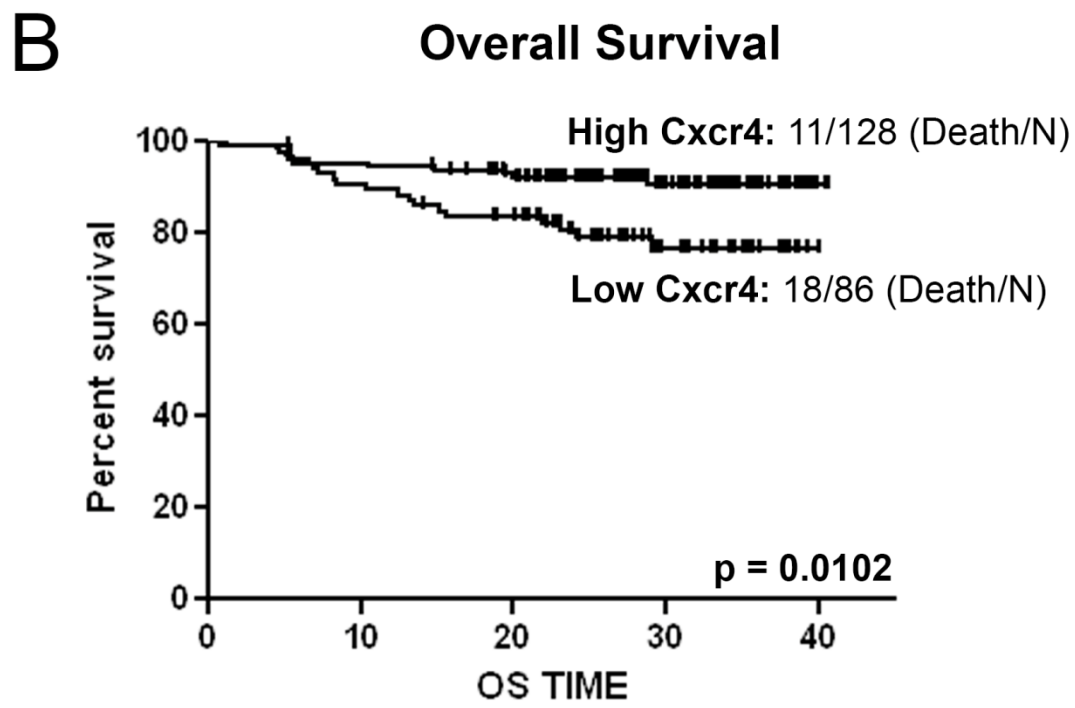
Overall Survival
High Cxcr4: 11/128 (Death/N)
Low Cxcr4: 18/86 (Death/N)
p = 0.0102
Percent survival
100
80
60
40
20
0
0
10
20
30
40
OS TIME

Supplemental Figure S4.

A. End-point RT-PCR analysis of *Xbp1* mRNA. Xbp1s (spliced) is represented by a 26 bp smaller spliced product compared to unspliced, Xbp1u. B. ELISA of intracellular Ig kappa light chain from lysates prepared following 72 hour LPS treatment. Cells were ficolled and incubated for an additional 24 hours. C. Array comparative genomic hybridization analysis highlighting the loss of light chain in the 589 BzR line.

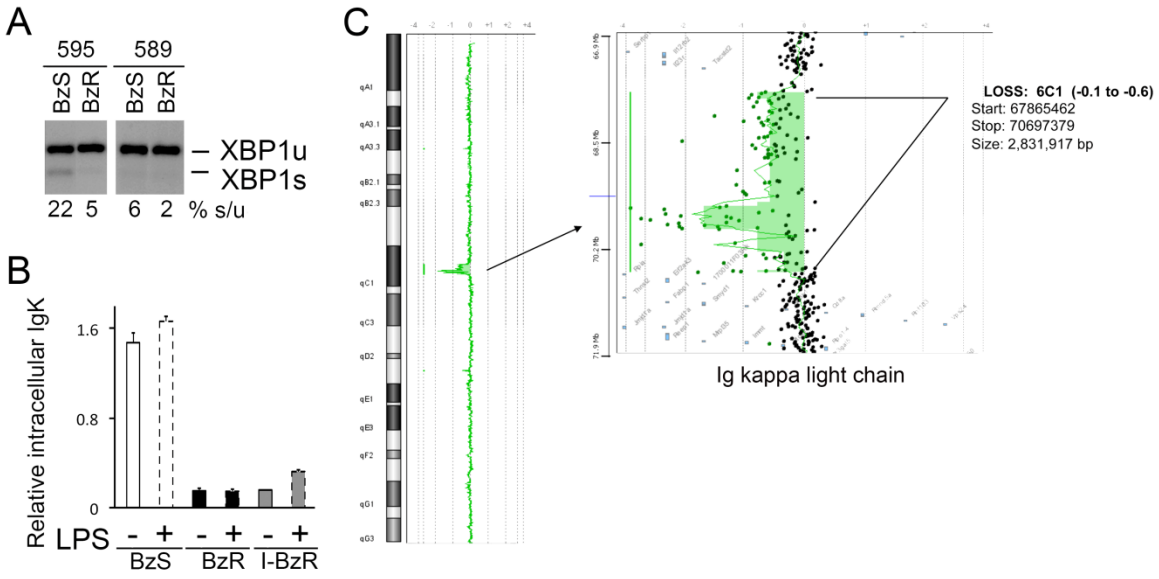
A
595
589
BzS
BzR
BzS
BzR
XBP1u
XBP1s
22 5 6 2 % s/u
B
Relative intracellular IgK
1.6
0.8
0
LPS - + - + - +
BzS
BzR
I-BzR
C
LOSS: 6C1 (-0.1 to -0.6)
Start: 67865462
Stop: 70697379
Size: 2,831,917 bp
Ig kappa light chain

Supplemental Figure S5.

A. Quantitative RT-PCR analysis of *Cd93* mRNA in 589 untreated cells and 72 hour LPS-treated cells. Values were normalized to *Gapd* mRNA and error bars represent PCR triplicates. Significance was determined using a one-tailed Student's t-test (*** $p < 0.001$). B. Fluorescence-activated cell sorting analysis of untreated BzS (top panel), BzR (middle panel) and I-BzR (bottom panel) and LPS-treated cells stained with CD93 and CD38.

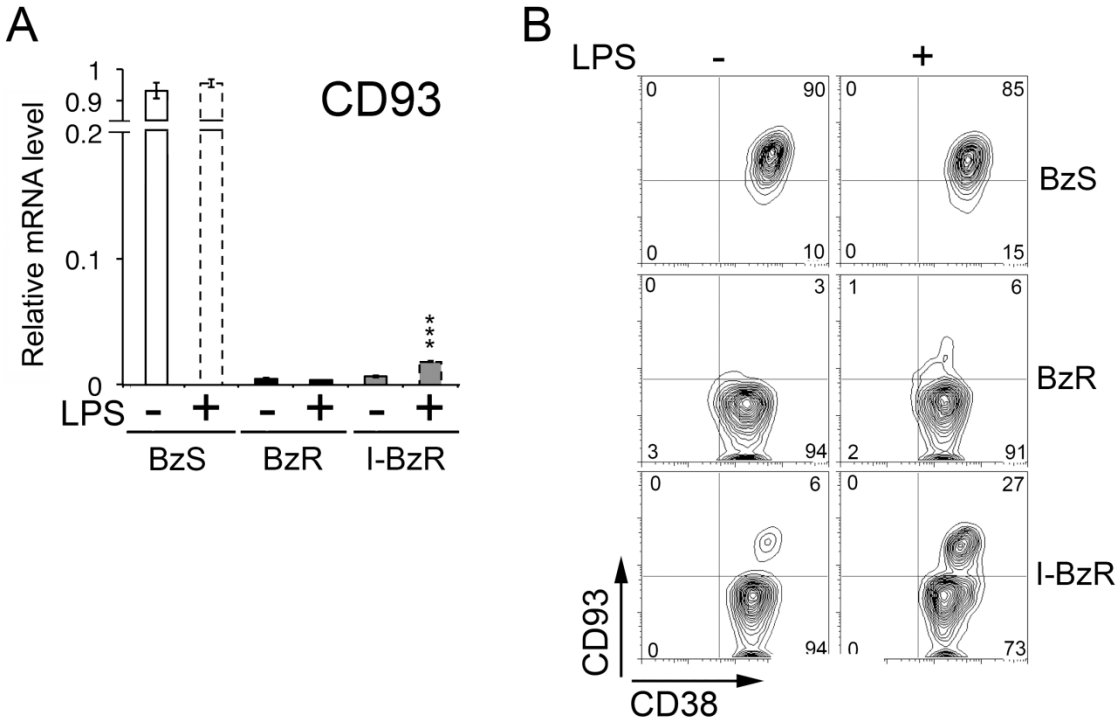
A
CD93
Relative mRNA level
1
0.9
0.2
0.1
0
***
LPS - + - + - +
BzS
BzR
I-BzR
B
LPS - +
0 90
0 10
0 85
0 15
BzS
0 3
3 94
1 6
2 91
BzR
0 6
0 94
0 27
0 73
I-BzR
CD93
CD38

CHAPTER 6

STABILIZATION OF AID BY BORTEZOMIB IN A BURKITT LYMPHOMA CELL LINE

Holly A. F. Stessman[1], Aatif Mansoor[1], Michael A. Linden[2], Brian G. Van Ness[1], Linda B. Baughn[1]*

From the [1]Department of Genetics, Cell Biology and Development and [2]Department of Laboratory Medicine and Pathology, University of Minnesota, Minneapolis, MN, USA.

Manuscript submitted for publication.

AUTHOR CONTRIBUTIONS

H. A. F. S. designed and performed *in vitro* experiments and wrote the manuscript.

A. M. performed *in vitro* experiments, designed the figure, and contributed to writing the manuscript.

M. A. L. edited the manuscript.

B. G. V. N. edited the manuscript.

L. B. B. designed the study, oversaw the project, performed *in vitro* experiments, and contributed to writing the manuscript.

ABSTRACT

Activation induced cytidine deaminase (AID) is a DNA-mutating enzyme that can promote the deamination of cytosine bases within single-stranded DNA, a function that is necessary for successful class switch recombination and somatic hypermutation but has been linked with acquired drug resistance in B cell malignancy. Burkitt lymphoma (BL), a type of non-Hodgkin lymphoma, shares many characteristics with germinal center B cells including the expression of AID. Previous work suggests that inhibition of the proteasome prevents AID degradation within BL cells. With the advent of proteasome inhibitors as a successful treatment for other B cell malignancies, the cellular consequences of AID stabilization by such compounds in BL may contribute to off-target mutations, potentially resulting in drug resistance. Here, we utilize a well-described, human BL cell line to show that short-term stabilization of AID protein does occur following treatment with a clinically relevant proteasome inhibitor, bortezomib (Bz). However, we find less on-target AID activity and no off-target mutations at the Bz active site following long-term Bz treatment. These results suggest that although AID is stabilized in the short-term by Bz, AID activity may be selected against by Bz and does not likely contribute to reduced Bz sensitivity in this case.

LETTER TO THE EDITOR

Burkitt lymphoma (BL) is a form of non-Hodgkin B cell lymphoma (NHL) that primarily affects children and is especially prevalent in endemic areas. Sporadic BL, the primary form of BL found in North America, accounts for 30-40% of all childhood NHL cases in the United States (449). A highly proliferative, clonal, B cell neoplasm, BL has characteristics of germinal center (GC) B cells including the expression of Bcl-6, CD10, IgM, and the DNA-mutating enzyme, activation induced cytidine deaminase (AID) (449). AID promotes mutagenesis by deamination of cytidine residues to uridines within single-stranded regions of DNA. The resultant G:U mismatch can be processed via replication, base excision repair, or mismatch repair in an error-prone manner.

On-target AID-induced mutations within the immunoglobulin (Ig) locus are necessary for the generation of a highly diverse antibody repertoire. AID induces a high rate of mutation both within the rearranged Ig variable region resulting in somatic hypermutation (SHM) and within switch regions enabling class switch recombination (CSR) (450). While it is known that AID prefers WRC/GYW hot spot motifs (showing the top and bottom strands where W=A/T, R=A/G, Y=C/T), the complete AID targeting mechanism remains unclear. Mistargeting of AID can promote mutations in off-target (non-Ig) genes such as proto-oncogenes and contribute to chromosomal translocations like those involving c-myc/IgH frequently associated with BL as well as other B cell malignancies (451, 452). Due to the mutagenic activity of AID, its expression is normally restricted to GC B cells. However, aberrant AID expression has been identified in malignant non-GC B cells and solid tumors (453). Approximately 85% of NHLs are thought to be a result of AID-induced mutations (454), and recently, multiple lines of evidence have suggested that aberrant expression of AID in cancer may contribute to

drug resistance. For example, in chronic myeloid leukemia, AID promotes imatinib mesylate/GLEEVEC® resistance through off-target mutagenesis within the BCR-ABL-1 target gene (455) demonstrating the important role that AID mistargeting plays in promoting B cell tumorigenesis and the acquisition of drug resistance, further underscoring the importance of its strict regulation.

The proteasome plays an essential role in regulating the nuclear abundance of AID by degrading excess AID protein (456, 457). This is especially important given that the dose of AID has been correlated with its level of mutagenic activity, particularly its ability to transform lymphocytes (458). Chemical inhibition of the 26S proteasome complex has been shown to stabilize AID protein (457). However, because the proteasome is also necessary for the degradation of regulatory proteins required for cellular homeostasis, targeting this complex has become a viable chemotherapeutic approach for cancer treatment. The boronic acid dipeptide, bortezomib/VELCADE® (Bz), was the first clinically approved reversible, specific inhibitor of the proteasome (459). Since its discovery, Bz has been primarily used in the treatment of multiple myeloma and relapsed mantle cell lymphoma but has also been tested for efficacy in other B cell malignancies including BL.

While Bz promotes cell cycle arrest and apoptosis by preventing the proteasomal degradation of cellular proteins, the specific mode of action for Bz toxicity remains unclear (459). Furthermore, patients treated with Bz eventually relapse due to drug resistance (459). Thus, it is critical that the cellular consequences of Bz treatment be deciphered in order to understand its mode of action and to develop novel approaches to combat drug resistance. Mutations have been identified within the active site of the proteasomal subunit *PSMB5*, the target of Bz, in *in vitro* models of Bz resistance (202)

suggesting that this could be a molecular mechanism for acquired resistance. The most common of these mutations, which result in substitutions of Ala49 and Ala50 within the PSMB5 protein occurs within AID hotspots (Supplemental Figure 1). Therefore, we hypothesize that the stabilization of AID protein upon Bz treatment may promote off-target mutations that contribute to acquired Bz resistance.

Here, we have utilized a previously published subclone of the AID-expressing, human BL cell line, Ramos 6 (Ramos), as a model system for this study (460). This cell line contains a nonsense mutation within the variable region of the Ig heavy chain gene, and can be used to monitor AID on-target activity by reversion of the mutation detected by surface IgM expression. As predicted, Ramos cells were highly sensitive to Bz-induced apoptosis *in vitro* (IC_{50}=11 nM) (Supplemental Figure 2A).

Because AID is degraded by the proteasome (456) we asked whether Bz treatment results in stabilization of AID protein. Ramos cells were treated with the indicated concentrations of Bz for 24 hours, and only viable cells were gated and analyzed for intracellular AID protein by flow cytometry. Bz treatment increased AID levels above the untreated control up to 2-fold in the 20 nM Bz treated samples (Figure 1A). Western blotting of the 0 and 10 nM treated cells, (Supplemental Figure 2A), also showed an approximate 2-fold increase in intracellular AID following Bz treatment (Figure 1B). The 20 nM Bz treated sample was eliminated from the Western analysis due to large-scale cell death. Cellular protein fractionation of the cytoplasmic and nuclear compartments showed that increased AID expression was present in both locations (data not shown). Quantitative RT-PCR did not show increased *AID* transcript following Bz treatment (data not shown), indicating that short-term proteasome inhibition

by Bz results in the stabilization of AID protein independent of transcriptional expression changes.

To analyze whether chronic long-term Bz treatment influences AID activity, Ramos cells were pulsed with 15 nM Bz, allowed to grow for one week, and the cycle was repeated for a total of ten weeks. Subsequently, IgM reversion (surface IgM^- to IgM^+) was measured as a marker of AID on-target activity (460). Because IgM^- and IgM^+ Ramos cells display similar Bz IC_{50} values (data not shown), differences in IgM reversion suggest alterations in AID activity. As expected, untreated Ramos cells showed increased surface IgM expression as a result of AID-dependent reversion of the nonsense mutation within the variable region of the heavy chain gene. Surprisingly, no reversion was observed in chronic Bz-treated (BzR) cells compared to untreated controls (Figure 1C) despite increases in AID levels during short-term Bz treatment (Figure 1B). Consistent with these results, when variable regions from the total cell pool were amplified, sequenced and scored for unique V region mutations (460), BzR cells had significantly fewer point mutations at the on-target IgM locus than their untreated Ramos counterparts (Figure 1D). In addition, BzR cells had reduced sensitivity to Bz compared to untreated controls with a 2.3-fold increase in the IC_{50} (Table I, Supplemental Figure 2B), yet displayed growth characteristics similar to the parental Ramos line (Supplemental Figure 2C). In this model system, reduced sensitivity to Bz also conferred a general reduced sensitivity to other proteasome inhibitors (carfilzomib/KYPROLIS®, MLN2238, and epoxomicin; Table I), while maintaining sensitivity to other classes of chemotherapeutic agents (data not shown). Array comparative genomic hybridization of these Bz-sensitive and BzR cells indicated the

presence of many copy number variations (data not shown), suggesting that genetic alterations had occurred or had been selected for as a result of Bz treatment.

To determine whether stabilization of AID by long-term Bz selection results in increased mutation frequency of *PSMB5*, we sequenced this off-target gene that when mutated confers reduced sensitivity to Bz. Despite the presence of AID hotspots, we identified no mutations within the off-target *PSMB5* gene in BzR cells (data not shown) that could explain their reduced Bz sensitivity. These data suggest that although there is ongoing genomic instability in chronically treated AID expressing Ramos BzR cells, AID stabilization by proteasome inhibition does not promote *IgM* or *PSMB5* mutations.

The data presented here show that proteasome inhibition of Ramos cells using Bz increases the abundance of intracellular AID. This AID is expressed both in the cytoplasmic but most importantly in the nuclear compartment where AID-induced damage is known to occur (450). However, this stabilization is likely short-term, as long-term chronically Bz treated cells do not express higher baseline levels of AID protein (data not shown) and lack increased AID activity at the on-target *IgM* locus. These results indicate that an interesting paradigm may be emerging where ongoing AID-induced DNA damage may be selected against under the pressure of Bz treatment. Indeed, AID expression has been shown to render B cells sensitive to apoptosis [(461)], thus it is possible that the AID-high, mutated Ramos cells were selectively eliminated from our chronically treated Ramos pool.

Bz is most commonly used to treat the B cell malignancy multiple myeloma (459), a plasma cell tumor of differentiated B cells that normally do not retain expression of AID, which is generally restricted to GC B cells (451). However, AID is a member of a larger superfamily of enzymes called cytidine deaminases which include the APOBEC

family of proteins. Having similar function to AID, the expression of APOBECs has been identified in a variety of solid tumors (462). Therefore, with current clinical trials aiming to utilize Bz for the treatment of a variety of tumors (459), determining what role, if any, APOBECs play in acquired Bz resistance may be an important future aim.

Table I. IC_{50} table comparing Bz-sensitive and -selected Ramos 6 cell lines.

Drug	**Fold increase in IC_{50} (Bz selected/sensitive)**
Bortezomib	2.3
Carfilzomib	3.0
MLN2238	2.0
Epoxomicin	3.3

Figure 1. Bz treatment results in AID protein stabilization but lower mutation frequency over long-term selection. A) Flow cytometry of intracellular AID protein following 24 hour Bz treatment with 0 (black line), 10 (dark gray line), or 20 (light gray line) nM Bz. All samples were normalized to an isotype control (filled gray peak) and quantified using FlowJo software (shown to the right). B) Western blotting of the 0 and 10 nM treated whole-cell lysates for AID normalized to β-actin expression at each Bz concentration quantified using Image Lab software (shown below). C) Surface IgM protein detected by flow cytometry on Ramos cells at weeks 0, 2, 10 and 17 over the course of weekly, 15 nM Bz treatments (total of ten weeks) compared to an untreated control. D) AID mutation frequency (number of mutations per total number of bases sequenced) within the variable region of the heavy chain locus between Ramos and RamosBzR cell lines. A total of 9522 bases were sequenced from untreated Ramos and 9108 bases were sequenced from chronically treated RamosBzR cells. Significance was determined using Pearson's chi-squared test where a p-value<0.05 was considered significant.

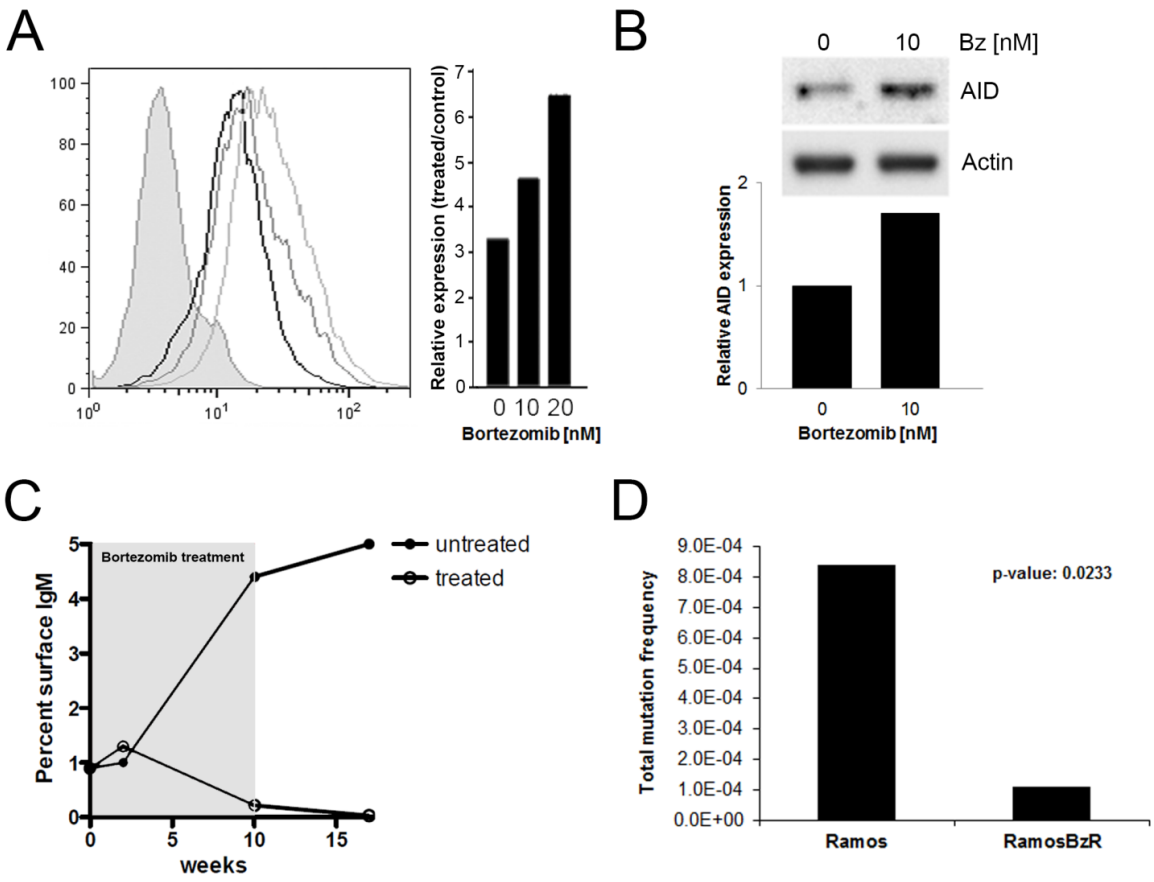
A
100
80
60
40
20
0
10^0
10^1
10^2
Relative expression (treated/control)
7
6
5
4
3
2
1
0
0 10 20
Bortezomib [nM]
B
0
10
Bz [nM]
AID
Actin
Relative AID expression
2
1
0
0
10
Bortezomib [nM]
C
Bortezomib treatment
untreated
treated
Percent surface IgM
5
4
3
2
1
0
0
5
10
15
weeks
D
Total mutation frequency
9.0E-04
8.0E-04
7.0E-04
6.0E-04
5.0E-04
4.0E-04
3.0E-04
2.0E-04
1.0E-04
0.0E+00
p-value: 0.0233
Ramos
RamosBzR

Supplemental Figure S1. Mutations identified in PSMB5 lie within predicted AID hotspots. Mutations identified previously (202) within the *PSMB5* gene target of Bz-selected cells. GCA and GCG code for Ala49 and Ala50, respectively, and are important for the chymotrypsin-like activity of PSMB5. The single mutations G322A and C323T as well as the combination of both mutations (highlighted in gray) identified lie in AID hotspots (460) (underlined), and, therefore, could be the result of off-target AID activity.

WT	GGC*G*CAG*C*GGAT
G322A	GGC*A*CAG*C*GGAT within the GCA hotspot
C323T	GGC*GT*AG*C*GGAT adjacent to the GCA hotspot
G322A/C326T	GGC*A*CAG*T*GGAT within both GCA and AGC hotspot

Supplemental Figure S2. Bz is cytotoxic to Ramos cells. A) Annexin V/propidium iodide (PI) analysis of Ramos cells treated with the indicated doses (left) of Bz for 48 hours. Analyses of cell cycle percentages (left panels) and percentages of cells that are Annexin V^+/PI^+ (right panels) at each concentration were performed using FlowJo software. B) Kill curve analysis of Ramos (filled circles) and RamosBzR (open circles) cell lines using the indicated doses of Bz over the course of 48 hours. All experiments were performed in triplicate and are shown as relative to an untreated control using GraphPad Prism software. C) PI analysis of Ramos and RamosBzR cells in the absence of Bz selection. Analysis of cell cycle percentages was performed using FlowJo software.

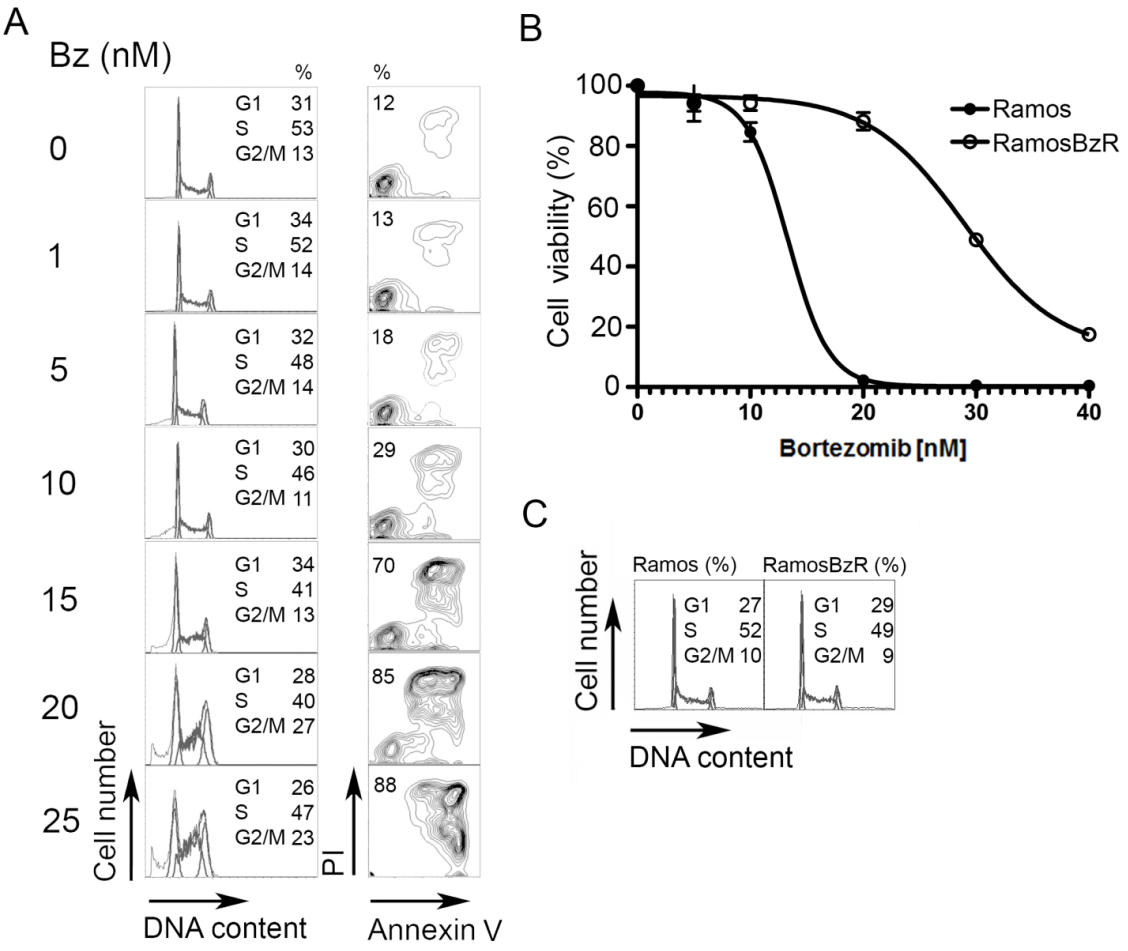
A
Bz (nM)
%
%
0
G1 31
S 53
G2/M 13
12
1
G1 34
S 52
G2/M 14
13
5
G1 32
S 48
G2/M 14
18
10
G1 30
S 46
G2/M 11
29
15
G1 34
S 41
G2/M 13
70
20
G1 28
S 40
G2/M 27
85
25
G1 26
S 47
G2/M 23
88
Cell number
PI
DNA content
Annexin V
B
Cell viability (%)
100
80
60
40
20
0
0
10
20
30
40
Bortezomib [nM]
Ramos
RamosBzR
C
Cell number
Ramos (%)
RamosBzR (%)
G1 27
S 52
G2/M 10
G1 29
S 49
G2/M 9
DNA content

Supplemental Methods and Methods

Protein extractions

Cellular protein fractionation was performed as a protocol adapted from the CellLytic NuCLEAR Extraction protocol (Sigma). Briefly, 5 x 10^6 cells were centrifuged at 450 x g for 5 minutes and washed twice with PBS. The pellet was resuspended in five times volume of isotonic lysis buffer (10 mM Tris-HCl, pH 7.5, 2 mM $MgCl_2$, 3 mM $CaCl_2$, and 0.3 M sucrose). The cells were lysed by the addition of 10% NP40 to 0.4%. Samples were centrifuged at 9000 x g for 30 seconds. Supernatants (cytoplasmic contents) were stored at -80° C. The remaining pellet was resuspended in nuclear extraction buffer (20 mM HEPES, pH 7.9, 1.5 mM $MgCl_2$, 0.6 M NaCl, 0.2 mM EDTA, 25% (w/v) glycerol, 10 mM DTT) supplemented with protease inhibitors. Samples were agitated on ice for 15 minutes and spun at 20,000 x g for 5 minutes at 4° C. Supernatants (nuclear contents) were stored at -80° C.

Whole-cell lysates were prepared by incubating cells in buffer containing 300 mM NaCl, 20 mM HEPES, 1 mM $MgCl_2$, 0.2% Nonidet P-40, 2.5 M glycerol, 1 mM DTT and complete protease inhibitor tablets.

AID expression

The following primers were used: AID, 5'-TCCTGCTCACTGGACTTCG-3' (5' primer), 5'-GCGTAGGAACAACAATTCCAC-3' (3' primer); Sybr green (Qiagen). The primers included in the Universal Human GAPD Gene Assay (Roche) were used as the reference gene. Data were analyzed using LightCycler 480 software (Roche) and relative fold changes were calculated using the $2^{-\Delta\Delta Ct}$ method with the GAPDH reference gene for normalization.

PCR Amplification, cloning and sequencing

The V region from Ramos cells were amplified using Pfu Turbo Cx Hotstart polymerase from genomic DNA by using 30 cycles of 95°C for 30 sec, 60°C for 30 sec and 72 °C for 1 min. Primers for the V region were 5'-TGTCTTCAGATCAGCAGCCTAAAG-3' (5' primer) and 5'-CATTCTTACCTGAGGAGACGGTG-3' (3' primer). PCR products were modified by A-tailing using Taq polymerase and cloned using the pGEM-T vector system. Minipreps were prepared and sequenced using the following V region primer: 5'-GCACAAGAACATGAAACACC-3'.

CHAPTER 7

DISCUSSION AND FUTURE AIMS

Cancer is a multi-faceted disease whose cure still remains elusive for the majority of cases. Although cancer-related deaths have decreased significantly over the past decade (463), there is still much that we do not understand about cancer, particularly how to eliminate minimal residual disease (MRD) that in most cases contributes to relapse and death. Of the cancer deaths that have been predicted for 2013, over 5% will likely be derived from a B cell of origin, of which, one-third will be MM patients (463). The elimination of MRD is particularly problematic in MM because these cells lack distinguishing and unique druggable targets compared to their normal PC counterparts (such as the Philadelphia chromosome in chronic myelogenous leukemia (464)). Therefore, further characterization of sensitivity and resistance to chemotherapeutic agents in MM is desperately needed for better personalized medicine approaches like those that are currently being used in some solid tumor types (*e.g.* Oncotype DX) (465). We believe that the culmination of these works specifically address this need and will contribute to the growing body of literature that will drive the utilization of new clinical approaches for the treatment of MM and other types of cancer.

For the majority of these studies, we have utilized a well-described mouse model of plasma cell malignancy to create a pipeline for secondary drug discovery which we present in Chapters 2 and 3. We have shown that we can isolate primary malignant mouse plasma cell lines in culture that can be further characterized and manipulated and injected back into syngeneic mice for *in vivo* validation of secondary therapies in the case of acquired Bz resistance. Importantly, this *in vivo* validation can be performed in

the presence of an active immune system. We currently have the only MM mouse model that harnesses this type of pipeline approach.

However, no model system is without limitations. For example, our mouse model likely only represents a subset of patients with aggressive disease and, therefore, does not allow us to study the entire genetic spectrum of MM patients. In addition, a current class of drugs that are being used regularly in the treatment of MM patients, the IMiDs, cannot be used in mice which lack the proper hepatic enzymes for drug activation. This further underscores the fact that homology is not 100% conserved between mice and humans meaning that we may identify genes that contribute to drug resistance in mice but not humans and perhaps some disease subsets but not others. However, the use of primary patient samples is also not trivial. Besides the rarity of MM patients, the process by which PCs are obtained from patients (*e.g.* bone marrow biopsy) involves a painful procedure that can produce sometimes only miniscule numbers of PCs. Furthermore, some have theorized that small "pockets" of clonal MM cells may reside at multiple independent sites within the bone marrow compartment (54, 110). Current reports regarding clonal evolution and the existence of potentially multiple MM clones within the same patient may further complicate the use of primary patient samples. We believe that given the advantages and disadvantages of both systems that the use of the mouse model provides the strongest tool for secondary drug discovery but that these new drugs must be further validated using patient data.

Within this mouse *in vitro* cell culture system, we use GEP to characterize how Bz-sensitive and -resistant cells respond differently to Bz treatment and use those data to predict secondary therapies that may be especially effective in combating refractory disease. Using CMAP we identified three distinct patterns of prediction: 1) drugs with

consistent correlation to the Bz-induced signature, 2) drugs with consistent anti-correlation to the Bz-induced signature, and 3) drugs with unique predictions in certain cell lines but not others to the unique Bz-induced signatures. Those drugs with consistent correlation within this study provided a nice proof-of-principle for the mechanism of Bz action. Indeed in Chapter 4, the investigation of the mode of action for the unknown compound VRC2 using correlating signatures from CMAP is proving particularly useful. Because the anti-correlated signatures are less well-described in the literature, we chose to investigate the utility of these predictions further in Chapter 4. Interestingly, the overlap of Topo inhibitors predicted by the CMAP approach and a high-throughput drug screening approach suggest that anti-correlated signatures might also have utility as secondary therapies in Bz-refractory MM. However, these studies are ongoing and need to be further validated using human MM cell lines and patient samples.

In Chapter 3, we show that perhaps those correlations with the most predictive power may be those with clear and conserved patterns of prediction in some but not all samples. In this study we highlighted a unique HDAC inhibitor correlation as predictive of an advantageous response to these drugs as secondary therapies in some but not all Bz-refractory disease. The optimization of this pipeline could have tremendous pre-clinical impact. However, one current limitation of this approach is a lack of MM specificity within the CMAP database. Currently, this database is populated with transcriptional responses to many drugs using four, well-described solid tumor cell lines. MM, apart from not being a solid tumor, is a unique and complex disease that currently is not represented in CMAP. We propose, as a future aim of these studies, to create a MM CMAP database to refine the predictive power of this approach using a combination

of clinical trial and HMCL data that is publicly available (Figure 1). However, in this current climate of exponential genome technology advancement, the combination of these available data into a database may be increasingly difficult. As array technology becomes an approach of the past making way for RNA-seq and exome sequencing, our best approach may be to focus on recreating some of these data using these newer approaches which will require both money and time. However, we believe that these costs may provide a much larger benefit to the clinical community by providing a database that can continually be annotated with new patient data providing stronger predictive power.

We also identify that in the absence of drug treatment that Bz-sensitive and -resistant cells have different homing properties *in vivo* in Chapter 3. Where the Bz-sensitive cells created the characteristic bone marrow "hot spots" by PET imaging, the Bz-resistant cells were more dispersed and infiltrated the extramedullary tissues. This is particularly interesting given that extramedullary disease has been observed in Bz relapse in MM patients (187, 466). When we queried our GEP for differences that might explain changes in cell homing, we identified that *Cxcr4* expression was differentially expressed between Bz-sensitive and -resistant cells. In Chapter 5, we show that based on CXCR4 expression alone we can predict significant differences in survival in MM patients on a Bz-only drug regimen. Another cell type within MM cell patients that has shown decreased sensitivity to Bz and extramedullary homing properties is the clonotypic B cell-like population that some have proposed may serve as the MM CSC population. These cells are thought to express cell markers that are representative of a more GC B-cell-like origin including decreased expression of CXCR4 which, when expressed, aids in migration to the bone marrow compartment (447).

We show that decreased expression of CXCR4 is associated with both the loss of plasma cell maturation markers as well as an increase in TFs known to regulate the GC B-cell phenotype within our mouse model system. However, whether the starting population is heterogeneous and these cells are simply selected for or whether Bz itself is inducing such changes remains unknown. Perhaps in some cases, as is the case with the loss of CD93, both scenarios may contribute to the loss of this marker in Bz-resistant cells. We show that CD93 status, in the mouse system, can be used to isolate primary Bz-refractory cells. These innate resistant cells also show a loss of PC maturation markers and an increase in a GC B-cell-like immunophenotype, similar to acquired Bz-resistant cells. However, little work has been done comparing primary refractory disease (PRD) and refractory disease following drug treatment. If in fact these cell types are similar, our characterization of refractory disease may further inform the treatment of drug naïve patients that may be identified in advance as having PRD guiding clinicians toward alternative therapies. Regardless to whether PRD and refractory disease are similar or dissimilar, further characterization of these cells is needed to create diagnostic tests with the utility to distinguish both.

Additional studies have associated Bz resistance with changes in B-cell differentiation. Interestingly, in models of MCL, a pre-GC disease, the Bz-resistant phenotype was associated with the upregulation of the plasmacytic differentiation markers IRF4, CD38 and CD138, but this was not accompanied by a corresponding increase in Ig secretion (354). These data in combination with our own observations suggest that Bz-resistance may intersect at a GC-B cell-like stage of differentiation that can be reached by forward differentiation (in the case of MCL) or by reversion (in the case of MM). This phenotype may be similar to the proposed CSC, although how similar

has yet to be defined. However, if there is a Bz-resistant immunophenotype common to both MCL and MM, the further characterization of these cells may reveal unique druggable targets for the elimination of the CSC population and MRD.

Although Chapters 3 through 5 focused on the characterization of Bz-resistance and -sensitivity with the goal of identifying secondary therapies, Chapter 6 explores one potential mechanism by which Bz-resistance may be acquired in an additional type of B cell malignancy, BL. In this particular cell type, malignant cells retain the expression of the DNA mutator, AID, normally responsible for SHM and CSR in the GC B cell of origin. The expression of AID in BL has been associated with acquired Gleevec resistance due to off-target activity (455). We find that AID protein is stabilized by Bz treatment, but that AID activity may in fact be downregulated in those cells that survive long-term drug selection. In addition, even though AID hotspots were identified in the Bz active site, mutations at these sites did not contribute to reduced Bz sensitivity following long-term selection. It is, therefore, unlikely that AID contributes to Bz-resistance in NHLs where it is expressed. However, there have been recent reports of aberrant expression of AID in MM (467). The expression of AID in this case may be mediated by simulation from neighboring dendritic cells within the bone marrow niche. This increased expression of AID in MM cells has been shown to increase the amount of DSBs in both HMCLs and primary MM patient samples. Furthermore, related DNA-damaging enzymes, the APOBEC family, have been reported in many types of cancer and may contribute genomic instability that leads to drug resistance (468-470). These reports suggest that a more comprehensive study of the expression of AID and APOBEC proteins with regard to their potential contributions to acquired drug resistance and disease progression in MM is warranted.

The next decade of research, which will likely merge genomics with novel drug modeling, will surely provide exponentially greater amounts of information that may be utilized for more personalized clinical approaches. Already, researchers are collecting exome and copy number information in serial relapse samples from diagnosis to plasma cell leukemic stages in MM patients (356). However, the number of these samples remains small likely due to a lack of bioinformatic support which will be required to process the terabytes of information that may be collected for each patient. However, this is an obstacle that must be overcome given that the availability of genome sequencing to the general public is on the horizon and approaching quickly. Indeed, new approaches have shown that copy number variation can now be imputed from exome sequencing data (471), and new technologies may also allow methylation patterns to be detected during real-time sequencing (472). Implementation of these approaches may mean that RNA-seq experiments will provide exome sequencing, gene expression, copy number, and epigenetic information all in one run making each sample a gold mine of information. By combining these patient data into publicly available databases together with clinical treatment information, we will be able to identify signatures related to drug sensitivity and resistance (Figure 1). We might also glean information that helps us to better understand clonal evolution and how this might contribute to drug sensitivity in MM. However, tremendous foresight and planning will be required to organize and collect such data. Common platforms and techniques must be adopted. Also, we must consider carefully which reference sequence we will use for analyzing these data. For example, a comparison of each patient's tumor sample to their germline sequence may eliminate genetic factors that contribute to primary refractory disease. The potential of these combined approaches, although complex, will

provide a larger picture of the tumor genome that will inform the future treatment of MM patients, perhaps even providing, in some cases, a cure.

The culmination of the studies presented in this thesis would not have been possible without a team approach. Although I designed and organized these interactive projects, our *in vivo* mouse studies would not have been feasible without Dr. Siegfried Janz and our other colleagues at the University of Iowa, Carver College of Medicine. Similarly, the combined *in silico* and high-throughput drug screening approaches were made possible through collaborating laboratories within the University of Minnesota Computer Science and Engineering Department and at Penn State Hershey Medical Center. In creating this MM working group, we have utilized multiple areas of expertise to contribute preclinical data toward individualized medicine approaches in MM.

Figure 1. Proposed pipeline approach for therapy prediction in MM patients. A diagram depicting the potential application of the combined approaches used in this thesis for individualized medicine approaches for MM patients. All patients will receive a bone marrow (BM) biopsy at diagnosis (or relapse) from which plasma cells (PCs) will be isolated and analyzed by *in silico* (MM CMAP = Myeloma-specific Connectivity Map database) and high-throughput drug screening methodologies for combined signatures and predictions of effective therapeutic options. The serial collection of patient samples from diagnosis through each relapse will provide individualized therapeutic data for each patient while helping to populate the MM CMAP database creating greater predictive power with each enrolled patient.

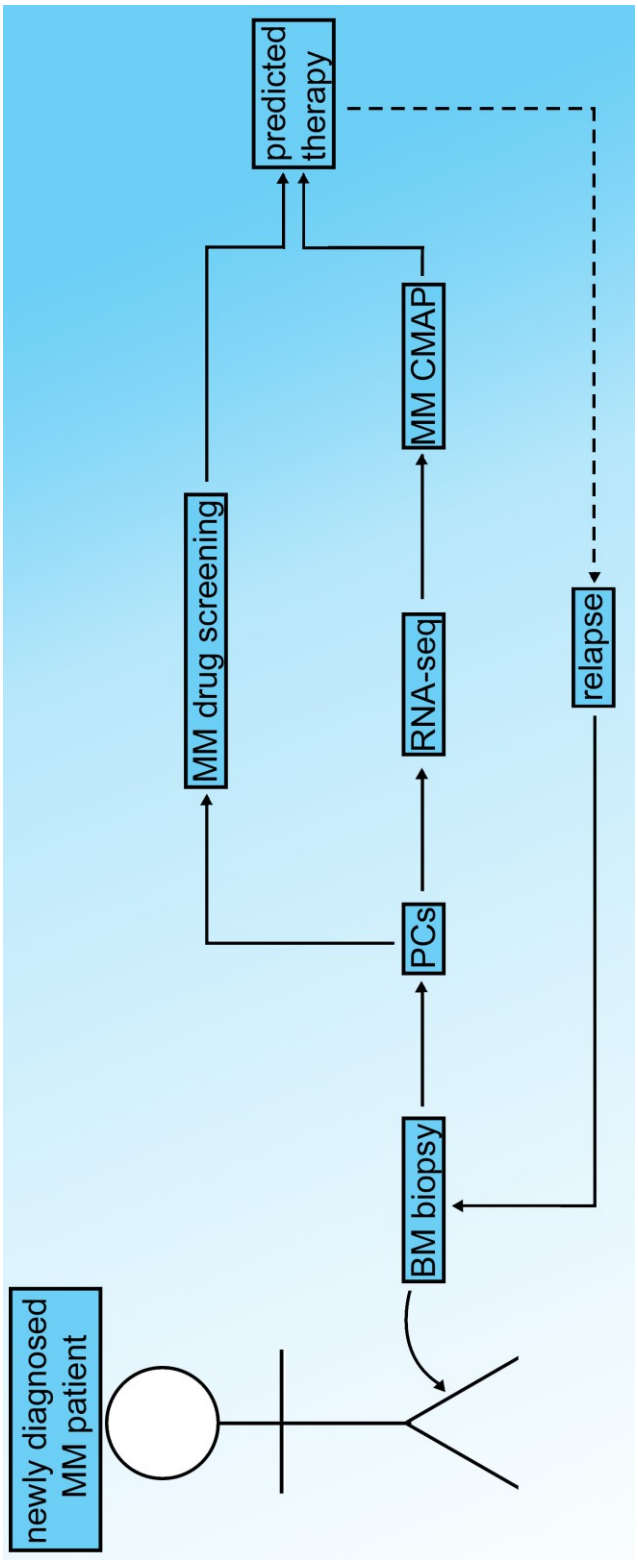
predicted therapy
MM drug screening
MM CMAP
RNA-seq
relapse
PCs
BM biopsy
newly diagnosed MM patient

BIBLIOGRAPHY

1. Johnson, K., Shapiro-Shelef, M., Tunyaplin, C., and Calame, K. 2005. Regulatory events in early and late B-cell differentiation. *Mol Immunol* 42:749-761.
2. Shaffer, A.L., Rosenwald, A., and Staudt, L.M. 2002. Lymphoid malignancies: the dark side of B-cell differentiation. *Nat Rev Immunol* 2:920-932.
3. Cooper, B. 2011. The origins of bone marrow as the seedbed of our blood: from antiquity to the time of Osler. *Proc (Bayl Univ Med Cent)* 24:115-118.
4. Rector, K., Liu, Y., and Van Zant, G. 2013. Comprehensive hematopoietic stem cell isolation methods. *Methods Mol Biol* 976:1-15.
5. Allman, D., Li, J., and Hardy, R.R. 1999. Commitment to the B lymphoid lineage occurs before DH-JH recombination. *J Exp Med* 189:735-740.
6. Li, Y.S., Wasserman, R., Hayakawa, K., and Hardy, R.R. 1996. Identification of the earliest B lineage stage in mouse bone marrow. *Immunity* 5:527-535.
7. Ogawa, M., ten Boekel, E., and Melchers, F. 2000. Identification of CD19(-)B220(+)c-Kit(+)Flt3/Flk-2(+)cells as early B lymphoid precursors before pre-B-I cells in juvenile mouse bone marrow. *Int Immunol* 12:313-324.
8. Kondo, M., Weissman, I.L., and Akashi, K. 1997. Identification of clonogenic common lymphoid progenitors in mouse bone marrow. *Cell* 91:661-672.
9. Wiken, M., Bjorck, P., Axelsson, B., and Perlmann, P. 1989. Studies on the role of CD43 in human B-cell activation and differentiation. *Scand J Immunol* 29:353-361.
10. Bassing, C.H., Swat, W., and Alt, F.W. 2002. The mechanism and regulation of chromosomal V(D)J recombination. *Cell* 109 Suppl:S45-55.
11. Fugmann, S.D., Lee, A.I., Shockett, P.E., Villey, I.J., and Schatz, D.G. 2000. The RAG proteins and V(D)J recombination: complexes, ends, and transposition. *Annu Rev Immunol* 18:495-527.
12. Hardy, R.R., Carmack, C.E., Shinton, S.A., Kemp, J.D., and Hayakawa, K. 1991. Resolution and characterization of pro-B and pre-pro-B cell stages in normal mouse bone marrow. *J Exp Med* 173:1213-1225.
13. Borghesi, L., Hsu, L.Y., Miller, J.P., Anderson, M., Herzenberg, L., Schlissel, M.S., Allman, D., and Gerstein, R.M. 2004. B lineage-specific regulation of V(D)J recombinase activity is established in common lymphoid progenitors. *J Exp Med* 199:491-502.
14. Johnson, K., Pflugh, D.L., Yu, D., Hesslein, D.G., Lin, K.I., Bothwell, A.L., Thomas-Tikhonenko, A., Schatz, D.G., and Calame, K. 2004. B cell-specific loss of histone 3 lysine 9 methylation in the V(H) locus depends on Pax5. *Nat Immunol* 5:853-861.
15. Mostoslavsky, R., Alt, F.W., and Bassing, C.H. 2003. Chromatin dynamics and locus accessibility in the immune system. *Nat Immunol* 4:603-606.
16. Nussenzweig, M.C., Shaw, A.C., Sinn, E., Danner, D.B., Holmes, K.L., Morse, H.C., 3rd, and Leder, P. 1987. Allelic exclusion in transgenic mice that express the membrane form of immunoglobulin mu. *Science* 236:816-819.
17. Krangel, M.S. 2003. Gene segment selection in V(D)J recombination: accessibility and beyond. *Nat Immunol* 4:624-630.

18. Franklin, A. 2006. Hypothesis: a biological role for germline transcription in the mechanism of V(D)J recombination--implications for initiation of allelic exclusion. *Immunol Cell Biol* 84:396-403.
19. Nossal, G.J. 1994. Negative selection of lymphocytes. *Cell* 76:229-239.
20. Gay, D., Saunders, T., Camper, S., and Weigert, M. 1993. Receptor editing: an approach by autoreactive B cells to escape tolerance. *J Exp Med* 177:999-1008.
21. Marculescu, R., Le, T., Simon, P., Jaeger, U., and Nadel, B. 2002. V(D)J-mediated translocations in lymphoid neoplasms: a functional assessment of genomic instability by cryptic sites. *J Exp Med* 195:85-98.
22. Boehm, T., Mengle-Gaw, L., Kees, U.R., Spurr, N., Lavenir, I., Forster, A., and Rabbitts, T.H. 1989. Alternating purine-pyrimidine tracts may promote chromosomal translocations seen in a variety of human lymphoid tumours. *EMBO J* 8:2621-2631.
23. Welzel, N., Le, T., Marculescu, R., Mitterbauer, G., Chott, A., Pott, C., Kneba, M., Du, M.Q., Kusec, R., Drach, J., et al. 2001. Templated nucleotide addition and immunoglobulin JH-gene utilization in t(11;14) junctions: implications for the mechanism of translocation and the origin of mantle cell lymphoma. *Cancer Res* 61:1629-1636.
24. Shapiro-Shelef, M., and Calame, K. 2005. Regulation of plasma-cell development. *Nat Rev Immunol* 5:230-242.
25. Martin, F., Oliver, A.M., and Kearney, J.F. 2001. Marginal zone and B1 B cells unite in the early response against T-independent blood-borne particulate antigens. *Immunity* 14:617-629.
26. Shaffer, A.L., Yu, X., He, Y., Boldrick, J., Chan, E.P., and Staudt, L.M. 2000. BCL-6 represses genes that function in lymphocyte differentiation, inflammation, and cell cycle control. *Immunity* 13:199-212.
27. Shaffer, A.L., Rosenwald, A., Hurt, E.M., Giltnane, J.M., Lam, L.T., Pickeral, O.K., and Staudt, L.M. 2001. Signatures of the immune response. *Immunity* 15:375-385.
28. MacLennan, I.C. 1994. Germinal centers. [Review]. *Annual Review of Immunology* 12:117-139.
29. Calame, K.L. 2001. Plasma cells: finding new light at the end of B cell development. *Nat Immunol* 2:1103-1108.
30. Martins, G., and Calame, K. 2008. Regulation and functions of Blimp-1 in T and B lymphocytes. *Annu Rev Immunol* 26:133-169.
31. Driver, D.J., McHeyzer-Williams, L.J., Cool, M., Stetson, D.B., and McHeyzer-Williams, M.G. 2001. Development and maintenance of a B220- memory B cell compartment. *J Immunol* 167:1393-1405.
32. Falini, B., Fizzotti, M., Pucciarini, A., Bigerna, B., Marafioti, T., Gambacorta, M., Pacini, R., Alunni, C., Natali-Tanci, L., Ugolini, B., et al. 2000. A monoclonal antibody (MUM1p) detects expression of the MUM1/IRF4 protein in a subset of germinal center B cells, plasma cells, and activated T cells. *Blood* 95:2084-2092.
33. Slifka, M.K., and Ahmed, R. 1998. Long-lived plasma cells: a mechanism for maintaining persistent antibody production. *Curr Opin Immunol* 10:252-258.
34. Sze, D.M., Toellner, K.M., Garcia de Vinuesa, C., Taylor, D.R., and MacLennan, I.C. 2000. Intrinsic constraint on plasmablast growth and extrinsic limits of plasma cell survival. *J Exp Med* 192:813-821.

35. Van Snick, J. 1990. Interleukin-6: an overview. *Annu Rev Immunol* 8:253-278.
36. Mittrucker, H.W., Matsuyama, T., Grossman, A., Kundig, T.M., Potter, J., Shahinian, A., Wakeham, A., Patterson, B., Ohashi, P.S., and Mak, T.W. 1997. Requirement for the transcription factor LSIRF/IRF4 for mature B and T lymphocyte function. *Science* 275:540-543.
37. Schliephake, D.E., and Schimpl, A. 1996. Blimp-1 overcomes the block in IgM secretion in lipopolysaccharide/anti-mu F(ab')2-co-stimulated B lymphocytes. *Eur J Immunol* 26:268-271.
38. Lin, K.I., Angelin-Duclos, C., Kuo, T.C., and Calame, K. 2002. Blimp-1-dependent repression of Pax-5 is required for differentiation of B cells to immunoglobulin M-secreting plasma cells. *Mol Cell Biol* 22:4771-4780.
39. Lin, K.I., Lin, Y., and Calame, K. 2000. Repression of c-myc is necessary but not sufficient for terminal differentiation of B lymphocytes in vitro. *Mol Cell Biol* 20:8684-8695.
40. Lin, Y., Wong, K., and Calame, K. 1997. Repression of c-myc transcription by Blimp-1, an inducer of terminal B cell differentiation. *Science* 276:596-599.
41. Shapiro-Shelef, M., Lin, K.I., McHeyzer-Williams, L.J., Liao, J., McHeyzer-Williams, M.G., and Calame, K. 2003. Blimp-1 is required for the formation of immunoglobulin secreting plasma cells and pre-plasma memory B cells. *Immunity* 19:607-620.
42. Martins, G.A., Cimmino, L., Shapiro-Shelef, M., Szabolcs, M., Herron, A., Magnusdottir, E., and Calame, K. 2006. Transcriptional repressor Blimp-1 regulates T cell homeostasis and function. *Nat Immunol* 7:457-465.
43. Shaffer, A.L., Lin, K.I., Kuo, T.C., Yu, X., Hurt, E.M., Rosenwald, A., Giltnane, J.M., Yang, L., Zhao, H., Calame, K., et al. 2002. Blimp-1 orchestrates plasma cell differentiation by extinguishing the mature B cell gene expression program. *Immunity* 17:51-62.
44. Reimold, A.M., Iwakoshi, N.N., Manis, J., Vallabhajosyula, P., Szomolanyi-Tsuda, E., Gravallese, E.M., Friend, D., Grusby, M.J., Alt, F., and Glimcher, L.H. 2001. Plasma cell differentiation requires the transcription factor XBP-1. *Nature* 412:300-307.
45. Lee, A.H., Iwakoshi, N.N., Anderson, K.C., and Glimcher, L.H. 2003. Proteasome inhibitors disrupt the unfolded protein response in myeloma cells. *Proc Natl Acad Sci U S A* 100:9946-9951.
46. Harding, H.P., Calfon, M., Urano, F., Novoa, I., and Ron, D. 2002. Transcriptional and translational control in the Mammalian unfolded protein response. *Annu Rev Cell Dev Biol* 18:575-599.
47. Iwakoshi, N.N., Lee, A.H., Vallabhajosyula, P., Otipoby, K.L., Rajewsky, K., and Glimcher, L.H. 2003. Plasma cell differentiation and the unfolded protein response intersect at the transcription factor XBP-1. *Nat Immunol* 4:321-329.
48. van Anken, E., Romijn, E.P., Maggioni, C., Mezghrani, A., Sitia, R., Braakman, I., and Heck, A.J. 2003. Sequential waves of functionally related proteins are expressed when B cells prepare for antibody secretion. *Immunity* 18:243-253.
49. Fujita, N., Jaye, D.L., Geigerman, C., Akyildiz, A., Mooney, M.R., Boss, J.M., and Wade, P.A. 2004. MTA3 and the Mi-2/NuRD complex regulate cell fate during B lymphocyte differentiation. *Cell* 119:75-86.

50. Shapiro-Shelef, M., Lin, K.I., Savitsky, D., Liao, J., and Calame, K. 2005. Blimp-1 is required for maintenance of long-lived plasma cells in the bone marrow. *J Exp Med* 202:1471-1476.
51. Alizadeh, A.A., Eisen, M.B., Davis, R.E., Ma, C., Lossos, I.S., Rosenwald, A., Boldrick, J.C., Sabet, H., Tran, T., Yu, X., et al. 2000. Distinct types of diffuse large B-cell lymphoma identified by gene expression profiling. *Nature* 403:503-511.
52. Lossos, I.S., Alizadeh, A.A., Eisen, M.B., Chan, W.C., Brown, P.O., Botstein, D., Staudt, L.M., and Levy, R. 2000. Ongoing immunoglobulin somatic mutation in germinal center B cell-like but not in activated B cell-like diffuse large cell lymphomas. *Proc Natl Acad Sci U S A* 97:10209-10213.
53. Rosenwald, A., Wright, G., Chan, W.C., Connors, J.M., Campo, E., Fisher, R.I., Gascoyne, R.D., Muller-Hermelink, H.K., Smeland, E.B., Giltnane, J.M., et al. 2002. The use of molecular profiling to predict survival after chemotherapy for diffuse large-B-cell lymphoma. *N Engl J Med* 346:1937-1947.
54. Shapiro-Shelef, M., and Calame, K. 2004. Plasma cell differentiation and multiple myeloma. *Curr Opin Immunol* 16:226-234.
55. Bakkus, M.H., Heirman, C., Van Riet, I., Van Camp, B., and Thielemans, K. 1992. Evidence that multiple myeloma Ig heavy chain VDJ genes contain somatic mutations but show no intraclonal variation. *Blood* 80:2326-2335.
56. Sahota, S.S., Leo, R., Hamblin, T.J., and Stevenson, F.K. 1997. Myeloma VL and VH gene sequences reveal a complementary imprint of antigen selection in tumor cells. *Blood* 89:219-226.
57. Hummel, M., Tamaru, J., Kalvelage, B., and Stein, H. 1994. Mantle cell (previously centrocytic) lymphomas express VH genes with no or very little somatic mutations like the physiologic cells of the follicle mantle. *Blood* 84:403-407.
58. Pelicci, P.G., Knowles, D.M., 2nd, Magrath, I., and Dalla-Favera, R. 1986. Chromosomal breakpoints and structural alterations of the c-myc locus differ in endemic and sporadic forms of Burkitt lymphoma. *Proc Natl Acad Sci U S A* 83:2984-2988.
59. Rabbitts, T.H., Hamlyn, P.H., and Baer, R. 1983. Altered nucleotide sequences of a translocated c-myc gene in Burkitt lymphoma. *Nature* 306:760-765.
60. Goossens, T., Klein, U., and Kuppers, R. 1998. Frequent occurrence of deletions and duplications during somatic hypermutation: implications for oncogene translocations and heavy chain disease. *Proc Natl Acad Sci U S A* 95:2463-2468.
61. Pasqualucci, L., Migliazza, A., Fracchiolla, N., William, C., Neri, A., Baldini, L., Chaganti, R.S.K., Klein, U., Kuppers, R., Rajewsky, K., et al. 1998. BCL-6 Mutations in Normal Germinal Center B Cells: Evidence of Somatic Hypermutation Acting Outside Ig Loci. *Proc Natl Acad Sci USA* 95:11816-11821.
62. Shen, H.M., Peters, A., Baron, B., Zhu, X., and Storb, U. 1998. Mutation of BCL-6 gene in normal B cells by the process of somatic hypermutation of Ig genes. *Science* 280:1750-1752.
63. Pasqualucci, L., Neumeister, P., Goossens, T., Nanjangud, G., Chaganti, R.S., Kuppers, R., and Dalla-Favera, R. 2001. Hypermutation of multiple proto-oncogenes in B-cell diffuse large-cell lymphomas. *Nature* 412:341-346.

64. Neri, A., Barriga, F., Knowles, D.M., Magrath, I.T., and Dalla-Favera, R. 1988. Different regions of the immunoglobulin heavy-chain locus are involved in chromosomal translocations in distinct pathogenetic forms of Burkitt lymphoma. *Proc Natl Acad Sci U S A* 85:2748-2752.
65. Bergsagel, P.L., Chesi, M., Nardini, E., Brents, L.A., Kirby, S.L., and Kuehl, W.M. 1996. Promiscuous translocations into immunoglobulin heavy chain switch regions in multiple myeloma. *Proc Natl Acad Sci U S A* 93:13931-13936.
66. Levens, D. 2002. Disentangling the MYC web. *Proc Natl Acad Sci U S A* 99:5757-5759.
67. Siegel, R., Naishadham, D., and Jemal, A. Cancer statistics, 2012. *CA Cancer J Clin* 62:10-29.
68. Solly, S. 1844. Remarks on the pathology of mollities ossium; with cases. *Med Chir Trans* 27:435-498 438.
69. Bence Jones, H. 1847. Chemical pathology. *Lancet* 2:88-92.
70. Wright, J.H. 1900. A Case of Multiple Myeloma. *J Boston Soc Med Sci* 4:195-204 195.
71. Edelman, G.M., and Gally, J.A. 1962. The nature of Bence-Jones proteins. Chemical similarities to polypetide chains of myeloma globulins and normal gamma-globulins. *J Exp Med* 116:207-227.
72. Longsworth, L.G., Shedlovsky, T., and Macinnes, D.A. 1939. Electrophoretic Patterns of Normal and Pathological Human Blood Serum and Plasma. *J Exp Med* 70:399-413.
73. Waldenstrom, J. 1961. Studies on conditions associated with disturbed gamma globulin formation (gammopathies). *Harvey Lectures* 56:211-231.
74. Kyle, R.A., and Rajkumar, S.V. 2004. Multiple myeloma. *N Engl J Med* 351:1860-1873.
75. Giuliani, N., Colla, S., Morandi, F., Lazzaretti, M., Sala, R., Bonomini, S., Grano, M., Colucci, S., Svaldi, M., and Rizzoli, V. 2005. Myeloma cells block RUNX2/CBFA1 activity in human bone marrow osteoblast progenitors and inhibit osteoblast formation and differentiation. *Blood* 106:2472-2483.
76. Standal, T., Abildgaard, N., Fagerli, U.M., Stordal, B., Hjertner, O., Borset, M., and Sundan, A. 2007. HGF inhibits BMP-induced osteoblastogenesis: possible implications for the bone disease of multiple myeloma. *Blood* 109:3024-3030.
77. Kyle, R.A., Gertz, M.A., Witzig, T.E., Lust, J.A., Lacy, M.Q., Dispenzieri, A., Fonseca, R., Rajkumar, S.V., Offord, J.R., Larson, D.R., et al. 2003. Review of 1027 patients with newly diagnosed multiple myeloma. *Mayo Clin Proc* 78:21-33.
78. Oyajobi, B.O. 2007. Multiple myeloma/hypercalcemia. *Arthritis Res Ther* 9 Suppl 1:S4.
79. Cohen, G., and Horl, W.H. 2009. Free immunoglobulin light chains as a risk factor in renal and extrarenal complications. *Semin Dial* 22:369-372.
80. Landgren, O., Kyle, R.A., Pfeiffer, R.M., Katzmann, J.A., Caporaso, N.E., Hayes, R.B., Dispenzieri, A., Kumar, S., Clark, R.J., Baris, D., et al. 2009. Monoclonal gammopathy of undetermined significance (MGUS) consistently precedes multiple myeloma: a prospective study. *Blood* 113:5412-5417.
81. Kyle, R.A., and Rajkumar, S.V. 2007. Monoclonal gammopathy of undetermined significance and smouldering multiple myeloma: emphasis on risk factors for progression. *Br J Haematol* 139:730-743.

82. Blade, J., Rosinol, L., Cibeira, M.T., and de Larrea, C.F. 2008. Pathogenesis and progression of monoclonal gammopathy of undetermined significance. *Leukemia* 22:1651-1657.
83. Kyle, R.A., Therneau, T.M., Rajkumar, S.V., Offord, J.R., Larson, D.R., Plevak, M.F., and Melton, L.J., 3rd. 2002. A long-term study of prognosis in monoclonal gammopathy of undetermined significance. *N Engl J Med* 346:564-569.
84. 2003. Criteria for the classification of monoclonal gammopathies, multiple myeloma and related disorders: a report of the International Myeloma Working Group. *Br J Haematol* 121:749-757.
85. Kyle, R.A., Remstein, E.D., Therneau, T.M., Dispenzieri, A., Kurtin, P.J., Hodnefield, J.M., Larson, D.R., Plevak, M.F., Jelinek, D.F., Fonseca, R., et al. 2007. Clinical course and prognosis of smoldering (asymptomatic) multiple myeloma. *N Engl J Med* 356:2582-2590.
86. Cesana, C., Klersy, C., Barbarano, L., Nosari, A.M., Crugnola, M., Pungolino, E., Gargantini, L., Granata, S., Valentini, M., and Morra, E. 2002. Prognostic factors for malignant transformation in monoclonal gammopathy of undetermined significance and smoldering multiple myeloma. *J Clin Oncol* 20:1625-1634.
87. Bartl, R., Frisch, B., Burkhardt, R., Fateh-Moghadam, A., Mahl, G., Gierster, P., Sund, M., and Kettner, G. 1982. Bone marrow histology in myeloma: its importance in diagnosis, prognosis, classification and staging. *Br J Haematol* 51:361-375.
88. Network, N.C.C. 2009. NCCN clinical practice guidelines in oncology. In *Multiple Myeloma*.
89. Zhan, F., Huang, Y., Colla, S., Stewart, J.P., Hanamura, I., Gupta, S., Epstein, J., Yaccoby, S., Sawyer, J., Burington, B., et al. 2006. The molecular classification of multiple myeloma. *Blood* 108:2020-2028.
90. Bartel, T.B., Haessler, J., Brown, T.L., Shaughnessy, J.D., Jr., van Rhee, F., Anaissie, E., Alpe, T., Angtuaco, E., Walker, R., Epstein, J., et al. 2009. F18-fluorodeoxyglucose positron emission tomography in the context of other imaging techniques and prognostic factors in multiple myeloma. *Blood* 114:2068-2076.
91. Abildgaard, N., Brixen, K., Eriksen, E.F., Kristensen, J.E., Nielsen, J.L., and Heickendorff, L. 2004. Sequential analysis of biochemical markers of bone resorption and bone densitometry in multiple myeloma. *Haematologica* 89:567-577.
92. Fonseca, R., Barlogie, B., Bataille, R., Bastard, C., Bergsagel, P.L., Chesi, M., Davies, F.E., Drach, J., Greipp, P.R., Kirsch, I.R., et al. 2004. Genetics and cytogenetics of multiple myeloma: a workshop report. *Cancer Res* 64:1546-1558.
93. Yeung, J., and Chang, H. 2008. Genomic aberrations and immunohistochemical markers as prognostic indicators in multiple myeloma. *J Clin Pathol* 61:832-836.
94. Smadja, N.V., Fruchart, C., Isnard, F., Louvet, C., Dutel, J.L., Cheron, N., Grange, M.J., Monconduit, M., and Bastard, C. 1998. Chromosomal analysis in multiple myeloma: cytogenetic evidence of two different diseases. *Leukemia* 12:960-969.
95. Fonseca, R., Bergsagel, P.L., Drach, J., Shaughnessy, J., Gutierrez, N., Stewart, A.K., Morgan, G., Van Ness, B., Chesi, M., Minvielle, S., et al. 2009. International Myeloma Working Group molecular classification of multiple myeloma: spotlight review. *Leukemia* 23:2210-2221.

96. Debes-Marun, C.S., Dewald, G.W., Bryant, S., Picken, E., Santana-Davila, R., Gonzalez-Paz, N., Winkler, J.M., Kyle, R.A., Gertz, M.A., Witzig, T.E., et al. 2003. Chromosome abnormalities clustering and its implications for pathogenesis and prognosis in myeloma. *Leukemia* 17:427-436.
97. Chng, W.J., Winkler, J.M., Greipp, P.R., Jalal, S.M., Bergsagel, P.L., Chesi, M., Trendle, M.C., Ahmann, G.J., Henderson, K., Blood, E., et al. 2006. Ploidy status rarely changes in myeloma patients at disease progression. *Leuk Res* 30:266-271.
98. Avet-Loiseau, H., Attal, M., Moreau, P., Charbonnel, C., Garban, F., Hulin, C., Leyvraz, S., Michallet, M., Yakoub-Agha, I., Garderet, L., et al. 2007. Genetic abnormalities and survival in multiple myeloma: the experience of the Intergroupe Francophone du Myelome. *Blood* 109:3489-3495.
99. Carrasco, D.R., Tonon, G., Huang, Y., Zhang, Y., Sinha, R., Feng, B., Stewart, J.P., Zhan, F., Khatry, D., Protopopova, M., et al. 2006. High-resolution genomic profiles define distinct clinico-pathogenetic subgroups of multiple myeloma patients. *Cancer Cell* 9:313-325.
100. Shaughnessy, J.D., Jr., Zhan, F., Burington, B.E., Huang, Y., Colla, S., Hanamura, I., Stewart, J.P., Kordsmeier, B., Randolph, C., Williams, D.R., et al. 2007. A validated gene expression model of high-risk multiple myeloma is defined by deregulated expression of genes mapping to chromosome 1. *Blood* 109:2276-2284.
101. Fonseca, R., Debes-Marun, C.S., Picken, E.B., Dewald, G.W., Bryant, S.C., Winkler, J.M., Blood, E., Oken, M.M., Santana-Davila, R., Gonzalez-Paz, N., et al. 2003. The recurrent IgH translocations are highly associated with nonhyperdiploid variant multiple myeloma. *Blood* 102:2562-2567.
102. Gabrea, A., Bergsagel, P.L., Chesi, M., Shou, Y., and Kuehl, W.M. 1999. Insertion of excised IgH switch sequences causes overexpression of cyclin D1 in a myeloma tumor cell. *Mol Cell* 3:119-123.
103. Shaughnessy, J., Jr., Gabrea, A., Qi, Y., Brents, L., Zhan, F., Tian, E., Sawyer, J., Barlogie, B., Bergsagel, P.L., and Kuehl, M. 2001. Cyclin D3 at 6p21 is dysregulated by recurrent chromosomal translocations to immunoglobulin loci in multiple myeloma. *Blood* 98:217-223.
104. Chesi, M., Nardini, E., Lim, R.S., Smith, K.D., Kuehl, W.M., and Bergsagel, P.L. 1998. The t(4;14) translocation in myeloma dysregulates both FGFR3 and a novel gene, MMSET, resulting in IgH/MMSET hybrid transcripts. *Blood* 92:3025-3034.
105. Chesi, M., Brents, L.A., Ely, S.A., Bais, C., Robbiani, D.F., Mesri, E.A., Kuehl, W.M., and Bergsagel, P.L. 2001. Activated fibroblast growth factor receptor 3 is an oncogene that contributes to tumor progression in multiple myeloma. *Blood* 97:729-736.
106. Chesi, M., Bergsagel, P.L., Shonukan, O.O., Martelli, M.L., Brents, L.A., Chen, T., Schrock, E., Ried, T., and Kuehl, W.M. 1998. Frequent dysregulation of the c-maf proto-oncogene at 16q23 by translocation to an Ig locus in multiple myeloma. *Blood* 91:4457-4463.
107. Hurt, E.M., Wiestner, A., Rosenwald, A., Shaffer, A.L., Campo, E., Grogan, T., Bergsagel, P.L., Kuehl, W.M., and Staudt, L.M. 2004. Overexpression of c-maf is

a frequent oncogenic event in multiple myeloma that promotes proliferation and pathological interactions with bone marrow stroma. *Cancer Cell* 5:191-199.
108. Bergsagel, P.L., Kuehl, W.M., Zhan, F., Sawyer, J., Barlogie, B., and Shaughnessy, J., Jr. 2005. Cyclin D dysregulation: an early and unifying pathogenic event in multiple myeloma. *Blood* 106:296-303.
109. Bergsagel, P.L., and Kuehl, W.M. 2005. Molecular pathogenesis and a consequent classification of multiple myeloma. *J Clin Oncol* 23:6333-6338.
110. Kuehl, W.M., and Bergsagel, P.L. 2002. Multiple myeloma: evolving genetic events and host interactions. *Nat Rev Cancer* 2:175-187.
111. Hanamura, I., Stewart, J.P., Huang, Y., Zhan, F., Santra, M., Sawyer, J.R., Hollmig, K., Zangarri, M., Pineda-Roman, M., van Rhee, F., et al. 2006. Frequent gain of chromosome band 1q21 in plasma-cell dyscrasias detected by fluorescence in situ hybridization: incidence increases from MGUS to relapsed myeloma and is related to prognosis and disease progression following tandem stem-cell transplantation. *Blood* 108:1724-1732.
112. Laubach, J., Richardson, P., and Anderson, K. 2011. Multiple myeloma. *Annu Rev Med* 62:249-264.
113. Derksen, P.W., Tjin, E., Meijer, H.P., Klok, M.D., MacGillavry, H.D., van Oers, M.H., Lokhorst, H.M., Bloem, A.C., Clevers, H., Nusse, R., et al. 2004. Illegitimate WNT signaling promotes proliferation of multiple myeloma cells. *Proc Natl Acad Sci U S A* 101:6122-6127.
114. Dutta-Simmons, J., Zhang, Y., Gorgun, G., Gatt, M., Mani, M., Hideshima, T., Takada, K., Carlson, N.E., Carrasco, D.E., Tai, Y.T., et al. 2009. Aurora kinase A is a target of Wnt/beta-catenin involved in multiple myeloma disease progression. *Blood* 114:2699-2708.
115. Davies, F.E., Dring, A.M., Li, C., Rawstron, A.C., Shammas, M.A., O'Connor, S.M., Fenton, J.A., Hideshima, T., Chauhan, D., Tai, I.T., et al. 2003. Insights into the multistep transformation of MGUS to myeloma using microarray expression analysis. *Blood* 102:4504-4511.
116. Tian, E., Zhan, F., Walker, R., Rasmussen, E., Ma, Y., Barlogie, B., and Shaughnessy, J.D., Jr. 2003. The role of the Wnt-signaling antagonist DKK1 in the development of osteolytic lesions in multiple myeloma. *N Engl J Med* 349:2483-2494.
117. Gonzalez-Paz, N., Chng, W.J., McClure, R.F., Blood, E., Oken, M.M., Van Ness, B., James, C.D., Kurtin, P.J., Henderson, K., Ahmann, G.J., et al. 2007. Tumor suppressor p16 methylation in multiple myeloma: biological and clinical implications. *Blood* 109:1228-1232.
118. Mitsiades, C.S., Mitsiades, N.S., McMullan, C.J., Poulaki, V., Shringarpure, R., Hideshima, T., Akiyama, M., Chauhan, D., Munshi, N., Gu, X., et al. 2004. Transcriptional signature of histone deacetylase inhibition in multiple myeloma: biological and clinical implications. *Proc Natl Acad Sci U S A* 101:540-545.
119. Pichiorri, F., Suh, S.S., Ladetto, M., Kuehl, M., Palumbo, T., Drandi, D., Taccioli, C., Zanesi, N., Alder, H., Hagan, J.P., et al. 2008. MicroRNAs regulate critical genes associated with multiple myeloma pathogenesis. *Proc Natl Acad Sci U S A* 105:12885-12890.
120. Smith, E.M., Boyd, K., and Davies, F.E. 2010. The potential role of epigenetic therapy in multiple myeloma. *Br J Haematol* 148:702-713.

121. Keats, J.J., Fonseca, R., Chesi, M., Schop, R., Baker, A., Chng, W.J., Van Wier, S., Tiedemann, R., Shi, C.X., Sebag, M., et al. 2007. Promiscuous mutations activate the noncanonical NF-kappaB pathway in multiple myeloma. *Cancer Cell* 12:131-144.
122. Bezieau, S., Devilder, M.C., Avet-Loiseau, H., Mellerin, M.P., Puthier, D., Pennarun, E., Rapp, M.J., Harousseau, J.L., Moisan, J.P., and Bataille, R. 2001. High incidence of N and K-Ras activating mutations in multiple myeloma and primary plasma cell leukemia at diagnosis. *Hum Mutat* 18:212-224.
123. Carrasco, D.R., Sukhdeo, K., Protopopova, M., Sinha, R., Enos, M., Carrasco, D.E., Zheng, M., Mani, M., Henderson, J., Pinkus, G.S., et al. 2007. The differentiation and stress response factor XBP-1 drives multiple myeloma pathogenesis. *Cancer Cell* 11:349-360.
124. Boylan, K.L., Gosse, M.A., Staggs, S.E., Janz, S., Grindle, S., Kansas, G.S., and Van Ness, B.G. 2007. A transgenic mouse model of plasma cell malignancy shows phenotypic, cytogenetic, and gene expression heterogeneity similar to human multiple myeloma. *Cancer Res* 67:4069-4078.
125. Chesi, M., Robbiani, D.F., Sebag, M., Chng, W.J., Affer, M., Tiedemann, R., Valdez, R., Palmer, S.E., Haas, S.S., Stewart, A.K., et al. 2008. AID-dependent activation of a MYC transgene induces multiple myeloma in a conditional mouse model of post-germinal center malignancies. *Cancer Cell* 13:167-180.
126. Shaffer, A.L., Emre, N.C., Lamy, L., Ngo, V.N., Wright, G., Xiao, W., Powell, J., Dave, S., Yu, X., Zhao, H., et al. 2008. IRF4 addiction in multiple myeloma. *Nature* 454:226-231.
127. Shaffer, A.L., Emre, N.C., Romesser, P.B., and Staudt, L.M. 2009. IRF4: Immunity. Malignancy! Therapy? *Clin Cancer Res* 15:2954-2961.
128. Hoogstraten, B., Sheehe, P.R., Cuttner, J., Cooper, T., Kyle, R.A., Oberfield, R.A., Townsend, S.R., Harley, J.B., Hayes, D.M., Costa, G., et al. 1967. Melphalan in multiple myeloma. *Blood* 30:74-83.
129. Oken, M.M., Harrington, D.P., Abramson, N., Kyle, R.A., Knospe, W., and Glick, J.H. 1997. Comparison of melphalan and prednisone with vincristine, carmustine, melphalan, cyclophosphamide, and prednisone in the treatment of multiple myeloma: results of Eastern Cooperative Oncology Group Study E2479. *Cancer* 79:1561-1567.
130. Alexanian, R., Haut, A., Khan, A.U., Lane, M., McKelvey, E.M., Migliore, P.J., Stuckey, W.J., Jr., and Wilson, H.E. 1969. Treatment for multiple myeloma. Combination chemotherapy with different melphalan dose regimens. *JAMA* 208:1680-1685.
131. 1998. Combination chemotherapy versus melphalan plus prednisone as treatment for multiple myeloma: an overview of 6,633 patients from 27 randomized trials. Myeloma Trialists' Collaborative Group. *J Clin Oncol* 16:3832-3842.
132. Koreth, J., Cutler, C.S., Djulbegovic, B., Behl, R., Schlossman, R.L., Munshi, N.C., Richardson, P.G., Anderson, K.C., Soiffer, R.J., and Alyea, E.P., 3rd. 2007. High-dose therapy with single autologous transplantation versus chemotherapy for newly diagnosed multiple myeloma: A systematic review and meta-analysis of randomized controlled trials. *Biol Blood Marrow Transplant* 13:183-196.

133. Bensinger, W.I. 2002. Allogeneic hematopoietic cell transplantation for multiple myeloma. *Biomed Pharmacother* 56:133-138.
134. Maloney, D.G., Molina, A.J., Sahebi, F., Stockerl-Goldstein, K.E., Sandmaier, B.M., Bensinger, W., Storer, B., Hegenbart, U., Somlo, G., Chauncey, T., et al. 2003. Allografting with nonmyeloablative conditioning following cytoreductive autografts for the treatment of patients with multiple myeloma. *Blood* 102:3447-3454.
135. Samson, D., Gaminara, E., Newland, A., Van de Pette, J., Kearney, J., McCarthy, D., Joyner, M., Aston, L., Mitchell, T., Hamon, M., et al. 1989. Infusion of vincristine and doxorubicin with oral dexamethasone as first-line therapy for multiple myeloma. *Lancet* 2:882-885.
136. Dimopoulos, M.A., San-Miguel, J.F., and Anderson, K.C. 2011. Emerging therapies for the treatment of relapsed or refractory multiple myeloma. *Eur J Haematol* 86:1-15.
137. Anderson, K.C. 2005. Lenalidomide and thalidomide: mechanisms of action--similarities and differences. *Semin Hematol* 42:S3-8.
138. Anargyrou, K., Dimopoulos, M.A., Sezer, O., and Terpos, E. 2008. Novel anti-myeloma agents and angiogenesis. *Leuk Lymphoma* 49:677-689.
139. Palumbo, A., Bringhen, S., Caravita, T., Merla, E., Capparella, V., Callea, V., Cangialosi, C., Grasso, M., Rossini, F., Galli, M., et al. 2006. Oral melphalan and prednisone chemotherapy plus thalidomide compared with melphalan and prednisone alone in elderly patients with multiple myeloma: randomised controlled trial. *Lancet* 367:825-831.
140. Rajkumar, S.V., Blood, E., Vesole, D., Fonseca, R., and Greipp, P.R. 2006. Phase III clinical trial of thalidomide plus dexamethasone compared with dexamethasone alone in newly diagnosed multiple myeloma: a clinical trial coordinated by the Eastern Cooperative Oncology Group. *J Clin Oncol* 24:431-436.
141. Chauhan, D., Singh, A.V., Aujay, M., Kirk, C.J., Bandi, M., Ciccarelli, B., Raje, N., Richardson, P., and Anderson, K.C. 2010. A novel orally active proteasome inhibitor ONX 0912 triggers in vitro and in vivo cytotoxicity in multiple myeloma. *Blood* 116:4906-4915.
142. Hideshima, T., Mitsiades, C., Akiyama, M., Hayashi, T., Chauhan, D., Richardson, P., Schlossman, R., Podar, K., Munshi, N.C., Mitsiades, N., et al. 2003. Molecular mechanisms mediating antimyeloma activity of proteasome inhibitor PS-341. *Blood* 101:1530-1534.
143. Hideshima, T., Richardson, P., Chauhan, D., Palombella, V.J., Elliott, P.J., Adams, J., and Anderson, K.C. 2001. The proteasome inhibitor PS-341 inhibits growth, induces apoptosis, and overcomes drug resistance in human multiple myeloma cells. *Cancer Res* 61:3071-3076.
144. LeBlanc, R., Catley, L.P., Hideshima, T., Lentzsch, S., Mitsiades, C.S., Mitsiades, N., Neuberg, D., Goloubeva, O., Pien, C.S., Adams, J., et al. 2002. Proteasome inhibitor PS-341 inhibits human myeloma cell growth in vivo and prolongs survival in a murine model. *Cancer Res* 62:4996-5000.
145. Richardson, P.G., Sonneveld, P., Schuster, M.W., Irwin, D., Stadtmauer, E.A., Facon, T., Harousseau, J.L., Ben-Yehuda, D., Lonial, S., Goldschmidt, H., et al.

2005. Bortezomib or high-dose dexamethasone for relapsed multiple myeloma. *N Engl J Med* 352:2487-2498.
146. Dispenzieri, A., and Kyle, R.A. 2005. Neurological aspects of multiple myeloma and related disorders. *Best Pract Res Clin Haematol* 18:673-688.
147. Richardson, P.G., Briemberg, H., Jagannath, S., Wen, P.Y., Barlogie, B., Berenson, J., Singhal, S., Siegel, D.S., Irwin, D., Schuster, M., et al. 2006. Frequency, characteristics, and reversibility of peripheral neuropathy during treatment of advanced multiple myeloma with bortezomib. *J Clin Oncol* 24:3113-3120.
148. Barlogie, B., van Rhee, F., Shaughnessy, J.D., Jr., Epstein, J., Yaccoby, S., Pineda-Roman, M., Hollmig, K., Alsayed, Y., Hoering, A., Szymonifka, J., et al. 2008. Seven-year median time to progression with thalidomide for smoldering myeloma: partial response identifies subset requiring earlier salvage therapy for symptomatic disease. *Blood* 112:3122-3125.
149. San Miguel, J.F., Schlag, R., Khuageva, N.K., Dimopoulos, M.A., Shpilberg, O., Kropff, M., Spicka, I., Petrucci, M.T., Palumbo, A., Samoilova, O.S., et al. 2008. Bortezomib plus melphalan and prednisone for initial treatment of multiple myeloma. *N Engl J Med* 359:906-917.
150. Stewart, A.K., and Fonseca, R. 2005. Prognostic and therapeutic significance of myeloma genetics and gene expression profiling. *J Clin Oncol* 23:6339-6344.
151. Jagannath, S., Richardson, P.G., Sonneveld, P., Schuster, M.W., Irwin, D., Stadtmauer, E.A., Facon, T., Harousseau, J.L., Cowan, J.M., and Anderson, K.C. 2007. Bortezomib appears to overcome the poor prognosis conferred by chromosome 13 deletion in phase 2 and 3 trials. *Leukemia* 21:151-157.
152. Otsuka, M., Mizuki, M., Fujita, J., Kang, S., and Kanakura, Y. 2011. Constitutively active FGFR3 with Lys650Glu mutation enhances bortezomib sensitivity in plasma cell malignancy. *Anticancer Res* 31:113-122.
153. Zheng, W., Guan, M., Zhu, L., Cai, Z., Chung, V., Huang, H., and Yen, Y. 2010. Bortezomib therapeutic effect is associated with expression and mutation of FGFR3 in human lymphoma cells. *Anticancer Res* 30:1921-1930.
154. Guan, M., Zhu, L., Somlo, G., Hughes, A., Zhou, B., and Yen, Y. 2009. Bortezomib therapeutic effect is associated with expression of FGFR3 in multiple myeloma cells. *Anticancer Res* 29:1-9.
155. Khong, T., and Spencer, A. 2011. Targeting HSP 90 induces apoptosis and inhibits critical survival and proliferation pathways in multiple myeloma. *Mol Cancer Ther* 10:1909-1917.
156. Roue, G., Perez-Galan, P., Mozos, A., Lopez-Guerra, M., Xargay-Torrent, S., Rosich, L., Saborit-Villarroya, I., Normant, E., Campo, E., and Colomer, D. The Hsp90 inhibitor IPI-504 overcomes bortezomib resistance in mantle cell lymphoma in vitro and in vivo by down-regulation of the prosurvival ER chaperone BiP/Grp78. *Blood* 117:1270-1279.
157. Meister, S., Frey, B., Lang, V.R., Gaipl, U.S., Schett, G., Schlotzer-Schrehardt, U., and Voll, R.E. 2010. Calcium channel blocker verapamil enhances endoplasmic reticulum stress and cell death induced by proteasome inhibition in myeloma cells. *Neoplasia* 12:550-561.
158. Richardson, P.G., Chanan-Khan, A.A., Lonial, S., Krishnan, A.Y., Carroll, M.P., Alsina, M., Albitar, M., Berman, D., Messina, M., and Anderson, K.C. 2011.

Tanespimycin and bortezomib combination treatment in patients with relapsed or relapsed and refractory multiple myeloma: results of a phase 1/2 study. *Br J Haematol* 153:729-740.
159. Balsas, P., Galan-Malo, P., Marzo, I., and Naval, J. 2012. Bortezomib resistance in a myeloma cell line is associated to PSMbeta5 overexpression and polyploidy. *Leuk Res* 36:212-218.
160. Barbone, D., Cheung, P., Battula, S., Busacca, S., Gray, S.G., Longley, D.B., Bueno, R., Sugarbaker, D.J., Fennell, D.A., and Broaddus, V.C. 2012. Vorinostat Eliminates Multicellular Resistance of Mesothelioma 3D Spheroids via Restoration of Noxa Expression. *PLoS One* 7:e52753.
161. Maiso, P., Carvajal-Vergara, X., Ocio, E.M., Lopez-Perez, R., Mateo, G., Gutierrez, N., Atadja, P., Pandiella, A., and San Miguel, J.F. 2006. The histone deacetylase inhibitor LBH589 is a potent antimyeloma agent that overcomes drug resistance. *Cancer Res* 66:5781-5789.
162. Kikuchi, J., Wada, T., Shimizu, R., Izumi, T., Akutsu, M., Mitsunaga, K., Noborio-Hatano, K., Nobuyoshi, M., Ozawa, K., Kano, Y., et al. 2010. Histone deacetylases are critical targets of bortezomib-induced cytotoxicity in multiple myeloma. *Blood* 116:406-417.
163. Badros, A., Burger, A.M., Philip, S., Niesvizky, R., Kolla, S.S., Goloubeva, O., Harris, C., Zwiebel, J., Wright, J.J., Espinoza-Delgado, I., et al. 2009. Phase I study of vorinostat in combination with bortezomib for relapsed and refractory multiple myeloma. *Clin Cancer Res* 15:5250-5257.
164. Richardson, P.G., Sonneveld, P., Schuster, M., Irwin, D., Stadtmauer, E., Facon, T., Harousseau, J.L., Ben-Yehuda, D., Lonial, S., Goldschmidt, H., et al. 2007. Extended follow-up of a phase 3 trial in relapsed multiple myeloma: final time-to-event results of the APEX trial. *Blood* 110:3557-3560.
165. Grigorieva, I., Thomas, X., and Epstein, J. 1998. The bone marrow stromal environment is a major factor in myeloma cell resistance to dexamethasone. *Exp Hematol* 26:597-603.
166. Rowley, M., Liu, P., and Van Ness, B. 2000. Heterogeneity in therapeutic response of genetically altered myeloma cell lines to interleukin 6, dexamethasone, doxorubicin, and melphalan. *Blood* 96:3175-3180.
167. Mitsiades, C.S., Mitsiades, N., Poulaki, V., Schlossman, R., Akiyama, M., Chauhan, D., Hideshima, T., Treon, S.P., Munshi, N.C., Richardson, P.G., et al. 2002. Activation of NF-kappaB and upregulation of intracellular anti-apoptotic proteins via the IGF-1/Akt signaling in human multiple myeloma cells: therapeutic implications. *Oncogene* 21:5673-5683.
168. Chauhan, D., Uchiyama, H., Akbarali, Y., Urashima, M., Yamamoto, K., Libermann, T.A., and Anderson, K.C. 1996. Multiple myeloma cell adhesion-induced interleukin-6 expression in bone marrow stromal cells involves activation of NF-kappa B. *Blood* 87:1104-1112.
169. Hideshima, T., Chauhan, D., Schlossman, R., Richardson, P., and Anderson, K.C. 2001. The role of tumor necrosis factor alpha in the pathophysiology of human multiple myeloma: therapeutic applications. *Oncogene* 20:4519-4527.
170. Roodman, G.D. 2010. Pathogenesis of myeloma bone disease. *J Cell Biochem* 109:283-291.

171. Ribatti, D., Nico, B., and Vacca, A. 2006. Importance of the bone marrow microenvironment in inducing the angiogenic response in multiple myeloma. *Oncogene* 25:4257-4266.
172. Yaccoby, S., Pearse, R.N., Johnson, C.L., Barlogie, B., Choi, Y., and Epstein, J. 2002. Myeloma interacts with the bone marrow microenvironment to induce osteoclastogenesis and is dependent on osteoclast activity. *Br J Haematol* 116:278-290.
173. Andersen, T.L., Boissy, P., Sondergaard, T.E., Kupisiewicz, K., Plesner, T., Rasmussen, T., Haaber, J., Kolvraa, S., and Delaisse, J.M. 2007. Osteoclast nuclei of myeloma patients show chromosome translocations specific for the myeloma cell clone: a new type of cancer-host partnership? *J Pathol* 211:10-17.
174. Hideshima, T., Mitsiades, C., Tonon, G., Richardson, P.G., and Anderson, K.C. 2007. Understanding multiple myeloma pathogenesis in the bone marrow to identify new therapeutic targets. *Nat Rev Cancer* 7:585-598.
175. Caers, J., Van Valckenborgh, E., Menu, E., Van Camp, B., and Vanderkerken, K. 2008. Unraveling the biology of multiple myeloma disease: cancer stem cells, acquired intracellular changes and interactions with the surrounding micro-environment. *Bull Cancer* 95:301-313.
176. Urashima, M., Chauhan, D., Uchiyama, H., Freeman, G.J., and Anderson, K.C. 1995. CD40 ligand triggered interleukin-6 secretion in multiple myeloma. *Blood* 85:1903-1912.
177. Hideshima, T., Bergsagel, P.L., Kuehl, W.M., and Anderson, K.C. 2004. Advances in biology of multiple myeloma: clinical applications. *Blood* 104:607-618.
178. Zang, M.R., Li, F., An, G., Xie, Z.Q., Li, C.H., Yu, Z., Xu, Y., Qiu, L.G., and Hao, M. 2012. [Regulation of miRNA-15a/-16 expression on the drug resistance of myeloma cells]. *Zhonghua Yi Xue Za Zhi* 92:1100-1103.
179. Hao, M., Zhang, L., An, G., Meng, H., Han, Y., Xie, Z., Xu, Y., Li, C., Yu, Z., Chang, H., et al. 2011. Bone marrow stromal cells protect myeloma cells from bortezomib induced apoptosis by suppressing microRNA-15a expression. *Leuk Lymphoma* 52:1787-1794.
180. Wang, X., Li, C., Ju, S., Wang, Y., Wang, H., and Zhong, R. 2011. Myeloma cell adhesion to bone marrow stromal cells confers drug resistance by microRNA-21 up-regulation. *Leuk Lymphoma* 52:1991-1998.
181. Kalitin, N.N., Kostyukova, M.N., Kakpakova, E.S., Tupitsyn, N.N., and Karamysheva, A.F. 2012. Expression of vascular endothelial growth factor receptors VEGFR1 in cultured multiple myeloma cells: correlation with immunophenotype and drug resistance. *Bull Exp Biol Med* 153:882-885.
182. Kuhn, D.J., Berkova, Z., Jones, R.J., Woessner, R., Bjorklund, C.C., Ma, W., Davis, R.E., Lin, P., Wang, H., Madden, T.L., et al. 2012. Targeting the insulin-like growth factor-1 receptor to overcome bortezomib resistance in preclinical models of multiple myeloma. *Blood* 120:3260-3270.
183. Tai, Y.T., Li, X., Tong, X., Santos, D., Otsuki, T., Catley, L., Tournilhac, O., Podar, K., Hideshima, T., Schlossman, R., et al. 2005. Human anti-CD40 antagonist antibody triggers significant antitumor activity against human multiple myeloma. *Cancer Res* 65:5898-5906.

184. Tai, Y.T., Li, X.F., Catley, L., Coffey, R., Breitkreutz, I., Bae, J., Song, W., Podar, K., Hideshima, T., Chauhan, D., et al. 2005. Immunomodulatory drug lenalidomide (CC-5013, IMiD3) augments anti-CD40 SGN-40-induced cytotoxicity in human multiple myeloma: clinical implications. *Cancer Res* 65:11712-11720.
185. Azab, A.K., Runnels, J.M., Pitsillides, C., Moreau, A.S., Azab, F., Leleu, X., Jia, X., Wright, R., Ospina, B., Carlson, A.L., et al. 2009. CXCR4 inhibitor AMD3100 disrupts the interaction of multiple myeloma cells with the bone marrow microenvironment and enhances their sensitivity to therapy. *Blood* 113:4341-4351.
186. Zhao, M., and Vuori, K. 2011. The docking protein p130Cas regulates cell sensitivity to proteasome inhibition. *BMC Biol* 9:73.
187. Moriuchi, M., Ohmachi, K., Kojima, M., Tsuboi, K., Ogawa, Y., Nakamura, N., and Ando, K. 2010. Three cases of bortezomib-resistant multiple myeloma with extramedullary masses. *Tokai J Exp Clin Med* 35:17-20.
188. Pirrotta, M.T., Gozzetti, A., Cerase, A., Bucalossi, A., Bocchia, M., Defina, M., and Lauria, F. 2008. Unusual discordant responses in two multiple myeloma patients during bortezomib treatment. *Onkologie* 31:45-47.
189. Bergsagel, P.L., and Kuehl, W.M. 2003. Critical roles for immunoglobulin translocations and cyclin D dysregulation in multiple myeloma. *Immunol Rev* 194:96-104.
190. Adams, J. 2004. The proteasome: a suitable antineoplastic target. *Nat Rev Cancer* 4:349-360.
191. Lichter, D.I., Danaee, H., Pickard, M.D., Tayber, O., Sintchak, M., Shi, H., Richardson, P.G., Cavenagh, J., Blade, J., Facon, T., et al. 2012. Sequence analysis of beta-subunit genes of the 20S proteasome in patients with relapsed multiple myeloma treated with bortezomib or dexamethasone. *Blood*.
192. Verbrugge, S.E., Al, M., Assaraf, Y.G., Niewerth, D., van Meerloo, J., Cloos, J., van der Veer, M., Scheffer, G.L., Peters, G.J., Chan, E.T., et al. 2013. Overcoming bortezomib resistance in human B cells by anti-CD20/rituximab-mediated complement-dependent cytotoxicity and epoxyketone-based irreversible proteasome inhibitors. *Exp Hematol Oncol* 2:2.
193. Verbrugge, S.E., Assaraf, Y.G., Dijkmans, B.A., Scheffer, G.L., Al, M., den Uyl, D., Oerlemans, R., Chan, E.T., Kirk, C.J., Peters, G.J., et al. 2012. Inactivating PSMB5 mutations and P-glycoprotein (multidrug resistance-associated protein/ATP-binding cassette B1) mediate resistance to proteasome inhibitors: ex vivo efficacy of (immuno)proteasome inhibitors in mononuclear blood cells from patients with rheumatoid arthritis. *J Pharmacol Exp Ther* 341:174-182.
194. Suzuki, E., Demo, S., Deu, E., Keats, J., Arastu-Kapur, S., Bergsagel, P.L., Bennett, M.K., and Kirk, C.J. 2011. Molecular mechanisms of bortezomib resistant adenocarcinoma cells. *PLoS One* 6:e27996.
195. de Wilt, L.H., Jansen, G., Assaraf, Y.G., van Meerloo, J., Cloos, J., Schimmer, A.D., Chan, E.T., Kirk, C.J., Peters, G.J., and Kruyt, F.A. 2012. Proteasome-based mechanisms of intrinsic and acquired bortezomib resistance in non-small cell lung cancer. *Biochem Pharmacol* 83:207-217.
196. Li, X., Wood, T.E., Sprangers, R., Jansen, G., Franke, N.E., Mao, X., Wang, X., Zhang, Y., Verbrugge, S.E., Adomat, H., et al. 2010. Effect of noncompetitive

proteasome inhibition on bortezomib resistance. *J Natl Cancer Inst* 102:1069-1082.
197. Franke, N.E., Niewerth, D., Assaraf, Y.G., van Meerloo, J., Vojtekova, K., van Zantwijk, C.H., Zweegman, S., Chan, E.T., Kirk, C.J., Geerke, D.P., et al. 2012. Impaired bortezomib binding to mutant beta5 subunit of the proteasome is the underlying basis for bortezomib resistance in leukemia cells. *Leukemia* 26:757-768.
198. Lu, S.Q., Yang, J.M., Huang, C.M., Xu, X.Q., Zhou, H., Song, N.X., and Wang, J.M. 2011. [Comparison of protein expression profiles between bortezomib-resistant JurkatB cells with PSMB5 mutation and their parent cells]. *Zhongguo Shi Yan Xue Ye Xue Za Zhi* 19:869-873.
199. Ri, M., Iida, S., Nakashima, T., Miyazaki, H., Mori, F., Ito, A., Inagaki, A., Kusumoto, S., Ishida, T., Komatsu, H., et al. 2010. Bortezomib-resistant myeloma cell lines: a role for mutated PSMB5 in preventing the accumulation of unfolded proteins and fatal ER stress. *Leukemia* 24:1506-1512.
200. Lu, S., Chen, Z., Yang, J., Chen, L., Gong, S., Zhou, H., Guo, L., and Wang, J. 2008. Overexpression of the PSMB5 gene contributes to bortezomib resistance in T-lymphoblastic lymphoma/leukemia cells derived from Jurkat line. *Exp Hematol* 36:1278-1284.
201. Lu, S., Yang, J., Chen, Z., Gong, S., Zhou, H., Xu, X., and Wang, J. 2009. Different mutants of PSMB5 confer varying bortezomib resistance in T lymphoblastic lymphoma/leukemia cells derived from the Jurkat cell line. *Exp Hematol* 37:831-837.
202. Lu, S., Yang, J., Song, X., Gong, S., Zhou, H., Guo, L., Song, N., Bao, X., Chen, P., and Wang, J. 2008. Point mutation of the proteasome beta5 subunit gene is an important mechanism of bortezomib resistance in bortezomib-selected variants of Jurkat T cell lymphoblastic lymphoma/leukemia line. *J Pharmacol Exp Ther* 326:423-431.
203. Oerlemans, R., Franke, N.E., Assaraf, Y.G., Cloos, J., van Zantwijk, I., Berkers, C.R., Scheffer, G.L., Debipersad, K., Vojtekova, K., Lemos, C., et al. 2008. Molecular basis of bortezomib resistance: proteasome subunit beta5 (PSMB5) gene mutation and overexpression of PSMB5 protein. *Blood* 112:2489-2499.
204. Shuqing, L., Jianmin, Y., Chongmei, H., Hui, C., and Wang, J. 2011. Upregulated expression of the PSMB5 gene may contribute to drug resistance in patient with multiple myeloma when treated with bortezomib-based regimen. *Exp Hematol* 39:1117-1118.
205. Politou, M., Karadimitris, A., Terpos, E., Kotsianidis, I., Apperley, J.F., and Rahemtulla, A. 2006. No evidence of mutations of the PSMB5 (beta-5 subunit of proteasome) in a case of myeloma with clinical resistance to Bortezomib. *Leuk Res* 30:240-241.
206. Wang, L., Kumar, S., Fridley, B.L., Kalari, K.R., Moon, I., Pelleymounter, L.L., Hildebrandt, M.A., Batzler, A., Eckloff, B.W., Wieben, E.D., et al. 2008. Proteasome beta subunit pharmacogenomics: gene resequencing and functional genomics. *Clin Cancer Res* 14:3503-3513.
207. Yeom, S.Y., Lee, S.J., Kim, W.S., and Park, C. 2012. Rad knockdown induces mitochondrial apoptosis in bortezomib resistant leukemia and lymphoma cells. *Leuk Res* 36:1172-1178.

208. Zhang, L., Littlejohn, J.E., Cui, Y., Cao, X., Peddaboina, C., and Smythe, W.R. 2010. Characterization of bortezomib-adapted I-45 mesothelioma cells. *Mol Cancer* 9:110.
209. Ling, X., Calinski, D., Chanan-Khan, A.A., Zhou, M., and Li, F. 2010. Cancer cell sensitivity to bortezomib is associated with survivin expression and p53 status but not cancer cell types. *J Exp Clin Cancer Res* 29:8.
210. Hu, J., Dang, N., Menu, E., De Bryune, E., Xu, D., Van Camp, B., Van Valckenborgh, E., and Vanderkerken, K. 2012. Activation of ATF4 mediates unwanted Mcl-1 accumulation by proteasome inhibition. *Blood* 119:826-837.
211. Smith, A.J., Dai, H., Correia, C., Takahashi, R., Lee, S.H., Schmitz, I., and Kaufmann, S.H. 2011. Noxa/Bcl-2 protein interactions contribute to bortezomib resistance in human lymphoid cells. *J Biol Chem* 286:17682-17692.
212. Liu, P., Xu, B., Li, J., and Lu, H. 2009. BAG3 gene silencing sensitizes leukemic cells to Bortezomib-induced apoptosis. *FEBS Lett* 583:401-406.
213. Yang, T.M., Barbone, D., Fennell, D.A., and Broaddus, V.C. 2009. Bcl-2 family proteins contribute to apoptotic resistance in lung cancer multicellular spheroids. *Am J Respir Cell Mol Biol* 41:14-23.
214. Xu, D., Hu, J., De Bruyne, E., Menu, E., Schots, R., Vanderkerken, K., and Van Valckenborgh, E. 2012. Dll1/Notch activation contributes to bortezomib resistance by upregulating CYP1A1 in multiple myeloma. *Biochem Biophys Res Commun* 428:518-524.
215. Kim, A., Park, S., Lee, J.E., Jang, W.S., Lee, S.J., Kang, H.J., and Lee, S.S. 2012. The dual PI3K and mTOR inhibitor NVP-BEZ235 exhibits anti-proliferative activity and overcomes bortezomib resistance in mantle cell lymphoma cells. *Leuk Res* 36:912-920.
216. Hegde, G.V., Nordgren, T.M., Munger, C.M., Mittal, A.K., Bierman, P.J., Weisenburger, D.D., Vose, J.M., Sharp, J.G., and Joshi, S.S. 2012. Novel therapy for therapy-resistant mantle cell lymphoma: multipronged approach with targeting of hedgehog signaling. *Int J Cancer* 131:2951-2960.
217. Jung, H.J., Chen, Z., Wang, M., Fayad, L., Romaguera, J., Kwak, L.W., and McCarty, N. 2012. Calcium blockers decrease the bortezomib resistance in mantle cell lymphoma via manipulation of tissue transglutaminase activities. *Blood* 119:2568-2578.
218. Markovina, S., Callander, N.S., O'Connor, S.L., Xu, G., Shi, Y., Leith, C.P., Kim, K., Trivedi, P., Kim, J., Hematti, P., et al. 2010. Bone marrow stromal cells from multiple myeloma patients uniquely induce bortezomib resistant NF-kappaB activity in myeloma cells. *Mol Cancer* 9:176.
219. Markovina, S., Callander, N.S., O'Connor, S.L., Kim, J., Werndli, J.E., Raschko, M., Leith, C.P., Kahl, B.S., Kim, K., and Miyamoto, S. 2008. Bortezomib-resistant nuclear factor-kappaB activity in multiple myeloma cells. *Mol Cancer Res* 6:1356-1364.
220. Yang, D.T., Young, K.H., Kahl, B.S., Markovina, S., and Miyamoto, S. 2008. Prevalence of bortezomib-resistant constitutive NF-kappaB activity in mantle cell lymphoma. *Mol Cancer* 7:40.
221. Landowski, T.H., Olashaw, N.E., Agrawal, D., and Dalton, W.S. 2003. Cell adhesion-mediated drug resistance (CAM-DR) is associated with activation of NF-kappa B (RelB/p50) in myeloma cells. *Oncogene* 22:2417-2421.

222. Hazlehurst, L.A., Damiano, J.S., Buyuksal, I., Pledger, W.J., and Dalton, W.S. 2000. Adhesion to fibronectin via beta1 integrins regulates p27kip1 levels and contributes to cell adhesion mediated drug resistance (CAM-DR). *Oncogene* 19:4319-4327.
223. Shi, L., Wang, S., Zangari, M., Xu, H., Cao, T.M., Xu, C., Wu, Y., Xiao, F., Liu, Y., Yang, Y., et al. 2010. Over-expression of CKS1B activates both MEK/ERK and JAK/STAT3 signaling pathways and promotes myeloma cell drug-resistance. *Oncotarget* 1:22-33.
224. Que, W., Chen, J., Chuang, M., and Jiang, D. 2012. Knockdown of c-Met enhances sensitivity to bortezomib in human multiple myeloma U266 cells via inhibiting Akt/mTOR activity. *APMIS* 120:195-203.
225. Filipczak, P.T., Piglowski, W., Glowala-Kosinska, M., Krawczyk, Z., and Scieglinska, D. 2012. HSPA2 overexpression protects V79 fibroblasts against bortezomib-induced apoptosis. *Biochem Cell Biol* 90:224-231.
226. Mozos, A., Roue, G., Lopez-Guillermo, A., Jares, P., Campo, E., Colomer, D., and Martinez, A. 2011. The expression of the endoplasmic reticulum stress sensor BiP/GRP78 predicts response to chemotherapy and determines the efficacy of proteasome inhibitors in diffuse large b-cell lymphoma. *Am J Pathol* 179:2601-2610.
227. Rushworth, S.A., Bowles, K.M., and MacEwan, D.J. 2011. High basal nuclear levels of Nrf2 in acute myeloid leukemia reduces sensitivity to proteasome inhibitors. *Cancer Res* 71:1999-2009.
228. Kern, J., Untergasser, G., Zenzmaier, C., Sarg, B., Gastl, G., Gunsilius, E., and Steurer, M. 2009. GRP-78 secreted by tumor cells blocks the antiangiogenic activity of bortezomib. *Blood* 114:3960-3967.
229. Du, Z.X., Zhang, H.Y., Meng, X., Guan, Y., and Wang, H.Q. 2009. Role of oxidative stress and intracellular glutathione in the sensitivity to apoptosis induced by proteasome inhibitor in thyroid cancer cells. *BMC Cancer* 9:56.
230. Chauhan, D., Li, G., Shringarpure, R., Podar, K., Ohtake, Y., Hideshima, T., and Anderson, K.C. 2003. Blockade of Hsp27 overcomes Bortezomib/proteasome inhibitor PS-341 resistance in lymphoma cells. *Cancer Res* 63:6174-6177.
231. Shringarpure, R., Catley, L., Bhole, D., Burger, R., Podar, K., Tai, Y.T., Kessler, B., Galardy, P., Ploegh, H., Tassone, P., et al. 2006. Gene expression analysis of B-lymphoma cells resistant and sensitive to bortezomib. *Br J Haematol* 134:145-156.
232. Jia, L., Gopinathan, G., Sukumar, J.T., and Gribben, J.G. 2012. Blocking autophagy prevents bortezomib-induced NF-kappaB activation by reducing I-kappaBalpha degradation in lymphoma cells. *PLoS One* 7:e32584.
233. Rzymski, T., Milani, M., Singleton, D.C., and Harris, A.L. 2009. Role of ATF4 in regulation of autophagy and resistance to drugs and hypoxia. *Cell Cycle* 8:3838-3847.
234. Milani, M., Rzymski, T., Mellor, H.R., Pike, L., Bottini, A., Generali, D., and Harris, A.L. 2009. The role of ATF4 stabilization and autophagy in resistance of breast cancer cells treated with Bortezomib. *Cancer Res* 69:4415-4423.
235. Potter, M., and Wax, J.S. 1981. Genetics of susceptibility to pristane-induced plasmacytomas in BALB/cAn: reduced susceptibility in BALB/cJ with a brief description of pristane-induced arthritis. *J Immunol* 127:1591-1595.

236. Potter, M. 1997. Experimental plasmacytomagenesis in mice. *Hematol Oncol Clin North Am* 11:323-347.
237. Mitsiades, C.S., Anderson, K.C., and Carrasco, D.R. 2007. Mouse models of human myeloma. *Hematol Oncol Clin North Am* 21:1051-1069, viii.
238. Dib, A., Gabrea, A., Glebov, O.K., Bergsagel, P.L., and Kuehl, W.M. 2008. Characterization of MYC translocations in multiple myeloma cell lines. *J Natl Cancer Inst Monogr*:25-31.
239. Chng, W.J., Huang, G.F., Chung, T.H., Ng, S.B., Gonzalez-Paz, N., Troska-Price, T., Mulligan, G., Chesi, M., Bergsagel, P.L., and Fonseca, R. 2011. Clinical and biological implications of MYC activation: a common difference between MGUS and newly diagnosed multiple myeloma. *Leukemia* 25:1026-1035.
240. Kuehl, W.M., and Bergsagel, P.L. 2012. MYC addiction: a potential therapeutic target in MM. *Blood* 120:2351-2352.
241. Brown, R.D., Pope, B., Luo, X.F., Gibson, J., and Joshua, D. 1994. The oncoprotein phenotype of plasma cells from patients with multiple myeloma. *Leuk Lymphoma* 16:147-156.
242. Cheung, W.C., Kim, J.S., Linden, M., Peng, L., Van Ness, B., Polakiewicz, R.D., and Janz, S. 2004. Novel targeted deregulation of c-Myc cooperates with Bcl-X(L) to cause plasma cell neoplasms in mice. *J Clin Invest* 113:1763-1773.
243. Radl, J., Hollander, C.F., van den Berg, P., and de Glopper, E. 1978. Idiopathic paraproteinaemia. I. Studies in an animal model--the ageing C57BL/KaLwRij mouse. *Clin Exp Immunol* 33:395-402.
244. Radl, J., De Glopper, E.D., Schuit, H.R., and Zurcher, C. 1979. Idiopathic paraproteinemia. II. Transplantation of the paraprotein-producing clone from old to young C57BL/KaLwRij mice. *J Immunol* 122:609-613.
245. Libouban, H., Moreau, M.F., Basle, M.F., Bataille, R., and Chappard, D. 2004. Selection of a highly aggressive myeloma cell line by an altered bone microenvironment in the C57BL/KaLwRij mouse. *Biochem Biophys Res Commun* 316:859-866.
246. Vanderkerken, K., De Greef, C., Asosingh, K., Arteta, B., De Veerman, M., Vande Broek, I., Van Riet, I., Kobayashi, M., Smedsrod, B., and Van Camp, B. 2000. Selective initial in vivo homing pattern of 5T2 multiple myeloma cells in the C57BL/KalwRij mouse. *Br J Cancer* 82:953-959.
247. Vanderkerken, K., De Raeve, H., Goes, E., Van Meirvenne, S., Radl, J., Van Riet, I., Thielemans, K., and Van Camp, B. 1997. Organ involvement and phenotypic adhesion profile of 5T2 and 5T33 myeloma cells in the C57BL/KaLwRij mouse. *Br J Cancer* 76:451-460.
248. Heath, D.J., Vanderkerken, K., Cheng, X., Gallagher, O., Prideaux, M., Murali, R., and Croucher, P.I. 2007. An osteoprotegerin-like peptidomimetic inhibits osteoclastic bone resorption and osteolytic bone disease in myeloma. *Cancer Res* 67:202-208.
249. Asosingh, K. 2003. Migration, adhesion and differentiation of malignant plasma cells in the 5T murine model of myeloma. *Verh K Acad Geneeskd Belg* 65:127-134.
250. Asosingh, K., De Raeve, H., Croucher, P., Goes, E., Van Riet, I., Van Camp, B., and Vanderkerken, K. 2001. In vivo homing and differentiation characteristics of

mature (CD45-) and immature (CD45+) 5T multiple myeloma cells. *Exp Hematol* 29:77-84.
251. Asosingh, K., Gunthert, U., De Raeve, H., Van Riet, I., Van Camp, B., and Vanderkerken, K. 2001. A unique pathway in the homing of murine multiple myeloma cells: CD44v10 mediates binding to bone marrow endothelium. *Cancer Res* 61:2862-2865.
252. Asosingh, K., Menu, E., Van Valckenborgh, E., Vande Broek, I., Van Riet, I., Van Camp, B., and Vanderkerken, K. 2002. Mechanisms involved in the differential bone marrow homing of CD45 subsets in 5T murine models of myeloma. *Clin Exp Metastasis* 19:583-591.
253. Asosingh, K., Vankerkhove, V., Van Riet, I., Van Camp, B., and Vanderkerken, K. 2003. Selective in vivo growth of lymphocyte function- associated antigen-1-positive murine myeloma cells. Involvement of function-associated antigen-1-mediated homotypic cell-cell adhesion. *Exp Hematol* 31:48-55.
254. Van Valckenborgh, E., Bakkus, M., Munaut, C., Noel, A., St Pierre, Y., Asosingh, K., Van Riet, I., Van Camp, B., and Vanderkerken, K. 2002. Upregulation of matrix metalloproteinase-9 in murine 5T33 multiple myeloma cells by interaction with bone marrow endothelial cells. *Int J Cancer* 101:512-518.
255. Van Valckenborgh, E., De Raeve, H., Devy, L., Blacher, S., Munaut, C., Noel, A., Van Marck, E., Van Riet, I., Van Camp, B., and Vanderkerken, K. 2002. Murine 5T multiple myeloma cells induce angiogenesis in vitro and in vivo. *Br J Cancer* 86:796-802.
256. Vanderkerken, K., Vande Broek, I., Eizirik, D.L., Van Valckenborgh, E., Asosingh, K., Van Riet, I., and Van Camp, B. 2002. Monocyte chemoattractant protein-1 (MCP-1), secreted by bone marrow endothelial cells, induces chemoattraction of 5T multiple myeloma cells. *Clin Exp Metastasis* 19:87-90.
257. Menu, E., Asosingh, K., Indraccolo, S., De Raeve, H., Van Riet, I., Van Valckenborgh, E., Vande Broek, I., Fujii, N., Tamamura, H., Van Camp, B., et al. 2006. The involvement of stromal derived factor 1alpha in homing and progression of multiple myeloma in the 5TMM model. *Haematologica* 91:605-612.
258. Menu, E., De Leenheer, E., De Raeve, H., Coulton, L., Imanishi, T., Miyashita, K., Van Valckenborgh, E., Van Riet, I., Van Camp, B., Horuk, R., et al. 2006. Role of CCR1 and CCR5 in homing and growth of multiple myeloma and in the development of osteolytic lesions: a study in the 5TMM model. *Clin Exp Metastasis* 23:291-300.
259. Asosingh, K., De Raeve, H., de Ridder, M., Storme, G.A., Willems, A., Van Riet, I., Van Camp, B., and Vanderkerken, K. 2005. Role of the hypoxic bone marrow microenvironment in 5T2MM murine myeloma tumor progression. *Haematologica* 90:810-817.
260. Mittelman, M., Neumann, D., Peled, A., Kanter, P., and Haran-Ghera, N. 2001. Erythropoietin induces tumor regression and antitumor immune responses in murine myeloma models. *Proc Natl Acad Sci U S A* 98:5181-5186.
261. Henry, J.M., Morley, A.A., and Sykes, P.J. 2001. Purging of myeloma cells using all-trans retinoic acid in a mouse model. *Exp Hematol* 29:315-321.

262. Manning, L.S., and Radin, N.S. 1999. Effects of the glucolipid synthase inhibitor, P4, on functional and phenotypic parameters of murine myeloma cells. *Br J Cancer* 81:952-958.
263. Menu, E., Jernberg-Wiklund, H., Stromberg, T., De Raeve, H., Girnita, L., Larsson, O., Axelson, M., Asosingh, K., Nilsson, K., Van Camp, B., et al. 2006. Inhibiting the IGF-1 receptor tyrosine kinase with the cyclolignan PPP: an in vitro and in vivo study in the 5T33MM mouse model. *Blood* 107:655-660.
264. Edwards, C.M., Mueller, G., Roelofs, A.J., Chantry, A., Perry, M., Russell, R.G., Van Camp, B., Guyon-Gellin, Y., Niesor, E.J., Bentzen, C.L., et al. 2007. Apomine, an inhibitor of HMG-CoA-reductase, promotes apoptosis of myeloma cells in vitro and is associated with a modulation of myeloma in vivo. *Int J Cancer* 120:1657-1663.
265. Libouban, H., Moreau, M.F., Basle, M.F., Bataille, R., and Chappard, D. 2003. Increased bone remodeling due to ovariectomy dramatically increases tumoral growth in the 5T2 multiple myeloma mouse model. *Bone* 33:283-292.
266. Croucher, P.I., De Hendrik, R., Perry, M.J., Hijzen, A., Shipman, C.M., Lippitt, J., Green, J., Van Marck, E., Van Camp, B., and Vanderkerken, K. 2003. Zoledronic acid treatment of 5T2MM-bearing mice inhibits the development of myeloma bone disease: evidence for decreased osteolysis, tumor burden and angiogenesis, and increased survival. *J Bone Miner Res* 18:482-492.
267. Croucher, P.I., Shipman, C.M., Van Camp, B., and Vanderkerken, K. 2003. Bisphosphonates and osteoprotegerin as inhibitors of myeloma bone disease. *Cancer* 97:818-824.
268. Radl, J., Croese, J.W., Zurcher, C., van den Enden-Vieveen, M.H., Brondijk, R.J., Kazil, M., Haaijman, J.J., Reitsma, P.H., and Bijvoet, O.L. 1985. Influence of treatment with APD-bisphosphonate on the bone lesions in the mouse 5T2 multiple myeloma. *Cancer* 55:1030-1040.
269. Mitsiades, C.S., Mitsiades, N., Munshi, N.C., and Anderson, K.C. 2004. Focus on multiple myeloma. *Cancer Cell* 6:439-444.
270. van den Akker, T.W., Radl, J., Franken-Postma, E., and Hagemeijer, A. 1996. Cytogenetic findings in mouse multiple myeloma and Waldenstrom's macroglobulinemia. *Cancer Genet Cytogenet* 86:156-161.
271. Radl, J., Punt, Y.A., van den Enden-Vieveen, M.H., Bentvelzen, P.A., Bakkus, M.H., van den Akker, T.W., and Benner, R. 1990. The 5T mouse multiple myeloma model: absence of c-myc oncogene rearrangement in early transplant generations. *Br J Cancer* 61:276-278.
272. Tong, A.W., Huang, Y.W., Zhang, B.Q., Netto, G., Vitetta, E.S., and Stone, M.J. 1993. Heterotransplantation of human multiple myeloma cell lines in severe combined immunodeficiency (SCID) mice. *Anticancer Res* 13:593-597.
273. Lentzsch, S., Rogers, M.S., LeBlanc, R., Birsner, A.E., Shah, J.H., Treston, A.M., Anderson, K.C., and D'Amato, R.J. 2002. S-3-Amino-phthalimido-glutarimide inhibits angiogenesis and growth of B-cell neoplasias in mice. *Cancer Res* 62:2300-2305.
274. Chauhan, D., Hideshima, T., and Anderson, K.C. 2006. A novel proteasome inhibitor NPI-0052 as an anticancer therapy. *Br J Cancer* 95:961-965.
275. Sydor, J.R., Normant, E., Pien, C.S., Porter, J.R., Ge, J., Grenier, L., Pak, R.H., Ali, J.A., Dembski, M.S., Hudak, J., et al. 2006. Development of 17-allylamino-17-

demethoxygeldanamycin hydroquinone hydrochloride (IPI-504), an anti-cancer agent directed against Hsp90. *Proc Natl Acad Sci U S A* 103:17408-17413.
276. Hideshima, T., Catley, L., Yasui, H., Ishitsuka, K., Raje, N., Mitsiades, C., Podar, K., Munshi, N.C., Chauhan, D., Richardson, P.G., et al. 2006. Perifosine, an oral bioactive novel alkylphospholipid, inhibits Akt and induces in vitro and in vivo cytotoxicity in human multiple myeloma cells. *Blood* 107:4053-4062.
277. Trudel, S., Ely, S., Farooqi, Y., Affer, M., Robbiani, D.F., Chesi, M., and Bergsagel, P.L. 2004. Inhibition of fibroblast growth factor receptor 3 induces differentiation and apoptosis in t(4;14) myeloma. *Blood* 103:3521-3528.
278. Trudel, S., Li, Z.H., Wei, E., Wiesmann, M., Chang, H., Chen, C., Reece, D., Heise, C., and Stewart, A.K. 2005. CHIR-258, a novel, multitargeted tyrosine kinase inhibitor for the potential treatment of t(4;14) multiple myeloma. *Blood* 105:2941-2948.
279. Trudel, S., Stewart, A.K., Li, Z., Shu, Y., Liang, S.B., Trieu, Y., Reece, D., Paterson, J., Wang, D., and Wen, X.Y. 2007. The Bcl-2 family protein inhibitor, ABT-737, has substantial antimyeloma activity and shows synergistic effect with dexamethasone and melphalan. *Clin Cancer Res* 13:621-629.
280. Trudel, S., Stewart, A.K., Rom, E., Wei, E., Li, Z.H., Kotzer, S., Chumakov, I., Singer, Y., Chang, H., Liang, S.B., et al. 2006. The inhibitory anti-FGFR3 antibody, PRO-001, is cytotoxic to t(4;14) multiple myeloma cells. *Blood* 107:4039-4046.
281. Mitsiades, C.S., Treon, S.P., Mitsiades, N., Shima, Y., Richardson, P., Schlossman, R., Hideshima, T., and Anderson, K.C. 2001. TRAIL/Apo2L ligand selectively induces apoptosis and overcomes drug resistance in multiple myeloma: therapeutic applications. *Blood* 98:795-804.
282. Podar, K., Tonon, G., Sattler, M., Tai, Y.T., Legouill, S., Yasui, H., Ishitsuka, K., Kumar, S., Kumar, R., Pandite, L.N., et al. 2006. The small-molecule VEGF receptor inhibitor pazopanib (GW786034B) targets both tumor and endothelial cells in multiple myeloma. *Proc Natl Acad Sci U S A* 103:19478-19483.
283. Navas, T.A., Nguyen, A.N., Hideshima, T., Reddy, M., Ma, J.Y., Haghnazari, E., Henson, M., Stebbins, E.G., Kerr, I., O'Young, G., et al. 2006. Inhibition of p38alpha MAPK enhances proteasome inhibitor-induced apoptosis of myeloma cells by modulating Hsp27, Bcl-X(L), Mcl-1 and p53 levels in vitro and inhibits tumor growth in vivo. *Leukemia* 20:1017-1027.
284. Lin, B., Catley, L., LeBlanc, R., Mitsiades, C., Burger, R., Tai, Y.T., Podar, K., Wartmann, M., Chauhan, D., Griffin, J.D., et al. 2005. Patupilone (epothilone B) inhibits growth and survival of multiple myeloma cells in vitro and in vivo. *Blood* 105:350-357.
285. Yan, H., Frost, P., Shi, Y., Hoang, B., Sharma, S., Fisher, M., Gera, J., and Lichtenstein, A. 2006. Mechanism by which mammalian target of rapamycin inhibitors sensitize multiple myeloma cells to dexamethasone-induced apoptosis. *Cancer Res* 66:2305-2313.
286. Suzuki, H., Yasukawa, K., Saito, T., Goitsuka, R., Hasegawa, A., Ohsugi, Y., Taga, T., and Kishimoto, T. 1992. Anti-human interleukin-6 receptor antibody inhibits human myeloma growth in vivo. *Eur J Immunol* 22:1989-1993.
287. Ozaki, S., Kosaka, M., Harada, M., Nishitani, H., Odomi, M., and Matsumoto, T. 1998. Radioimmunodetection of human myeloma xenografts with a monoclonal

antibody directed against a plasma cell specific antigen, HM1.24. *Cancer* 82:2184-2190.
288. Urashima, M., Chen, B.P., Chen, S., Pinkus, G.S., Bronson, R.T., Dedera, D.A., Hoshi, Y., Teoh, G., Ogata, A., Treon, S.P., et al. 1997. The development of a model for the homing of multiple myeloma cells to human bone marrow. *Blood* 90:754-765.
289. Yaccoby, S., Barlogie, B., and Epstein, J. 1998. Primary myeloma cells growing in SCID-hu mice: a model for studying the biology and treatment of myeloma and its manifestations. *Blood* 92:2908-2913.
290. Yaccoby, S., Johnson, C.L., Mahaffey, S.C., Wezeman, M.J., Barlogie, B., and Epstein, J. 2002. Antimyeloma efficacy of thalidomide in the SCID-hu model. *Blood* 100:4162-4168.
291. Pearse, R.N., Sordillo, E.M., Yaccoby, S., Wong, B.R., Liau, D.F., Colman, N., Michaeli, J., Epstein, J., and Choi, Y. 2001. Multiple myeloma disrupts the TRANCE/ osteoprotegerin cytokine axis to trigger bone destruction and promote tumor progression. *Proc Natl Acad Sci U S A* 98:11581-11586.
292. Sordillo, E.M., and Pearse, R.N. 2003. RANK-Fc: a therapeutic antagonist for RANK-L in myeloma. *Cancer* 97:802-812.
293. Hideshima, T., Neri, P., Tassone, P., Yasui, H., Ishitsuka, K., Raje, N., Chauhan, D., Podar, K., Mitsiades, C., Dang, L., et al. 2006. MLN120B, a novel IkappaB kinase beta inhibitor, blocks multiple myeloma cell growth in vitro and in vivo. *Clin Cancer Res* 12:5887-5894.
294. Zhu, K., Gerbino, E., Beaupre, D.M., Mackley, P.A., Muro-Cacho, C., Beam, C., Hamilton, A.D., Lichtenheld, M.G., Kerr, W.G., Dalton, W., et al. 2005. Farnesyltransferase inhibitor R115777 (Zarnestra, Tipifarnib) synergizes with paclitaxel to induce apoptosis and mitotic arrest and to inhibit tumor growth of multiple myeloma cells. *Blood* 105:4759-4766.
295. Tassone, P., Goldmacher, V.S., Neri, P., Gozzini, A., Shammas, M.A., Whiteman, K.R., Hylander-Gans, L.L., Carrasco, D.R., Hideshima, T., Shringarpure, R., et al. 2004. Cytotoxic activity of the maytansinoid immunoconjugate B-B4-DM1 against CD138+ multiple myeloma cells. *Blood* 104:3688-3696.
296. Tassone, P., Neri, P., Burger, R., Savino, R., Shammas, M., Catley, L., Podar, K., Chauhan, D., Masciari, S., Gozzini, A., et al. 2005. Combination therapy with interleukin-6 receptor superantagonist Sant7 and dexamethasone induces antitumor effects in a novel SCID-hu In vivo model of human multiple myeloma. *Clin Cancer Res* 11:4251-4258.
297. Araki, K., Sangai, T., Miyamoto, S., Maeda, H., Zhang, S.C., Nakamura, M., Ishii, G., Hasebe, T., Kusaka, H., Akiyama, T., et al. 2006. Inhibition of bone-derived insulin-like growth factors by a ligand-specific antibody suppresses the growth of human multiple myeloma in the human adult bone explanted in NOD/SCID mouse. *Int J Cancer* 118:2602-2608.
298. Epstein, J., and Yaccoby, S. 2005. The SCID-hu myeloma model. *Methods Mol Med* 113:183-190.
299. Tassone, P., Gozzini, A., Goldmacher, V., Shammas, M.A., Whiteman, K.R., Carrasco, D.R., Li, C., Allam, C.K., Venuta, S., Anderson, K.C., et al. 2004. In vitro and in vivo activity of the maytansinoid immunoconjugate huN901-N2'-

deacetyl-N2'-(3-mercapto-1-oxopropyl)-maytansine against CD56+ multiple myeloma cells. *Cancer Res* 64:4629-4636.
300. Yata, K., and Yaccoby, S. 2004. The SCID-rab model: a novel in vivo system for primary human myeloma demonstrating growth of CD138-expressing malignant cells. *Leukemia* 18:1891-1897.
301. Tsunenari, T., Koishihara, Y., Nakamura, A., Moriya, M., Ohkawa, H., Goto, H., Shimazaki, C., Nakagawa, M., Ohsugi, Y., Kishimoto, T., et al. 1997. New xenograft model of multiple myeloma and efficacy of a humanized antibody against human interleukin-6 receptor. *Blood* 90:2437-2444.
302. Mitsiades, C.S., Mitsiades, N.S., McMullan, C.J., Poulaki, V., Shringarpure, R., Akiyama, M., Hideshima, T., Chauhan, D., Joseph, M., Libermann, T.A., et al. 2004. Inhibition of the insulin-like growth factor receptor-1 tyrosine kinase activity as a therapeutic strategy for multiple myeloma, other hematologic malignancies, and solid tumors. *Cancer Cell* 5:221-230.
303. Baughn, L.B., Di Liberto, M., Wu, K., Toogood, P.L., Louie, T., Gottschalk, R., Niesvizky, R., Cho, H., Ely, S., Moore, M.A., et al. 2006. A novel orally active small molecule potently induces G1 arrest in primary myeloma cells and prevents tumor growth by specific inhibition of cyclin-dependent kinase 4/6. *Cancer Res* 66:7661-7667.
304. Wu, K.D., Cho, Y.S., Katz, J., Ponomarev, V., Chen-Kiang, S., Danishefsky, S.J., and Moore, M.A. 2005. Investigation of antitumor effects of synthetic epothilone analogs in human myeloma models in vitro and in vivo. *Proc Natl Acad Sci U S A* 102:10640-10645.
305. Wu, K.D., Zhou, L., Burtrum, D., Ludwig, D.L., and Moore, M.A. 2007. Antibody targeting of the insulin-like growth factor I receptor enhances the anti-tumor response of multiple myeloma to chemotherapy through inhibition of tumor proliferation and angiogenesis. *Cancer Immunol Immunother* 56:343-357.
306. Mitsiades, C.S., Mitsiades, N.S., McMullan, C.J., Poulaki, V., Kung, A.L., Davies, F.E., Morgan, G., Akiyama, M., Shringarpure, R., Munshi, N.C., et al. 2006. Antimyeloma activity of heat shock protein-90 inhibition. *Blood* 107:1092-1100.
307. Xin, X., Abrams, T.J., Hollenbach, P.W., Rendahl, K.G., Tang, Y., Oei, Y.A., Embry, M.G., Swinarski, D.E., Garrett, E.N., Pryer, N.K., et al. 2006. CHIR-258 is efficacious in a newly developed fibroblast growth factor receptor 3-expressing orthotopic multiple myeloma model in mice. *Clin Cancer Res* 12:4908-4915.
308. Carlo-Stella, C., Guidetti, A., Di Nicola, M., Longoni, P., Cleris, L., Lavazza, C., Milanesi, M., Milani, R., Carrabba, M., Farina, L., et al. 2006. CD52 antigen expressed by malignant plasma cells can be targeted by alemtuzumab in vivo in NOD/SCID mice. *Exp Hematol* 34:721-727.
309. Namba, M., Ohtsuki, T., Mori, M., Togawa, A., Wada, H., Sugihara, T., Yawata, Y., and Kimoto, T. 1989. Establishment of five human myeloma cell lines. *In Vitro Cell Dev Biol* 25:723-729.
310. Lombardi, L., Poretti, G., Mattioli, M., Fabris, S., Agnelli, L., Bicciato, S., Kwee, I., Rinaldi, A., Ronchetti, D., Verdelli, D., et al. 2007. Molecular characterization of human multiple myeloma cell lines by integrative genomics: insights into the biology of the disease. *Genes Chromosomes Cancer* 46:226-238.
311. Hjorth-Hansen, H., Seifert, M.F., Borset, M., Aarset, H., Ostlie, A., Sundan, A., and Waage, A. 1999. Marked osteoblastopenia and reduced bone formation in a

model of multiple myeloma bone disease in severe combined immunodeficiency mice. *J Bone Miner Res* 14:256-263.
312. Mitsiades, C.S., Mitsiades, N.S., Bronson, R.T., Chauhan, D., Munshi, N., Treon, S.P., Maxwell, C.A., Pilarski, L., Hideshima, T., Hoffman, R.M., et al. 2003. Fluorescence imaging of multiple myeloma cells in a clinically relevant SCID/NOD in vivo model: biologic and clinical implications. *Cancer Res* 63:6689-6696.
313. Dewan, M.Z., Watanabe, M., Terashima, K., Aoki, M., Sata, T., Honda, M., Ito, M., Yamaoka, S., Watanabe, T., Horie, R., et al. 2004. Prompt tumor formation and maintenance of constitutive NF-kappaB activity of multiple myeloma cells in NOD/SCID/gammacnull mice. *Cancer Sci* 95:564-568.
314. Mazars, G.R., Portier, M., Zhang, X.G., Jourdan, M., Bataille, R., Theillet, C., and Klein, B. 1992. Mutations of the p53 gene in human myeloma cell lines. *Oncogene* 7:1015-1018.
315. Portier, M., Moles, J.P., Mazars, G.R., Jeanteur, P., Bataille, R., Klein, B., and Theillet, C. 1992. p53 and RAS gene mutations in multiple myeloma. *Oncogene* 7:2539-2543.
316. Li, X., Pennisi, A., Zhan, F., Sawyer, J.R., Shaughnessy, J.D., and Yaccoby, S. 2007. Establishment and exploitation of hyperdiploid and non-hyperdiploid human myeloma cell lines. *Br J Haematol* 138:802-811.
317. Zhu, Y.X., Tiedemann, R., Shi, C.X., Yin, H., Schmidt, J.E., Bruins, L.A., Keats, J.J., Braggio, E., Sereduk, C., Mousses, S., et al. 2011. RNAi screen of the druggable genome identifies modulators of proteasome inhibitor sensitivity in myeloma including CDK5. *Blood* 117:3847-3857.
318. Bergsagel, D.E., and Valeriote, F.A. 1968. Growth characteristics of a mouse plasma cell tumor. *Cancer Res* 28:2187-2196.
319. Park, C.H., Bergsagel, D.E., and McCulloch, E.A. 1971. Mouse myeloma tumor stem cells: a primary cell culture assay. *J Natl Cancer Inst* 46:411-422.
320. Drewinko, B., Alexanian, R., Boyer, H., Barlogie, B., and Rubinow, S.I. 1981. The growth fraction of human myeloma cells. *Blood* 57:333-338.
321. Hamburger, A., and Salmon, S.E. 1977. Primary bioassay of human myeloma stem cells. *J Clin Invest* 60:846-854.
322. Hamburger, A.W., Kim, M.B., and Salmon, S.E. 1979. The nature of cells generating human myeloma colonies in vitro. *J Cell Physiol* 98:371-376.
323. Szczepek, A.J., Seeberger, K., Wizniak, J., Mant, M.J., Belch, A.R., and Pilarski, L.M. 1998. A high frequency of circulating B cells share clonotypic Ig heavy-chain VDJ rearrangements with autologous bone marrow plasma cells in multiple myeloma, as measured by single-cell and in situ reverse transcriptase-polymerase chain reaction. *Blood* 92:2844-2855.
324. Bergsagel, P.L., Smith, A.M., Szczepek, A., Mant, M.J., Belch, A.R., and Pilarski, L.M. 1995. In multiple myeloma, clonotypic B lymphocytes are detectable among CD19+ peripheral blood cells expressing CD38, CD56, and monotypic Ig light chain. *Blood* 85:436-447.
325. Chen, B.J., and Epstein, J. 1996. Circulating clonal lymphocytes in myeloma constitute a minor subpopulation of B cells. *Blood* 87:1972-1976.
326. Rasmussen, T. 2001. The presence of circulating clonal CD19+ cells in multiple myeloma. *Leuk Lymphoma* 42:1359-1366.

327. Rasmussen, T., Lodahl, M., Hancke, S., and Johnsen, H.E. 2004. In multiple myeloma clonotypic CD38- /CD19+ / CD27+ memory B cells recirculate through bone marrow, peripheral blood and lymph nodes. *Leuk Lymphoma* 45:1413-1417.
328. Sanderson, R.D., and Yang, Y. 2008. Syndecan-1: a dynamic regulator of the myeloma microenvironment. *Clin Exp Metastasis* 25:149-159.
329. Yang, Y., Macleod, V., Miao, H.Q., Theus, A., Zhan, F., Shaughnessy, J.D., Jr., Sawyer, J., Li, J.P., Zcharia, E., Vlodavsky, I., et al. 2007. Heparanase enhances syndecan-1 shedding: a novel mechanism for stimulation of tumor growth and metastasis. *J Biol Chem* 282:13326-13333.
330. Ikeda, H., Hideshima, T., Fulciniti, M., Lutz, R.J., Yasui, H., Okawa, Y., Kiziltepe, T., Vallet, S., Pozzi, S., Santo, L., et al. 2009. The monoclonal antibody nBT062 conjugated to cytotoxic Maytansinoids has selective cytotoxicity against CD138-positive multiple myeloma cells in vitro and in vivo. *Clin Cancer Res* 15:4028-4037.
331. Matsui, W., Huff, C.A., Wang, Q., Malehorn, M.T., Barber, J., Tanhehco, Y., Smith, B.D., Civin, C.I., and Jones, R.J. 2004. Characterization of clonogenic multiple myeloma cells. *Blood* 103:2332-2336.
332. Gooding, R.P., Bybee, A., Cooke, F., Little, A., Marsh, S.G., Coelho, E., Gupta, D., Samson, D., and Apperley, J.F. 1999. Phenotypic and molecular analysis of six human cell lines derived from patients with plasma cell dyscrasia. *Br J Haematol* 106:669-681.
333. Matsui, W., Wang, Q., Barber, J.P., Brennan, S., Smith, B.D., Borrello, I., McNiece, I., Lin, L., Ambinder, R.F., Peacock, C., et al. 2008. Clonogenic multiple myeloma progenitors, stem cell properties, and drug resistance. *Cancer Res* 68:190-197.
334. Clarke, M.F., and Fuller, M. 2006. Stem cells and cancer: two faces of eve. *Cell* 124:1111-1115.
335. Peacock, C.D., Wang, Q., Gesell, G.S., Corcoran-Schwartz, I.M., Jones, E., Kim, J., Devereux, W.L., Rhodes, J.T., Huff, C.A., Beachy, P.A., et al. 2007. Hedgehog signaling maintains a tumor stem cell compartment in multiple myeloma. *Proc Natl Acad Sci U S A* 104:4048-4053.
336. Dierks, C., Grbic, J., Zirlik, K., Beigi, R., Englund, N.P., Guo, G.R., Veelken, H., Engelhardt, M., Mertelsmann, R., Kelleher, J.F., et al. 2007. Essential role of stromally induced hedgehog signaling in B-cell malignancies. *Nat Med* 13:944-951.
337. Epstein, J. 1997. Myeloma stem cell phenotype. Implications for treatment. *Hematol Oncol Clin North Am* 11:43-49.
338. Berenson, J.R., Vescio, R.A., and Said, J. 1998. Multiple myeloma: the cells of origin--a two-way street. *Leukemia* 12:121-127.
339. Mitterer, M., Oduncu, F., Lanthaler, A.J., Drexler, E., Amaddii, G., Fabris, P., Emmerich, B., Coser, P., and Straka, C. 1999. The relationship between monoclonal myeloma precursor B cells in the peripheral blood stem cell harvests and the clinical response of multiple myeloma patients. *Br J Haematol* 106:737-743.

340. Davies, F.E., Rawstron, A.C., Owen, R.G., and Morgan, G.J. 2000. Controversies surrounding the clonogenic origin of multiple myeloma. *Br J Haematol* 110:240-241.
341. Pilarski, L.M., and Jensen, G.S. 1992. Monoclonal circulating B cells in multiple myeloma. A continuously differentiating, possibly invasive, population as defined by expression of CD45 isoforms and adhesion molecules. *Hematol Oncol Clin North Am* 6:297-322.
342. Billadeau, D., Ahmann, G., Greipp, P., and Van Ness, B. 1993. The bone marrow of multiple myeloma patients contains B cell populations at different stages of differentiation that are clonally related to the malignant plasma cell. *J Exp Med* 178:1023-1031.
343. Bakkus, M.H., Van Riet, I., Van Camp, B., and Thielemans, K. 1994. Evidence that the clonogenic cell in multiple myeloma originates from a pre-switched but somatically mutated B cell. *Br J Haematol* 87:68-74.
344. Berenson, J.R., Vescio, R.A., Hong, C.H., Cao, J., Kim, A., Lee, C.C., Schiller, G., Berenson, R.J., and Lichtenstein, A.K. 1995. Multiple myeloma clones are derived from a cell late in B lymphoid development. *Curr Top Microbiol Immunol* 194:25-33.
345. Rasmussen, T., Kastrup, J., Knudsen, L.M., and Johnsen, H.E. 1999. High numbers of clonal CD19+ cells in the peripheral blood of a patient with multiple myeloma. *Br J Haematol* 105:265-267.
346. Pilarski, L.M., Szczepek, A.J., and Belch, A.R. 1997. Deficient drug transporter function of bone marrow-localized and leukemic plasma cells in multiple myeloma. *Blood* 90:3751-3759.
347. Pilarski, L.M., and Belch, A.R. 1994. Circulating monoclonal B cells expressing P glycoprotein may be a reservoir of multidrug-resistant disease in multiple myeloma. *Blood* 83:724-736.
348. Kiel, K., Cremer, F.W., Rottenburger, C., Kallmeyer, C., Ehrbrecht, E., Atzberger, A., Hegenbart, U., Goldschmidt, H., and Moos, M. 1999. Analysis of circulating tumor cells in patients with multiple myeloma during the course of high-dose therapy with peripheral blood stem cell transplantation. *Bone Marrow Transplant* 23:1019-1027.
349. Rottenburger, C., Kiel, K., Bosing, T., Cremer, F.W., Moldenhauer, G., Ho, A.D., Goldschmidt, H., and Moos, M. 1999. Clonotypic CD20+ and CD19+ B cells in peripheral blood of patients with multiple myeloma post high-dose therapy and peripheral blood stem cell transplantation. *Br J Haematol* 106:545-552.
350. Rasmussen, T., Jensen, L., Honore, L., and Johnsen, H.E. 2000. Frequency and kinetics of polyclonal and clonal B cells in the peripheral blood of patients being treated for multiple myeloma. *Blood* 96:4357-4359.
351. Peceliunas, V., Janiulioniene, A., Matuzeviciene, R., Zvirblis, T., and Griskevicius, L. 2012. Circulating plasma cells predict the outcome of relapsed or refractory multiple myeloma. *Leuk Lymphoma* 53:641-647.
352. Kawano, Y., Fujiwara, S., Wada, N., Izaki, M., Yuki, H., Okuno, Y., Iyama, K., Yamasaki, H., Sakai, A., Mitsuya, H., et al. 2012. Multiple myeloma cells expressing low levels of CD138 have an immature phenotype and reduced sensitivity to lenalidomide. *Int J Oncol* 41:876-884.

353. Gu, J.L., Li, J., Zhou, Z.H., Liu, J.R., Huang, B.H., Zheng, D., and Su, C. 2012. Differentiation induction enhances bortezomib efficacy and overcomes drug resistance in multiple myeloma. *Biochem Biophys Res Commun* 420:644-650.
354. Desai, S., Maurin, M., Smith, M.A., Bolick, S.C., Dessureault, S., Tao, J., Sotomayor, E., and Wright, K.L. 2010. PRDM1 is required for mantle cell lymphoma response to bortezomib. *Mol Cancer Res* 8:907-918.
355. Keats, J.J., Chesi, M., Egan, J.B., Garbitt, V.M., Palmer, S.E., Braggio, E., Van Wier, S., Blackburn, P.R., Baker, A.S., Dispenzieri, A., et al. 2012. Clonal competition with alternating dominance in multiple myeloma. *Blood*.
356. Egan, J.B., Shi, C.X., Tembe, W., Christoforides, A., Kurdoglu, A., Sinari, S., Middha, S., Asmann, Y., Schmidt, J., Braggio, E., et al. 2012. Whole-genome sequencing of multiple myeloma from diagnosis to plasma cell leukemia reveals genomic initiating events, evolution, and clonal tides. *Blood* 120:1060-1066.
357. Yuan, J., Shah, R., Kulharya, A., and Ustun, C. 2010. Near-tetraploidy clone can evolve from a hyperdiploidy clone and cause resistance to lenalidomide and bortezomib in a multiple myeloma patient. *Leuk Res* 34:954-957.
358. Morabito, F., Recchia, A.G., Mazzone, C., and Gentile, M. 2012. Targeted therapy of multiple myeloma: the changing paradigm at the beginning of the new millennium. *Curr Cancer Drug Targets*.
359. Balyasnikova, I.V., Ferguson, S.D., Han, Y., Liu, F., and Lesniak, M.S. 2011. Therapeutic effect of neural stem cells expressing TRAIL and bortezomib in mice with glioma xenografts. *Cancer Lett* 310:148-159.
360. Kahana, S., Finniss, S., Cazacu, S., Xiang, C., Lee, H.K., Brodie, S., Goldstein, R.S., Roitman, V., Slavin, S., Mikkelsen, T., et al. 2011. Proteasome inhibitors sensitize glioma cells and glioma stem cells to TRAIL-induced apoptosis by PKCepsilon-dependent downregulation of AKT and XIAP expressions. *Cell Signal* 23:1348-1357.
361. Bruning, A., Vogel, M., Mylonas, I., Friese, K., and Burges, A. 2011. Bortezomib targets the caspase-like proteasome activity in cervical cancer cells, triggering apoptosis that can be enhanced by nelfinavir. *Curr Cancer Drug Targets* 11:799-809.
362. Luo, P., Lin, M., Zhu, D., Wang, Z., Shen, J., Yang, B., and He, Q. 2010. Bortezomib induces apoptosis in human neuroblastoma CHP126 cells. *Pharmazie* 65:213-218.
363. Armstrong, M.B., Schumacher, K.R., Mody, R., Yanik, G.A., Opipari, A.W., Jr., and Castle, V.P. 2008. Bortezomib as a therapeutic candidate for neuroblastoma. *J Exp Ther Oncol* 7:135-145.
364. Pasquini, L., Petronelli, A., Petrucci, E., Saulle, E., Mariani, G., Scambia, G., Benedetti-Panici, P., Greggi, S., Cognetti, F., and Testa, U. 2010. Primary ovarian cancer cells are sensitive to the proaptotic effects of proteasome inhibitors. *Int J Oncol* 36:707-713.
365. Periyasamy-Thandavan, S., Jackson, W.H., Samaddar, J.S., Erickson, B., Barrett, J.R., Raney, L., Gopal, E., Ganapathy, V., Hill, W.D., Bhalla, K.N., et al. 2010. Bortezomib blocks the catabolic process of autophagy via a cathepsin-dependent mechanism, affects endoplasmic reticulum stress and induces caspase-dependent cell death in antiestrogen-sensitive and resistant ER+ breast cancer cells. *Autophagy* 6:19-35.

366. Bauer, S., Parry, J.A., Muhlenberg, T., Brown, M.F., Seneviratne, D., Chatterjee, P., Chin, A., Rubin, B.P., Kuan, S.F., Fletcher, J.A., et al. 2010. Proapoptotic activity of bortezomib in gastrointestinal stromal tumor cells. *Cancer Res* 70:150-159.
367. Goktas, S., Baran, Y., Ural, A.U., Yazici, S., Aydur, E., Basal, S., Avcu, F., Pekel, A., Dirican, B., and Beyzadeoglu, M. 2010. Proteasome inhibitor bortezomib increases radiation sensitivity in androgen independent human prostate cancer cells. *Urology* 75:793-798.
368. Christian, P.A., Thorpe, J.A., and Schwarze, S.R. 2009. Velcade sensitizes prostate cancer cells to TRAIL induced apoptosis and suppresses tumor growth in vivo. *Cancer Biol Ther* 8:73-80.
369. Chen, Z., Ricker, J.L., Malhotra, P.S., Nottingham, L., Bagain, L., Lee, T.L., Yeh, N.T., and Van Waes, C. 2008. Differential bortezomib sensitivity in head and neck cancer lines corresponds to proteasome, nuclear factor-kappaB and activator protein-1 related mechanisms. *Mol Cancer Ther* 7:1949-1960.
370. Li, C., Li, R., Grandis, J.R., and Johnson, D.E. 2008. Bortezomib induces apoptosis via Bim and Bik up-regulation and synergizes with cisplatin in the killing of head and neck squamous cell carcinoma cells. *Mol Cancer Ther* 7:1647-1655.
371. Croonquist, P.A., Linden, M.A., Zhao, F., and Van Ness, B.G. 2003. Gene profiling of a myeloma cell line reveals similarities and unique signatures among IL-6 response, N-ras-activating mutations, and coculture with bone marrow stromal cells. *Blood* 102:2581-2592.
372. Lee, E.C., Fitzgerald, M., Bannerman, B., Donelan, J., Bano, K., Terkelsen, J., Bradley, D.P., Subakan, O., Silva, M.D., Liu, R., et al. 2011. Antitumor activity of the investigational proteasome inhibitor MLN9708 in mouse models of B-cell and plasma cell malignancies. *Clin Cancer Res* 17:7313-7323.
373. Urashima, M., Ogata, A., Chauhan, D., Vidriales, M.B., Teoh, G., Hoshi, Y., Schlossman, R.L., DeCaprio, J.A., and Anderson, K.C. 1996. Interleukin-6 promotes multiple myeloma cell growth via phosphorylation of retinoblastoma protein. *Blood* 88:2219-2227.
374. Kubagawa, H., Vogler, L.B., Capra, J.D., Conrad, M.E., Lawton, A.R., and Cooper, M.D. 1979. Studies on the clonal origin of multiple myeloma. Use of individually specific (idiotype) antibodies to trace the oncogenic event to its earliest point of expression in B-cell differentiation. *J Exp Med* 150:792-807.
375. Chen, D., Frezza, M., Schmitt, S., Kanwar, J., and Dou, Q.P. 2011. Bortezomib as the first proteasome inhibitor anticancer drug: current status and future perspectives. *Curr Cancer Drug Targets* 11:239-253.
376. Richardson, P.G., Barlogie, B., Berenson, J., Singhal, S., Jagannath, S., Irwin, D., Rajkumar, S.V., Srkalovic, G., Alsina, M., Alexanian, R., et al. 2003. A phase 2 study of bortezomib in relapsed, refractory myeloma. *N Engl J Med* 348:2609-2617.
377. Mahindra, A., Laubach, J., Raje, N., Munshi, N., Richardson, P.G., and Anderson, K. 2012. Latest advances and current challenges in the treatment of multiple myeloma. *Nat Rev Clin Oncol* 9:135-143.
378. Orlowski, R.Z., and Kuhn, D.J. 2008. Proteasome inhibitors in cancer therapy: lessons from the first decade. *Clin Cancer Res* 14:1649-1657.

379. Ciechanover, A. 2005. Proteolysis: from the lysosome to ubiquitin and the proteasome. *Nat Rev Mol Cell Biol* 6:79-87.
380. Kisselev, A.F., van der Linden, W.A., and Overkleeft, H.S. 2012. Proteasome inhibitors: an expanding army attacking a unique target. *Chem Biol* 19:99-115.
381. Obeng, E.A., Carlson, L.M., Gutman, D.M., Harrington, W.J., Jr., Lee, K.P., and Boise, L.H. 2006. Proteasome inhibitors induce a terminal unfolded protein response in multiple myeloma cells. *Blood* 107:4907-4916.
382. Atadja, P. 2009. Development of the pan-DAC inhibitor panobinostat (LBH589): successes and challenges. *Cancer Lett* 280:233-241.
383. Pei, X.Y., Dai, Y., and Grant, S. 2004. Synergistic induction of oxidative injury and apoptosis in human multiple myeloma cells by the proteasome inhibitor bortezomib and histone deacetylase inhibitors. *Clin Cancer Res* 10:3839-3852.
384. Hideshima, T., Bradner, J.E., Wong, J., Chauhan, D., Richardson, P., Schreiber, S.L., and Anderson, K.C. 2005. Small-molecule inhibition of proteasome and aggresome function induces synergistic antitumor activity in multiple myeloma. *Proc Natl Acad Sci U S A* 102:8567-8572.
385. Catley, L., Weisberg, E., Kiziltepe, T., Tai, Y.T., Hideshima, T., Neri, P., Tassone, P., Atadja, P., Chauhan, D., Munshi, N.C., et al. 2006. Aggresome induction by proteasome inhibitor bortezomib and alpha-tubulin hyperacetylation by tubulin deacetylase (TDAC) inhibitor LBH589 are synergistic in myeloma cells. *Blood* 108:3441-3449.
386. Campbell, R.A., Sanchez, E., Steinberg, J., Shalitin, D., Li, Z.W., Chen, H., and Berenson, J.R. 2010. Vorinostat enhances the antimyeloma effects of melphalan and bortezomib. *Eur J Haematol* 84:201-211.
387. Ocio, E.M., Vilanova, D., Atadja, P., Maiso, P., Crusoe, E., Fernandez-Lazaro, D., Garayoa, M., San-Segundo, L., Hernandez-Iglesias, T., de Alava, E., et al. 2010. In vitro and in vivo rationale for the triple combination of panobinostat (LBH589) and dexamethasone with either bortezomib or lenalidomide in multiple myeloma. *Haematologica* 95:794-803.
388. Sanchez, E., Shen, J., Steinberg, J., Li, M., Wang, C., Bonavida, B., Chen, H., Li, Z.W., and Berenson, J.R. 2011. The histone deacetylase inhibitor LBH589 enhances the anti-myeloma effects of chemotherapy in vitro and in vivo. *Leuk Res* 35:373-379.
389. Sarver, A.L. 2010. Toward understanding the informatics and statistical aspects of micro-RNA profiling. *J Cardiovasc Transl Res* 3:204-211.
390. Shaughnessy, J.D., Jr., Qu, P., Usmani, S., Heuck, C.J., Zhang, Q., Zhou, Y., Tian, E., Hanamura, I., van Rhee, F., Anaissie, E., et al. 2011. Pharmacogenomics of bortezomib test-dosing identifies hyperexpression of proteasome genes, especially PSMD4, as novel high-risk feature in myeloma treated with total therapy 3. *Blood*.
391. Lamb, J. 2007. The Connectivity Map: a new tool for biomedical research. *Nat Rev Cancer* 7:54-60.
392. Wei, G., Twomey, D., Lamb, J., Schlis, K., Agarwal, J., Stam, R.W., Opferman, J.T., Sallan, S.E., den Boer, M.L., Pieters, R., et al. 2006. Gene expression-based chemical genomics identifies rapamycin as a modulator of MCL1 and glucocorticoid resistance. *Cancer Cell* 10:331-342.

393. Bookout, A.L., Cummins, C.L., Mangelsdorf, D.J., Pesola, J.M., and Kramer, M.F. 2006. High-throughput real-time quantitative reverse transcription PCR. *Curr Protoc Mol Biol* Chapter 15:Unit 15 18.
394. Altun, M., Galardy, P.J., Shringarpure, R., Hideshima, T., LeBlanc, R., Anderson, K.C., Ploegh, H.L., and Kessler, B.M. 2005. Effects of PS-341 on the activity and composition of proteasomes in multiple myeloma cells. *Cancer Res* 65:7896-7901.
395. Greenstein, S., Krett, N.L., Kurosawa, Y., Ma, C., Chauhan, D., Hideshima, T., Anderson, K.C., and Rosen, S.T. 2003. Characterization of the MM.1 human multiple myeloma (MM) cell lines: a model system to elucidate the characteristics, behavior, and signaling of steroid-sensitive and -resistant MM cells. *Exp Hematol* 31:271-282.
396. Weniger, M.A., Rizzatti, E.G., Perez-Galan, P., Liu, D., Wang, Q., Munson, P.J., Raghavachari, N., White, T., Tweito, M.M., Dunleavy, K., et al. Treatment-induced oxidative stress and cellular antioxidant capacity determine response to bortezomib in mantle cell lymphoma. *Clin Cancer Res* 17:5101-5112.
397. Perez-Galan, P., Mora-Jensen, H., Weniger, M.A., Shaffer, A.L., 3rd, Rizzatti, E.G., Chapman, C.M., Mo, C.C., Stennett, L.S., Rader, C., Liu, P., et al. 2010. Bortezomib resistance in mantle cell lymphoma is associated with plasmacytic differentiation. *Blood* 117:542-552.
398. Hideshima, T., Richardson, P.G., and Anderson, K.C. 2011. Mechanism of action of proteasome inhibitors and deacetylase inhibitors and the biological basis of synergy in multiple myeloma. *Mol Cancer Ther* 10:2034-2042.
399. Stewart, A.K. 2012. Novel therapeutics in multiple myeloma. *Hematology* 17 Suppl 1:S105-108.
400. Rao, R., Nalluri, S., Kolhe, R., Yang, Y., Fiskus, W., Chen, J., Ha, K., Buckley, K.M., Balusu, R., Coothankandaswamy, V., et al. 2010. Treatment with panobinostat induces glucose-regulated protein 78 acetylation and endoplasmic reticulum stress in breast cancer cells. *Mol Cancer Ther* 9:942-952.
401. Hideshima, T., and Anderson, K.C. 2011. Novel therapies in MM: from the aspect of preclinical studies. *Int J Hematol* 94:344-354.
402. Chauhan, D., Singh, A.V., Brahmandam, M., Carrasco, R., Bandi, M., Hideshima, T., Bianchi, G., Podar, K., Tai, Y.T., Mitsiades, C., et al. 2009. Functional interaction of plasmacytoid dendritic cells with multiple myeloma cells: a therapeutic target. *Cancer Cell* 16:309-323.
403. Mulligan, G., Mitsiades, C., Bryant, B., Zhan, F., Chng, W.J., Roels, S., Koenig, E., Fergus, A., Huang, Y., Richardson, P., et al. 2007. Gene expression profiling and correlation with outcome in clinical trials of the proteasome inhibitor bortezomib. *Blood* 109:3177-3188.
404. Goy, A., Bernstein, S.H., McDonald, A., Pickard, M.D., Shi, H., Fleming, M.D., Bryant, B., Trepicchio, W., Fisher, R.I., Boral, A.L., et al. 2010. Potential biomarkers of bortezomib activity in mantle cell lymphoma from the phase 2 PINNACLE trial. *Leuk Lymphoma* 51:1269-1277.
405. Jia, H., Ge, F., Lu, X., Zeng, H., Li, L., Chen, Z., and Lu, C. 2010. Proteomics of apoptosis of multiple myeloma cells induced by proteasome inhibitor PS-341. *Zhong Nan Da Xue Xue Bao Yi Xue Ban* 35:784-791.

406. Vande Broek, I., Leleu, X., Schots, R., Facon, T., Vanderkerken, K., Van Camp, B., and Van Riet, I. 2006. Clinical significance of chemokine receptor (CCR1, CCR2 and CXCR4) expression in human myeloma cells: the association with disease activity and survival. *Haematologica* 91:200-206.
407. Catley, L., Weisberg, E., Tai, Y.T., Atadja, P., Remiszewski, S., Hideshima, T., Mitsiades, N., Shringarpure, R., LeBlanc, R., Chauhan, D., et al. 2003. NVP-LAQ824 is a potent novel histone deacetylase inhibitor with significant activity against multiple myeloma. *Blood* 102:2615-2622.
408. Rao, R., Nalluri, S., Fiskus, W., Savoie, A., Buckley, K.M., Ha, K., Balusu, R., Joshi, A., Coothankandaswamy, V., Tao, J., et al. 2010. Role of CAAT/enhancer binding protein homologous protein in panobinostat-mediated potentiation of bortezomib-induced lethal endoplasmic reticulum stress in mantle cell lymphoma cells. *Clin Cancer Res* 16:4742-4754.
409. Kawaguchi, Y., Kovacs, J.J., McLaurin, A., Vance, J.M., Ito, A., and Yao, T.P. 2003. The deacetylase HDAC6 regulates aggresome formation and cell viability in response to misfolded protein stress. *Cell* 115:727-738.
410. Chesi, M., Matthews, G.M., Garbitt, V.M., Palmer, S.E., Shortt, J., Lefebure, M., Stewart, A.K., Johnstone, R.W., and Bergsagel, P.L. 2012. Drug response in a genetically engineered mouse model of multiple myeloma is predictive of clinical efficacy. *Blood* 120:376-385.
411. Iorio, F., Bosotti, R., Scacheri, E., Belcastro, V., Mithbaokar, P., Ferriero, R., Murino, L., Tagliaferri, R., Brunetti-Pierri, N., Isacchi, A., et al. 2010. Discovery of drug mode of action and drug repositioning from transcriptional responses. *Proc Natl Acad Sci U S A* 107:14621-14626.
412. Barlogie, B., Anaissie, E., van Rhee, F., Pineda-Roman, M., Zangari, M., Shaughnessy, J., Epstein, J., and Crowley, J. 2007. The Arkansas approach to therapy of patients with multiple myeloma. *Best Pract Res Clin Haematol* 20:761-781.
413. Lamb, J., Crawford, E.D., Peck, D., Modell, J.W., Blat, I.C., Wrobel, M.J., Lerner, J., Brunet, J.P., Subramanian, A., Ross, K.N., et al. 2006. The Connectivity Map: using gene-expression signatures to connect small molecules, genes, and disease. *Science* 313:1929-1935.
414. Hassane, D.C., Guzman, M.L., Corbett, C., Li, X., Abboud, R., Young, F., Liesveld, J.L., Carroll, M., and Jordan, C.T. 2008. Discovery of agents that eradicate leukemia stem cells using an in silico screen of public gene expression data. *Blood* 111:5654-5662.
415. Karube, K., Tsuzuki, S., Yoshida, N., Arita, K., Kato, H., Katayama, M., Ko, Y.H., Ohshimad, K., Nakamura, S., Kinoshita, T., et al. 2013. Comprehensive gene expression profiles of NK cell neoplasms identify vorinostat as an effective drug candidate. *Cancer Lett*.
416. Yu, G., Wang, L., Li, Y., and Ma, Z. 2013. Identification of drug candidates for osteoporosis by computational bioinformatics analysis of gene expression profile. *Eur J Med Res* 18:5.
417. Ushijima, M., Mashima, T., Tomida, A., Dan, S., Saito, S., Furuno, A., Tsukahara, S., Seimiya, H., Yamori, T., and Matsuura, M. 2013. Development of a gene expression database and related analysis programs for evaluation of anticancer compounds. *Cancer Sci* 104:360-368.

418. Stessman, H.A.F., Baughn, L.B., Sarver, A.L., Xia, T., Deshpande, R., Mansoor, A., Walsh, S., Sunderland, J., Dolloff, N., Linden, M., et al. Manuscript submitted for publication. Profiling bortezomib resistance identifies secondary therapies in a mouse myeloma model.
419. Congdon, L.M., Pourpak, A., Escalante, A.M., Dorr, R.T., and Landowski, T.H. 2008. Proteasomal inhibition stabilizes topoisomerase IIalpha protein and reverses resistance to the topoisomerase II poison ethonafide (AMP-53, 6-ethoxyazonafide). *Biochem Pharmacol* 75:883-890.
420. Chou, T.C. 2010. Drug combination studies and their synergy quantification using the Chou-Talalay method. *Cancer Res* 70:440-446.
421. Xie, X.Q., and Chen, J.Z. 2008. Data mining a small molecule drug screening representative subset from NIH PubChem. *J Chem Inf Model* 48:465-475.
422. Chou, T.C. 2008. Preclinical versus clinical drug combination studies. *Leuk Lymphoma* 49:2059-2080.
423. Pommier, Y., Leo, E., Zhang, H., and Marchand, C. 2010. DNA topoisomerases and their poisoning by anticancer and antibacterial drugs. *Chem Biol* 17:421-433.
424. Pommier, Y., Barcelo, J.M., Rao, V.A., Sordet, O., Jobson, A.G., Thibaut, L., Miao, Z.H., Seiler, J.A., Zhang, H., Marchand, C., et al. 2006. Repair of topoisomerase I-mediated DNA damage. *Prog Nucleic Acid Res Mol Biol* 81:179-229.
425. Heisig, P. 2009. Type II topoisomerases--inhibitors, repair mechanisms and mutations. *Mutagenesis* 24:465-469.
426. Lee, C.K., Barlogie, B., Munshi, N., Zangari, M., Fassas, A., Jacobson, J., van Rhee, F., Cottler-Fox, M., Muwalla, F., and Tricot, G. 2003. DTPACE: an effective, novel combination chemotherapy with thalidomide for previously treated patients with myeloma. *J Clin Oncol* 21:2732-2739.
427. Kraut, E.H., Ju, R., and Muller, M. 1998. The use of topoisomerase I inhibitors in multiple myeloma. *Semin Hematol* 35:32-38.
428. Kraut, E.H., Crowley, J.J., Wade, J.L., Laufman, L.R., Alsina, M., Taylor, S.A., and Salmon, S.E. 1998. Evaluation of topotecan in resistant and relapsing multiple myeloma: a Southwest Oncology Group study. *J Clin Oncol* 16:589-592.
429. Iyer, L., Das, S., Janisch, L., Wen, M., Ramirez, J., Karrison, T., Fleming, G.F., Vokes, E.E., Schilsky, R.L., and Ratain, M.J. 2002. UGT1A1*28 polymorphism as a determinant of irinotecan disposition and toxicity. *Pharmacogenomics J* 2:43-47.
430. Palomaki, G.E., Bradley, L.A., Douglas, M.P., Kolor, K., and Dotson, W.D. 2009. Can UGT1A1 genotyping reduce morbidity and mortality in patients with metastatic colorectal cancer treated with irinotecan? An evidence-based review. *Genet Med* 11:21-34.
431. Dimopoulos, M.A., Mateos, M.V., Richardson, P.G., Schlag, R., Khuageva, N.K., Shpilberg, O., Kropff, M., Spicka, I., Palumbo, A., Wu, K.L., et al. 2011. Risk factors for, and reversibility of, peripheral neuropathy associated with bortezomib-melphalan-prednisone in newly diagnosed patients with multiple myeloma: subanalysis of the phase 3 VISTA study. *Eur J Haematol* 86:23-31.
432. Chen-Kiang, S. 2003. Cell-cycle control of plasma cell differentiation and tumorigenesis. *Immunol Rev* 194:39-47.

433. Landis, S.H., Murray, T., Bolden, S., and Wingo, P.A. 1999. Cancer statistics, 1999. *CA Cancer J Clin* 49:8-31, 31.
434. Hershko, A., and Ciechanover, A. 1998. The ubiquitin system. *Annu Rev Biochem* 67:425-479.
435. Rajkumar, S.V., Richardson, P.G., Hideshima, T., and Anderson, K.C. 2005. Proteasome inhibition as a novel therapeutic target in human cancer. *J Clin Oncol* 23:630-639.
436. Adams, J., Palombella, V.J., Sausville, E.A., Johnson, J., Destree, A., Lazarus, D.D., Maas, J., Pien, C.S., Prakash, S., and Elliott, P.J. 1999. Proteasome inhibitors: a novel class of potent and effective antitumor agents. *Cancer Res* 59:2615-2622.
437. Richardson, P.G., Laubach, J., Mitsiades, C.S., Schlossman, R., Hideshima, T., Redman, K., Chauhan, D., Ghobrial, I.M., Munshi, N., and Anderson, K.C. 2011. Managing multiple myeloma: the emerging role of novel therapies and adapting combination treatment for higher risk settings. *Br J Haematol*.
438. Lonial, S. 2010. Presentation and risk stratification--improving prognosis for patients with multiple myeloma. *Cancer Treat Rev* 36 Suppl 2:S12-17.
439. Angelin-Duclos, C., Cattoretti, G., Lin, K.I., and Calame, K. 2000. Commitment of B lymphocytes to a plasma cell fate is associated with Blimp-1 expression in vivo. *J Immunol* 165:5462-5471.
440. Alsayed, Y., Ngo, H., Runnels, J., Leleu, X., Singha, U.K., Pitsillides, C.M., Spencer, J.A., Kimlinger, T., Ghobrial, J.M., Jia, X., et al. 2007. Mechanisms of regulation of CXCR4/SDF-1 (CXCL12)-dependent migration and homing in multiple myeloma. *Blood* 109:2708-2717.
441. Bhattacharya, D., Cheah, M.T., Franco, C.B., Hosen, N., Pin, C.L., Sha, W.C., and Weissman, I.L. 2007. Transcriptional profiling of antigen-dependent murine B cell differentiation and memory formation. *J Immunol* 179:6808-6819.
442. Chevrier, S., Genton, C., Kallies, A., Karnowski, A., Otten, L.A., Malissen, B., Malissen, M., Botto, M., Corcoran, L.M., Nutt, S.L., et al. 2009. CD93 is required for maintenance of antibody secretion and persistence of plasma cells in the bone marrow niche. *Proc Natl Acad Sci U S A* 106:3895-3900.
443. Kearney, J.F., Radbruch, A., Liesegang, B., and Rajewsky, K. 1979. A new mouse myeloma cell line that has lost immunoglobulin expression but permits the construction of antibody-secreting hybrid cell lines. *Journal of Immunology* 123:1548-1550.
444. Poltorak, A., He, X., Smirnova, I., Liu, M.Y., Van Huffel, C., Du, X., Birdwell, D., Alejos, E., Silva, M., Galanos, C., et al. 1998. Defective LPS signaling in C3H/HeJ and C57BL/10ScCr mice: mutations in Tlr4 gene. *Science* 282:2085-2088.
445. Poltorak, A., Smirnova, I., He, X., Liu, M.Y., Van Huffel, C., McNally, O., Birdwell, D., Alejos, E., Silva, M., Du, X., et al. 1998. Genetic and physical mapping of the Lps locus: identification of the toll-4 receptor as a candidate gene in the critical region. *Blood Cells Mol Dis* 24:340-355.
446. Meister, S., Schubert, U., Neubert, K., Herrmann, K., Burger, R., Gramatzki, M., Hahn, S., Schreiber, S., Wilhelm, S., Herrmann, M., et al. 2007. Extensive immunoglobulin production sensitizes myeloma cells for proteasome inhibition. *Cancer Res* 67:1783-1792.

447. Kunkel, E.J., and Butcher, E.C. 2003. Plasma-cell homing. *Nat Rev Immunol* 3:822-829.
448. Platica, M., and Hollander, V.P. 1985. Lipopolysaccharide stimulation of plasmacytoma cells. *J Natl Cancer Inst* 74:197-201.
449. Molyneux, E.M., Rochford, R., Griffin, B., Newton, R., Jackson, G., Menon, G., Harrison, C.J., Israels, T., and Bailey, S. 2012. Burkitt's lymphoma. *Lancet* 379:1234-1244.
450. Muramatsu, M., Kinoshita, K., Fagarasan, S., Yamada, S., Shinkai, Y., and Honjo, T. 2000. Class switch recombination and hypermutation require activation-induced cytidine deaminase (AID), a potential RNA editing enzyme. *Cell* 102:553-563.
451. Pasqualucci, L., Guglielmino, R., Houldsworth, J., Mohr, J., Aoufouchi, S., Polakiewicz, R., Chaganti, R.S., and Dalla-Favera, R. 2004. Expression of the AID protein in normal and neoplastic B cells. *Blood* 104:3318-3325.
452. Pasqualucci, L., Bhagat, G., Jankovic, M., Compagno, M., Smith, P., Muramatsu, M., Honjo, T., Morse, H.C., 3rd, Nussenzweig, M.C., and Dalla-Favera, R. 2008. AID is required for germinal center-derived lymphomagenesis. *Nat Genet* 40:108-112.
453. Mechtcheriakova, D., Svoboda, M., Meshcheryakova, A., and Jensen-Jarolim, E. 2012. Activation-induced cytidine deaminase (AID) linking immunity, chronic inflammation, and cancer. *Cancer Immunol Immunother* 61:1591-1598.
454. Okazaki, I.M., Kotani, A., and Honjo, T. 2007. Role of AID in Tumorigenesis. *Adv Immunol* 94:245-273.
455. Klemm, L., Duy, C., Iacobucci, I., Kuchen, S., von Levetzow, G., Feldhahn, N., Henke, N., Li, Z., Hoffmann, T.K., Kim, Y.M., et al. 2009. The B cell mutator AID promotes B lymphoid blast crisis and drug resistance in chronic myeloid leukemia. *Cancer Cell* 16:232-245.
456. Aoufouchi, S., Faili, A., Zober, C., D'Orlando, O., Weller, S., Weill, J.C., and Reynaud, C.A. 2008. Proteasomal degradation restricts the nuclear lifespan of AID. *J Exp Med* 205:1357-1368.
457. Orthwein, A., Patenaude, A.M., Affar el, B., Lamarre, A., Young, J.C., and Di Noia, J.M. 2010. Regulation of activation-induced deaminase stability and antibody gene diversification by Hsp90. *J Exp Med* 207:2751-2765.
458. Takizawa, M., Tolarova, H., Li, Z., Dubois, W., Lim, S., Callen, E., Franco, S., Mosaico, M., Feigenbaum, L., Alt, F.W., et al. 2008. AID expression levels determine the extent of cMyc oncogenic translocations and the incidence of B cell tumor development. *J Exp Med* 205:1949-1957.
459. Mujtaba, T., and Dou, Q.P. 2011. Advances in the understanding of mechanisms and therapeutic use of bortezomib. *Discov Med* 12:471-480.
460. Martin, A., Bardwell, P.D., Woo, C.J., Fan, M., Shulman, M.J., and Scharff, M.D. 2002. Activation-induced cytidine deaminase turns on somatic hypermutation in hybridomas. *Nature* 415:802-806.
461. Zaheen, A., Boulianne, B., Parsa, J.Y., Ramachandran, S., Gommerman, J.L., and Martin, A. 2009. AID constrains germinal center size by rendering B cells susceptible to apoptosis. *Blood* 114:547-554.
462. Navaratnam, N., and Sarwar, R. 2006. An overview of cytidine deaminases. *Int J Hematol* 83:195-200.

463. Siegel, R., Naishadham, D., and Jemal, A. 2013. Cancer statistics, 2013. *CA Cancer J Clin* 63:11-30.
464. Druker, B.J., Tamura, S., Buchdunger, E., Ohno, S., Segal, G.M., Fanning, S., Zimmermann, J., and Lydon, N.B. 1996. Effects of a selective inhibitor of the Abl tyrosine kinase on the growth of Bcr-Abl positive cells. *Nat Med* 2:561-566.
465. Dowsett, M., Cuzick, J., Wale, C., Forbes, J., Mallon, E.A., Salter, J., Quinn, E., Dunbier, A., Baum, M., Buzdar, A., et al. 2010. Prediction of risk of distant recurrence using the 21-gene recurrence score in node-negative and node-positive postmenopausal patients with breast cancer treated with anastrozole or tamoxifen: a TransATAC study. *J Clin Oncol* 28:1829-1834.
466. Koiso, H., Tahara, K., Osaki, Y., Mawatari, M., Sekigami, T., Yokohama, A., Saitoh, T., Uchiumi, H., Handa, H., Tsukamoto, N., et al. 2009. [Development of an extramedullary plasmacytoma despite disappearing M protein in multiple myeloma by bortezomib treatment]. *Rinsho Ketsueki* 50:78-82.
467. Koduru, S., Wong, E., Strowig, T., Sundaram, R., Zhang, L., Strout, M.P., Flavell, R.A., Schatz, D.G., Dhodapkar, K.M., and Dhodapkar, M.V. 2012. Dendritic cell-mediated activation-induced cytidine deaminase (AID)-dependent induction of genomic instability in human myeloma. *Blood* 119:2302-2309.
468. Burns, M.B., Lackey, L., Carpenter, M.A., Rathore, A., Land, A.M., Leonard, B., Refsland, E.W., Kotandeniya, D., Tretyakova, N., Nikas, J.B., et al. 2013. APOBEC3B is an enzymatic source of mutation in breast cancer. *Nature* 494:366-370.
469. Lada, A.G., Dhar, A., Boissy, R.J., Hirano, M., Rubel, A.A., Rogozin, I.B., and Pavlov, Y.I. 2012. AID/APOBEC cytosine deaminase induces genome-wide kataegis. *Biol Direct* 7:47; discussion 47.
470. Nik-Zainal, S., Alexandrov, L.B., Wedge, D.C., Van Loo, P., Greenman, C.D., Raine, K., Jones, D., Hinton, J., Marshall, J., Stebbings, L.A., et al. 2012. Mutational processes molding the genomes of 21 breast cancers. *Cell* 149:979-993.
471. Krumm, N., Sudmant, P.H., Ko, A., O'Roak, B.J., Malig, M., Coe, B.P., Quinlan, A.R., Nickerson, D.A., and Eichler, E.E. 2012. Copy number variation detection and genotyping from exome sequence data. *Genome Res* 22:1525-1532.
472. Flusberg, B.A., Webster, D.R., Lee, J.H., Travers, K.J., Olivares, E.C., Clark, T.A., Korlach, J., and Turner, S.W. 2010. Direct detection of DNA methylation during single-molecule, real-time sequencing. *Nat Methods* 7:461-465.